Mitochondrial Dysfunction in Dopaminergic Neurons and the Impact on Neurodegeneration in Parkinson's disease

I n a u g u r a l – D i s s e r t a t i o n

zur

Erlangung des Doktorgrades

der Mathematisch-Naturwissenschaftlichen Fakultät

der Universität zu Köln

vorgelegt von

Thomas Paß

aus Coesfeld

Köln, 2020

Berichterstatter/in: Prof. Dr. Peter Kloppenburg

Prof. Dr. Aleksandra Trifunovic

Tag der mündlichen Prüfung: 17.07.2020

Index of Contents

List of Figures

List of Abbreviations

6-OHDA	6-hydroxydopamine
α-Syn	alpha-Synuclein
ATP	adenosine triphosphate
ATP13A2	ATPase cation transporting 13A2
bp	base pair
Ca^{2+}	calcium
Ca_v	voltage-gated calcium channels
Ca_v1	L-type voltage-gated calcium channel
$Ca_v1.2$	L-type voltage-gated calcium channel subunit 1.2
$Ca_v1.3$	L-type voltage-gated calcium channel subunit 1.3
$Ca_v2.3$	R-type voltage-gated calcium channel subunit 2.3
CHCHD2	coiled-coil-helix-coiled-coil-helix domain containing 2
ClpP	caseinolytic mitochondrial matrix peptidase proteolytic subunit
CNS	central nervous system
COX	cytochrome c oxidase
CPu	caudate putamen
CSF	cerebrospinal fluid
Cre	cre recombinase
DA	dopamine
DaN	dopaminergic neuron
DAT	dopamine transporter
DBS	deep brain stimulation
DHP	dihydropyridines
DJ-1	parkinsonism associated deglycase
DNA	deoxyribonucleic acid
DOPAL	3,4-dihydroxyphenylacetaldehyde
DRP1	dynamin-related protein 1
E	embryonic day
ERK2	extracellular-signal-regulated protein kinase 2
NADPH phosphate	nicotinamide adenine dinucleotide
NCS-1	neuronal calcium sensor 1

ERK	extracellular-signal-regulated protein kinase 2
Fig	figure
GABA	γ-aminobutyric acid
GL	glomerular layer
GPi	globus pallidus pars interna
GPe	Globus pallidus pars externa
GPx	glutathione peroxidase
GR	glutathione reductase
GSH	glutathione, reduced form
GSSG	glutathione, oxidized form
H_2O_2	hydrogen peroxide
I_h	hyperpolarization-activated current
iPSC	induced pluripotent stem cell
K-ATP	ATP-sensitive potassium channel
KO	knockout
LAC	large axonic cell
L-DOPA	L-3,4-dihydroxyphenylalanine
LRRK2	leucine-rich repeat kinase 2
MAO	monoamine oxidase
MAO_B	monoamine oxidase type B
MDVs	mitochondrial-derived vesicles
MFN1	mitofusin 1
MFN2	mitofusin 2
MPP^+	1-methyl-4-phenylpyridinium
mPTP	mitochondrial permeability transition pore
MPTP	1-methyl-4-phenyl-1,2,3,6-tetrahydropyridine
mt	mitochondrial
mtDNA	mitochondrial DNA
MUL1	mitochondrial E3 ubiquitin ligase 1
NAcc	nucleus accumbens
NADH	nicotinamide adenine dinucleotide
NDP52	nuclear dot protein 52
O_2^-	superoxide

OB	olfactory bulb
OH⁻	hydroxyl radical
OMM	outer mitochondrial membrane
OPA1	optic atrophy 1
OPTN	optineurin
PARIS	parkin interacting substrate
PAX6	paired box 6
PCR	polymerase chain reaction
PET	positron emission tomography
PD	Parkinson's disease
PGC-1α	peroxisome proliferator-activated receptor gamma coactivator 1α
PINK1	PTEN-induced kinase 1
POLγ	mitochondrial DNA polymerase γ
RN	raphe nuclei
RNA	ribonucleic acid
ROS	reactive oxygen species
SC	small anaxonic cell
SDH	succinate dehydrogenase
SERT	serotonin transporter
SNc	substantia nigra pars compacta
SNCA	synuclein α
SNr	substantia nigra pars reticulata
STN	subthalamic nucleus
SVZ	subventricular zone
TFAM	mitochondrial transcription factory A
TOM	translocase of outer membrane
TOM20	translocase of outer membrane 20
VPS35	vacuolar protein sorting 35
VTA	ventral tegmental area

Abstract

Parkinson's disease (PD) is a neurodegenerative disorder affecting ~1% of the population above 60 years. It is primarily characterized by severe motor deficits following the progressive and selective loss of dopaminergic neurons (DaNs) in the *substantia nigra pars compacta* (SNc). Non-motor symptoms, such as hyposmia and depression, further arise in a prodromal manner. Mitochondrial dysfunction plays an essential role for the loss of SNc DaNs, as evidenced by mitochondrial complex I impairing toxins, an especially high accumulation rate of mitochondrial DNA (mtDNA) deletions as well as the wide variety of mitochondrial-related gene mutations in familial forms of PD. Given that neighboring DaNs in the *ventral tegmental area* (VTA) are relatively spared from neurodegeneration, however, cell-type specific factors must additionally contribute to the selective vulnerability in PD. In this work, data of three manuscripts are presented, confirming that distinct DaN populations respond differently to mitochondrial dysfunction following inactivation of mitochondrial transcription factor A (TFAM) in mice. In the olfactory bulb (OB), only small anaxonic DaNs (SCs) are mildly reduced in numbers, which is however associated with severe olfactory dysfunction and suggests a putative role for OB DaNs in the development of PD-related hyposmia. The midbrain reveals progressive and exclusive loss of SNc DaNs, which is accompanied by a severe decline of motor function. In contrast to the VTA, DaNs in the SNc die through a detrimental imbalance in the mitochondrial redox system, triggered by enhanced intracellular Ca^{2+} loads. Whereas SNc DaNs perish due to the rapid and continuous loss of mtDNA upon TFAM inactivation, they can adapt to impaired mtDNA replication, demonstrated after the expression of a mutated variant of the mitochondrial helicase TWINKLE (K320E). Despite similar severe neurodegeneration of both SNc and VTA DaNs, aged SNc DaNs preserve striatal innervation and thereby normal motor performance. Conversely, VTA DaN projections are lost, causing depressive-like behavior in these animals. Thus, identification and stimulation of ongoing compensatory mechanisms in aged SNc DaNs of K320E-Twinkle[DaN] mice host the potential to help the small number of remaining SNc DaNs in PD patients to escape from cell death and concurrently to recover motor performance through enhanced striatal innervation.

Zusammenfassung

Die Parkinson-Krankheit (PD) ist eine neurodegenerative Erkrankung und betrifft rund 1% der Bevölkerung über 60 Jahre. Sie äußert sich vor allem durch die motorischen Ausfälle infolge des progressiven und selektiven Verlusts von dopaminergen Neuronen (DaNs) in der *substantia nigra pars compacta* (SNc). Nichtmotorische Symptome, wie Geruchsverlust und Depression, treten dabei zusätzlich prodromal auf. Die mitochondriale Dysfunktion spielt beim Verlust von SNc DaNs eine entscheidende Rolle, wie durch Toxine, die den mitochondrialen Komplex I beeinträchtigen, einer sehr hohen Akkumulationsrate von mitochondrialen DNA (mtDNA) Deletionen sowie einem breiten Spektrum an mitochondrial-bezogenen Genmutationen bei familiären PD-Fällen gezeigt wird. Die Tatsache, dass benachbarte DaNs im *ventralen tegmentalen Areal* (VTA) vom Zelltod nahezu verschont bleiben, legt jedoch nahe, dass zusätzliche, zelltypspezifische Faktoren zu der selektiven Vulnerabilität bei PD beitragen. In dieser Arbeit werden die Daten dreier Manuskripte dargestellt, welche zeigen, dass DaNs verschiedener Populationen unterschiedlich auf mitochondriale Dysfunktion reagieren, die auf der Inaktivierung des mitochondrialen Transkriptionsfaktors A (TFAM) in Mäusen beruht. Im olfaktorischen Bulbus (OB) sind lediglich kleine, anaxonische DaNs (SCs) zahlenmäßig leicht reduziert, was jedoch mit einer schweren olfaktorischen Dysfunktion assoziiert ist und eine mutmaßliche Rolle von OB DaNs beim PD-bezogenen Geruchsverlust vermuten lässt. Das Mittelhirn zeigt hingegen einen progressiven und alleinigen Verlust von SNc DaNs, der mit einer starken Abnahme der motorischen Leistung einhergeht. Im Gegensatz zum VTA sterben DaNs der SNc durch ein verheerendes Ungleichgewicht im mitochondrialen Redox-System, das durch einen zu hohen Ca^{2+}-Gehalt in ebendiesen Zellen ausgelöst wird. Während SNc DaNs somit infolge eines schnellen sowie kontinuierlichen Verlusts von mtDNA sterben, können sie sich an eine Störung der mtDNA Replikation, in Form einer mutierten Variante der mitochondrialen Helikase TWINKLE (K320E), anpassen. Trotz schwerer Neurodegeneration sowohl von SNc als auch VTA DaNs schaffen es die überlebenden SNc DaNs ferner die striatale Innervierung und somit die motorische Aktivität der Mäuse zu erhalten. Auf der anderen Seite hingegen, verlieren VTA DaNs ihre Projektionen, was schließlich einen depressiven Phänotyp hervorruft. Somit könnten die kompensatorischen Mechanismen, die in den SNc DaNs alter K320E-Twinkle[DaN] Mäuse vonstattengehen, dazu verwendet werden, die geringe Anzahl überlebender SNc DaNs in PD-Erkrankten vor dem Tod zu bewahren und zugleich die motorische Leistung durch neue striatale Innervierungen wiederherzustellen.

1 Introduction

1.1 Mitochondrial Dysfunction and Parkinson's disease

Since its first association with the neurodegenerative disease through the discovery of a toxic agent almost 40 years ago, mitochondrial dysfunction has been intensively studied in the context of Parkinson's disease (PD). Reduced activity of mitochondrial complex I, which is the outcome of toxins related to PD, in the most affected brain area has for a long time been the crucial phenotype at the cellular level besides Lewy bodies. The huge number of mutated genes that are directly linked to mitochondrial function in familial cases, further highlights the essential role of mitochondria in the pathophysiology of PD.

1.1.1 Complex I Deficiency

The mitochondrial enzyme nicotinamide adenine dinucleotide (NADH) ubiquinone oxidoreductase, named complex I, is the first in the mitochondrial electron transport chain, and responsible for both the electron transfer from NADH to Q_{10} and proton pumping into the mitochondrial intermembrane space in order to ensure ATP production (Wirth et al. 2016). Reduced activity of mitochondrial complex I has been first described in the *substantia nigra pars compacta* (SNc) of *post mortem* brains from patients with idiopathic PD in 1989 (Schapira et al. 1989). The same observations have been made by analyzing isolated mitochondria from the striatum (Mizuno et al. 1989) as well as platelet mitochondria of those patients (Parker, Boyson, and Parks 1989). A reduced complex I activity in PD has been subsequently reported, by a variety of studies, to be a phenomenon that is restricted to the SNc (Hattori et al. 1991; Mann et al. 1992; Janetzky et al. 1994; Mann et al. 1994). Studies including other brain regions are limited and of contradictory results. Whereas some revealed decreased complex I activity in homogenates of frontal cortices from PD patients (Parker, Boyson, and Parks 1989; Keeney et al. 2006), others could not detect any differences compared to healthy individuals (Schapira, Mann, et al. 1990; Janetzky et al. 1994). A recent study presented unchanged complex I activity in the prefrontal cortex of PD patients, but a reduction in PD patients which additionally suffer from dementia, suggesting altered mitochondrial complex activity in this brain region to be rather linked to the combination of both conditions (Gatt et al. 2016). The analysis of enzyme activity or protein content in the cerebellum and striatum did not show any difference comparing PD patients and controls (Mizuno et al. 1989; Schapira, Mann, et al. 1990; Mann et al. 1992; Janetzky et al. 1994).

It is out of question that intact complex I activity is of great importance for mitochondrial functionality, especially for highly energy consuming synaptic processes in the projection area of SNc dopaminergic neurons (DaNs) (Telford, Kilbride, and Davey 2009; Kilbride, Telford, and Davey 2020). However, the significance of complex I deficiency in the development of PD is still disputed, since it is unclear whether this phenomenon is a primary causative event, or a

secondary response to disease-related modifications. Flønes et al. recently showed that complex I deficiency is indeed found throughout the PD brain, including the prefrontal cortex, hippocampus and putamen as well as regions which are spared from neurodegeneration, such as the cerebellum (Flones et al. 2018), questioning the pathogenic role of complex I impairment in PD.

1.1.2 Gene Mutations

A genetic correlation in PD has been first described almost 100 years ago (Bell and Clark 1926). Today we know that there is a wide range of genetic variants and modifications that is related to PD-like disorders or parkinsonism. In this chapter I will focus on the monogenic origin of PD. With only ~5 – 10% of all patients, only a minority of PD cases is caused by monogenic mutations (Lill 2016), many of them being directly linked to mitochondrial dysfunction (see Fig. 1-1). These mutations occur in an autosomal dominant and recessive manner.

1.1.2.1 SNCA

The first discovered autosomal dominant gene in PD is *SNCA* (synuclein alpha) (Polymeropoulos et al. 1997). Although rarely found among familial forms of PD (Scott et al. 1999), the discovery of *SNCA* subsequently led to the identification of its encoded protein α-Synuclein (α-Syn) as the main component of the intracellular Lewy bodies arising also in many cases of idiopathic PD (Spillantini et al. 1997). The function of α-Syn is still not fully understood, but it might be involved in the maintenance, trafficking as well as exocytosis of synaptic vesicle and thereby modulates neurotransmitter release (Bendor, Logan, and Edwards 2013; Lautenschlager, Kaminski, and Kaminski Schierle 2017; Lautenschlager et al. 2018).

In order to unravel its neurotoxic effect in aggregated form, α-Syn and its interactions with mitochondria are intensively studied. Although α-Syn does not possess a canonical mitochondrial targeting sequence, it has been reported to be localized to mitochondria, leading to reduced complex I activity (Devi et al. 2008). Mitochondrial binding is achieved via translocase of outer membrane 20 (TOM20) and impairs mitochondrial protein import (Di Maio et al. 2016). A recent study just showed that α-Syn is involved in the reduction of mitochondrial respiratory activity and neurodegeneration by suppressing the mitochondrial matrix protease ClpP (Hu et al. 2019). When localized to mitochondria-endoplasmic reticulum contact sites, α-Syn is reported to influence mitochondrial morphology (Guardia-Laguarta et al. 2014) as well as calcium (Ca^{2+}) signaling and thereby reduces energy production (Paillusson et al. 2017). Aggregates of α-Syn show an increased tendency to bind to mitochondria (Wang, Becker, et al. 2019) and induce cell death via the oxidation of the ATP synthase and the following increased opening probability of the mitochondrial permeability transition pore (mPTP) (Ludtmann et al. 2018). However, recent findings suggest that it is rather the formation of Lewy

bodies than solely α-Syn aggregation that causes neurodegeneration through mitochondrial damage (Mahul-Mellier et al. 2020).

1.1.2.2 LRRK2

Another autosomal dominant form is referred to the *LRRK2* (leucine-rich repeat kinase 2) gene, in which mutations are most frequently detected in PD (Paisan-Ruiz et al. 2004; Zimprich et al. 2004). Mutations in the *LRRK2* gene lead to increased kinase activity and have hence been classified as gain-of-function mutations (West et al. 2005; Greggio et al. 2006; Lu and Tan 2008; Sheng et al. 2012). Although the significance in PD is undisputed, the physiological role as well as the pathological mechanism of LRRK2 is still not fully understood. LRRK2 has been associated with a wide range of cellular processes, with many of them directly impacting mitochondrial functionality. LRRK2 interacts with microtubules and cytoskeleton proteins (Caesar et al. 2013; Beilina et al. 2014; Law et al. 2014) and is important for microtubule assembly (Parisiadou et al. 2009; Lin et al. 2010). In PD patients with LRRK2 mutation, a decrease in tubulin acetylation was detected (Esteves et al. 2015), which is important for organellar trafficking and axonal function (Reed et al. 2006; Esteves, Gozes, and Cardoso 2014). Together with the localization of LRRK2 on the mitochondrial outer membrane (West et al. 2005; Biskup et al. 2006), this raises the question whether in PD, mitochondrial transport might be affected by LRRK2 as well. Indeed, cells expressing a mutant *LRRK2* revealed impaired mitochondrial trafficking (Thomas et al. 2016), which could mechanistically be explained by the direct interaction of LRRK2 with Miro, an outer mitochondrial membrane protein anchoring the microtubule motors kinesin and dynein to mitochondria (Hsieh et al. 2016).

Furthermore, mitochondrial morphology is found to be altered in LRRK2 mutants (Yue et al. 2015), including elongated mitochondria (Mortiboys et al. 2010). However, most studies rather reported mitochondrial fragmentation which has been linked to reduced levels of the short form of OPA1 (Stafa et al. 2014) as well as direct interaction of LRRK2 with DRP1 (dynamin-related protein 1), thereupon promoting mitochondrial fission (Wang et al. 2012; Su and Qi 2013; Smith et al. 2016; Perez Carrion et al. 2018). Eventually, there is evidence that LRRK2 is involved in mitochondrial clearance via autophagy (Ramonet et al. 2011; Cherra et al. 2013; Hindle et al. 2013; Orenstein et al. 2013; Cookson 2016): While LRRK2 physiologically promotes the removal of Miro, mutated LRRK2 disrupts this function and delays the degradation of damaged mitochondria (Hsieh et al. 2016).

1.1.2.3 VPS35

VPS35 (vacuolar protein sorting 35) encodes the vacuolar protein sorting-associated protein 35 and mutations in this gene were first observed in European PD cases appearing in an autosomal dominant manner (Vilarino-Guell et al. 2011; Zimprich et al. 2011). VPS35 is one
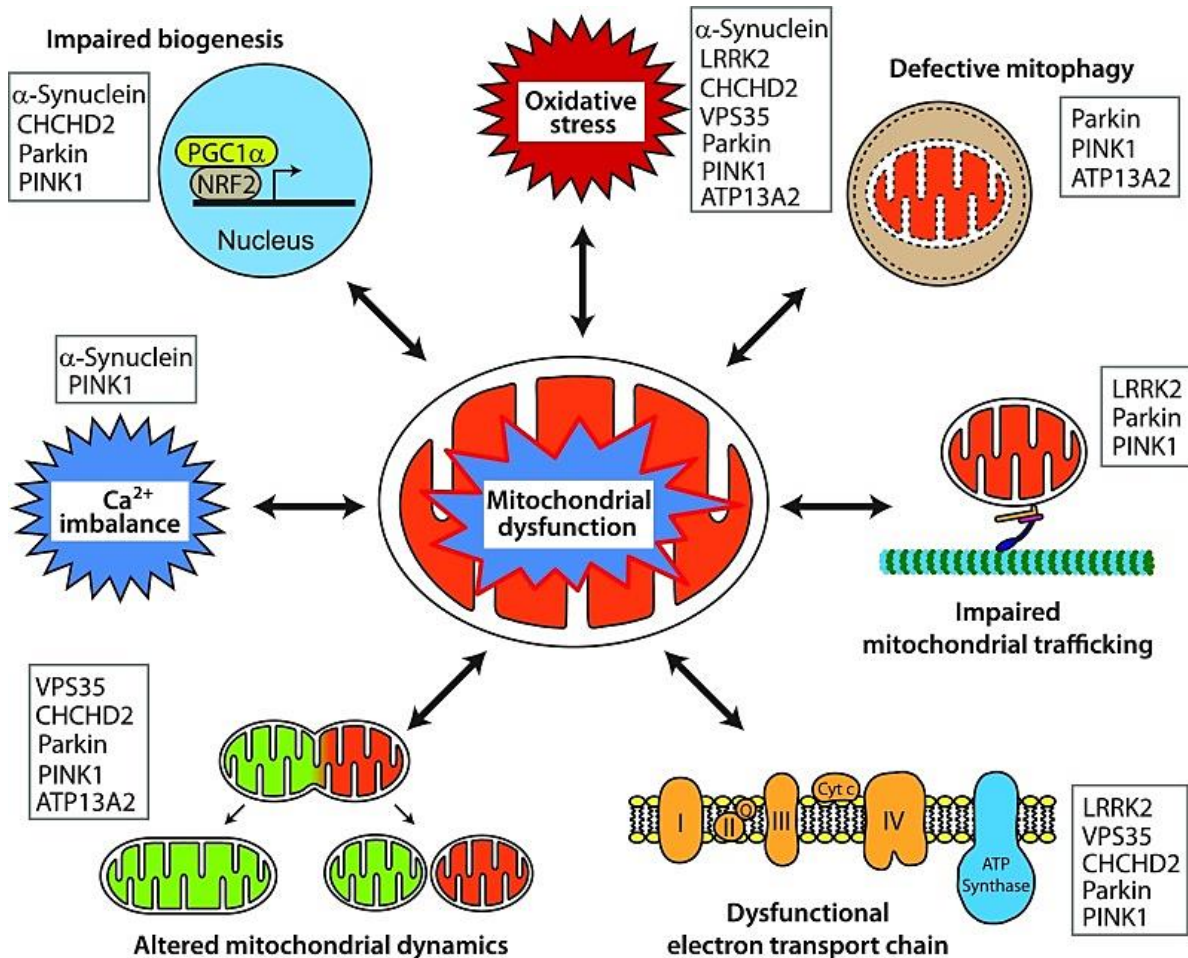
Fig. 1-1 Mitochondrial dysfunction upon PD-related gene mutations is linked to a variety of pathways. Monogenic mutations associated with PD can affect mitochondrial function, among others, via impaired mitochondrial biogenesis, enhanced ROS production, defective mitophagy, disrupted mitochondrial trafficking, deficient respiratory chain, modification of mitochondrial dynamics, imbalanced Ca^{2+} homeostasis and the combination of those, respectively (from Park et al. 2018).

part of the retromer complex, which is involved in intracellular protein trafficking. VPS35 by itself is responsible for binding and sorting of protein cargo (Hierro et al. 2007; Seaman 2012) and contributes to the formation of mitochondrial derived vesicles (MDVs), which shuttle mitochondrial cargo to peroxisomes or lysosomes (Soubannier et al. 2012; Sugiura et al. 2014) in order to degrade a selection of mitochondrial proteins instead of the entire organelle (McLelland et al. 2014). Regarding mitochondrial function, VSP35 has been primarily linked to fusion and fission. A mutant VSP35 caused mitochondrial fragmentation, which is explained by either decreased Mitofusin 2 (MFN2) levels in response to mitochondrial E3 ubiquitin ligase 1 (MUL1) degradation (Tang et al. 2015), or increased turnover of DRP1 complexes by MDVs and lysosomal degradation (Wang et al. 2016).

1.1.2.3 CHCHD2

CHCHD2 (coiled-coil-helix-coiled-coil-helix domain containing 2) mutations have been recently identified to be responsible for autosomal dominant, late-onset PD in three Japanese families (Funayama et al. 2015). However, other studies, including screening of Caucasians, south Italians (Jansen et al. 2015; Gagliardi et al. 2017) and Brazilians (Voigt et al. 2019), could not confirm this finding. It is believed that the localization of CHCHD2 to the mitochondrial intermembrane space maintains cristae structure and respiratory chain integrity, whereas impaired CHCHD2 function caused a reduced activity of complex III and IV and oxidative damage (Bannwarth et al. 2014; Meng et al. 2017), which could additionally be shown in fibroblasts from CHCHD2 mutant PD patients (Lee et al. 2018).

1.1.2.4 Parkin

With over 120 identified mutations so far (Lill 2016), *Parkin* (*PARK2*) mutations are the most common cause of autosomal recessive PD (Kitada et al. 1998) with predominantly early disease onset (Klein et al. 2003; Hedrich et al. 2004; Kilarski et al. 2012). Parkin is a cytosolic E3 ubiquitin ligase that regulates the degradation of mitochondria via mitophagy. It ubiquitinates a wide range of cytosolic as well as outer mitochondrial membrane (OMM) proteins upon mitochondrial damage, such as mitochondrial depolarization (Chan et al. 2011; Sarraf et al. 2013). The accumulation of polyubiquitin chains on mitochondria subsequently leads to the recruitment of autophagosomes and lysosomes (Geisler et al. 2010; Matsuda et al. 2010; Narendra et al. 2010). Under basal condition, the activity of Parkin is repressed (Chaugule et al. 2011; Riley et al. 2013; Trempe et al. 2013; Wauer and Komander 2013), probably via K6-linked ubiquitination-mediated degradation (Durcan et al. 2014).

Despite its conserved role in mediating mitophagy in diverse mammalian cell lines, the relevance of Parkin in neurons and especially in PD pathology has been questioned. Some studies showed an only moderate Parkin contribution to the degradation of damaged mitochondria in primary neurons (Cai et al. 2012; Grenier, McLelland, and Fon 2013), whereas others confirmed the importance of Parkin in mitophagy in these cells (Grenier, Kontogiannea, and Fon 2014) and especially axons (Ashrafi et al. 2014). Intriguingly, Parkin-deficient mice (Perez and Palmiter 2005) as well as rats (Dave et al. 2014) revealed no PD-related phenotype. However, in the context of mitochondrial dysfunction upon impaired replication of mitochondrial DNA (mtDNA), loss of Parkin caused DaN degeneration and L-3,4-dihydroxyphenylalanine (L-DOPA) reversible motor symptoms (Pickrell et al. 2015), highlighting the importance of Parkin-mediated mitochondrial quality control in DaNs.

Besides mitophagy, Parkin is suggested to play a role in the regulation of mitochondrial biogenesis (Scarffe et al. 2014) via the degradation of the parkin interacting substrate (PARIS), which, in the presence of mutated Parkin, can no longer suppress the activity of the peroxisome

proliferator-activated receptor gamma coactivator 1α (PGC-1α), the main transcriptional activator of mitochondrial genes (Shin et al. 2011). Local knockout (KO) of Parkin in the midbrain of mice via virus injection consequently led to reduced mitochondrial number and size as well as morphological abnormalities (Stevens et al. 2015). Other studies have linked Parkin to the turnover of synaptic vesicles, showing Parkin-mediated ubiquitination of synaptic vesicle proteins (Zhang et al. 2000; Huynh et al. 2003; Trempe et al. 2013; Cao et al. 2014) as well as proteins responsible for vesicle recycling (Fallon et al. 2002; Fallon et al. 2006; Joch et al. 2007). Hence, it is assumed that Parkin plays a role in synaptic transmission control. Moreover, studies including the *in vitro* investigation of DaNs that are directly derived from *Parkin* mutant patients via induced pluripotent stem cell (iPSC) technology confirm this assumption. Thus, iPSC-derived DaNs revealed excessive DA release as well as reduced DA uptake (Jiang et al. 2012) and large DA-induced bursting of spontaneous excitatory postsynaptic currents in contrast to iPSCs from normal subjects (Zhong et al. 2017). These results underscore an altered sensitivity of patient-derived DaNs towards DA. In order to understand the exact processes that are responsible for PD in *Parkin* mutant patients, further investigations are needed. The absence of α-Syn aggregations in most of the PD cases including a disrupted function of Parkin (Pramstaller et al. 2005; Doherty et al. 2013) points to a different mechanism compared to idiopathic cases of PD.

1.1.2.5 PINK1

The second most common cause of autosomal recessive PD are mutations in the *PINK1* (PTEN-induced putative kinase 1) gene (Valente et al. 2004) with loss-of-function mutations being associated with early-onset PD (Truban et al. 2017). PINK1 is a mitochondrial serine/threonine kinase and, besides Parkin, another key protein responsible for mitochondrial quality control via mitophagy. With intact mitochondrial function, PINK1 is imported into mitochondria via the TOM complex (Lazarou et al. 2012) and cleaved by mitochondrial proteases, such as PARL (Jin et al. 2010; Deas et al. 2011; Greene et al. 2012). In contrast, upon mitochondrial damage, the import of PINK1 is inhibited and the protein accumulates on the OMM (Lin and Kang 2008; Zhou et al. 2008). As a consequence, PINK1 activates Parkin and thus mediates mitochondrial clearance via autophagy (Vives-Bauza et al. 2010). The activation of Parkin is regulated by PINK1 via direct phosphorylation at Serine 65 (Kondapalli et al. 2012) and trans-activation by phosphorylation of ubiquitin at Serine 65, which is followed by binding to Parkin (Kane et al. 2014; Kazlauskaite et al. 2014; Koyano et al. 2014). Interestingly, PINK1 can initiate mitophagy even without Parkin while using alternative receptors, such as nuclear dot protein 52 (NDP52) and optineurin (OPTN) (Lazarou et al. 2015).

The loss of PINK1 activity has been primarily related to mitochondrial dysfunction, including the reduced activity of complex I and III (Amo et al. 2014), and to PD due to its leading role in

the regulation of mitophagy. However, mitochondrial Ca^{2+} overload-induced death of PINK1-deficient DaNs (Kostic et al. 2015) further suggests an involvement of PINK1 in Ca^{2+} handling. In addition, mitochondrial biogenesis via Parkin-mediated PARIS regulation (Lee et al. 2017) and fission (Pryde et al. 2016) were reported to be positively regulated by PINK1.

1.1.2.6 ATP13A2

A novel gene that has been identified to lead to a rare form of autosomal recessive juvenile-onset PD, the so called Kufor-Rakeb syndrome, is *ATP13A2* (ATPase cation transporting 13A2) (Park, Blair, and Sue 2015; Suleiman, Hamwi, and El-Hattab 2018). *ATP13A2* encodes the P5B ATPase, which mediates the transport of cations across endo/lyosomal membranes and is believed to be involved in vesicular transport (Park et al. 2014), endolysosomal activity (Sato et al. 2016; Rayaprolu et al. 2018) and indirectly glycolysis (Park et al. 2016). So far, studies using ATP13A2-deficient cells have presented lysosomal defects with corresponding disturbances in cation, especially Zn^{2+}, homeostasis. Moreover, these cells revealed impaired mitochondrial functionality in the form of reduced ATP conversion, mitochondrial fragmentation and reactive oxygen species (ROS) production (Ramonet et al. 2012; Park et al. 2014). However, further research needs to be conducted to decipher the exact consequences of *ATP13A2* mutations in patients.

1.1.2.7 DJ-1

Mutations in the DJ-1 encoding gene *PARK7* (parkinsonism associated deglycase) cause autosomal recessive early-onset PD (van Duijn et al. 2001; Bonifati et al. 2003) with a prevalence of only up to 1% of these cases (Maraganore et al. 2004; Alcalay et al. 2010; Sironi et al. 2013). DJ-1 is a ubiquitously expressed protein and implicated in a variety of cellular processes. Whereas the molecular mechanisms of DJ-1 functions remain elusive, there is a wide acceptance for its control of ROS and its neuroprotective effect upon oxidative damage (Taira et al. 2004; Surmeier et al. 2010; Cookson 2012). While mainly localized in the cytoplasm, DJ-1 can be translocated to mitochondria in response to oxidative stress (Irrcher et al. 2010; Kim et al. 2012). The loss of DJ-1 has been connected to reduced autophagic activity and mitochondrial dysfunction in fibroblasts (Krebiehl et al. 2010), to mitochondrial fragmentation and reduced mitochondrial membrane potential in human dopaminergic cells (Thomas et al. 2016), and more importantly, to the loss of SNc DaNs in mice (Rousseaux et al. 2012). There is recent evidence, that DJ-1 is additionally involved in the regulation of mitochondrial Ca^{2+} handling by direct interaction with the mitochondria-ER coupling complex (Basso, Marchesan, and Ziviani 2020).

1.1.3   Toxins

The discovery of PD-related toxins led to the first connection of the neurodegenerative disease with impaired mitochondrial function. It opened the door for a plethora of studies that

deciphered the pathological mechanisms during the course of PD. Today, these toxins are mainly used in animal models to assess the potential neuroprotective effects of newly identified drugs on the survival of DaNs and related motor symptoms.

1.1.3.1 MPTP

The very first association of PD with mitochondrial dysfunction was enabled by the discovery of 1-methyl-4-phenyl-1,2,3,6-tetrahydropyridine (MPTP). Nearly 40 years ago, MPTP was found to induce parkinsonian-like symptoms in drug users consuming self-produced heroine-like substances (Langston et al. 1983; Langston and Ballard 1983). Through its lipophilic property, MPTP crosses the blood-brain-barrier and is subsequently converted into its toxic form 1-methyl-4-phenylpyridinium (MPP$^+$) via the astrocytic monoamine oxidase (MAO) (Levitt, Pintar, and Breakefield 1982). Once its released via the organic transporter-3 from astrocytes (Cui et al. 2009), MPP$^+$ is preferentially taken up by DaNs due to its high affinity to the DA transporter (DAT) (Javitch et al. 1985; Gainetdinov et al. 1997), accumulates inside mitochondria due to its lipophilic charge and has been shown to inhibit complex I, finally causing selective degeneration of SNc DaNs in both mice and humans (Langston and Ballard 1983; Heikkila et al. 1985; Nicklas, Vyas, and Heikkila 1985).

Besides affecting complex I activity, MPP$^+$ is believed to compete with DA for being stored in vesicles, thus provoking DA extrusion and subsequent conversion into compounds with oxidative damage potential, such as 3,4-dihydroxyphenylacetaldehyde (DOPAL) (Panneton et al. 2010). In support of this, oxidative stress together with neuroinflammation have been found to occur in *post mortem* PD brains (Langston et al. 1999). However, many symptoms that are typical for idiopathic PD were absent upon MPTP consumption, including the Lewy pathology and the impairment of other brain regions as well as non-dopaminergic cells.

1.1.3.2 Rotenone

In 1987, an epidemiological study reported for the first time about an increased prevalence of PD in rural areas where certain pesticides were used (Barbeau et al. 1987). However, subsequent contradictory studies did not allow a conclusive confirmation of this observed phenomenon, probably caused by its limitations on the investigation of entire classes of pesticides instead of specific agents (Nandipati and Litvan 2016). One of these naturally occurring pesticides is rotenone, which can be extracted from roots of *Lonchocarpus* and *Derris* plants (Soloway 1976). It mechanistically acts like MPTP and inhibits complex I causing progressive loss of midbrain DaNs (Betarbet et al. 2000). Its highly lipophilic features and independence of transporters allow a direct and fast cell penetrance of rotenone, even through the blood-brain-barrier (Martinez and Greenamyre 2012). Therefore, it can be administered via different routes, including intraperitoneally, intravenously, subcutaneously and stereotactically, in order to induce histopathological features and motor symptoms according to PD (Johnson

and Bobrovskaya 2015). However, whereas rotenone exposure is known to be one of the greatest risks to develop PD in humans, inhalation did not cause an impairment in the nigrostriatal system in rodents (Rojo et al. 2007).

Mitochondrial dysfunction upon impaired complex I activity through rotenone treatment is referred to cause ROS production and reduced glutathione levels (Duty and Jenner 2011; Martinez and Greenamyre 2012) and sensitizes DaNs to further oxidative damage (Milusheva et al. 2005). Correspondingly, reduced DJ-1 levels have been detected in homogenates of different brain regions, including the SNc, from rats treated with rotenone (Sonia Angeline et al. 2012). The same study presented a decreased Parkin expression, which could either simply be accompanied with the severe loss of DaNs or point to impaired mitochondrial quality control in the SNc upon rotenone exposure. Moreover, rotenone-induced dopaminergic cell death is believed to be initiated by the activation of mitochondrial-dependent caspases, which in turn induce apoptosis (Chung, Miranda, and Maier 2007).

Like MPTP, rotenone treatment reproduces many features of PD, including selective loss of SNc DaNs, striatal DA depletion and motor impairment. Furthermore, rotenone induces α-Syn pathology (Betarbet et al. 2000; Biskup et al. 2006; Marella et al. 2008; Cannon et al. 2009; Ferris et al. 2013), which is not observed when using MPTP. However, it must be noted that the rotenone model is limited in the number of animals that develop the loss of the nigrostriatal system, in the location of the lesion, the degree of lesion severity, and the mortality rate (Cicchetti, Drouin-Ouellet, and Gross 2009; Greenamyre et al. 2010). It is further not clear, whether the motor decline is solely due to the impaired DA system or to diffuse mitochondrial dysfunction in other cell types and brain regions, respectively, as shown when using different doses of rotenone (Fleming et al. 2004; Richter, Hamann, and Richter 2007).

1.1.3.3 6-OHDA

6-Hydroxydopamine (6-OHDA) is an established neurotoxin structurally similar to DA and used to induce the degeneration of the nigrostriatal system in rodents. Due to its low penetrance of the blood-brain-barrier, the necessity of a direct injection into the brain where it is taken up by catecholaminergic neurons (Luthman et al. 1989), has been reported already over 50 years ago (Ungerstedt 1968). In order to provoke DaN damage only, noradrenaline reuptake inhibitors are additionally applied (Waddington 1980). 6-OHDA is either injected unilaterally into the medial forebrain bundle and the SNc, respectively, where anterograde (nigrostriatal) DaN degeneration is starting within 24 h (Faull and Laverty 1969; Jeon, Jackson-Lewis, and Burke 1995), or into the dorsal striatum with retrograde (striatonigral) loss of DaNs occurring within one to three weeks (Sauer and Oertel 1994; Przedborski et al. 1995). This way by, usage of unilateral lesions resulted in circumventing the high death rate of bilaterally treated mice as

well as concurrently generating an intrinsic control by the uninjured hemisphere (Thiele, Warre, and Nash 2012).

6-OHDA-mediated neuron death is thought to be mainly caused by oxidative damage through auto-oxidation of 6-OHDA and subsequent generation of various ROS (Soto-Otero et al. 2000). However, the role of mitochondrial dysfunction in this toxin-induced loss of DaNs is debated as well. Whereas the impact of 6-OHDA on mitochondrial function *in vivo* is not clear, there is strong evidence in cultured cells. Thus, 6-OHDA treatment has been shown to induce mitochondrial fragmentation via upregulation of Drp1 expression (Gomez-Lazaro et al. 2008) as well as reduced expression of Mfn1, Mfn2 and OPA1 (Xi et al. 2018). It further leads to decreased mitochondrial membrane potential (Ren et al. 2019) and increased mitophagy upon extracellular-signal-regulated protein kinase 2 (ERK2) accumulation (Dagda et al. 2008; Zhu et al. 2007) via the externalization of cardiolipin (Chu et al. 2013). Moreover, axonal transport of vesicles as well as mitochondria is impaired after 6-OHDA treatment, which is probably due to ROS damage (Lu et al. 2014). These findings suggest, that it is the oxidative damage in the first place, that causes 6-OHDA-mediated degeneration of DaNs, with mitochondrial malfunction being of secondary importance.

1.1.4 mtDNA Deletions

After being first described in neuromuscular disorders in the late 1980s (Holt, Harding, and Morgan-Hughes 1988; Wallace et al. 1988; Shoffner et al. 1990), mutations of the mtDNA attracted more and more attention to be a potential cause of complex I deficiency and mitochondrial dysfunction in PD patients (Schapira 1994). Sequence analysis of mtDNA did not reveal specific mutations associated with PD, and parkinsonism-like symptoms were only sporadically found in mitochondrial disease patients (Rana et al. 2000; Thyagarajan et al. 2000). However, based on the recognition that heteroplasmic mtDNA deletions are able to cause myopathy (Holt, Harding, and Morgan-Hughes 1988) as well as Kearn-Sayres syndrome (Zeviani et al. 1988), the presence of mtDNA deletions in brains of PD patients was investigated as well. Whereas the amount of deleted molecules was too low to be detected via southern blot (Lestienne et al. 1990; Schapira, Holt, et al. 1990), mtDNA deletions could be indeed presented in the striatum of *post mortem* PD brains by using the at this time newly developed polymerase chain reaction (PCR) (Ikebe et al. 1990; Ozawa et al. 1990). Interestingly, striatal mtDNA deletions were also verified in age-matched controls in contrast to other brain regions, although to a lesser extent than in PD (Ozawa et al. 1990). Subsequent studies confirmed this observation in the dorsal striatum and extended it to the SNc (Soong et al. 1992), suggesting DaN-enriched regions to be hotspots for mtDNA deletions during normal aging and especially in PD (Melov et al. 1999; Gu et al. 2002). Later on, laser microdissection of single cells from *post mortem* brains revealed elevated levels of mtDNA deletions (~50% of mtDNA molecules carry deletions) in the SNc in healthy aged individuals (Kraytsberg et al.

2006) and even more abundant in PD patients (Bender et al. 2006). These studies further showed that respiratory chain deficiency of SNc DaNs correlated with increased mtDNA deletions, providing a direct link between accumulating deletions and mitochondrial dysfunction (see Fig. 1-2).

MtDNA deletions in SNc DaNs vary widely in size (~2000 – 9500bp) and are thought to be somatically acquired via clonal expansion (Reeve et al. 2008). Their accumulation is driven by the catecholamine metabolism (Neuhaus et al. 2014; Neuhaus et al. 2017), explaining why especially DaNs are hotspots for such alterations in the mtDNA. A possible mechanistic explanation for the differential outcome during normal ageing and PD was provided by the groups of Tzoulis and Bindoff: Whereas in SNc DaNs of healthy individuals, the population of wild-type mtDNA is maintained by increased total mtDNA copy number upon deletion accumulation, this compensatory upregulation fails and results in depletion of the wild-type mtDNA population in PD patients (Dolle et al. 2016). These findings could be confirmed by two established mouse models with impaired mtDNA maintenance and mtDNA replication,
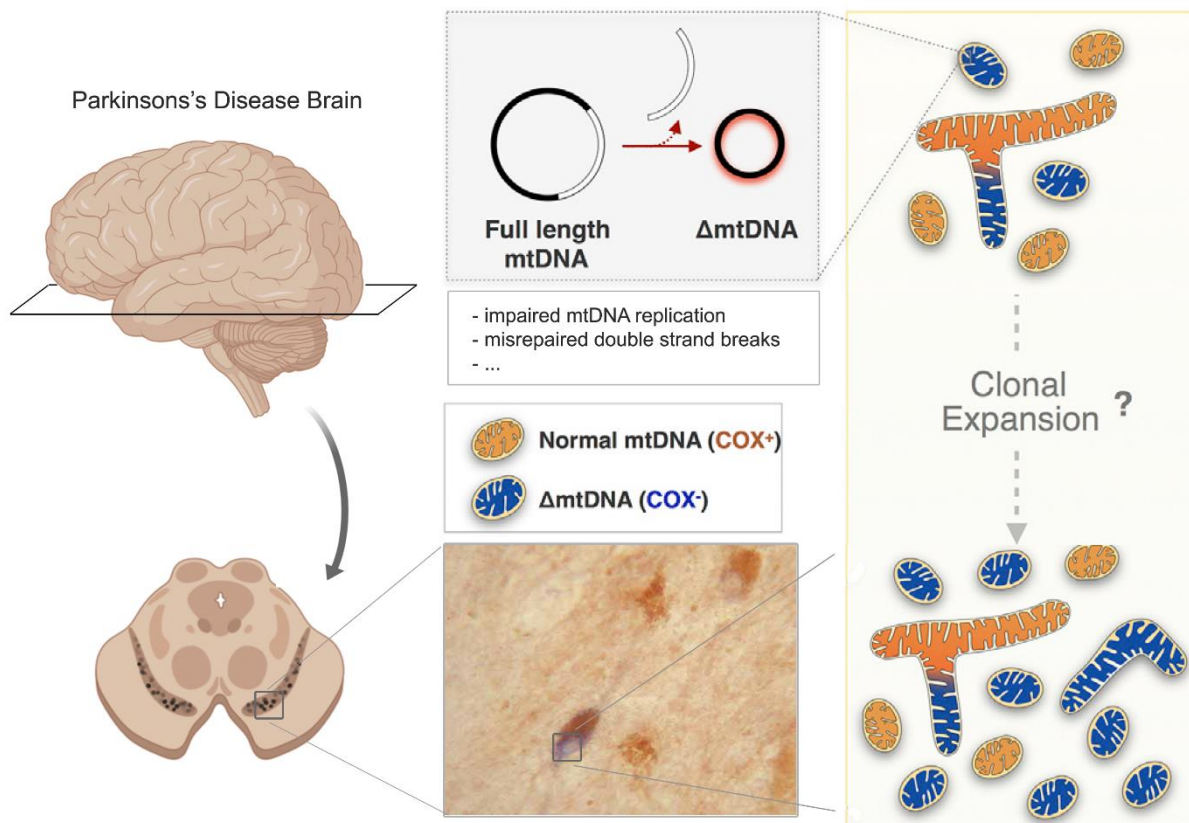
Fig. 1-2 Accumulation of mtDNA deletions in SNc DaNs of PD patients. With increasing age, SNc DaNs accumulate deletions of mtDNA, a process which is accelerated in PD. Deletion accumulation is associated with mitochondrial dysfunction, presented by COX deficiency (blue stained neuron). Defective replication as well as misrepaired double strand breaks of mtDNA are proposed to result in deletion formation. Deleted molecules are thought to accumulate via clonal expansion over time, whereas underlying mechanisms remain unclear (Figure was generated according to Picard et al. 2016 by using BioRender tools. Image illustrating COX-deficient SNc neuron was taken from Bender et al. 2006, 20X magnification).

respectively. Depletion of mtDNA in DaNs via cell type-specific KO of the mitochondrial transcription factor A (TFAM) has been shown to mimic the key features of PD pathology in mice. These so called MitoPark mice revealed selective neurodegeneration and progressive motor impairment (Ekstrand et al. 2007). Furthermore, DaNs were able to compensate multiple mtDNA deletions upon mutation of *mitochondrial DNA polymerase γ* (*POLγ*) by the upregulation of mtDNA copy number (Trifunovic et al. 2004; Perier et al. 2013). However, crossing these Mutator mice with Parkin KO mice, which do not show any impairment of DaNs (Perez and Palmiter 2005), caused selective loss of DaNs and an accompanied motor dysfunction (Pickrell et al. 2015). This highlights that the success of the compensatory increase in mtDNA copy number upon deletion accumulation further depends on functional mitochondrial quality control. SNc DaNs of idiopathic PD patients have been further shown to reveal low TFAM levels, accompanied with reduced mtDNA copy number and complex I deficiency (Grunewald et al. 2016). It is thereby likely that in PD, the significant pathological event is the depletion of wild-type mtDNA as a result of accumulating deletions, rather than solely the presence of mtDNA deletions. If balancing the amount of wild-type mtDNA and mtDNA deletions, by increasing mtDNA copy number and holding the amount of deleted mtDNA molecules at tolerable levels, fails in SNc DaNs, this will inevitably cause mitochondrial dysfunction and subsequently provoke neuron death.

The mechanism for the formation of mtDNA deletions is still not fully understood. For a long period of time, incorrect mtDNA replication in the form of strand displacement has been thought to be primarily responsible (Clayton 1982). The contribution of the replication machinery on deletion formation in general is evidenced by a variety of studies reporting multiple mtDNA deletions in patients with mutations in genes that are responsible for mtDNA replication, such as *Twinkle* (Suomalainen et al. 1992; Hudson et al. 2005; Hanisch et al. 2015) and *POLγ* (Di Fonzo et al. 2003; Ferreira et al. 2011; Nissanka et al. 2018). However, this scenario was challenged to also occur in SNc DaNs (Reeve et al. 2008). Simultaneously, mtDNA deletions were suggested to rather arise as a consequence of misrepaired double strand breaks upon mtDNA damage (Krishnan et al. 2008). The connection between deletion formation and mtDNA double strand breaks has been subsequently confirmed in neurons *in vitro* (Fukui and Moraes 2009) as well as *in vivo* (Fukui and Moraes 2009), including DaNs (Pickrell et al. 2011). The fact that mtDNA double strand breaks are promoted by ROS (Pinto et al. 2017), could further explain the accumulation of mtDNA deletions in healthy individuals, with regard to increasing ROS-induced mtDNA damage with normal ageing. Thereby, mtDNA deletions underscore the significance of ageing in the development of PD (Liu 2014; Rizzo et al. 2016; Collier, Kanaan, and Kordower 2017).

The potential of measuring mtDNA levels as a putative biomarker for PD has been intensively studied by various groups in recent years. After the identification of reduced levels of circulating

cell-free mtDNA in the cerebrospinal fluid (CSF) in Alzheimer's disease patients (Podlesniy et al. 2013), those results could be shown in PD patients as well (Pyle et al. 2015) and seem to be further influenced upon treatment (Lowes et al. 2020). This indicates that alterations in the amount of CSF mtDNA could rather be used for the diagnosis of ongoing neurodegeneration in general than specifically for PD. Reduced mtDNA copy number has been further detected in peripheral blood cells and SNc DaNs of PD patients, in contrast to healthy individuals (Pyle, Anugrha, et al. 2016), however, these findings could not be repeated in PD patients with depression (Pyle, Lowes, et al. 2016). A recent study confirmed that blood mtDNA copy number is unchanged in PD patients and controls, indicating that it is not an adequate biomarker for PD (Davis et al. 2020). Correspondingly, fibroblasts from idiopathic PD patients as well as patients with a LRRK2 mutation background did not show any changes in mtDNA copy number (Podlesniy et al. 2019). In face of the unsolved mechanistic relation between neurodegeneration and reduced circulating cell-free mtDNA as well as the majority of data reporting no alterations of the mtDNA copy number in diverse biopsies of PD patients, mtDNA levels are currently no promising candidate for reliable PD diagnosis.

1.1.5 Oxidative Stress

Oxidative stress is a widespread term characterizing a pathophysiological cellular state with increased presence of ROS not balanced by the cellular anti-oxidative systems. The three main ROS are superoxide (O_2^-), hydrogen peroxide (H_2O_2) and hydroxyl radical (OH^-), all being produced from molecular oxygen (O_2) (Collin 2019). Mitochondria are the primary intracellular source of ROS through the interaction of unpaired electrons with molecular O_2 at the respiratory chain (Cadenas and Davies 2000; Andreyev, Kushnareva, and Starkov 2005). In particular, complex I and III have been shown to be the major ROS producers in isolated mitochondria (Kudin et al. 2004; Kudin, Debska-Vielhaber, and Kunz 2005; Kussmaul and Hirst 2006). Increased O_2^- production at complex I is observed upon high matrix NADH concentrations and high mitochondrial membrane potential, respectively, whereas at complex III, high O_2^- levels are induced by selective inhibition. Thus, ROS contribution by complex III is rather thought to be of secondary importance (Murphy 2009).

Mitochondria possess their own antioxidant system in order to counteract increased ROS levels. Reduced glutathione (GSH) can scavenge ROS and thereby protects biomolecules from oxidative damage (Ruszkiewicz and Albrecht 2015). Moreover, mitochondrial matrix enzymes with antioxidant activity, such as manganese-dependent superoxide dismutase (MnSOD), are able to convert O_2^- into H_2O_2 (Miriyala, Holley, and St Clair 2011). Glutathione peroxidase (GPx) subsequently transforms H_2O_2 into H_2O while oxidizing GSH. The oxidized form, GSSG, is in turn reduced back to GSH by glutathione reductase (GR) and the usage of NADPH (Ruszkiewicz and Albrecht 2015). In addition, peroxiredoxins can directly eliminate H_2O_2 and modulate redox signalling (Rhee, Chae, and Kim 2005). Accordingly, the

mitochondria-located isoform peroxiredoxin 5 has been reported to protect cells from neurodegeneration upon treatment with MPTP (De Simoni et al. 2013) and rotenone (Wang, Huang, et al. 2019), respectively.

Constantly keeping mitochondrially-derived ROS at low levels, DaNs additionally have to face another source, since the metabolism of DA is associated with the production of a variety of ROS and hence impede antioxidant processes in this cell type (Delcambre, Nonnenmacher, and Hiller 2016). Consequently, signs of oxidative damage (Dexter et al. 1989; Alam et al. 1997; Floor and Wetzel 1998; Bosco et al. 2006) as well as low GSH concentrations (Sofic et al. 1992; Sian et al. 1994; Jenner and Olanow 1996) have been detected early in the SNc of PD patients. In addition, the deficiency of complex I, the primary ROS producer (Murphy 2009), in SNc DaNs leads to elevated ROS levels, thereby causing a vicious circle that might greatly contribute to cell death in PD (Dias, Junn, and Mouradian 2013). The importance of oxidative stress in PD pathology is further confirmed by the fact that mutations in *CHCHD2* or DJ-1 encoded by *PARK7* as well as treatment with MPTP, Rotenone and 6-OHDA (see above) are associated with oxidative damage and degeneration of DaNs.

1.2   Dopaminergic Neurons in Parkinson's disease

Cardinal symptoms in PD only occur with the loss of DaNs in the SNc to a certain degree. The 'shaking palsy', as it was initially termed by James Parkinson in 1817 (Parkinson 2002), considerably improved our understanding of voluntary movement control. Besides the SNc, other DA-enriched brain regions are affected in PD and linked to prodromal non-motor symptoms, such as hyposmia and depression (Postuma, Aarsland, et al. 2012). However, though multiple and promising insights have been gained up to now, the especially severe vulnerability of nigral DaNs is not fully understood and treatments to slow down neurodegeneration are still lacking.

1.2.1   Selective Vulnerability

PD is a complex neurological disorder that occurs in a heterogeneous manner and includes the loss of differential neuronal subtypes in a variety of areas in the brain. In addition to the SNc mentioned above, among others, neurons in the locus coeruleus, nucleus basalis of Meynert, pedunculopontine nucleus, raphe nucleus, dorsal motor nucleus of the vagus, olfactory bulb (OB), amygdala and hypothalamus are also affected (Dickson 2012). Thus, neurodegeneration in PD is not only restricted to DaNs but also involves serotonergic, noradrenergic, cholinergic, GABAergic and glutamatergic neurons (Brichta, Greengard, and Flajolet 2013). This heterogeneous damage of diverse neurological systems is primarily linked to non-motor symptoms which can precede motor impairment by up to ten years (Martinez-Martin et al. 2011; Postuma, Aarsland, et al. 2012; Khoo et al. 2013; Duncan et al. 2014).

However, motor symptoms remain the key pathology and the pivotal event for diagnosis of PD. Motor dysfunction is primarily caused by the loss of DaNs in the SNc and the accompanying depletion of DA in the dorsal striatum (Michel, Hirsch, and Hunot 2016; Obeso et al. 2017). It is the DaNs that are therefore in the focus of potential cell replacement therapies (Sonntag et al. 2018). Interestingly, a neighboring DaN-enriched midbrain region, the ventral tegmental area (VTA), is much less affected (Alberico, Cassell, and Narayanan 2015) although both SNc and VTA DaNs are closely related with only <1% (Grimm et al. 2004) and <3% (Greene, Dingledine, and Greenamyre 2005), respectively, of genes being differentially expressed. This selectivity in the death of DaNs is occupying scientists since decades. Whereas the favored loss of SNc DaNs upon treatment with MPTP and 6-OHDA, which rely on cell penetrance via DAT, could be explained by the lower expression of the transporter in VTA DaNs (Lammel et al. 2008), the explanation for rotenone, which should be able to access any cell but still causes selective DaN death via diverse routes of administration, is more complex. Monogenic mutations causing familial forms of PD are widespread in the brain and complex I deficiency has been shown to occur throughout the whole brain of idiopathic PD patients (Flones et al. 2018). Furthermore, both SNc and VTA DaNs of wildtype mice have been shown to equally accumulate mtDNA deletions with increasing age (Neuhaus et al. 2014). Consequently, there must be further cell-type specific factors rendering SNc DaNs highly vulnerable to mitochondrial dysfunction (see Fig. 1-3).

Investigation of electrophysiological patterns of both midbrain DaN populations has greatly contributed to a better understanding of the selective vulnerability. SNc as well as VTA DaNs demonstrate autonomous pacemaking (Grace and Bunney 1984; Puopolo, Raviola, and Bean 2007; Khaliq and Bean 2010). In juvenile SNc DaNs and generally in VTA DaNs, voltage-dependent Na^+ channels are mainly responsible for pacemaker activity, while in adult SNc DaNs, L-type voltage-gated Ca^{2+} channels [Ca_v1 (Catterall et al. 2005)] contribute to the autonomous firing (Chan et al. 2007). Whereas Ca_v1 activity is not essential for pacemaking (Guzman et al. 2009; Poetschke et al. 2015), it is associated with somatodendritic Ca^{2+} oscillations (Chan et al. 2007) and on the one hand thought to assist pacemaker activity and directly boost oxidative phosphorylation (Surmeier, Guzman, and Sanchez-Padilla 2010). On the other hand, however, Ca^{2+} oscillations are a disservice to SNc DaNs, as they cause oxidative stress by unknown mechanisms (Guzman et al. 2010). Ca^{2+} entry via Ca_v1 channels might be further promoted in PD via the inhibition of the hyperpolarization-activated current (I_h). MPTP treatment blocked I_h in SNc DaNs (Masi et al. 2013) and thereby increased neuronal activity (Masi et al. 2015) as well as elevated intracellular Ca^{2+} levels (Carbone et al. 2017). The metabolic challenge upon increased Ca^{2+} concentrations in SNc DaNs, in contrast to VTA DaNs (Philippart et al. 2016), is thought to render these neurons more vulnerable to neurodegeneration (Surmeier et al. 2012; Duda, Potschke, and Liss 2016). Consistently,
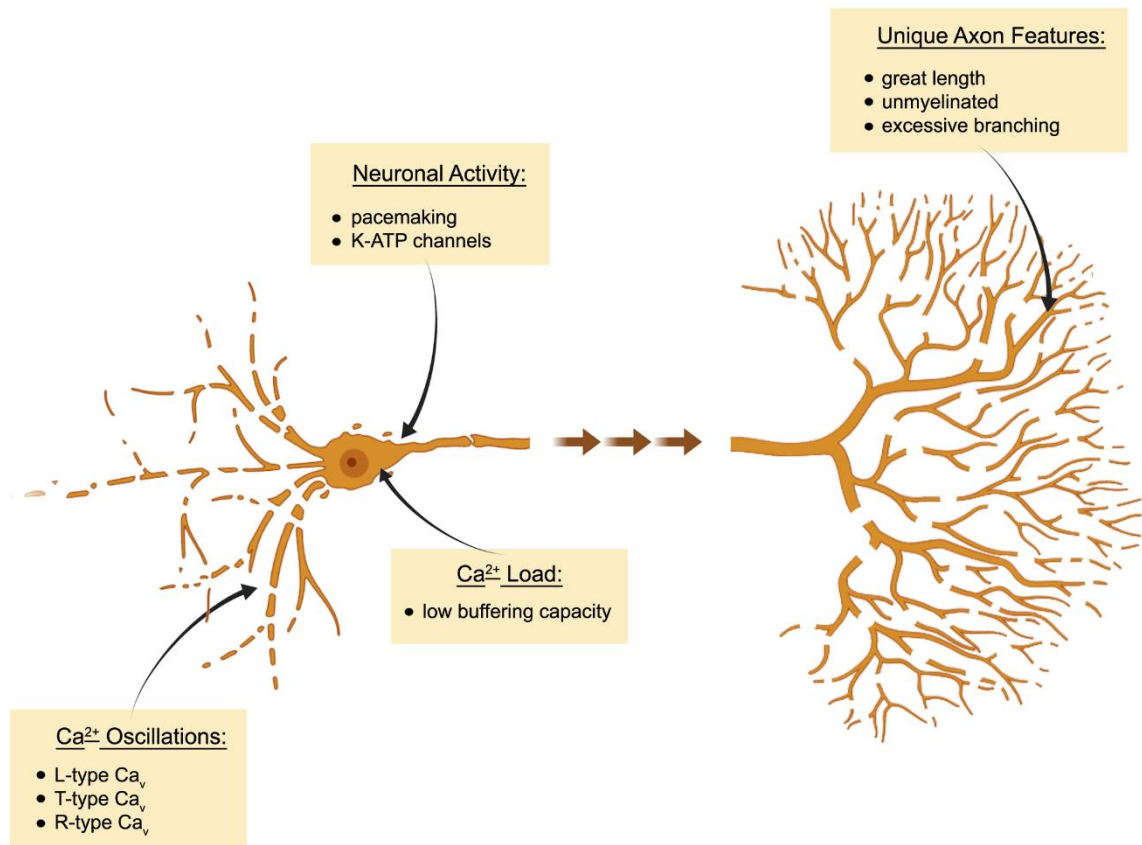
Fig. 1-3 Cell-autonomous factors contributing to the vulnerability of SNc DaNs to mitochondrial dysfunction. Schematic summary of selected cellular key features that contribute to the selective vulnerability of SNc DaNs in PD upon mitochondrial dysfunction. Autonomous pacemaking is associated with Ca^{2+} oscillations mediated by distinct voltage-gated Ca^{2+} channels (Ca_V). Low Ca^{2+} buffering capacity further contributes to enhanced intracellular Ca^{2+} load, which in turn causes oxidative stress by unknown mechanisms. SNc DaNs have a long, unmyelinated axon which is extremely branched, leading to high energetic demands and a strong dependence on functional mitochondria. ATP-sensitive potassium (K-ATP) channels open in metabolic demand situations, and thereby connect neuronal activity with the energetic state of the cell. When mitochondrial function is impaired, however, hyperactivity of K-ATP channels can result in the complete loss of neuronal excitability and contributes to neuron death (Figure was generated by using BioRender, according to Surmeier et al. 2017).

epidemiological studies revealed a 20-30% lower risk for the development of PD in patients treated for high blood pressure with Ca_V1 inhibitors (Lang, Gong, and Fan 2015), so called dihydropyridines (DHP) which block both $Ca_V1.2$ and $Ca_V1.3$ channels (Koschak et al. 2001; Xu and Lipscombe 2001). Despite controversial *in vivo* results regarding dose efficiency as well as specificity, the DHP isradipine, has been tested in a phase III clinical trial on PD patients (Biglan et al. 2017). This clinical trial failed ('Isradipine Versus Placebo in Early Parkinson Disease: A Randomized Trial' 2020), supporting recent concerns about the dosage's efficiency (Ortner et al. 2017).

Other voltage-gated Ca^{2+} channels have been linked to increased cytosolic Ca^{2+} levels and the accompanying vulnerability of SNc DaNs. T-type voltage-gated Ca^{2+} channels have been shown to contribute to Ca^{2+} oscillations (Guzman et al. 2018) and to drive degeneration of SNc DaNs in a familial form of PD (Tabata et al. 2018). In addition, a recent study identified the R-type channel $Ca_V2.3$ to be most strongly expressed among all voltage-gated Ca^{2+} channels in

mouse SNc DaNs. The KO of this channel revealed neuroprotective effects upon MPTP treatment through the reduction of activity-associated Ca^{2+} signals and upregulation of the neuronal Ca^{2+} sensor (NCS-1) (Benkert et al. 2019). NCS-1 in turn promotes DA-induced auto-inhibition (Boeckel and Ehrlich 2018) via binding to DA D2-autoreceptors (Dragicevic et al. 2014; Ford 2014; Philippart and Khaliq 2018) and is thereby believed to protect SNc DaNs from activity-dependent Ca^{2+} overload (Catoni, Cali, and Brini 2019).

The importance of the prevention of increased cytosolic Ca^{2+} levels is underscored by the severe loss of those ventrolateral DaNs in the SNc of PD patients (Halliday et al. 1996; Braak et al. 2003), which do not express the intracellular Ca^{2+}-buffering protein calbindin (Damier et al. 1999). However, the neuroprotective potential of calbindin is still inconclusive. Whereas, besides in PD patients, calbindin-positive SNc DaNs were spared in MPTP-treated monkeys as well (German et al. 1992; Dopeso-Reyes et al. 2014), the lack of calbindin did not modify its sensitivity to MPTP toxicity (Airaksinen, Thoenen, and Meyer 1997). Calbindin overexpression (Yuan et al. 2013), however, as well as viral vector-mediated gene delivery of calbindin (Inoue et al. 2019) attenuated MPTP-induced selective neurodegeneration and further reduced the number of α-Syn expressing DaNs. It is therefore likely that the presence of α-Syn aggregates and Lewy bodies in PD is linked to increased intracellular Ca^{2+} levels in SNc DaNs in the first place (Post, Lieberman, and Mosharov 2018). This regulatory role of Ca^{2+} is mediated by the Ca^{2+}-activated protease calpain, of which a higher activity was found in *post mortem* PD brains (Crocker et al. 2003). In addition, calpain levels were increased in cells and mouse striatum upon MPTP treatment (Singh et al. 2019). Interestingly, calpain activity is attenuated by calbindin and reduction of calpain activity prevents DaNs from increased α-Syn aggregation and synaptic impairment (Diepenbroek et al. 2014) as well as from MPTP-induced cell death (Choi et al. 2008). These findings support the potential neuroprotective effect of the presence of calbindin, and once more, the significance of maintaining intracellular Ca^{2+} homeostasis in SNc DaNs.

Apart from voltage-gated Ca^{2+} channels, other ion channels have been implicated in the vulnerability of SNc DaNs. ATP-sensitive potassium (K-ATP) channels are metabolic sensors, as their open probability is higher in metabolic demand situations, followed by membrane hyperpolarization and inhibition of neuronal activity in order to reduce energetic costs (Liss and Roeper 2001). Under physiological conditions, these channels hence protect the cell from overexcitability and excitotoxicity. Conversely, K-ATP channels have been shown to activate SNc DaNs by controlling burst activity to maintain goal-directed behavior for food seeking, among others (Schiemann et al. 2012). Upon MPTP treatment, however, K-ATP channels of SNc DaNs open and cause a complete loss of electrophysiological activity, in contrast to VTA DaNs. DaN death was rescued upon genetic inactivation of K-ATP channels (Liss et al. 2005).

This suggests a breakdown of the SNc DaN neuronal activity following complex I deficiency in face of enhanced energy demands.

The high as well as consistent energetic demands of SNc DaNs become apparent when considering the unique axonal architecture. In contrast to the VTA, DaNs located in the SNc possess unusually large and extremely branched axons that are connected to a large number of nerve cells. The axon of a single SNc DaN is estimated to give rise to up to 245,000 synapses in rats and 2.4 million synapses in humans, respectively (Bolam and Pissadaki 2012). The architecture of these concurrently unmyelinated axons (Braak et al. 2004) is accompanied by an extremely high energetic demand in order to maintain ion homeostasis for continuous action potential propagation and synaptic processes (Pacelli et al. 2015). Consequently, SNc DaNs are vulnerable to additional stressors influencing the energetic balance of the cell, and especially the impairment of mitochondrial function.

1.2.2   Motor Symptoms

Since the initial description by James Parkinson 200 years ago (Parkinson 2002), motor symptoms are still the cardinal, clinical component of PD. Bradykinesia is the essential feature in PD and occurs in combination with either resting tremor, rigidity, or both (Postuma et al. 2015). It is the 'palsy' part of the 'shaking palsy' as originally termed, and defined as the slowness of movement and decrement in amplitude or speed as movements are continued (Postuma et al. 2015; Berg et al. 2018; Bologna et al. 2020). Tremor, the rhythmic oscillation of a body part (Bhatia et al. 2018), is also present in the essential tremor disease, however, the unilateral onset and appearance at rest is considered to be specific for PD (Reich 2020). The third motor component, rigidity, is defined as the resistance to passive movements independent of velocity. In order to distinguish rigidity from spasticity, this resistance should not be restricted to failure in relaxing with regard to diagnosis (Postuma et al. 2015).

Voluntary movement control is explained by the basal ganglia model. Regarding the classical model, the main input component of the basal ganglia is the dorsal striatum (Albin, Young, and Penney 1989; DeLong 1990), where most of SNc DaNs are projecting to (Liss and Roeper 2008; Watabe-Uchida et al. 2012). In humans, the dorsal striatum is composed of the caudate nucleus and the putamen (Ghandili and Munakomi 2020), whereas it is seen as one structure, called the caudate putamen (CPu), in mice (Allen Institute 2020). The major output regions of the basal ganglia are the *globus pallidus pars interna* (GPi) and the *substantia nigra pars reticulata* (SNr). These brain areas project to the thalamus and thereby regulate the activity of the motor cortices (Obeso et al. 2000). In the 'direct pathway', the GPi and the SNr are inhibited. Thus, they allow the thalamus to activate the motor cortices (see Fig. 1-4). In contrast, the 'indirect pathway' further includes inhibitory projections of the *globus pallidus pars externa* (GPe) as well as excitatory projections of the subthalamic nucleus (STN), which both
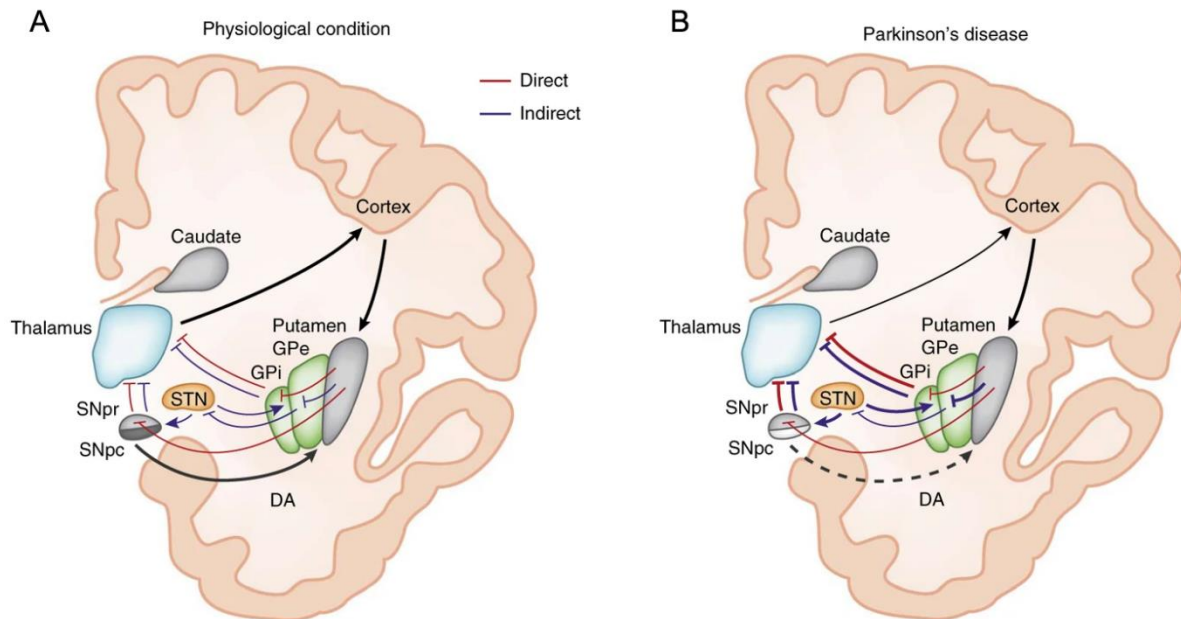
Fig. 1-4 Voluntary movement control under physiological conditions and during Parkinson's disease. A) According to the basal ganglia model, SNc DaNs innervate the dorsal striatum (putamen) and activate D1-expressing striatal medium spiny neurons of the direct pathway (red lines) and inhibit D2--expressing striatal neurons of the indirect pathway (blue lines), respectively. The major output regions, GPi and SNr, project to the thalamus, which in turn stimulates the motor cortices. B) In PD, the progressive loss of SNc DaNs results in insufficient striatal DA supply and leads to an imbalance between the direct and indirect pathway. As a result, thalamo-cortical motor systems are inhibited via both pathways, which affects movement preparation as well as execution (Modified from Calabresi et al. 2014).

target the main output components of the basal ganglia (GPi/SNr). This results in GPi and SNr activation and subsequent thalamus inhibition. Thus, the net outcome of the indirect pathway is the inactivation of the motor centers (Albin, Young, and Penney 1989; DeLong 1990; Benarroch 2016). Notably, these two pathways seem to be simultaneously rather than consecutively activated during movement initiation (Cui et al. 2013). A third pathway, the so called 'hyperdirect pathway', is characterized by a projection from the cortex to the STN and considered to be responsible for outcome optimization (Nambu, Tokuno, and Takada 2002; Aron et al. 2016).

In PD, the lack of DA in the dorsal striatum upon the loss of SNc DaNs reduces the activity of the direct pathway, which is initiated by striatal activation via D1 receptors. Concurrently, the indirect pathway is promoted (Wichmann and DeLong 1996). As a consequence, the activity of the main output components of the basal ganglia (GPi/SNr) is enhanced by both the lack of inhibition from the direct pathway, as well as increased activation from the indirect pathway due to the reduced firing of GPe neurons and subsequent STN disinhibition (Pan and Walters 1988; Bergman et al. 1994; Hutchison et al. 1994; Sterio et al. 1994; Wichmann et al. 1999; Kita and Kita 2011). Thalamo-cortical and brainstem motor systems are consequently inhibited via both pathways, impairing preparation and execution of voluntary movement (Wichmann

and DeLong 1996). Thus, motor symptoms in PD are related to the depletion of DA in the main input component of the basal ganglia upon DaN loss in the SNc. However, it is believed that the cerebellum also plays a role in bradykinesia formation (Bostan and Strick 2018) and that compensatory hyperactivity of pyramidal neurons in the premotor cortex might further contribute to rigidity (Yu et al. 2007).

When ~30-50% of SNc DaNs are perished, motor symptoms of PD patients become apparent (Obeso et al. 2017). At this time point, DA release in the dorsal striatum is already reduced by ~50-60% (Fearnley and Lees 1990; Ehringer and Hornykiewicz 1998). Since striatal nerve terminals have been shown to degenerate before their cell bodies (Chu et al. 2012; Kordower et al. 2013), loss of SNc DaNs in PD is thought to occur in a striatonigral (retrograde) manner. PD-related mouse models reveal motor impairment at dopaminergic loss rates comparable to humans, while the spontaneous motor activity is classically assessed by the open field test (Seibenhener and Wooten 2015). When ~40-60% of SNc DaNs are perished, genetically as well as pharmacologically induced, mice show impaired motor behavior (Crocker et al. 2003; Ekstrand et al. 2007; Wakamatsu et al. 2007; Lu et al. 2009; Chen et al. 2012; Rousseaux et al. 2012; Becker et al. 2018; Zeng, Geng, and Jia 2018).

Motor symptoms of PD patients can nowadays be treated with a range of drugs, including the well-known blood-brain barrier permeable L-DOPA, DA agonists and MAO type B (MAO_B) inhibitors. The overall aim is to increase or maintain striatal DA levels, either by the DA precursor, DA agonists and inhibition of DA breakdown, respectively (Kalia and Lang 2015). In the early phase of PD, L-DOPA is currently the first choice of treatment with low doses at the beginning and subsequent titration to therapeutic threshold, while DA agonists and MAO_B blockers are reserved for intervention at later stages of the disease (de Bie et al. 2020). Though the mechanism of L-DOPA is still not fully understood and the traditional idea of a DA precursor has been challenged since it does not explain the fading pharmacological efficiency (Obeso et al. 2017), L-DOPA has been demonstrated to improve, and more importantly, not to worsen the progression of PD in the long run (Fahn et al. 2004). However, motor dyskinesias present a serious problem (Aquino and Fox 2015; Vijayakumar and Jankovic 2016) as occurring in ~30% of PD patients after the first year of L-DOPA treatment ('Impact of deprenyl and tocopherol treatment on Parkinson's disease in DATATOP patients requiring levodopa. Parkinson Study Group' 1996) and additional ~10% with each following year (Ahlskog and Muenter 2001). Thus, the development of new formulations of L-DOPA and novel delivery techniques is still ongoing (Obeso et al. 2017). When L-DOPA and DA agonists have eventually failed and dyskinesia becomes disabling, surgical intervention by deep brain stimulation (DBS) of the STN and GPi is the next candidate for the treatment of motor impairment. DBS improves motor symptoms by modifying the dynamics of basal ganglia circuits from persistent synchronized activity to a more dynamic activity pattern (Hahn et al.

2008; Vitek et al. 2012; Cleary et al. 2013; Muller and Robinson 2018). Whereas due to the prior pharmacological treatments the average age of PD patients treated with DBS is about 10-13 years after disease diagnosis, DBS could be performed earlier in future interventions, regarding the positive results after application in the early disease phase (Schuepbach et al. 2013).

1.2.3 Hyposmia

In contrast to many other neurodegenerative diseases, the advantage hallmark of PD is the occurrence of non-motor prodromal symptoms (Postuma, Lang, et al. 2012). One of these prodromes is hyposmia, which is found in ~95% of PD patients and can precede motor impairment by up to ten years (Haehner, Hummel, and Reichmann 2009; Lang 2011; Doty 2012). Though the vast majority of people with hyposmia will never develop PD (Abbott et al. 2005), olfactory dysfunction probably possesses the best potential of all non-motor symptoms for PD prediction (Beach et al. 2010; Obeso et al. 2017). The mechanisms causing PD-related hyposmia are still not understood. However, first pathological changes in PD, including the presence of Lewy bodies, are observed in olfactory systems, such as the anterior olfactory nucleus and the OB (Braak et al. 2003). Recently, impaired olfactory behavior has been presented upon α-Syn inclusions in the OB of transgenic mice (Taguchi et al. 2020). This might explain the early appearance of dysfunctional olfaction and further supports a long standing hypothesis of an infectious agent (Braak et al. 2004), affecting olfactory nerve terminals first followed by spreading throughout the central nervous system (CNS), to be the initial cause of PD (Breen, Halliday, and Lang 2019).

Besides their prominent roles in the striatonigral and mesolimbic system, DaNs are additionally present in the OB. They make up about 5% of the neuronal OB population and are primarily located in the glomerular layer (GL) (Cave and Baker 2009). As interneurons, DaNs are involved in the discrimination of odors rather than the detection (Tillerson et al. 2006; Escanilla et al. 2009). In particular, they modulate the activity of both olfactory sensory fibers (Berkowicz and Trombley 2000; Wachowiak et al. 2005) and mitral cells by D2 receptor-mediated inhibition (Nagayama, Homma, and Imamura 2014; Banerjee et al. 2015) as well as via contacts with external tufted cells (Liu et al. 2013). In spite of a variety of literature reporting about different categorizations, DaNs in the OB can be clearly divided into small (5-10 μm) anaxonic (SCs) and large (10-15 μm) axonic cells (LACs) (Pignatelli and Belluzzi 2017). Notably, SCs can be generated throughout life in both humans and mice (Kosaka et al. 1987; Vergano-Vera et al. 2006; Bovetti et al. 2009; Kosaka and Kosaka 2009; Galliano et al. 2018). This neurogenic process is initiated by the presence of progenitor cells in the dorsolateral region of the subventricular zone (SVZ) (Fiorelli et al. 2015). These cells are characterized by the transcription factor paired box 6 (PAX6), which is required for DaN phenotype development (Merkle, Mirzadeh, and Alvarez-Buylla 2007; Young et al. 2007; Brill et al. 2008). Only 5% of

the ~20,000-30,000 daily generated new-born progenitor cells migrate to the GL, whereas the vast majority differentiates into interneurons in the granule cell layer (Codega et al. 2014; Bonaguidi et al. 2016).

Regarding the general vulnerability of DaNs in PD as well as early pathological changes in the DaN-enriched OB, it would be obvious that hyposmia is linked to a reduced number or an altered functionality of DaNs. However, there are both limited and contradictory results concerning the fate of DaNs in the OB of PD patients. Whereas even elevated numbers of DaNs in the GL were reported as a result of potential compensatory mechanisms (Mundinano et al. 2011), no differences could be detected by other groups when comparing PD patients and healthy individuals (Huisman, Uylings, and Hoogland 2008; Cave et al. 2016). Hence, there are currently no data revealing a mechanistic explanation for PD-related hyposmia or the contribution of OB DaNs to this pathology. Furthermore, it is not known whether DaNs in the OB are as vulnerable to mitochondrial dysfunction as their midbrain counterparts.

1.2.4 Depression

Depression is a common non-motor symptom associated with PD, arising with a prevalence of 15-50% (Obeso et al. 2017). It can occur at any time during the course of PD, whereas development in the early phase is associated with an increased risk for more severe motor deficits (Pfeiffer 2016). While being a complex interplay of psychological and neurobiological factors, depression frequently correlates with anxiety, which can be expressed by generalized anxiety disorder, panic attacks and social phobia (Berg et al. 2015). Besides its contribution to resting tremor and L-DOPA-induced dyskinesias (Doder et al. 2003; Rylander et al. 2010; Politis et al. 2014), impairment of serotonergic signalling is the main cause of depressive behavior. Hence, additional antidepressant therapy, including serotonin reuptake inhibitors, is quite common in PD (Richard et al. 2012).

Brainstem raphe nuclei (RN) are highly enriched in serotonin-expressing neurons, which project to the basal ganglia, amygdala, hippocampus, and diverse cortical areas (Parent et al. 2011; Wallman, Gagnon, and Parent 2011). While presenting Lewy pathology in the early course of PD (Braak et al. 2003), *post mortem* investigations further revealed severe degeneration of serotonergic neurons in the RN (Halliday et al. 1990) correlating with diagnosed depression in these patients (Paulus and Jellinger 1991). Commensurately, reduced serotonin levels have been found in RN projection areas, including the basal ganglia, hypothalamus, hippocampus and prefrontal cortex (Fahn, Libsch, and Cutler 1971; Shannak et al. 1994). However, *in vivo* imaging studies mainly using the positron emission tomography (PET) technique did not show consistent results. Striatal serotonin transporter (SERT) density was found to be reduced in PD patients (Kerenyi et al. 2003), but binding features of SERT were similar comparing PD patients with and without depression (Kim et al. 2003; Guttman et

al. 2007). In contrast, another study detected increased SERT availability in the RN and the limbic cortex of depressive PD patients, which were referred to compensatory enhanced serotonin binding upon the progressive loss of the serotonergic system (Politis et al. 2010). Intriguingly, investigation of DA and noradrenaline transporters revealed lower binding capacity in the locus coeruleus and areas of the limbic system, such as the ventral striatum, when comparing depressed and non-depressed PD patients (Remy et al. 2005). This suggests that besides serotonergic denervation, PD-related depression is further caused by the depletion of DA in the ventral striatum. Indeed, depressive behavior can be reproduced in primates and rodents when the dopaminergic mesolimbic pathway, including projections originating from the VTA to the *nucleus accumbens* (NAcc), is impaired (Brown et al. 2012; Furlanetti, Coenen, and Dobrossy 2016; Nobili et al. 2017).

2   Aim of the Thesis

The contribution of mitochondrial dysfunction to the loss of SNc DaNs in PD is undisputed. However, it is still unsolved why particularly this dopaminergic subpopulation degenerates upon mitochondrial damage. In contrast to the less affected VTA (Alberico, Cassell, and Narayanan 2015), pacemaker activity in SNc DaNs is associated with Ca^{2+} oscillations (Chan et al. 2007), which are causing oxidative stress (Guzman et al. 2010) and are thought to render these highly energy demanding neurons (Pacelli et al. 2015) more vulnerable to neurodegeneration through the metabolic challenge upon increased Ca^{2+} levels (Surmeier et al. 2012; Duda, Potschke, and Liss 2016). The potential consequences of impaired intracellular Ca^{2+} homeostasis in SNc DaNs are further underscored by the severe loss of calbindin-negative cells in the ventrolateral SNc of PD patients (Damier et al. 1999). However, a mechanistic link between mitochondrial dysfunction and intracellular Ca^{2+} handling in PD is still missing. Thus, the first manuscript of the thesis focused on studying the impact of neuronal Ca^{2+} handling on the selective vulnerability of SNc DaNs upon mitochondrial dysfunction by using the MitoPark mouse model.

In the second manuscript, the same mouse model was used to investigate the influence of mitochondrial dysfunction on DaNs that are located in the OB as well as the olfactory-related behavior. Despite hyposmia being an important PD-related prodromal non-motor symptom (Beach et al. 2010; Obeso et al. 2017), little is known about the vulnerability of this dopaminergic subpopulation in PD and there are contradictory results regarding the number of OB DaNs in patients (Huisman, Uylings, and Hoogland 2008; Mundinano et al. 2011; Cave et al. 2016).

In the MitoPark model, DaN-specific TFAM depletion leads to the rapid loss of mtDNA encoded transcripts. However, rather than progressively losing mtDNA, SNc DaNs have been reported to accumulate mtDNA deletions with increasing age and even more abundantly in PD (Bender et al. 2006; Kraytsberg et al. 2006; Reeve et al. 2008; Elstner et al. 2011; Dolle et al. 2016). In our lab, we make use of mice expressing a mutated, dominant-negative variant of the mitochondrial helicase Twinkle (K320E mutation) in a cell-specific manner, in order to study the impact of accumulating mtDNA deletions on the function of various tissues (Baris et al. 2015; Weiland et al. 2018; Holzer et al. 2019). We consequently generated mice in which K320E is exclusively expressed in DaNs. Accordingly, the third manuscript of this thesis includes the outcome of impaired mtDNA replication on survival as well as mitochondrial function of DaNs in these animals.

The content of the manuscripts was kept in its original form. However, integration of figures and corresponding figure legends into the text, consecutive labeling of figures as well as uniform font style were applied in order to improve readability of the thesis. The aim of was to

present the three manuscripts and eventually discuss their findings in a coherent manner. This led to the following key questions of this thesis:

1. How are distinct subpopulations of DaNs differently affected upon the loss of TFAM followed by mitochondrial dysfunction?
2. What are the differences between the early-onset MitoPark and the delayed-onset K320E-Twinkle^{DaN} mouse model regarding loss of mitochondrial function, DaN survival, striatal innervation and behavioral phenotype?
3. Which clinical relevance do these mouse models have?

2.1 Manuscript Declaration

The manuscripts included in this thesis report about degeneration of DaNs following mitochondrial dysfunction in mice induced by differential genetic impairment of mtDNA maintenance. The first two manuscripts deal with the well-established MitoPark mouse model, which is characterized by the DaN-specific loss of TFAM and mimics the course of PD within weeks. The one published in the Journal of Neuroscience reveals that upon mitochondrial dysfunction, high Ca^{2+} loads lead to an imbalance in the antioxidant system of vulnerable SNc DaNs right before the onset of neurodegeneration, in contrast to their VTA counterparts. The second, published in Molecular Neurobiology, contrasts the impact of mitochondrial defects in midbrain DaNs to DaNs located in the OB and further presents the consequence for olfactory-related behavior in MitoPark mice. The third manuscript, which is in preparation for submission, includes the newly generated K320E-Twinkle^{DaN} mouse model. In contrast to the MitoPark mouse model, K320E-Twinkle^{DaN} animals reveal a delayed, non-selective degeneration of midbrain DaNs following mitochondrial dysfunction, induced by the expression of a mutated form of the mitochondrial replicative helicase Twinkle (K320E). However, dopaminergic striatal projections are differentially affected, causing a depressive-like behavior but normal motor performance in these mice. Hence, the three manuscript provide insights into vulnerability but also compensatory potential of SNc DaNs upon differentially induced mitochondrial dysfunction.

3 Publications and Manuscripts

3.1 Mitochondrial Dysfunction Combined with High Calcium Load Leads to Impaired Antioxidant Defense Underlying the Selective Loss of Nigral Dopaminergic Neurons

Konrad M. Ricke[1][*], Thomas Paß[1][*], Sammy Kimoloi[1], Kai Fährmann[1], Christian Jüngst[2], Astrid Schauss[2], Olivier R. Baris[1], Marijana Aradjanski[2,3], Aleksandra Trifunovic[2,3,4], Therese M. Eriksson Faelker[2], Matteo Bergami[2,4] and Rudolf J. Wiesner[1,2,4]

* K.M.R. and T.P. contributed equally as co-first authors.

Author Contribution:

Konrad M. Ricke: Methodology, Validation, Formal Analysis, Investigation, Data Curation, Writing - Original Draft, Writing - Review & Editing, Visualization **Thomas Paß**: Validation, Formal Analysis, Investigation, Data Curation, Writing – Review & Editing, Visualization **Sammy Kimoloi**: Writing - Review & Editing **Kai Fährmann**: Investigation **Christian Jüngst**: Methodology, Resources **Astrid Schauss**: Software, Resources **Olivier R. Baris**: Writing - Review & Editing **Marijana Aradjanski**: Methodology **Aleksandra Trifunovic**: Methodology, Resources, Writing - Review Editing **Therese M. Eriksson Faelker**: Methodology, Resources **Matteo Bergami**: Methodology, Resources, Writing - Review Editing **Rudolf J. Wiesner**: Conceptualization, Methodology, Writing - Review & Editing, Supervision, Funding Acquisition

Author involvement listed according to the structured Contributor Role Taxonomy (CRediT) in order to transparently visualize individual contribution.

3.2 The Impact of Mitochondrial Dysfunction on Dopaminergic Neurons in the Olfactory Bulb and Odor Detection

Thomas Paß[1], Marlene Aßfalg[1], Marianna Tolve[3], Sandra Blaess[3], Markus Rothermel[4], Rudolf J. Wiesner[1,2] and Konrad M. Ricke[1]

Author Contribution:

Thomas Paß: Methodology, Validation, Formal Analysis, Investigation, Data Curation, Writing - Original Draft, Writing - Review & Editing, Visualization **Marlene Aßfalg**:

Methodology, Formal Analysis, Investigation, Visualization, Resources **Marianna Tolve**: Methodology, Investigation **Sandra Blaess**: Methodology, Investigation, Writing - Review & Editing **Markus Rothermel**: Writing - Review Editing **Rudolf J. Wiesner**: Writing - Review & Editing, Supervision, Funding Acquisition **Konrad M. Ricke**: Conceptualization, Methodology, Writing - Review & Editing, Supervision

Author involvement listed according to the structured Contributor Role Taxonomy (CRediT) in order to visualize individual contribution.

3.3   Preserved Striatal Innervation and Motor Function Despite Severe Neurodegeneration of Nigral Dopaminergic Neurons Upon Slow Progressive Impairment of mtDNA Replication

Thomas Paß[1], Konrad Ricke[1], Olivier Baris[1] and Rudolf J. Wiesner[1,2]

Manuscript ready for submission

Author Contribution:

Thomas Paß: Methodology, Validation, Formal Analysis, Investigation, Data Curation, Writing - Original Draft, Writing - Review & Editing, Visualization **Konrad M. Ricke**: Methodology, Validation, Formal Analysis, Investigation, Writing - Review & Editing **Olivier R. Baris**: Methodology, Resources, Writing - Review & Editing **Rudolf J. Wiesner**: Conceptualization, Methodology, Writing - Review & Editing, Supervision, Funding Acquisition

Author involvement listed according to the structured Contributor Role Taxonomy (CRediT) in order to visualize individual contribution.

3.1 Mitochondrial Dysfunction Combined with High Calcium Load Leads to Impaired Antioxidant Defense Underlying the Selective Loss of Nigral Dopaminergic Neurons

Short title: Low mitochondrial GSH causes dopaminergic neuron death

Konrad M. Ricke[1*], Thomas Paß[1*], Sammy Kimoloi[1], Kai Fährmann[1], Christian Jüngst[2], Astrid Schauss[2], Olivier R. Baris[1], Marijana Aradjanski[2,3], Aleksandra Trifunovic[2,3,4], Therese M. Eriksson Faelker[2], Matteo Bergami[2,4] and Rudolf J. Wiesner[1,2,4]

[1]Center for Physiology and Pathophysiology, Institute of Vegetative Physiology, University of Köln, 50931 Köln, Germany
[2]Cologne Excellence Cluster on Cellular Stress Responses in Aging-associated Diseases (CECAD), University of Köln, 50931 Köln, Germany
[3]Institute for Mitochondrial Diseases and Aging, Medical Faculty, University of Köln, 50931 Köln, Germany
[4]Center for Molecular Medicine Cologne, University of Köln, 50931 Köln, Germany

Corresponding authors:
Prof. Dr. Rudolf J. Wiesner
rudolf.wiesner@uni-koeln.de
or
Konrad M. Ricke, PhD
kricke@uottawa.ca
or
Thomas Paß, M. Sc.
thomas.pass@uk-koeln.de

* K.M.R. and T.P. contributed equally as co-first authors.

Abstract

Mitochondrial dysfunction is critically involved in Parkinson's disease, characterized by loss of dopaminergic neurons (DaNs) in the *Substantia nigra* (SNc), while DaNs in the neighboring ventral tegmental area (VTA) are much less affected. In contrast to VTA, SNc DaNs engage calcium channels to generate action potentials, which leads to oxidant stress by yet unknown pathways. To determine the molecular mechanisms linking calcium load with selective cell death in the presence of mitochondrial deficiency, we analyzed the mitochondrial redox state and the mitochondrial membrane potential in mice of both sexes with genetically induced, severe mitochondrial dysfunction in DaNs (MitoPark mice), at the same time expressing a redox-sensitive GFP targeted to the mitochondrial matrix. Despite mitochondrial insufficiency in all DaNs, exclusively SNc neurons showed an oxidized RedOx-system, i.e. a low GSH/GSSG ratio. This was mimicked by cyanide, but not by rotenone or antimycin A, making the involvement of reactive oxygen species (ROS) rather unlikely. Surprisingly, a high mitochondrial inner membrane potential was maintained in MitoPark SNc DaNs. Antagonizing calcium influx into the cell and into mitochondria, respectively, rescued the disturbed RedOx-ratio and induced further hyperpolarization of the inner mitochondrial membrane. Our data therefore show that the constant calcium load in SNc DaNs is counterbalanced by a high mitochondrial inner membrane potential, even under conditions of severe mitochondrial dysfunction, but triggers a detrimental imbalance in the mitochondrial redox system, which will lead to neuron death. Our findings thus reveal a new mechanism, redox imbalance, which underlies the differential vulnerability of DaNs to mitochondrial defects.

Key words: Parkinson's disease, mitochondrial dysfunction, selective neuron loss, redox imbalance, mitochondrial membrane potential

Significance Statement

Parkinson's disease (PD) is characterized by the preferential degeneration of dopaminergic neurons (DaNs) of the *substantia nigra pars compacta* (SNc), resulting in the characteristic hypokinesia in patients. Ubiquitous pathological triggers cannot be responsible for the selective neuron loss. Here we show that mitochondrial impairment together with elevated calcium burden destabilize the mitochondrial defense only in SNc DaNs, and thus promote the increased vulnerability of this neuron population.

Introduction

The motor symptoms of Parkinson's disease (PD) are caused by the selective degeneration of dopaminergic neurons (DaNs) in the substantia nigra pars compacta (SNc) (Dauer and Przedborski, 2003; Sulzer, 2007; Obeso et al., 2017). Mitochondrial dysfunction is a central feature of idiopathic PD, but also a large percentage of genetic forms is due to mutations of proteins involved in quality control of the mitochondrial pool (Pickrell and Youle, 2015).

The probability to develop idiopathic PD strongly increases with age (De Lau and Breteler, 2006). At the same time, dopaminergic midbrain regions are hot spots for the accumulation of mitochondrial DNA (mtDNA) deletions (Cortopassi et al., 1992; Meissner et al., 2008), which reach detrimental levels in single DaNs with increasing age (Bender et al., 2006; Kraytsberg et al., 2006; Dölle et al., 2016). Thus, it is tempting to speculate that these two aging-related phenomena are causally connected. We have shown that it is catecholamine metabolism which drives the enhanced generation of mtDNA deletions (Neuhaus et al., 2014; Neuhaus et al., 2017), and leads to mitochondrial dysfunction (Burbulla et al., 2017), explaining why cells producing dopamine are mostly affected by these mtDNA alterations.

While there is a general aging-related decline of neurons in the SNc, surprisingly the DaNs in the neighboring ventral tegmental area (VTA) are more or less spared (Reeve et al., 2014), although we have clearly shown that they also accumulate mtDNA deletions (Neuhaus et al., 2014). This specific decline can be further observed in PD patients (Hirsch et al., 1988; Damier et al., 1999), as well as in rodents, where the same specific neuron loss is induced by mitochondrial toxins like MPTP (German et al., 1992) or rotenone (Betarbet et al., 2000). Several reasons have been proposed to explain this puzzling differential vulnerability. One hypothesis is that DaNs of the SNc are unusually large neurons with an extremely branched axonal network which connects to a very high number of other nerve cells. These axonal branches are even unmyelinated (Braak et al., 2004), thus the energy demand to maintain ion homeostasis for action potential propagation and to supply synaptic processes is extremely high (Bolam and Pissadaki, 2012; Pacelli et al., 2015). Roeper and Liss, on the other hand, have shown that this metabolic "stress" triggers activity of K-ATP channels and NMDA receptors, promoting action potential bursting in vivo and propelling excitotoxicity, but only in SNc DaNs (Schiemann et al., 2012; Duda et al., 2016), since in VTA DaNs, mitochondria are mildly uncoupled, potentially preventing K-ATP channel-mediated vulnerability (Liss et al., 2005). Last but probably most attractive, the differential vulnerability of VTA and SNc neurons has been linked to their different modes of pacemaking: While SNc DaNs use L-type calcium channels as well as sodium channels (Chan et al., 2007; Philippart et al., 2016; Ortner et al., 2017), VTA neurons exclusively use sodium channels (Betarbet et al., 2000). Therefore, the maintenance of steep calcium concentration gradients across membranes may again place a

much higher energy demand on SNc DaNs. Moreover, their well-known low intrinsic calcium buffering capacity (German et al., 1992; Damier et al., 1999; Schiemann et al., 2012), together with α-synuclein- and L-type calcium channel-dependent increase in cytosolic calcium (Lieberman et al., 2017) causes "oxidant stress" in mitochondria of vulnerable SNc DaNs, promoting their specific death (Guzman et al., 2010; Dryanovski et al., 2013).

In order to further explain why two closely related neuron subtypes respond so differently to mitochondrial dysfunction, we investigated the changes in their mitochondrial redox state and inner membrane potential, respectively, in vivo. To achieve this, we targeted a redox-sensitive GFP to the matrix (mito-roGFP) (Guzman et al., 2010) in MitoPark mice. MitoPark mice display COX-deficiency in DaNs (12 weeks) followed by degeneration of the dopaminergic system and motor impairment, which becomes more pronounced with increasing age (from 13 to 20 weeks) (Ekstrand et al., 2007). The mito-roGFP probe is sensitive to the ratio of reduced/oxidized glutathione (GSH/GSSG) (Dooley et al., 2004) in the mitochondrial matrix, which in turn depends on the NAD(P)H/NAD(P) + ratio (Nelson and Cox, 2005), which again is closely linked to respiratory chain activity.

Materials and methods

Experimental model

Experiments were performed in agreement with European and German guidelines and approved (LANUV NRW, Recklinghausen, Germany; 84-02.04.2013-A141). All experiments were carried out with male or female mice of the strain C57/BL6N. TfamloxP/loxP and Dat-cre mice were provided by Nils-Göran Larsson (Max-Planck-Institute for Biology of Ageing, Köln, Germany). MitoPark mice (TfamloxP/loxP +/Dat-cre) were bred as described previously (Ekstrand et al., 2007) and TfamloxP/WT or TfamloxP/loxP mice were used as controls. Mito-roGFP mice were provided by James D. Surmeier (Northwestern University Feinberg School of Medicine, Chicago IL 60611, USA). MitoPark x mito-roGFP mice were generated by crossing TfamloxP/WT +/Dat-cre mito-roGFP males with TfamloxP/loxP females.

Genotyping

All genetic lines were identified by qualitative PCR-approaches using genomic DNA either from tail tip or ear punch biopsies. Tissue lysis was done in 75 µL lysis buffer (10 mM NaOH, 0.2 mM EDTA) at 96 °C for 45 min. After adding 75 µL of neutralization buffer (40 mM Tris-HCl, pH 7.6), lysates were centrifuged (1 min, 3000 rpm) and stored at -20 °C. Cycling conditions and primer sequences for the genetic lines are available upon request. Agarose gels containing 1.2 or 1.5% agarose (Tfam PCR: 1.5%, DatCre and mito-roGFP PCR: 1.2%) and 0.8 µg/mL ethidium bromide in TAE buffer (40 mM Tris base, 20 mM Acetic acid, 1mM EDTA, pH 8) were used to illustrate PCR products under UV-light.

Histology

All immunohistochemical approaches were performed on 5 µm paraffin sections. Striatal tyrosine hydroxylase (TH) immunoreactivity was done using a TH antibody (polyclonal rabbit, Abcam, #ab112, 1:750) and a biotinylated secondary antibody (donkey anti-rabbit, dianova, #111-065-006, 1:500). Fluorescence stainings of midbrain sections were performed with primary antibodies against TH (polyclonal rabbit, Abcam, #ab112, 1:1500), mitochondrial complex IV SU1 (COX I, monoclonal mouse, Abcam, #ab14705, 1:1000) or calbindin-D28k (Cb-D28k, monoclonal mouse, Swant, #300, 1:150) and fluorochrome-conjugated secondary antibodies (Goat anti-rabbit TRITC-conjugated, AffiniPure, #111-025-144, 1:2000, Goat anti-mouse DyLight488-conjugated, Jackson-ImmunoResearch, #115-485-003, 1:400). Visualization of Cytochrome c Oxidase (COX) deficiency was performed by COX-SDH enzymatic activity staining at Bregma -3.08 mm similar to Lotter et al., 2017, but incubation with SDH solution was performed for 180 min.

Bright-field microscopy was done with a slidescanner (SCN400, Leica) equipped with a 40x objective. TH-positive striatal fiber density was determined by optical density analysis using ImageJ-software with 2 sections/mouse at Bregma +0.74 mm. Fluorescence images were obtained with an inverse confocal microscope (TCS SP8 gSTED, Leica) with a 10x objective (Cb-D28k) or a 40x oil objective (COX) at Bregma -3.08 mm. COX-signal intensity was measured in the perikarya of TH-positive neurons and normalized to the COX-signal of a TH-negative area. Cb-D28k and TH double stainings were done on 2 midbrain sections/mouse, followed by identification of double-positive and TH-positive neurons similar to (Liang et al., 1996).

Two-photon laser scanning microscopy

Two-photon laser scanning microscopy (2PLSM) recordings were performed in 300 µm thick coronal midbrain sections. 10 to 12 week-old mice were anaesthetized with isoflurane and afterwards decapitated. The brain was quickly removed and brain sections were prepared with a vibratome (Leica VT1000 S or Thermo Scientific HM 650 V) in ice-cold, carbonated artificial cerebrospinal fluid (ACSF, 125 mM NaCl, 2.5 mM KCl, 25 mM NaHCO3, 1.25 mM NaH2PO4 x H2O, 25 mM Glucose, 2 mM MgCl2, 2 mM CaCl2 x 2 H2O).

2PLSM analysis was adapted from (Guzman et al., 2010). Ex vivo 2PLSM measurements in midbrain sections were conducted using a two-photon excitation microscope (TCS SP8 MP-OPO, IR APO L25x/0.95 objective, Leica). Before recordings, sections were incubated for at least 20 min at room temperature. Sections were transferred into the recording chamber of the imaging setup containing ~ 0.5 mL ACSF (37°C) and continuously perfused with carbonated ACSF. Solutions were applied at a flow rate of 4 to 5 mL per minute. Analysis of the mitochondrial RedOx-ratio in intact cells is enabled by the use of a redox-sensitive variant of

the green fluorescent protein (roGFP; (Vevea et al., 2013)). In the analyzed mouse line, expression of mito-roGFP is driven by the TH promoter (Guzman et al., 2010; Dryanovski et al., 2013), restricting the origin of any mito-roGFP signal to dopaminergic neurons. SNc and VTA DaNs were identified according to their location in the slice. Mito-roGFP excitation was done with 920 nm wavelength (Chameleon Vision II) and fluorescence detection between 500 to 550 nm. Fluorescence intensity in perikarya of single cells was measured using ImageJ-software. The fluorescence intensity from a GFP negative region was subtracted from each DaN signal, to remove mito-roGFP unspecific noise. Previous 2PLSM analysis of mito-roGFP mice (Guzman et al., 2010; Dryanovski et al., 2013) was presented as levels of "relative oxidation" and the mito-roGFP signal was detected on a single focus level, excluding a considerable fraction of the mitochondrial network. Here we analyzed the fluorescence of the entire mitochondrial network in perikarya by stacking approximately 45 focus planes (z-stacks, Figure 3-4, 3-4-1 and 3-4-2). Z-stacks covered a tissue depth of 45 µm. Neurons which were located at the surface of the slice were excluded from analysis. Discrete mito-roGFP recordings were performed with the multiphoton laser being activated at 4 time points: 1) At the beginning of the recording (0 minutes), 2) at 20 minutes to define the baseline, 3) after application of DTT at 30 minutes and 4) after application of ALD at 40 minutes. The fluorescence intensity after DTT application was interpreted as the mito-roGFP response at minimal oxidation or maximal reduction (RedOx-ratio = 0). The signal intensity after application of ALD was taken as response at maximal oxidation (RedOx-ratio = 1). The mitochondrial RedOx-ratio of DaNs was calculated using the following formula: RedOx-ratio = (roGFP-F ACSF, 20 min - roGFP-F DTT, 30 min)/ (roGFP-F ALD, 40 min - roGFP-F DTT, 30 min).

Conditions for TMRM 2PLSM recordings for the analysis of the DaN mitochondrial membrane potential were identical to mito-roGFP experiments. Sections were incubated with 100 nM TMRM for 30 min (37°C). TMRM recordings were conducted with TMRM-free ACSF. TMRM excitation was performed at 830 nm with laser intensities between 0.1 to 0.4% and fluorescence detected at 565 to 605 nm. DaNs were identified by their mito roGFP signal elicited with 920 nm. TMRM fluorescence was analyzed sequentially in perikarya of neurons in a fixed focus level and was detected at the beginning of each session. Only neurons with stable fluorescence traces were considered for TMRM signal quantification. At the end of each recording, sections were perfused with 5 mM KCN for 20 min and the difference between TMRM fluorescence before and after KCN was calculated (ΔTMRM-FKCN = TMRM-FACSF, 20 min - TMRM-FKCN, 40 min). Thus, low TMRM signal intensities induced by KCN are reflected by high ΔTMRM-FKCN values. A high ΔTMRM-FKCN value, in turn, represents a high mitochondrial membrane potential. Background signal was detected by analogous recordings of brain slices without TMRM and subtracted from the TMRM signal emitted by DaNs.

Spherical GFP aggregates were observed in MitoPark mito-roGFP midbrain sections. It was previously reported that these aggregates are mitochondria with a severely disturbed morphology (Sterky et al., 2011). The GFP aggregates in our MitoPark mice were primarily, yet not exclusively, observed in the SNc and those neurons were excluded from the analysis to eliminate their potential impact on 2PLSM readouts.

For blockade of calcium channels, sections were incubated with 300 nM isradipine or 20 µM Ru360 for at least 30 minutes.

COX-SDH staining

Visualization of Cytochrome c Oxidase (COX) deficiency was performed by COX-SDH enzymatic activity staining (Sciacco and Bonilla, 1996). COX is a respiratory chain (RC) complex which is partially encoded by mtDNA, while succinate dehydrogenase (SDH), another RC enzyme, is entirely encoded by nuclear DNA. Impaired integrity of mtDNA results in COX-deficiency, but sustained SDH-activity. Cells with decreased COX-activity will stain blue, while cells with normal COX-activity will appear brown. Mice were killed by cervical dislocation. Following dissection, brains were embedded (O.C.T. Tissue-Tek), frozen on dry ice and stored at -80 °C. Cryostat (Leica CM3050 S) sections of 7 µm were stored at -80 °C. Coronal midbrain cryosections at Bregma -3.08 mm were air dried and treated with COX incubation solution (100 µM Cytochrome C, 4 mM diaminobenzidine, 4400 U catalase in 0.1 M phosphate buffer) for 40 min at 37 °C. Afterwards, sections were washed in ddH2O (3 x 30 sec) and treated with SDH incubation solution (1.5 mM Nitroblue tetrazolium, 130 mM sodium succinate, 200 µM phenazine methosulfate, 1 mM sodium azide) for 180 min at 37 °C. Sections were washed again in ddH2O (3 x 30 sec), dehydrated in 95% (2 x 2 min) and 100% ethanol (10 min), air dried and mounted with glycerol-gelatine.

Immunohistochemistry

Anaesthetized mice (ketamine/xylazine: 100/10 mg/kg body weight, intraperitoneally) were intracardially perfused with PBS (GIBCO; 140 mM NaCl, 10 mM sodium phosphate, 2.68 mM KCl, pH 7.4) for 3 min and 4% PFA in PBS for 15 min. Brains were dissected and immersion-fixed in 4% PFA in PBS overnight. Afterwards tissues were dehydrated in a series of ethanol solutions (ethanol percentages are given): 70%, 90%, 2x 100% (15 min each), 100% (30 min) and 100% (45 min, Leica ASP300, CMMC Tissue Embedding Facility) and embedded in paraffin (Leica EG1150 H, CMMC Tissue Embedding Facility). Coronal 5 µm striatal sections were cut with a microtome (Leica RM2125 RTS). Sections were deparaffinized in xylene (2 x 5 min), washed in a series of ethanol solutions (100%, 95%, 70% and 50%, 1 min each) and afterwards washed in ddH$_2$O (5 min). For epitope retrieval, sections were heated in citrate buffer (10 mM citric acid monohydrate, pH 6) using a microwave oven.

Brightfield microscopy: Sections were washed in TBS (10 mM Tris base, 150 mM NaCl, pH 7.6, 3 x 5 min), quenched with 0.3% H_2O_2/TBS solution and washed again in TBS (3 x 5 min). Subsequently, sections were blocked in 10% normal goat serum in TBS (45 min, RT) and afterwards incubated with the tyrosine hydroxylase (TH) antibody (polyclonal rabbit, Abcam, #ab112, 1:750 in 3% skim milk powder/TBS, overnight, 4°C). After another TBS washing step (3 x 5 min), sections were incubated with the secondary biotinylated antibody (donkey anti-rabbit, dianova, #111-065-006, 1:500 in 3% skim milk powder/TBS, 30 min, RT), followed by avidin/biotin Vectastain Elite ABC HRP Kit (Vector Laboratories). Visualization was performed using DAB solution (0.46 mM 3,3'-Diaminobenzidine tetrahydrochloride, 7.3 mM Imidazole, 15.2 mM Ammonium nickel (II) sulfate hexahydrate, 0.015% H_2O_2 in TBS, pH 7.1, 6 min). Following a short washing in ddH$_2$O (1 sec), sections were dehydrated in 50%, 70% (1 sec each), 95% and 100% ethanol (1 min each), cleared in xylene (2 x 10 min) and mounted with Entellan.

Fluorescence stainings: Sections were rinsed in 0.2% Triton-X 100 in TBS (3 x 5 min) after the epitope retrieval and incubated with the primary antibodies (TH polyclonal rabbit, Abcam, #ab112, 1:1500, mitochondrial complex IV SU1 (COX I) monoclonal mouse, Abcam, #ab14705, 1:1000 or calbindin-D28k (Cb-D28k) monoclonal mouse, Swant, #300, 1:150 in Dako antibody diluent, overnight, 4°C). Sections were washed in 0.2% Triton-X 100 in TBS (3 x 5 min) and incubated with fluorochrome-conjugated secondary antibodies (Goat anti-rabbit TRITC-conjugated, AffiniPure, #111-025-144, 1:2000, Goat anti-mouse DyLight488-conjugated, Jackson-ImmunoResearch, #115-485-003, 1:400, overnight, 4°C). Following another washing step in 0.2% Triton-X 100 in TBS (3 x 5 min), midbrain sections were counterstained with DAPI (1 µg/mL in ddH$_2$O, 1 min), washed again in 0.2% Triton-X 100 in TBS (3 x 5 min) and mounted with Fluoromount.

Stereological quantification of dopaminergic neurons

For the counting of DaNs, tyrosine hydroxylase stainings of serial coronal paraffin midbrain sections were performed similar to stainings in the striatum. Sections were incubated with DAB solution (0.46 mM 3,3'-Diaminobenzidine tetrahydrochloride, 7.3 mM Imidazole, 15.2 mM Ammonium nickel (II) sulfate hexahydrate, 0.015% H2O2 in TBS, pH 7.1) for 14 min and counterstained with nuclear fast red (NFR, 0.1% in 5% aluminium dissolved 1:5 in ddH2O). Stereological quantification of DaNs was conducted with the physical fractionator approach, which is typically used for the quantification of large neuron numbers in brain nuclei using thin, paired tissue sections (Gundersen et al., 1988; Ma et al., 2003; Glaser et al., 2007). The region of interest was confined either to the SNc or to the VTA using the mouse brain atlas (Paxinos and Franklin, 2001) on sections between Bregma -2.54 mm and -3.88 mm. Neurons Q were only counted, if their TH- and NFR-positive profiles appeared in the reference section but not in the lookup section. In addition, neurons had to be located either within the counting frame,

or touching the open frame, but not touching the forbidden frame. The height sampling fraction hsf (section thickness/dissection height = 5 µm/5 µm = 1) and the area sampling fraction asf (area of counting frame/area of sampling grid = 42.9 µm²/191.82 µm² = 0.223647) were given as constants. The section sampling fraction ssf was set by the number of sections between the analyzed section pairs (typically 21 sections). Total dopaminergic neuron numbers N were calculated by means of the following formula (Dorph-Petersen et al., 2001; Howard and Reed, 2005): N = Q x 1/hsf x 1/asf x 1/ssf.

Spontaneous motor activity

Beam break experiments were performed to examine the spontaneous horizontal and vertical movement (rearing behaviour) of mice. The activity measurements were done in home-made beam break detector cages. Before the experiments, cages were cleaned with ethanol. Horizontal movement and vertical activity were detected by infrared beams. Interruptions on the horizontal and vertical level were recorded during a tracking period of 60 minutes. The total counts after 60 minutes are presented as percentages of control animals. All experiments were conducted between 12:00 and 17:00 p.m.

Oxygen consumption measurements

Polarographic measurements were performed in 300 µm thick coronal brain sections. 10 to 20 week-old mice were killed by cervical dislocation and the brain was quickly removed. Sections were prepared with a vibratome (Leica VT1000 S) in ice-cold, carbonated artificial cerebrospinal fluid (ACSF: 125 mM NaCl, 2.5 mM KCl, 25 mM NaHCO$_3$, 1.25 mM NaH$_2$PO$_4$ x H$_2$O, 25 mM Glucose, 2 mM MgCl$_2$, 2 mM CaCl$_2$ x 2 H$_2$O). Tested compounds were dissolved freshly or prepared from stock solutions (stored at -80 °C) on the day of the experiment. Oxygen consumption of midbrain sections was measured at 37 °C using a Clark-type oxygen electrode (Hansatech oxyview system) in a closed glass chamber containing 1 mL uncarbonated recording ACSF. An initial zero calibration with sodium dithionite was performed before the measurement. Mitochondrial respiratory chain inhibitors were applied to midbrain sections with a micro syringe. Mitochondrial oxygen consumption was stopped by adding 5 mM potassium cyanide at the end of the recordings. Relative values of oxygen content given by the measurement were converted into absolute values using reference oxygen values of electrolyte solutions at defined conditions (http://water.usgs.gov/software/DOTABLES/, 37.5 °C solution temperature, 760 mmHg barometric pressure and 12‰ salinity). Mean oxygen consumption was determined over a period of 5 to 10 minutes. Oxygen consumption during application of potassium cyanide was averaged over a period of 2 minutes in order to measure non-mitochondrial oxygen consumption. After oxygen consumption measurements, midbrain sections were snap frozen in liquid nitrogen and stored at -20 °C. Brain material was thawed on ice and lysed in TOTEX (20 mM Hepes, 400 mM NaCl, 20% Glycerol, 1% NP-40, 1 mM

MgCl$_2$, 0.5 mM EDTA, 0.1 mM EGTA, 10 mM α-glycerophosphat, 5 mM DTT, 10% Roche complete Protease Inhibitor, pH 7.9) buffer with fourfold volume of the sample volume. Lysates were frozen at -80 °C to rupture membranes. For the measurement of the protein content, lysates were thawed on ice again, centrifuged (15 min, 4 °C, 14,000 rpm) and supernatants were carefully removed. Protein concentrations of the supernatants were determined using Bradford assay with a BSA standard. Oxygen consumption values of midbrain sections were normalized to their protein content and presented as percentages of control measurements. Values of sample size (n) represent the number of investigated brain sections.

Experimental Design and Statistical Analysis

Statistical analysis was done with GraphPad Prism 4. Quantified Data is presented as mean + SEM. Values of sample size (n) refer to mouse numbers or, in COX-immunohistochemistry and in 2PLSM experiments, to neuron numbers. Unpaired *t* tests, one-way or two-way ANOVA with *post hoc* comparisons (Kruskal-Wallis with Dunn`s or Bonferroni *post hoc* test) were used to determine differences between groups. A significance level of 0.05 was accepted for all statistical tests. Asterisks mark P-values of 0.05 (*), 0.01 (**), 0.001 (***) or 0.0001 (****).

Results

MitoPark mice recapitulate the differential vulnerability of the dopaminergic system following mitochondrial impairment

In PD patients, degeneration of dopaminergic projections is primarily observed in the caudate putamen region (CPu) of the striatum (Miller et al., 1997), which is innervated by SNc DaNs (Liss and Roeper, 2008). In contrast, the nucleus accumbens (NAc), which is a major projection area for VTA DaNs, is more or less spared (Miller et al., 1997). A similar pattern of differential fiber loss was also observed in the striatum of MitoPark mice (Figure 3-1A). There was no reduction of dopaminergic projections in the nucleus accumbens of 12 and 14 week-old MitoPark mice (Figure 3-1B, 12 week-old MitoPark mice 105% ± 2% TH-positive fiber density compared to controls, P=0.9656, n.s., 14 week-old MitoPark mice 104% ± 3%, P>0.9999, n.s.), and only a minor reduction in 20 week-old MitoPark mice (85% ± 3%; P=0.0226). However, there was rapid degeneration of dopaminergic projections in the caudate putamen: A severe loss of fibers was observed already at 14 weeks (Figure 3-1C, fibers remaining: 53% ± 9%, P<0.0001) and even more at 20 weeks (16% ± 3%; P<0.0001) in MitoPark mice, underlining also in this genetic PD model the striking differential vulnerability of dopaminergic projections to mitochondrial dysfunction.

This differential vulnerability was also clearly observed when counting neurons in the midbrain. In aging MitoPark mice, SNc DaNs die earlier than VTA DaNs (Figure 3-1D, 20-week-old MitoPark mice: VTA 81% ± 5%, SNc 32% ± 3%, P=0.0001) and neurodegeneration starts at
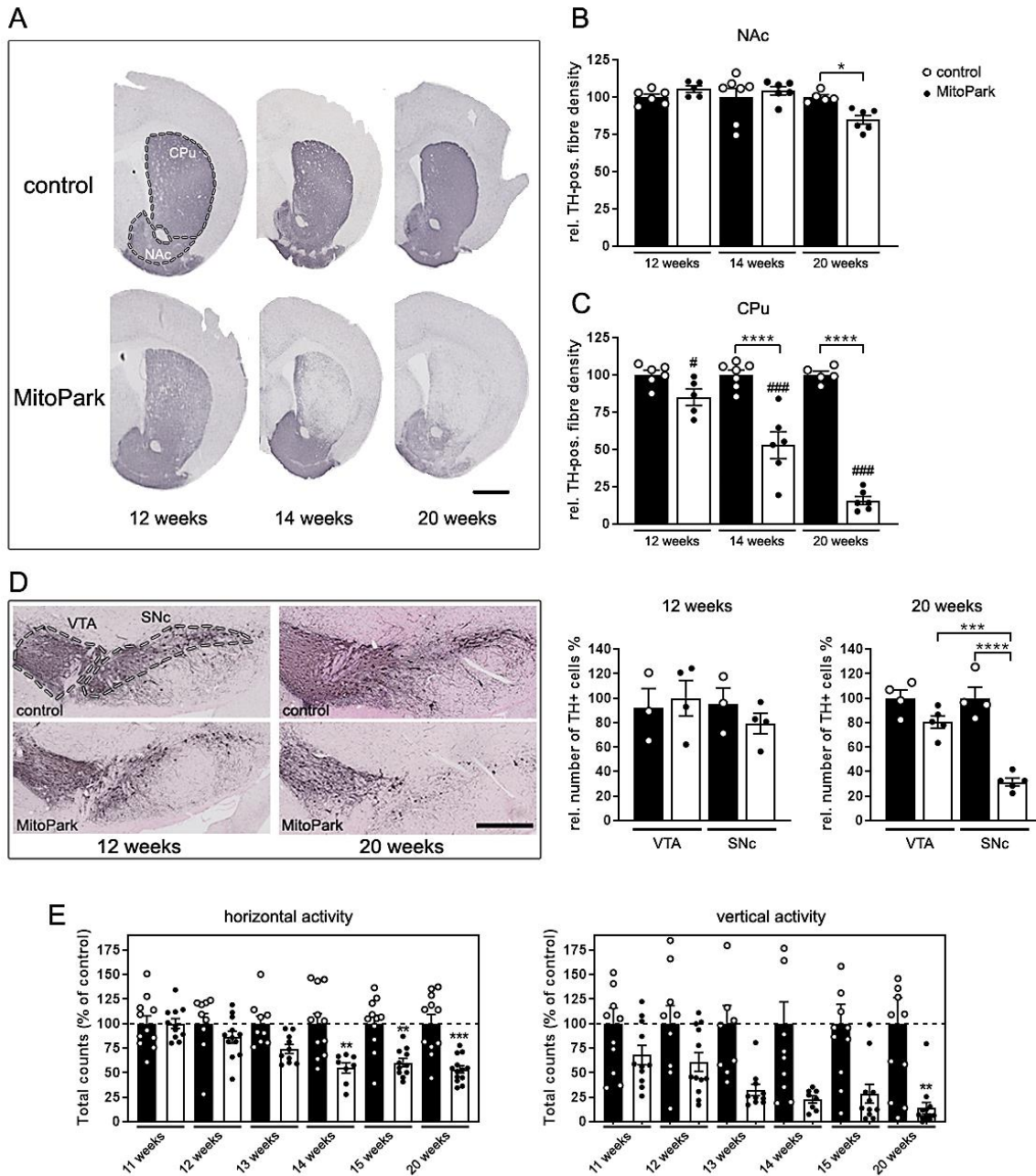
Fig. 3-1 Degeneration of the nigro-striatal system in MitoPark mice. A) Tyrosine hydroxylase (TH) immunohistochemistry in the striatum (CPu and NAc, marked by the dashed line) of 12-, 14- and 20-week-old MitoPark and age-matched control mice. Scale bar, 1 mm. B) Quantification of the striatal TH signal revealed minor degeneration of dopaminergic projections with increasing age in the NAc of MitoPark mice (black dots on white bars). C) In contrast, there was a dramatic loss of the dopaminergic projections in the CPu of aging MitoPark mice (Control mice: n = 5-7, MitoPark mice: n = 5-6, # indicates significances between CPu and NAc of MitoPark mice). D) Immunohistochemical staining of TH-positive neurons in the VTA and SNc in 12- and 20-week-old MitoPark and control mice (VTA and SNc delimitated by dashed lines). Scale bar, 500 µm. DaN numbers (TH+ neurons) in both midbrain regions of MitoPark (black dots on white bars, n = 4-6) and control mice (white dots on black bars, n = 4) were estimated by stereological quantification. E) Beam break events are presented on the horizontal and vertical levels to show the spontaneous motoric activity of MitoPark mice (black dots on white bars, n = 8-13) in comparison to control mice (white dots on black bars, n = 9-11). Data are represented as mean ± SEM; * p < 0.05, ** p < 0.01, *** p < 0.001, **** p < 0.0001, ### p < 0.0001.

12 weeks and becomes pronounced at 20 weeks (20 weeks: control SNc 100% ±9%, MitoPark SNc 32% ± 3%, P<0.0001). Nigro-striatal degeneration causes impairment of spontaneous movement, starting at 14 weeks (Figure 3-1E, horizontal 55% ± 5%, P=0.0040). Reflecting the progressive development of the PD phenotype, motor behaviour of MitoPark mice was further decreased over time (horizontal 15 weeks 60% ± 4%, P=0.0067, 20 weeks ± 53% 4%, P=0.0002, vertical 20 weeks 14% ± 6%, P=0.0036). Next, we asked if the selective vulnerability P=0.0002, vertical 20 weeks 14% ± 6%, P=0.0036). Next, we asked if the selective vulnerability observed in MitoPark mice is due to a different time course in the loss of the respiratory chain (RC), which is represented by the mtDNA-encoded subunit I of cytochrome *c* oxidase (COX), essential for activity as well as assembly (Figure 3-2A and B). Interestingly, somata of DaNs of control mice exhibited a higher COX-signal compared to the surrounding tissue (VTA: 134% ± 15%, SNc: 129% ± 8%). The COX-signal was clearly reduced, however to a similar extent in
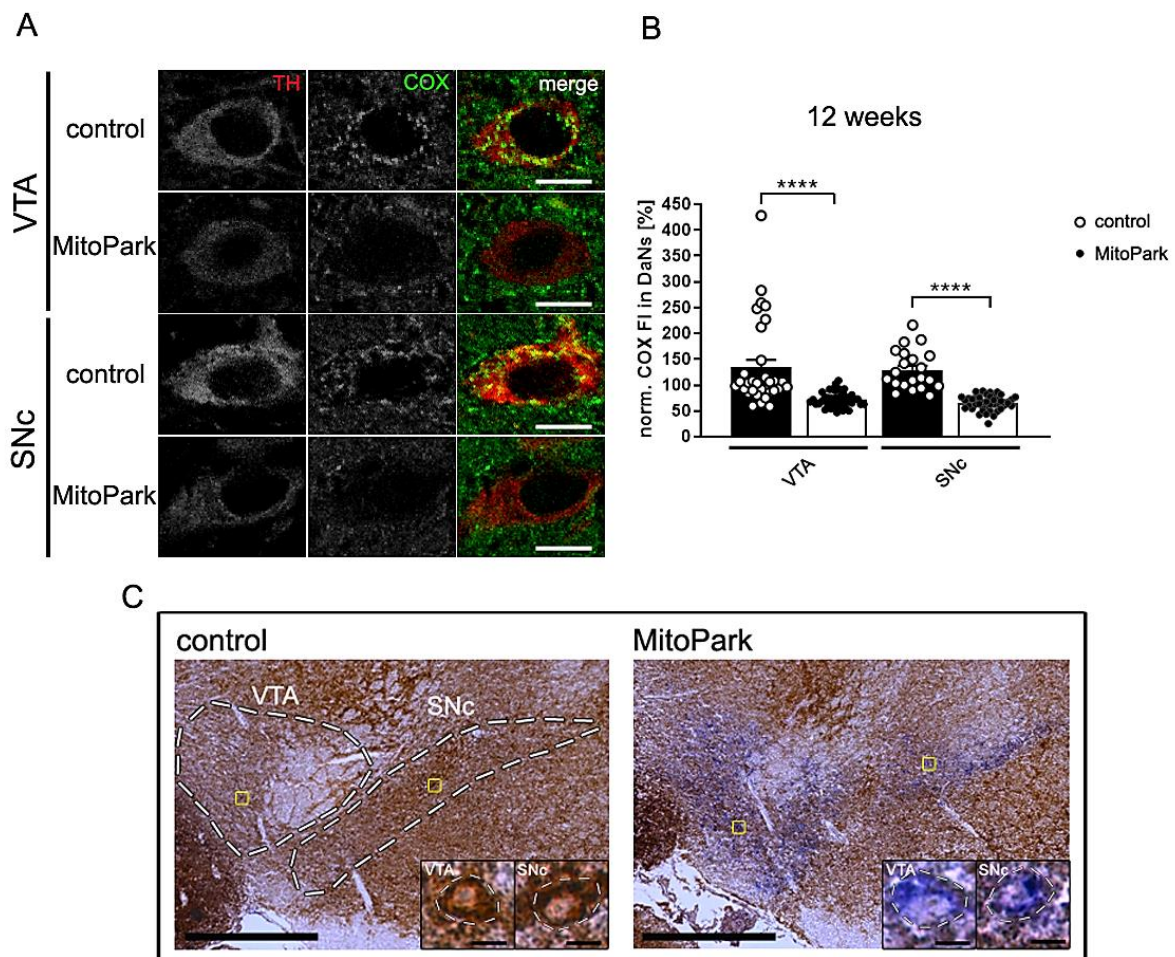
Fig. 3-2 Mitochondrial respiratory chain integrity is lost in dopaminergic neurons of MitoPark mice. A) The signal of the COX immunostaining (green) was analyzed in TH-positive (red) neurons in the VTA and SNc of 12 week-old control and MitoPark mice. Scale bars, 10 µm. B) The fluorescence intensity of the COX-staining (norm. COX-FI) was dramatically decreased in both, VTA and SNc DaNs of MitoPark mice (control mice: white dots on black bars, n = 21-32 neurons, 4 mice, MitoPark mice: black dots on white bars, n = 45-47 neurons, 6 mice). C) Neurons with reduced activity of COX in the VTA and the SNc in 12-week-old MitoPark mice were unraveled by COX-SDH staining (dashed lines delimitate the dopamine midbrain regions in the overview with 500 µm scale bars and single neurons in the close-ups with 10 µm scale bars). Data are represented as mean ± SEM; **** p < 0.0001.

both, VTA and SNc of MitoPark mice at 12 weeks, at the onset of neurodegeneration (VTA: 72% ± 2%, P<0.0001, SNc: 66% ± 2%, P<0.0001). In addition, a severe deficiency of enzymatic COX-activity was detected by histochemistry in DaNs in the SNc, but, importantly, again similarly in the VTA of MitoPark mice (Figure 3-2C). Therefore, both dopaminergic midbrain regions displayed comparable and severe mitochondrial dysfunction, implying that other SNc DaN specific characteristics must be responsible for their enhanced vulnerability.

Calbindin-D28k expression increases the probability for survival of dopaminergic neurons in MitoPark mice

The higher vulnerability of SNc DaNs to mitochondrial dysfunction might be linked to differential expression of calcium-binding proteins, since mitochondria are importantly involved in calcium handling: Indeed, in *post mortem* PD patient samples those midbrain regions which are prone to neurodegeneration contain fewer calbindin-expressing neurons than areas with low susceptibility (Yamada et al., 1990). Therefore, the presence of calbindin was investigated in the surviving fraction of DaNs in MitoPark mice (Figure 3-3A). In the VTA, the proportion of calbindin-positive neurons did not differ between control and MitoPark mice (Figure 3-3B, 12 weeks: control 25% ± 1%, MitoPark 39% ± 5%, P=0.1600, n.s.; 14 weeks: control 26% ± 5%, MitoPark 39% ± 9%, P=0.3068, n.s.; 20 weeks: control 21% ± 2%, MitoPark 40% ± 7%; P=0.0671, n.s.). In addition, in the VTA the amount of calbindin-positive neurons of control and MitoPark mice did not significantly change over time. However, in the SNc, we observed a higher fraction of remaining, calbindin-positive DaNs in 20 week-old MitoPark mice compared to controls (control 9% ± 3%, MitoPark 29% ± 9%, P=0.0262), strongly suggesting that the presence of this protein is protective in the context of severe general neuron loss (Figure 3-1D).

The inhibition of mitochondrial complex IV increases the RedOx-ratio of SNc DaNs

TH-mito-roGFP mice (here referred to as mito-roGFP) express a redox-sensitive GFP variant in the mitochondrial matrix of DaNs, and thus can be used to assess changes of the redox system, more specifically the GSH/GSSG ratio, in situ. Surmeier and colleagues used this fluorescence sensor to estimate "oxidant stress" of the mitochondrial matrix in DaNs (Guzman et al., 2010). The reducing compound dithiotreitol (DTT) and the oxidizing compound aldrithiol (ALD) were sequentially applied during 2PLSM experiments in order to calibrate the redox-sensitive GFP signal (Guzman et al., 2010; Dryanovski et al., 2013). In order to optimize our RedOx calibration protocol, in a first experiment, DTT and ALD were applied to midbrain sections for 10 minutes whilst the 2PLSM laser was inactive (Figure 3-4-1). DTT induced a strong increase (VTA: +0.34 ± 0.06-fold change, SNc: +0.32 ± 0.04-fold change) and ALD a strong decrease of the fluorescence intensity (VTA: -0.35 ± 0.02-fold change, SNc: -0.42 ±
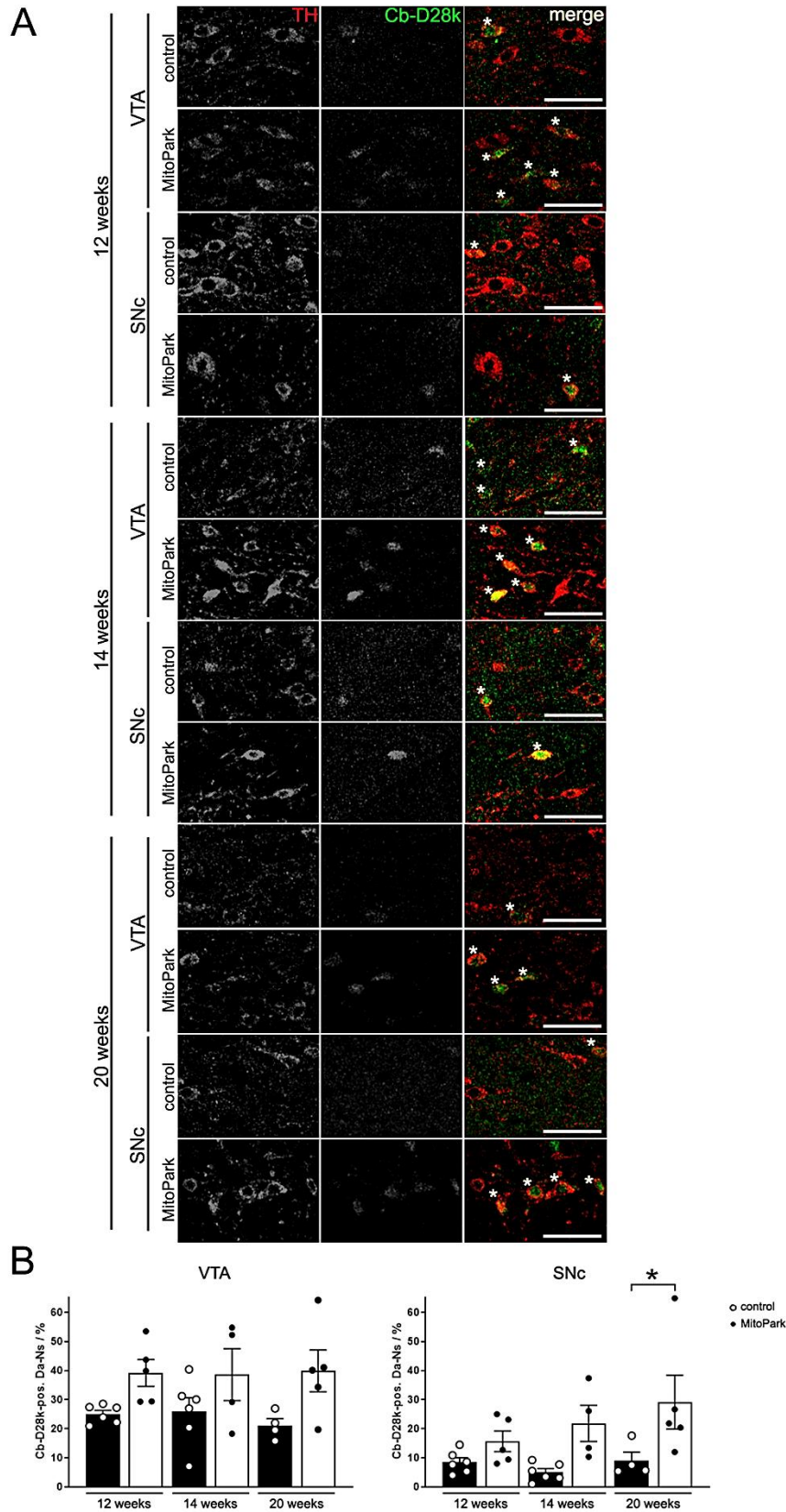
Fig. 3-3 Colocalization of TH and calbindin-D28k (Cb-D28k) in the midbrain of 12-, 14-, and 20-week-old MitoPark mice. A) Merged TH (red, 1st column) and Cb-D28k (green, 2nd column) fluorescence immunostainings depict Cb-D28k-expressing DaNs (yellow, marked by asterisks). Scale bar, 50 μm. B) There were significantly more Cb-D28k positive DaNs in the SNc of 20-week-old MitoPark mice compared with control mice. Data are represented as mean ± SEM (Control mice: white dots on black bars, n = 4-6, MitoPark mice: black dots on white bars, n = 4-5; * p < 0.05).

0.04-fold change) measured after this time. Also, application of H2O2 resulted in a pronounced decrease of the fluorescence intensity in both, VTA (-0.66 ± 0.04-fold change) and SNc DaNs (-0.65 ± 0.03-fold change). In addition, a kinetic analysis was performed in 2PLSM experiments with a continuously active laser (Figure 3-4-2). The normalized mito-roGFP fluorescence (F/Fo) displayed a constant loss of intensity over time (Figure 3-4-3A). Application of DTT (Figure 3-4-2B) induced a pronounced increase of the fluorescence intensity which reached a plateau after 10 minutes of application (127% ± 5%; P<0.001). The mito-roGFP signal reached the initial level (99% ± 4%) after 10 further minutes of DTT application. A rapid loss of the fluorescence intensity (46% ± 2%; P<0.01) was observed when application of DTT was followed by ALD (Figure 3-4-2C). Thus, the mito-roGFP signal can be maximally increased by a 10-minute application of DTT and maximally decreased by a consecutive 10-minute application of ALD. These application intervals were used in follow-up experiments to gain reference values for signal intensity. Since we observed a permanent signal loss in the continuous recording mode, we evaluated the signal in "discrete" experiments, with the laser being inactive for most of the time. The laser was active at the beginning of the recording (0 minutes), at 20 minutes, after application of DTT at 30 minutes and after application of ALD at 40 minutes (Figure 3-4-2D). The signal loss after 20 minutes during this protocol was considerably lower compared to continuous recordings (Figure 3-4-2E). Few neurons which displayed a rundown by more than 40% after 20 minutes were excluded from analysis. In remaining neurons, DTT and ALD caused prominent changes of the fluorescence intensity (Figure 3-4-2D).

After optimizing the recording conditions, selective RC inhibitors were applied to acute midbrain sections of Th-mito-roGFP wild type mice in order to investigate how defects of the RC change the RedOx-ratio of the glutathione system. In order to prove their efficiency, we confirmed that Rotenone, antimycin A and potassium cyanide (KCN) significantly reduced oxygen consumption of similarly isolated midbrain sections at the same concentrations used in 2PLSM (Figure 3-4-3, rotenone: 36% ± 3% of control measurements, P=0.0019, antimycin A: 23% ± 3%, P=0.0016, KCN: 6% ± 2%, P<0.0001). Rotenone was used at its maximal solubility and a higher concentration of antimycin A (200 µM) did not further reduce oxygen consumption (data not shown). Oligomycin at maximal concentration, probably due to its high lipophilicity and the myelin rich brain slice, displayed extremely slow wash in kinetics and did
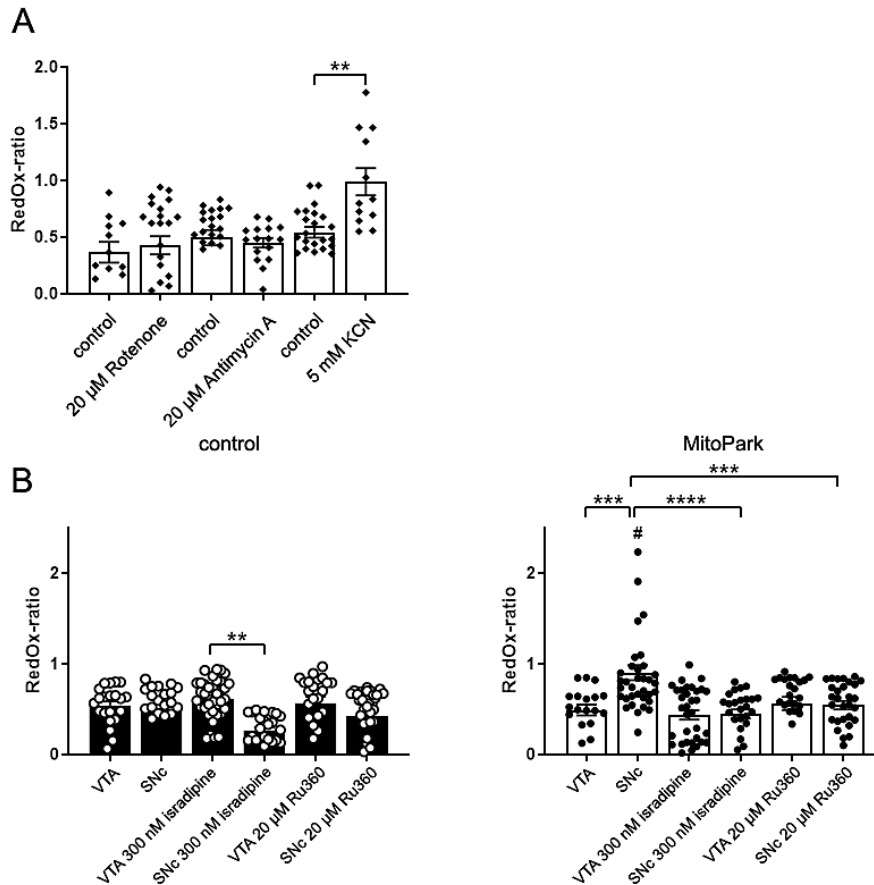
Fig. 3-4 The mitochondrial RedOx-ratio of SNc DaNs is reduced by application of isradipine or Ru360 in MitoPark mice. A) Only application of 5 mM potassium cyanide (KCN) induced an increase of the mitochondrial RedOx-ratio. B) Incubation of midbrain mito-roGFP sections with 300 nM isradipine (similar to Dragicevic et al., 2014; Ortner et al., 2017) for at least 30 min induced a reduction of the RedOx-ratio in SNc DaNs of control mice, but not in VTA DaNs. Treatment with 20 μM Ru360 only induced a small decrease of the RedOx-ratio in control SNc neurons. On the contrary, the RedOx-ratio was elevated in SNc, but not in VTA neurons of 10 – 12-week-old MitoPark mice. This SNc-specific high RedOx-ratio in MitoPark mice was diminished by isradipine and Ru360. Data are represented as mean ± SEM (A: Rotenone control: n = 12, rotenone: n = 23, antimycin A control: n =2 2, antimycin A: n = 16, KCN control: n = 23, KCN: n = 22, 3-5 mice per condition; B: control VTA n = 21, control SNc n = 22, control VTA + isradipine n = 36, control SNc + isradipine n=25, control VTA + Ru360 n = 23, control SNc + Ru360 n = 37, MitoPark VTA n=19, MitoPark SNc n = 35, MitoPark VTA + isradipine n = 34, MitoPark SNc + isradipine n=26, MitoPark VTA + Ru360 n = 25, MitoPark SNc + Ru360 n = 23, 3-5 mice per condition, # indicates significance between SNc DaNs of MitoPark and control mice); ** $p < 0.01$, *** $p < 0.001$, **** $p < 0.0001$.

not significantly reduce oxygen consumption (59% ± 8%, P>0.9999, n.s.). Also, the inner membrane uncoupler CCCP did not increase oxygen consumption (91% ± 6%, P>0.9999, n.s.), because mitochondria in mouse brain seem to utilize oxygen at maximal rate which cannot be further increased by uncouplers, as shown recently also by others (Dias et al., 2018). Surprisingly, only KCN increased the RedOx-ratio of SNc DaNs (Figure 3-4A, RedOx-ratio rotenone control: 0.37 ± 0.09, rotenone: 0.43 ± 0.08; antimycin A control: 0.50 ± 0.07, antimycin A: 0.45 ± 0.04; KCN control: 0.54 ± 0.05, KCN: 0.90 ± 0.09, P=0.0004), indicating that the level of GSH in the matrix is decreased by the inhibition of COX. Importantly, inhibition of complex I and III by rotenone and antimycin A, respectively, which is established to result in pronounced production of reactive oxygen species (ROS) (Murphy, 2009), did not change this ratio.

Calcium influx is responsible for the high RedOx-ratio of vulnerable SNc DaNs

2PLSM experiments showed that, in control mice, both VTA and SNc DaNs display almost identical mitochondrial RedOx-ratios (Figure 3-4B, VTA: 0.54 ± 0.05, SNc: 0.50 ± 0.07, P>0.9999, n.s.). Neither blockade of plasma membrane calcium channels by the selective inhibitor isradipine, nor inhibition of the mitochondrial calcium uniporter (MCU) with Ru360 induced changes in SNc and VTA DaNs of control animals (SNc + 300 nM isradipine 0.26 ± 0.04, P>0.9999, n.s., VTA + 300 nM isradipine 0.62 ± 0.04, P>0.9999, n.s.; SNc 20 µM Ru360 0.42 ± 0.05, P>0.9999, n.s., VTA 20 µM Ru360 0.57 ± 0.07, P>0.9999, n.s.).

Importantly, there was a much higher RedOx-ratio in MitoPark SNc DaNs (Figure 3-4B, 0.90 ± 0.08) at the age of 12 weeks, i.e. at the onset of neurodegeneration, compared to MitoPark VTA DaNs (0.49 ± 0.06, P=0.0009), but also compared to control SNc DaNs (P=0.0004). This high RedOx-ratio was robustly decreased in MitoPark SNc when treating sections with isradipine (0.45 ± 0.05, P<0.0001), but no effect was seen in MitoPark VTA DaNs (0.44 ± 0.05, P>0.9999, n.s.). Also, when MitoPark midbrain sections were incubated with Ru360, the RedOx-ratio of SNc DaNs was again significantly lowered (0.42 ± 0.05, P=0.0010).

In conclusion, an elevated RedOx-ratio, indicating a low GSH/GSSG ratio in the mitochondrial matrix, was found to be a hallmark of SNc, but not VTA DaNs in MitoPark mice, preceding the onset of severe neurodegeneration. This high RedOx-ratio could be rescued by reducing neuronal as well as mitochondrial calcium influx.

Mitochondrial membrane potential is hyperpolarized in MitoPark SNc DaNs and is further elevated when calcium influx is blocked

The electrochemical potential of the inner mitochondrial membrane was assessed in midbrain sections loaded with TMRM, in order to better understand how mitochondrial dysfunction affects the RedOx-ratio. Initial experiments showed that, quite surprisingly, the TMRM signal was lower in the somata of midbrain neurons compared to the surrounding tissue (Figure 3-5A), in contrast to the higher signal for COXI protein (Figure 3-2A), indicating that mitochondria in the somata have a lower inner membrane potential than those in other cell types and neurites. The mitochondrial network was clearly visualized by TMRM as shown in mouse fibroblasts (Figure 3-5B). As expected, the TMRM signal of identified DaNs, but also of mitochondria in surrounding neurites, was dramatically reduced by KCN (Figure 3-5C). TMRE, another fluorescent dye sensitive to the inner membrane potential displayed a signal similar to TMRM and its intensity was likewise decreased by KCN (Figure 3-5-1). It was not possible to decrease these signals by the uncoupler CCCP, as usually used as a control, again probably due to its high lipophilicity and the myelin rich brain sections. Therefore, we decided to use the deflection of the TMRM signal upon maximal RC inhibition by KCN as a convenient readout
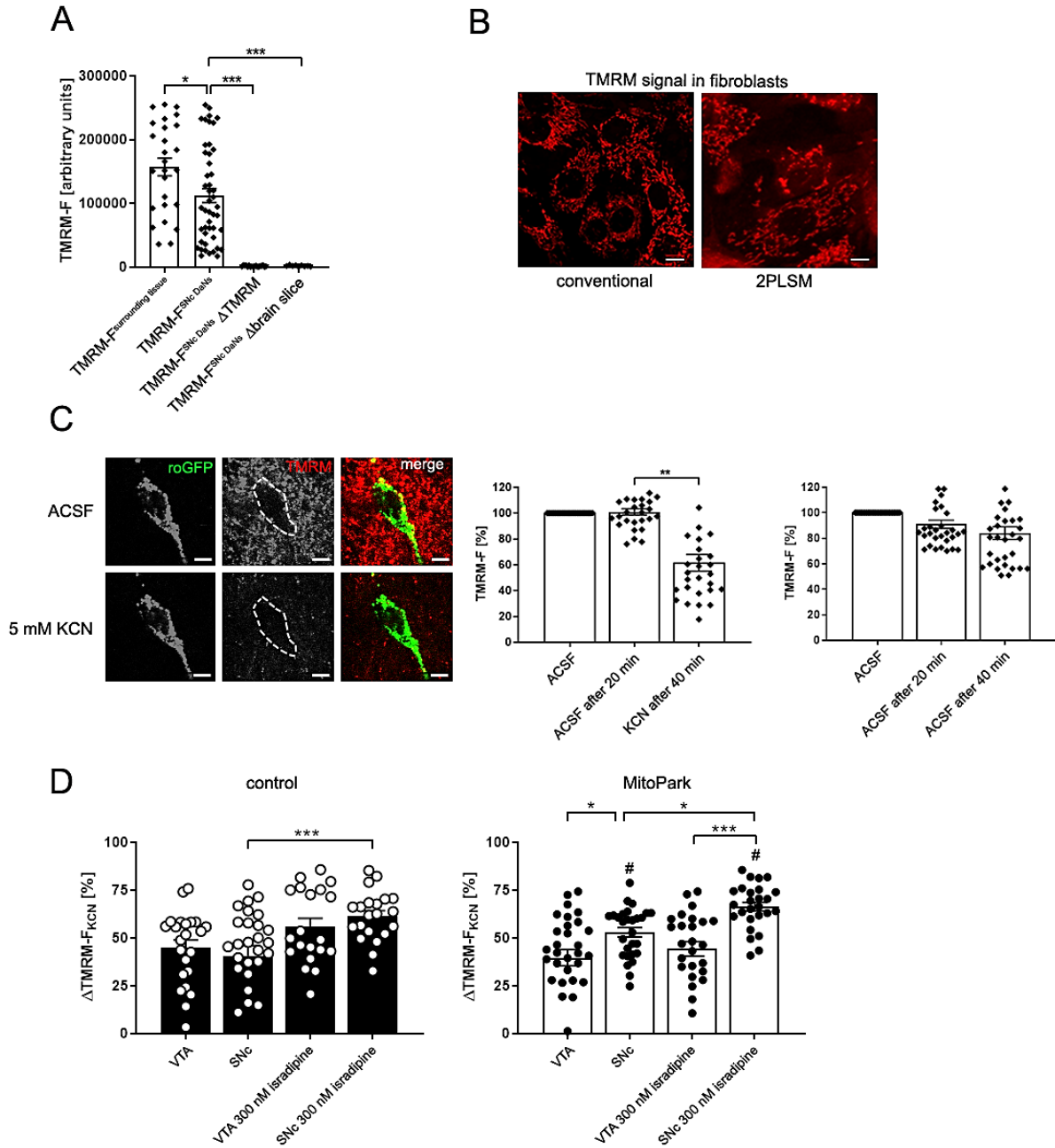
Fig. 3-5 KCN induces an increase of ΔTMRM-F$_{KCN}$ in MitoPark SNc DaNs. A) Quantitative data presenting a high fluorescent TMRM signal in the surrounding of cell somata and midbrain DaNs, compared to DaNs from sections that were not loaded with TMRM and ACSF containing TMRM without tissue, respectively. B) TMRM visualizes the mitochondrial network in mouse fibroblasts. Pictures were taken by using both conventional fluorescent microscope and 2PLSM. Scale bar, 10 μm. C) TMRM signal of a mito-roGFP expressing midbrain DaN before and after application of KCN. Scale bar, 10 μm. KCN (5 mM) induced a significant reduction of the TMRM signal in the soma of DaNs. D) Reduction of the TMRM signal after KCN application was used to calculate the difference between TMRM fluorescence before and after KCN (ΔTMRM-F$_{KCN}$ = TMRM-F$_{ACSF, 20\ min}$ - TMRM-F$_{KCN, 40\ min}$). Low TMRM signal intensities induced by KCN are reflected by high ΔTMRM-F$_{KCN}$ values. A high ΔTMRM-F$_{KCN}$ value, in turn, represents a high mitochondrial membrane potential. ΔTMRM-F$_{KCN}$ did not differ between VTA and SNc DaNs in control animals. However, in MitoPark mice, SNc DaNs showed a significantly higher ΔTMRM-F$_{KCN}$ deflection compared to MitoPark VTA and control SNc DaNs. Administration of KCN to midbrain sections preincubated with 300 nM isradipine led to a significant elevation of ΔTMRM-F$_{KCN}$ in control and MitoPark SNc DaNs. In contrast, the use of isradipine did not alter the TMRM signal in both control and MitoPark VTA DaNs. Data are represented as mean ± SEM (control VTA n = 23 neurons, MitoPark VTA n = 31 neurons, control VTA + 300 nM isradipine n = 20 neurons, MitoPark VTA + 300 nM isradipine n = 26 neurons, control SNc n = 28 neurons, control SNc + 300 nM isradipine n = 21 neurons, MitoPark SNc n = 28 neurons, MitoPark SNc + 300 nM isradipine n = 26 neurons, 3-6 mice per group); * $p < 0.05$, ** $p < 0.01$, *** $p < 0.001$, # $p < 0.05$.

for the actual inner mitochondrial membrane potential present *in situ*, before addition of KCN. VTA and SNc DaNs of control mice revealed a similar ΔTMRM-F_{KCN} value (Figure 3-5D, SNc: 40.7 ± 5.1, VTA: 45.1 ± 3.9, P>0.9999, n.s.), indicating that the inner mitochondrial membrane potential is similar in these DaN populations. In addition, there was no difference in ΔTMRM-F_{KCN} between control (45.1 ± 3.9) and MitoPark VTA DaNs (39.7 ± 4.2, P=0.3670, n.s.), indicating that the mitochondrial membrane potential remained similar in the latter neurons, even in the presence of severe mitochondrial dysfunction. Interestingly, inhibition of complex IV by KCN led to an increase of ΔTMRM-F_{KCN} in MitoPark SNc DaNs (53.0 ± 2.5) compared to MitoPark VTA (39.7 ± 4.2, P=0.0278) and control SNc DaNs (40.7 ± 5.1, P=0.0352). This quite unexpectedly indicates that a high mitochondrial inner membrane potential was present in SNc DaNs of MitoPark mice *in situ*.

Last, L-type plasma membrane calcium channels were blocked by isradipine to investigate if and how the elevated mitochondrial membrane potential of MitoPark SNc DaNs is affected by calcium fluxes. Isradipine induced a significant increase of ΔTMRM-F_{KCN} in control as well as in MitoPark SNc DaNs (Figure 3-5D, control + 300 nM isradipine: 61.5 ± 2.9, P=0.0052, MitoPark + 300 nM isradipine: 66.4 ± 2.3, P=0.0392), but not in VTA DaNs, showing that the mitochondrial membrane potential in SNc DaNs of both control and MitoPark mice is further elevated when cytosolic calcium influx is inhibited. This suggests that a high mitochondrial membrane potential is established in SNc DaNs of control, but surprisingly also in MitoPark mice, in order to electrogenically remove and thus buffer cytosolic calcium, even when RC function is severely impaired, and consequently reaches an even higher maximal value when calcium influx is blocked.

Discussion

In order to answer the question how mitochondrial impairment leads to the selective degeneration of SNc DaNs, the mitochondrial RedOx-ratio and the inner membrane potential was analyzed in MitoPark mice with preferential degeneration of the nigrostriatal system, similar to patients (Hirsch et al., 1988; Miller et al., 1997; Damier et al., 1999) (Figure 3-1A and Figure 3-1D). COXI-expression was reduced to the same degree in VTA and SNc, and neurons with low COX activity were detected in both midbrain regions of MitoPark mice (Figure 3-2), showing that the respiratory chain was affected to a similar extent. Substantial loss of COX did not lead to significant neuron death at 12 weeks (compare Figure 3-1D and Figure 3-2), implying that other factors than simply energy-deprivation are involved.

Calcium-binding proteins buffer excessive cytosolic calcium, shape calcium transients and contribute to calcium homeostasis (Baimbridge et al., 1992). In PD patients, SNc with few Cb-D28k-expressing DaNs suffers more from neuron loss than the Cb-D28k-enriched VTA (Yamada et al., 1990; German et al., 1992; Reyes et al., 2012). Supporting these results,

colocalization experiments of TH and Cb-D28k in MPTP-treated mice revealed predominant survival of calbindin-positive DaNs, suggesting that the presence of calbindin confers protection (Liang et al., 1996). Indeed, also our experiments revealed more calbindin-expressing DaNs remaining in both regions in 12- and 14-week-old MitoPark mice, and significantly more in SNc of 20 week-old MitoPark mice (Figure 3-3B). Interestingly, the calbindin mRNA content in pooled single substantia nigra DaNs from PD patients was found to be six fold higher compared to healthy individuals (Schiemann et al., 2012), potentially indicating a response to mitochondrial defects. In summary, our colocalization experiments show that calbindin may render midbrain DaNs more resistant against neurodegeneration induced by mitochondrial dysfunction.

The substantia nigra of PD patients contains high levels of oxidized and damaged molecules (Dexter et al., 1994; Alam et al., 1997a; Alam et al., 1997b), correlating with low concentrations of the ROS-scavenging GSH molecule (Sian et al., 1994). Thus, mtDNA deletions leading to mitochondrial dysfunction, a high calcium load and oxidative stress due to changes in the antioxidant defense system might be causally linked and ultimately lead to SNc DaN death.

Inhibitors were applied to midbrain sections to investigate if and how impaired activity of the different RC complexes results in changes of the RedOx-ratio (Figure 3-4A). Despite reducing oxygen consumption, as expected (Figure 3-4-3), neither antimycin A nor rotenone altered the mitochondrial RedOx-ratio of DaNs. Superoxide (O_2•-) is increased by the complex III inhibitor antimycin A (Zhang et al., 1998) or the complex I inhibitor rotenone (Kushnareva et al., 2002), summarized in (Murphy, 2009), in SNc DaNs at even lower concentrations than used by us (Freestone et al., 2009). Therefore, the mito-roGFP signal is not sensitive to increased ROS-production from RC complexes and our data make ROS rather unlikely as the cause of neuron death.

In contrast, KCN considerably increased the RedOx-ratio (Figure 3-4A). KCN results in increased autofluorescence in substantia nigra DaNs (Tucker et al., 2016), which is generally used as a readout for enhanced levels of reduced NAD(P)H. Elevated NAD(P)H should increase the GSH/GSSG ratio (Nelson and Cox, 2005), which should lower the RedOx-ratio (Dooley et al., 2004). However, our high RedOx-ratio after KCN implies that inhibition of complex IV decreases levels of GSH in DaNs. We postulate that the pool of NAD(P)H in mitochondria is slowly consumed upon inhibition, without being further replenished by the Krebs cycle dehydrogenases.

After having established these relations, the RedOx-ratio was analyzed in MitoPark DaNs (Figure 3-4B) at the age of 12 weeks, before wide-spread neuron death, but with severe COX deficiency (compare Figure 3-1D and Figure 3-2). SNc DaNs, but not VTA DaNs of MitoPark mice presented with an increased RedOx-ratio, similar to KCN treatment, showing that

additional, SNc-specific factors must account for this outcome. Since isradipine rescued the elevated RedOx-ratio in MitoPark SNc DaNs (Figure 3-4B), we postulate that calcium influx through Cav1.3 channels (Chan et al., 2007; Guzman et al., 2009; Ortner et al., 2017) is responsible for mitochondrial "relative oxidation" in mitochondrially impaired SNc DaNs. Isradipine did not decrease the RedOx-ratio in VTA neurons, since their pacemaking activity is predominantly driven by sodium channels (Khaliq and Bean, 2010).

Although isradipine at 300 nM, as we used, has been shown to completely block pacemaking by ablating Cav1.3-mediated calcium influx in SNc DaNs (Ortner et al., 2017), it remains a matter of debate to which extent the magnitude of intracellular calcium is altered by this inhibitor, as indicated by fluorescent calcium probes: Isradipine at lower concentrations (30 nM) did not alter somatic calcium fluctuations (Ortner et al., 2017), while higher levels of isradipine (5 µM) were sufficient to minimize dendritic calcium oscillations in SNc DaNs (Guzman et al., 2009). Blockade of calcium-driven pacemaking may significantly lower the energy demand of neurons, which may have caused the observed changes in mito-roGFP fluorescence. However, Ru360, the inhibitor of the mitochondrial calcium uniporter MCU, also reduced the RedOx-ratio in MitoPark SNc DaNs (Figure 3-4B), which was also observed in dendrites of SNc DaNs in control mice (Guzman et al., 2010), but not in their somata. Thus, in our hands, reduction of mitochondrial calcium uptake by Ru360 is not sufficient to reduce the RedOx-ratio in functional mitochondria, while it does so in DaNs with a defective respiratory chain.

Elevated mitochondrial calcium leads to an increased rate of production of NADH by enhancing the activity of dehydrogenases and thus Krebs cycle flux (Denton, 2009), which should result in elevated GSH/GSSG. However, in SNc DaNs of MitoPark mice, reduction of mitochondrial calcium influx resulted in a decrease of the RedOx-ratio and thus high levels of mitochondrial GSH.

In addition, and counterintuitively, although complex IV was reduced in both DaN types before the onset of neuron death (Figure 3-2), MitoPark SNc DaNs had maintained a high mitochondrial inner membrane potential (Figure 3-5D), even higher than SNc DaNs in controls. We postulate that this is achieved by bringing in a net negative charge by importing ATP^{4-}, produced by glycolysis, from the cytosol via the adenine nucleotide transporter. ATP is hydrolyzed by ATP synthase operating in reverse mode, followed by export of ATP^{2-} + Pi^-. This mechanism of generating an inner membrane potential is well established in cell lines lacking mtDNA and thus a functioning respiratory chain (Buchet and Godinot, 1998; Appleby et al., 2001), however has not yet been shown in vivo to our knowledge. RC deficient SNc DaNs in MitoPark mice might maintain a high inner membrane potential - even at the expense of precious glycolytic ATP - in order to be able to pump calcium from the cytosol into the negative matrix via MCU. This is substantiated by our finding that inhibiting calcium influx

through plasma membrane channels by isradipine further hyperpolarizes the inner membrane potential, both in control as well as in MitoPark mice (Figure 3-5D), since, under this condition, the depolarizing cation influx into the matrix is blocked. In conclusion, even under conditions of a severe respiratory chain dysfunction, SNc DaNs in MitoPark mice maintain a high inner membrane potential in order to preserve calcium homeostasis.

The question remains how a high inner membrane potential, driving a constant calcium influx into the matrix, relates to the redox system changes we observed. The drop of the RedOx-ratio after isradipine or Ru360 (Figure 3-4B) shows that calcium influx contributed to the reduced GSH levels in SNc DaNs of MitoPark mice. Mammalian mitochondria contain two isocitrate dehydrogenase (IDH) isoforms, specific for $NAD+$ (IDH3) and $NADP+$ (IDH2), respectively, which catalyze the conversion of isocitrate to α-ketoglutarate (α-KG) (Denton, 2009). Importantly, calcium is known to increase the activity of only IDH3, by lowering its Km for isocitrate (Denton et al., 1978; Rutter and Denton, 1988; Rutter and Denton, 1989; Denton, 2009; Llorente-Folch et al., 2015). Therefore, mitochondrial calcium influx would enhance IDH3, but not IDH2 activity, with a resultant decrease in NADPH generation. We therefore hypothesize that the blockage of mitochondrial calcium influx by isradipine and Ru360 in our studies has decreased the activity of IDH3, thereby enhancing NADPH generation by IDH2, resulting in a normalization of the RedOx-ratio. Alternatively, the teams of Mosharov and Sulzer have shown in primary mouse DaNs that the mitochondrial toxin MPP+ activates a cascade of increased cytosolic dopamine and calcium, followed by an elevation of mitochondrial calcium and activation of mitochondrial nitric oxide synthase, so generation of NO may also contribute to the disturbed mitochondrial redox system (Lieberman et al., 2017).

In summary, we hypothesize that mitochondrial dysfunction in SNc DaNs, in combination with their high mitochondrial calcium load, in contrast to the VTA, impairs the mitochondrial antioxidant defense system, which finally promotes their preferential degeneration.

Acknowledgements

Conflict of Interests

The authors declare no conflict of interests.

References

Alam, Z.I., Daniel, S.E., Lees, A.J., Marsden, D.C., Jenner, P., Halliwell, B. A Generalised Increase in Protein Carbonyls in the Brain in Parkinson's but Not Incidental Lewy Body Disease. Journal of Neurochemistry 1997a; 69: 1326-1329.

Alam, Z.I., Jenner, A., Daniel, S.E., Lees, A.J., Cairns, N., Marsden, C.D., et al. Oxidative DNA Damage in the Parkinsonian Brain: An Apparent Selective Increase in 8-Hydroxyguanine Levels in Substantia Nigra. Journal of Neurochemistry 1997b; 69: 1196-1203.

Appleby, R.D., Porteous, W.K., Hughes, G., James, A.M., Shannon, D., Wei, Y.-H., et al. Quantitation and origin of the mitochondrial membrane potential in human cells lacking mitochondrial DNA. European Journal of Biochemistry 2001; 262: 108-116.

Baimbridge, K.G., Celio, M.R., Rogers, J.H. Calcium-binding proteins in the nervous system. Trends in Neurosciences 1992; 15: 303-308.

Bender, A., Krishnan, K.J., Morris, C.M., Taylor, G.A., Reeve, A.K., Perry, R.H., et al. High levels of mitochondrial DNA deletions in substantia nigra neurons in aging and Parkinson disease. Nat Genet 2006; 38: 515-517.

Betarbet, R., Sherer, T.B., MacKenzie, G., Garcia-Osuna, M., Panov, A.V., Greenamyre, J.T. Chronic systemic pesticide exposure reproduces features of Parkinson's disease. Nat Neurosci 2000; 3: 1301-1306.

Bolam, J.P., Pissadaki, E.K. Living on the edge with too many mouths to feed (Braak et al. 2004)d: Why dopamine neurons die. Movement Disorders 2012; 27: 1478-1483.

Braak, H., Ghebremedhin, E., Rüb, U., Bratzke, H., Del Tredici, K. Stages in the development of Parkinson's disease-related pathology. Cell and Tissue Research 2004; 318: 121-134.

Buchet, K., Godinot, C. Functional F1-ATPase Essential in Maintaining Growth and Membrane Potential of Human Mitochondrial DNA-depleted ρ° Cells. Journal of Biological Chemistry 1998; 273: 22983-22989.

Burbulla, L.F., Song, P., Mazzulli, J.R., Zampese, E., Wong, Y.C., Jeon, S., et al. Dopamine oxidation mediates mitochondrial and lysosomal dysfunction in Parkinson's disease. Science 2017; 357: 1255-1261.

Chan, C.S., Guzman, J.N., Ilijic, E., Mercer, J.N., Rick, C., Tkatch, T., et al. 'Rejuvenation' protects neurons in mouse models of Parkinson's disease. Nature 2007; 447: 1081–1086.

Cortopassi, G.A., Shibata, D., Soong, N.W., Arnheim, N. A pattern of accumulation of a somatic deletion of mitochondrial DNA in aging human tissues. Proceedings of the National Academy of Sciences of the United States of America 1992; 89: 7370-7374.

Damier, P., Hirsch, E.C., Agid, Y., Graybiel, A.M. The substantia nigra of the human brain: II. Patterns of loss of dopamine-containing neurons in Parkinson's disease. Brain 1999; 122: 1437-1448.

Dauer, W., Przedborski, S. Parkinson's Disease: Mechanisms and Models. Neuron 2003; 39: 889-909.

De Lau, L.M.L., Breteler, M.M.B. Epidemiology of Parkinson's disease. The Lancet Neurology 2006; 5: 525-535.

Denton, R.M., Richards, D.A., Chin, J.G. Calcium ions and the regulation of NAD+-linked isocitrate dehydrogenase from the mitochondria of rat heart and other tissues. The Biochemical journal 1978; 176: 899-906.

Denton, R.M. Regulation of mitochondrial dehydrogenases by calcium ions. Biochimica et Biophysica Acta (BBA) - Bioenergetics 2009; 1787: 1309-1316.

Dexter, D.T., Holley, A.E., Flitter, W.D., Slater, T.F., Wells, F.R., Daniel, S.E., et al. Increased levels of lipid hydroperoxides in the parkinsonian substantia nigra: An HPLC and ESR study. Movement Disorders 1994; 9: 92-97.

Dias, C., Lourenço, C.F., Barbosa, R.M., Laranjinha, J., Ledo, A. Analysis of respiratory capacity in brain tissue preparations: high-resolution respirometry for intact hippocampal slices. Analytical Biochemistry 2018; 551: 43-50.

Dölle, C., Flønes, I., Nido, G.S., Miletic, H., Osuagwu, N., Kristoffersen, S., et al. Defective mitochondrial DNA homeostasis in the substantia nigra in Parkinson disease. Nature communications 2016; 7: 13548-13548.

Dooley, C.T., Dore, T.M., Hanson, G.T., Jackson, W.C., Remington, S.J., Tsien, R.Y. Imaging Dynamic Redox Changes in Mammalian Cells with Green Fluorescent Protein Indicators. Journal of Biological Chemistry 2004; 279: 22284-22293.

Dorph-Petersen, K.A., Nyengaard, J.R., Gundersen, H.J.G. Tissue shrinkage and unbiased stereological estimation of particle number and size. Journal of Microscopy 2001; 204: 232-246.

Dragicevic, E., Poetschke, C., Duda, J., Schlaudraff, F., Lammel, S., Schiemann, J., et al. Cav1.3 channels control D2-autoreceptor responses via NCS-1 in substantia nigra dopamine neurons. Brain 2014; 137: 2287-2302.

Dryanovski, D.I., Guzman, J.N., Xie, Z., Galteri, D.J., Volpicelli-Daley, L.A., Lee, V.M.-Y., et al. Calcium Entry and α-Synuclein Inclusions Elevate Dendritic Mitochondrial Oxidant Stress in Dopaminergic Neurons. The Journal of Neuroscience 2013; 33: 10154-10164.

Duda, J., Pötschke, C., Liss, B. Converging roles of ion channels, calcium, metabolic stress, and activity pattern of Substantia nigra dopaminergic neurons in health and Parkinson's disease. Journal of Neurochemistry 2016; 139: 156-178.

Ekstrand, M.I., Terzioglu, M., Galter, D., Zhu, S., Hofstetter, C., Lindqvist, E., et al. Progressive parkinsonism in mice with respiratory-chain-deficient dopamine neurons. Proceedings of the National Academy of Sciences of the United States of America 2007; 104: 1325-1330.

Freestone, P.S., Chung, K.K.H., Guatteo, E., Mercuri, N.B., Nicholson, L.F.B., Lipski, J. Acute action of rotenone on nigral dopaminergic neurons – involvement of reactive oxygen species and disruption of Ca2+ homeostasis. European Journal of Neuroscience 2009; 30: 1849-1859.

German, D.C., Manaye, K.F., Sonsalla, P.K., Brooks, B.A. Midbrain Dopaminergic Cell Loss in Parkinson's Disease and MPTP-Induced Parkinsonism: Sparing of Calbindin-D28k-Containing Cells. Annals of the New York Academy of Sciences 1992; 648: 42-62.

Glaser, J., Greene, G., Hendricks, S. Stereology for biological research with focus on neurobiology. MBF Press 2007.

Gundersen, H.J.G., Bagger, P., Bendtsen, T.F., Evans, S.M., Korbo, L., Marcussen, N., et al. The new stereological tools: Disector, fractionator, nucleator and point sampled intercepts and their use in pathological research and diagnosis. APMIS 1988; 96: 857-881.

Guzman, J.N., Sánchez-Padilla, J., Chan, C.S., Surmeier, D.J. Robust Pacemaking in Substantia Nigra Dopaminergic Neurons. The Journal of Neuroscience 2009; 29: 11011-11019.

Guzman, J.N., Sanchez-Padilla, J., Wokosin, D., Kondapalli, J., Ilijic, E., Schumacker, P.T., et al. Oxidant stress evoked by pacemaking in dopaminergic neurons is attenuated by DJ-1. Nature 2010; 468: 696-700.

Hirsch, E., Graybiel, A.M., Agid, Y.A. Melanized dopaminergic neurons are differentially susceptible to degeneration in Parkinson's disease. Nature 1988; 334: 345-348.

Howard, V.C., Reed, M.R. Unbiased Stereology - Threedimensional Measurement in Microscopy 2005: 2nd edition, The optical fractionator, 95-96.

Khaliq, Z.M., Bean, B.P. Pacemaking in Dopaminergic Ventral Tegmental Area Neurons: Depolarizing Drive from Background and Voltage-Dependent Sodium Conductances. The Journal of Neuroscience 2010; 30: 7401-13.

Kraytsberg, Y., Kudryavtseva, E., McKee, A.C., Geula, C., Kowall, N.W., Khrapko, K. Mitochondrial DNA deletions are abundant and cause functional impairment in aged human substantia nigra neurons. Nat Genet 2006; 38: 518-20.

Kushnareva, Y., Murphy, A.N., Andreyev, A. Complex I-mediated reactive oxygen species generation: modulation by cytochrome c and NAD(P)+ oxidation–reduction state. Biochemical Journal 2002; 368: 545-53.

Liang, C.-L., Sinton, C.M., Sonsalla, P.K., German, D.C. Midbrain Dopaminergic Neurons in the Mouse that Contain Calbindin-D28kExhibit Reduced Vulnerability to MPTP-induced Neurodegeneration. Neurodegeneration 1996; 5: 313-318.

Lieberman, O. J., Choi, S. J., Kanter, E., Saverchenko, A., Fier, M. D., Fiore, G. M., Wu, M., Kondapalli, J., Zampese, E., Surmeier, D. J., Sulzer, D., Mosharov, E. V. alpha-synuclein-dependent calcium entry underlies differential sensitivity of cultured SN and VTA dopaminergic neurons to a parkinsonian neurotoxin. eNeuro 2017; 6: 1-22.

Liss, B., Haeckel, O., Wildmann, J., Miki, T., Seino, S., Roeper, J. K-ATP channels promote the differential degeneration of dopaminergic midbrain neurons. Nat Neurosci 2005; 8: 1742-1751.

Liss, B., Roeper, J. Individual dopamine midbrain neurons: Functional diversity and flexibility in health and disease. Brain Research Reviews 2008; 58: 314-321.

Llorente-Folch, I., Rueda, C.B., Pardo, B., Szabadkai, G., Duchen, M.R., Satrustegui, J. The regulation of neuronal mitochondrial metabolism by calcium. The Journal of Physiology 2015; 593: 3447-3462.

Lotter, S., Aradjanski, M., Hermans, S., Dogan, S.A., Trifunovic, A., Wang, S., et al. DARS2 protects against neuroinflammation and apoptotic neuronal loss, but is dispensable for myelin producing cells. Human Molecular Genetics 2017; 26: 4181-4189.

Ma, S.Y., Longo, F., Röyttä, M., Collan, Y. Modern stereological evaluation in the aging human substantia nigra. Image Analysis and Stereology 2003; 22: 73-80.

Meissner, C., Bruse, P., Mohamed, S.A., Schulz, A., Warnk, H., Storm, T., et al. The 4977 bp deletion of mitochondrial DNA in human skeletal muscle, heart and different areas of the brain: A useful biomarker or more? Experimental Gerontology 2008; 43: 645-652.

Miller, G.W., Staley, J.K., Heilman, C.J., Perez, J.T., Mash, D.C., Rye, D.B., et al. Immunochemical analysis of dopamine transporter protein in Parkinson's disease. Annals of Neurology 1997; 41: 530-539.

Murphy, Michael P. How mitochondria produce reactive oxygen species. Biochemical Journal 2009; 417: 1-13.

Nelson, D.L., Cox, M.M., 2005. In: Lehninger - Principles of Biochemistry. Vol., ed.^eds., pp. 722.

Neuhaus, J.F., Baris, O.R., Hess, S., Moser, N., Schroder, H., Chinta, S.J., et al. Catecholamine metabolism drives generation of mitochondrial DNA deletions in dopaminergic neurons. Brain 2014; 137: 354-65.

Neuhaus, J.F.G., Baris, O.R., Kittelmann, A., Becker, K., Rothschild, M.A., Wiesner, R.J. Catecholamine Metabolism Induces Mitochondrial DNA Deletions and Leads to Severe Adrenal Degeneration during Aging. Neuroendocrinology 2017; 104: 72-84.

Obeso, J.A., Stamelou, M., Goetz, C.G., Poewe, W., Lang, A.E., Weintraub, D., et al. Past, present, and future of Parkinson's disease: A special essay on the 200th Anniversary of the Shaking Palsy. Movement Disorders 2017; 32: 1264-1310.

Ortner, N.J., Bock, G., Dougalis, A., Kharitonova, M., Duda, J., Hess, S., et al. Lower Affinity of Isradipine for L-Type Ca^{2+} Channels during Substantia Nigra Dopamine Neuron-Like Activity: Implications for Neuroprotection in Parkinson's Disease. The Journal of Neuroscience 2017; 37: 6761-6777.

Pacelli, C., Giguère, N., Bourque, M.-J., Lévesque, M., Slack, Ruth S., Trudeau, L.-É. Elevated Mitochondrial Bioenergetics and Axonal Arborization Size Are Key Contributors to the Vulnerability of Dopamine Neurons. Current Biology 2015; 25: 2349-2360.

Paxinos, G., Franklin, K.B.J., 2001. The Mouse Brain in Stereotaxic Coordinates, Vol.

Philippart, F., Destreel, G., Merino-Sepúlveda, P., Henny, P., Engel, D., Seutin, V. Differential Somatic Ca^{2+} Channel Profile in Midbrain Dopaminergic Neurons. The Journal of Neuroscience 2016; 36: 7234-45.

Reeve, A., Simcox, E., Turnbull, D. Ageing and Parkinson's disease: Why is advancing age the biggest risk factor? Ageing Research Reviews 2014; 14: 19-30.

Reyes, S., Fu, Y., Double, K., Thompson, L., Kirik, D., Paxinos, G., et al. GIRK2 expression in dopamine neurons of the substantia nigra and ventral tegmental area. The Journal of Comparative Neurology 2012; 520: 2591-2607.

Rutter, G.A., Denton, R.M. Regulation of NAD+-linked isocitrate dehydrogenase and 2-oxoglutarate dehydrogenase by Ca^{2+} ions within toluene-permeabilized rat heart mitochondria. Interactions with regulation by adenine nucleotides and NADH/NAD+ ratios. The Biochemical journal 1988; 252: 181-189.

Rutter, G.A., Denton, R.M. The binding of Ca^{2+} ions to pig heart NAD+-isocitrate dehydrogenase and the 2-oxoglutarate dehydrogenase complex. The Biochemical journal 1989; 263: 453-462.

Schiemann, J., Schlaudraff, F., Klose, V., Bingmer, M., Seino, S., Magill, P.J., et al. K-ATP channels in dopamine substantia nigra neurons control bursting and novelty-induced exploration. Nat Neurosci 2012; 15: 1272-1280.

Sciacco, M., Bonilla, E., 1996. Cytochemistry and immunocytochemistry of mitochondria in tissue sections. In: Methods in Enzymology. Vol. 264, ed.^eds. Academic Press, pp. 509-521.

Sian, J., Dexter, D.T., Lees, A.J., Daniel, S., Agid, Y., Javoy-Agid, F., et al. Alterations in glutathione levels in Parkinson's disease and other neurodegenerative disorders affecting basal ganglia. Annals of Neurology 1994; 36: 348-355.

Sterky, F.H., Lee, S., Wibom, R., Olson, L., Larsson, N.-G. Impaired mitochondrial transport and Parkin-independent degeneration of respiratory chain-deficient dopamine neurons in vivo. Proceedings of the National Academy of Sciences of the United States of America 2011; 108: 12937-12942.

Sulzer, D. Multiple hit hypotheses for dopamine neuron loss in Parkinson's disease. Trends in Neurosciences 2007; 30: 244-250.

Tucker, K.R., Cavolo, S.L., Levitan, E.S. Elevated mitochondria-coupled NAD(P)H in endoplasmic reticulum of dopamine neurons. Molecular Biology of the Cell 2016; 27: 3214-3220.

Vevea, J.D., Alessi Wolken, D.M., Swayne, T.C., White, A.B., Pon, L.A. Ratiometric biosensors that measure mitochondrial redox state and ATP in living yeast cells. Journal of visualized experiments: JoVE 2013: 10.3791/50633.

Yamada, T., McGeer, P.L., Baimbridge, K.G., McGeer, E.G. Relative sparing in Parkinson's disease of substantia nigra dopamine neurons containing calbindin-D28K. Brain Research 1990; 526: 303-307.

Zhang, L., Yu, L., Yu, C.-A. Generation of Superoxide Anion by Succinate-Cytochrome c Reductase from Bovine Heart Mitochondria. Journal of Biological Chemistry 1998; 273: 33972-33976.

Supplementary Material
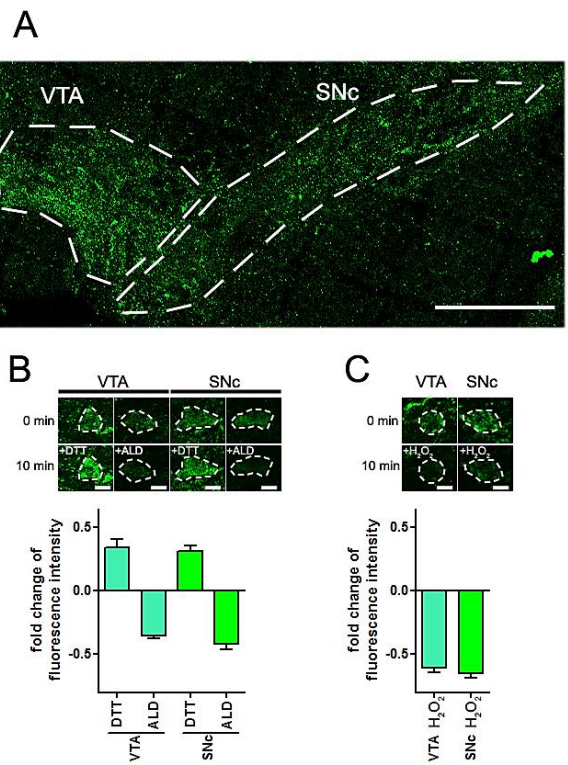
Fig. 3-4-1 Reducing and oxidizing agents alter the mito-roGFP fluorescence intensity during 2PLSM experiments. A) Mito-roGFP expressing DaNs were either selected in the ventral tegmental area (VTA) or in the substantia nigra pars compacta (SNc, dashed lines enframe Da regions, 500 µm scale bar). B) Application of 2 mM DTT for 10 minutes led to a strong increase and 1 mM ALD to a strong decrease of the mito-roGFP fluorescence intensity. C) Application of 10 mM H_2O_2 also induced a strong decrease of the mito-roGFP fluorescence intensity. Data are represented as mean ± SEM (dashed lines delimitate single DaNs, 10 µm scale bars, VTA: turquoise bars, n = 17-18, SNc: green bars, n = 13-19, 3 mice per condition).
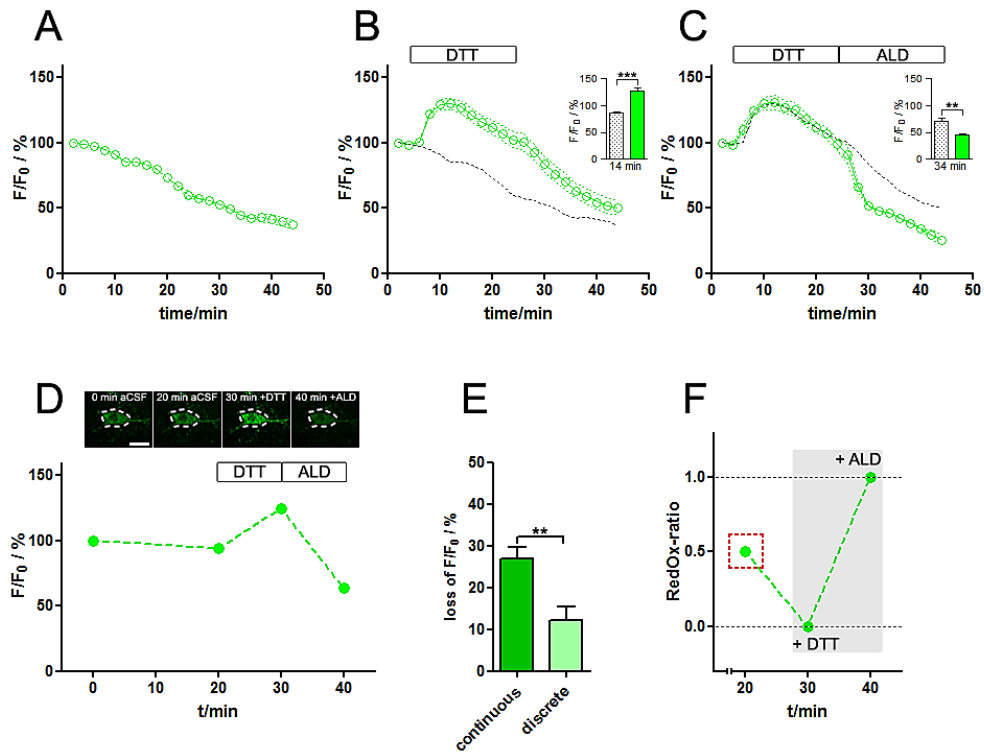
Fig. 3-4-2 RedOx-ratio imaging protocol during 2PLSM experiments. A) There was a constant decrease of the normalized mito-roGFP fluorescence intensity (F/F_0) during continuous 2PLSM recordings. B) 2 mM DTT induced a strong increase of the mito-roGFP fluorescence intensity, reaching a plateau after roughly 10 minutes of application. C) The mito-roGFP signal decreased dramatically, when application of 2 mM DTT was followed by 1 mM ALD. Data are represented as mean ± SEM (green traces represent mean fluorescence intensities, grey dashed lines indicate mean values of prior experiment: grey line in B) = mean of A), grey line in C) = mean of B) n = 13-20, 3 mice per condition). D) Application of 2 mM DTT from 20 to 30 minutes resulted in a strong increase and application of 1 mM ALD from 30 to 40 minutes induced a strong decrease of the mito-roGFP fluorescence intensity in DaNs during discrete recordings (DaNs marked by dashed line, 20 μm scale bar, fluorescence intensities of a single neuron plotted as green dots). E) Continuous recordings (dark green bar, n = 20) with a permanent activated 2PLSM laser displayed a higher loss of mito-roGFP fluorescence intensity than discrete recordings (light green bar, n=21, 3 mice per condition). The loss of fluorescence intensity was calculated after 20 minutes. Data are represented as mean ± SEM; ** $p < 0.01$. F) RedOx-ratio values of the mitochondrial network in Da-Ns (values of the same neuron as in D) plotted as green dots) were calculated using the following formula: RedOx-ratio = $(F_{20\,min} - F_{DTT,\,30\,min})/(F_{ALD,\,40\,min} - F_{DTT,\,30\,min})$. Quantification of RedOx-ratios was performed with values obtained at 20 minutes (marked by dashed red square).
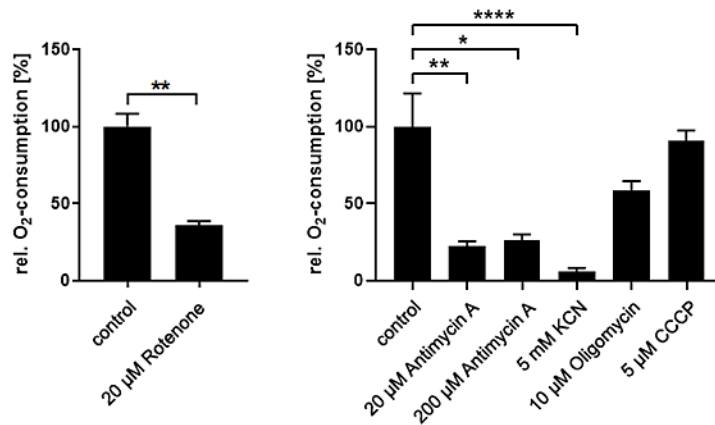
Fig. 3-4-3 Oxygen consumption of midbrain sections. A) Polarographic measurements with fresh brain sections revealed that oxygen consumption of midbrain sections was, as expected, significantly reduced by 20 µM rotenone in comparison to DMSO control experiments (DMSO: striped blue bar, n=3, rotenone: blue bar, n=3). B) Mitochondrial oxygen consumption was, as expected, significantly reduced by 20 µM antimycin A and 5 mM KCN, but not by 10 µM oligomycin or 5 µM CCCP. Higher concentrations of rotenone were not possible due to limited solubility, higher concentrations of antimycin A did not further decrease oxygen consumption (data not shown). Data are represented as mean ± SEM (control: n = 10, antimycin A: n = 8, KCN: n = 10, oligomycin: n = 2, CCCP: n = 2); * p < 0.05, ** p < 0.01, **** p < 0.0001.
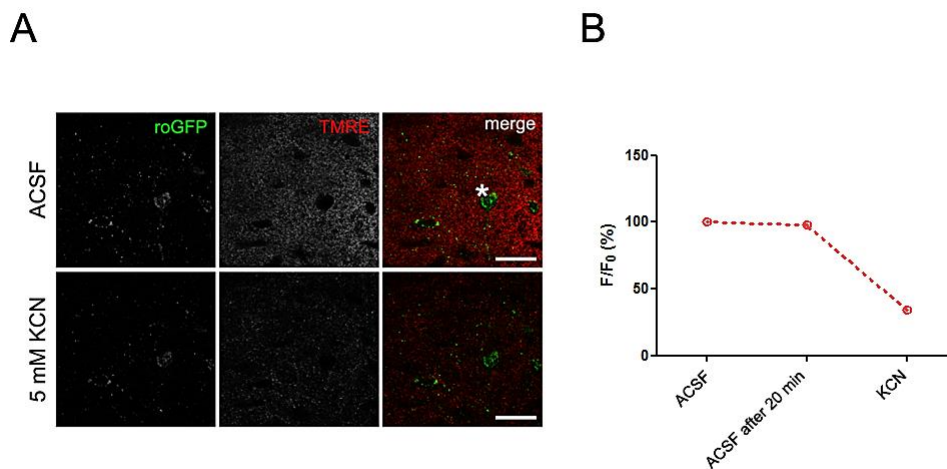
Fig. 3-5-1 TMRE fluorescent signal is similarly responding to KCN. A) KCN reduced the signal intensity of TMRE, another inner membrane potential probe. B) Quantification of KCN-induced TMRE signal reduction is demonstrated in the representative DaN from A (asterisk, 50 µm scale bar).

3.2 The Impact of Mitochondrial Dysfunction on Dopaminergic Neurons in the Olfactory Bulb and Odor Detection

Thomas Paß[1], Marlene Aßfalg[1], Marianna Tolve[3], Sandra Blaess[3], Markus Rothermel[4], Rudolf J. Wiesner[1,2] and Konrad M. Ricke[1]

[1]Center for Physiology and Pathophysiology, Institute of Vegetative Physiology, University of Cologne, Cologne, Germany

[2]Cologne Excellence Cluster on Cellular Stress Responses in Aging-associated Diseases (CECAD), University of Cologne, Cologne, Germany

[3]Neurodevelopmental Genetics, Institute of Reconstructive Neurobiology, University of Bonn School of Medicine & University Hospital Bonn, Bonn, Germany

[4]Institute for Biology II, Dept. Chemosensation, AG Neuromodulation, RWTH Aachen University, Germany

Corresponding authors:
Konrad M. Ricke, PhD
Ottawa Hospital Research Institute
University of Ottawa
501 Smyth Rd.
Ottawa, ON K1H8M5, Canada
kricke@uottawa.ca
or
Thomas Paß, M. Sc.
Institute of Vegetative Physiology,
University of Köln,
Robert-Koch-Str. 39
50931 Köln
Germany
thomas.pass@uk-koeln.de
ORCID-ID: 0000-0002-9915-7360

Abstract

Understanding non-motor symptoms of Parkinson's disease is important in order to unravel the underlying molecular mechanisms of the disease. Olfactory dysfunction is an early stage, non-motor symptom which occurs in 95% of Parkinson's disease patients. Mitochondrial dysfunction is a key feature in Parkinson's disease and importantly contributes to the selective loss of dopaminergic neurons the *substantia nigra pars compacta*. The olfactory bulb, the first olfactory processing station, also contains dopaminergic neurons, which modulate odor information and thereby enable odor detection as well as odor discrimination. MitoPark mice are a genetic model for Parkinson's disease with severe mitochondrial dysfunction, reproducing the differential vulnerability of dopaminergic neurons in the midbrain. These animals were used to investigate the impact of mitochondrial dysfunction on olfactory-related behavior and olfactory bulb dopaminergic neuron survival. Odor detection was severely impaired in MitoPark mice. Interestingly, only the small anaxonic dopaminergic subpopulation, which is continuously replenished by neurogenesis, was moderately reduced in number, much less compared to dopaminergic neurons in the midbrain. As a potential compensatory response, an enhanced mobilization of progenitor cells was found in the subventricular zone. These results reveal a high robustness of dopaminergic neurons located in the olfactory bulb towards mitochondrial impairment, in striking contrast to their midbrain counterparts.

Introduction

Parkinson's disease (PD) is the most common movement disorder affecting 1% of the population above 60 years [1] characterized by the initial loss of midbrain dopaminergic neurons (DaNs) in the substantia nigra pars compacta (SNc). The depletion of striatal dopamine leads to progressive and irreversible motor impairment [2]. Besides the cardinal symptoms of PD, non-motor dysfunctions including depression, sleep disturbance and hyposmia have been described. Olfactory dysfunction is found in more than 95% of PD patients and can precede motor symptoms by up to ten years [3–5].

The olfactory bulb (OB) is the first station of sensory processing in the olfactory system. Besides the midbrain, DaNs are also present in the OB and make up 5% of the neuronal population [6]. They function as interneurons and are necessary for odor discrimination rather than for odor detection [7, 8]. They are primarily located in the glomerular layer (GL), where they modulate the activity of both olfactory sensory fibers [9, 10] and mitral cells by D2 receptor-mediated inhibition [11, 12] as well as via contacts with external tufted cells [13]. Despite of multiple as well as contradictory statements regarding their categorization, OB DaNs can be clearly divided into small (5 10 µm), anaxonic (SCs) and large (10 15 µm diameter), axonic cells (LACs) [14]. In contrast to LACs, SCs can be continuously generated throughout life by neurogenesis, in mice as well as in humans [15–19]. Progenitor cells are formed in the dorsolateral region of the subventricular zone (SVZ) [20] and are characterized by the expression of the transcription factor PAX6, required for development into the DaN phenotype [21–23]. The majority of progenitor cells in the OB differentiate into interneurons in the granule cell layer, while only 5% of the 20,000-30,000 new-born cells generated daily migrate to the GL [24, 25].

In PD, there are contradictory results according to the fate of DaNs in the OB. Luquin and colleagues reported elevated numbers of periglomerular DaNs, potentially displaying a compensatory mechanism induced by the early degeneration of other neurotransmitter systems and resulting in the olfactory dysfunction of patients [26]. In contrast, no difference in OB DaN numbers were found between PD patients and healthy individuals, implying that PD-related hyposmia is not due to alterations in the quantity of OB DaNs [27, 28].

Mitochondrial dysfunction is a central feature of PD, both in the common idiopathic as well as in the rare familiar forms caused by mutations, e.g. in the Parkin, Pink1, LRRK2 or DJ 1 genes. During normal aging, SNc DaNs accumulate high loads of deletions in mitochondrial DNA (mtDNA), present in thousands of copies in neurons. Interestingly, this is accompanied by an upregulation of mtDNA copy numbers in healthy humans, while this compensatory mechanism is disrupted in PD patients [29]. This indicates that a defective mtDNA maintenance system

and subsequent severe mitochondrial impairment is an important factor for the degeneration of SNc DaNs in PD.

The mitochondrial transcription factor A (TFAM) is crucial for mtDNA transcription and maintenance [30, 31]. Depletion of TFAM consequently leads to the loss of mtDNA encoded transcripts followed by a respiratory chain defect. MitoPark mice are lacking TFAM exclusively in DaNs, which culminates in progressive neuronal death and corresponding motor impairment starting from 14 weeks of age [32, 33]. The progression of PD is recapitulated in terms of both anatomical and behavioral malfunctions. However, the impact of mitochondrial dysfunction on OB DaNs has not been investigated so far. Therefore, olfactory-related behavior was explored in MitoPark mice. Furthermore, mice were used to study the impact of mitochondrial defects on OB DaN survival as well as adult neurogenesis.

Materials and Methods

Experimental model

All experiments were conducted in agreement with European and German guidelines and approved by local authorities (LANUV NRW; 81-02.04.2018-A210) (for breeding details, see supplementary methods). Experiments were carried out with male or female mice of the strain C57/BL6N. For the generation of MitoPark mice, DAT cre mice (Cre-gene inserted upstream of the translation start codon in exon 2 of the DAT gene) and animals with a loxP-flanked Tfam allele were crossed as described in detail previously [32]. MitoPark mice (genotype TfamloxP/loxP, +/DAT cre) show homozygous disruption of Tfam in dopaminergic neurons. TfamloxP/loxP and Dat-cre mice were provided by Nils-Göran Larsson (Max-Planck-Institute for Biology of Ageing, Köln, Germany). TfamloxP/WT or TfamloxP/loxP mice were used as controls.

COX-SDH staining

Visualization of Cytochrome c Oxidase (COX) deficiency was performed by COX-SDH enzymatic activity staining [34]. COX is a respiratory chain (RC) complex which is partially encoded by mtDNA, while succinate dehydrogenase (SDH), another respiratory chain enzyme, is entirely encoded by nuclear DNA. Impaired integrity of mtDNA results in COX-deficiency, but sustained SDH-activity. Cells with decreased COX-activity will stain blue, while cells with normal COX-activity will appear brown (for details, see supplementary methods). Quantification of COX-deficient cells was performed at Bregma +4.30 mm and +3.00 mm. Four images (33 x 50 µm) were taken from dorsal, ventral and lateral OB regions per slice each. Number of COX-deficient cells was defined per slice.

Immunohistochemistry

Brain sections were stained for tyrosine hydroxylase to visualize DaNs and their projections (for details, see supplementary methods).

Soma size quantification of OB DaN subpopulations: Soma sizes of DaNs stained for tyrosine hydroxylase were analyzed by using FIJI-software (https://imagej.net/Fiji/Downloads). Cells were selected and automatically measured by the Wand-Auto-Tool based on the black-white-contrast of the cells compared to background. The outline of the cell soma was detected and the area within the shape was automatically calculated. Two subpopulations of DaNs with distinct morphological characteristics have been described [35]. DaN somata in the GL were differentiated into areas of 20-80 µm2 for SCs and 80-180 µm2 for LACs. Two consecutive brain sections per mouse were analyzed at Bregma +4.3, +3.75 and +3.21. Images were taken from both dorsal and ventral OB regions (for details, see supplementary methods).

Analysis of immunohistochemical stainings

Automated bright-field microscopy was done with a slidescanner (SCN400, Leica) equipped with a 40x objective. High resolution images from the OB and striatum were generated by the Leica SlidePath Gateway and the Microsoft Image Composite Editor software. TH-positive striatal fiber density was determined by optical density (OD) analysis using FIJI-software (area fraction, https://imagej.net/Fiji/Downloads) with two consecutive sections per mouse at Bregma +0.74 mm. Non-specific background signal of the corpus callosum was subtracted from the striatal OD values. Fluorescence images were obtained by utilizing an inverse confocal microscope (TCS SP8 gSTED, Leica) with a 40x oil objective and the Leica Application Suite (LAS) 3 software. OB fluorescence microscopy was performed at Bregma +4.30 mm, +3.30 mm and +2.30 mm. TH- as well as PAX6-expressing cells were detected independently before merging the channels and quantifying the number of colocalizing cells, respectively. PAX6 expression in the SVZ was performed at Bregma +1.10 mm, +0.70 mm and +0.30 mm. Sections immunostained for EYFP/TH were imaged using with an inverted Zeiss AxioObserver Z1 microscope equipped with an ApoTome. Fluorescence images were acquired with Zeiss AxioCam MRm 1388 x 1040 pixels (Carl Zeiss). At 10X (EC PlnN 10x/0.3, Carl Zeiss) tile images were acquired with conventional epifluorescence. At 20X (EC PlnN 20x/0.5, Carl Zeiss) tile images were acquired using the ApoTome function.

Odor discrimination test

Odor discrimination ability was examined to analyze DaN functionality in the OB. In addition, the odor discrimination test provides an opportunity to investigate odor detection rather independently from motor activity (for details of the test, see supplementary methods).

Statistics

Statistical analysis was done with GraphPad Prism 4 for Windows. Quantified data in the figures and in the text is presented as mean + SEM. Relative data is shown as percentage of control experiments. Values of sample size (n) refer to mouse numbers. Unpaired *t* tests, one-way or two-way ANOVA with *post hoc* comparisons (Bonferroni *post hoc* test) were used to determine differences between groups. A significance level of 0.05 was accepted for all statistical tests. Asterisks mark P-values of 0.05 (*), 0.01 (**), 0.001 (***) or 0.0001 (****).

Results

Time course of TFAM loss in different DaN populations

To determine the onset of Cre-mediated recombination, and thus TFAM knockout, in DaNs in the DatCre mouse line, we crossed DatCre/+ mice with a reporter mouse line expressing enhanced yellow fluorescent protein (EYFP) (Rosa26loxP-stop-loxP-EYFP) [36]. In the midbrain, YFP expression starts in laterally located tyrosine hydroxylase-positive (TH-positive) DaNs at E13.5 and spreads to medial DaN populations by E15.5 (Fig. 3-6) [37]. In the OB, we could not detect any YFP-expression in TH-positive DaNs at E15.5 (Fig. 3-6) or P0 (not shown), although some TH-positive neurons were present. Only at 4 weeks of age, TH-positive DaNs expressed YFP, indicating that recombination in OB DaNs only occurs postnatally in DatCre mice. Consistent with this, RNA in situ hybridization data from the Allen Brain Atlas show that Dat is not expressed in the OB at P4 [38] while by P14, weak expression of DAT is detected in the OB and this is maintained into adulthood. These data suggest that inactivation of TFAM in the MitoPark model occurs at least two weeks later in OB DaNs than in midbrain DaNs.

MitoPark mice show dopaminergic nigro-striatal degeneration

TFAM depletion causes progressive motor impairment evoked by the loss of midbrain SNc DaNs and corresponding striatal fibres in the caudate putamen (CPu) starting from 14 weeks of age [32, 33]. Since Tfam inactivation in OB DaNs occurs later, 20- and 30-week-old MitoPark mice were used in this study. The severe degeneration of the nigro-striatal and the mesolimbic pathway was confirmed in 30-week-old MitoPark mice. In particular, the reduction of TH-positive cells in the SNc and ventral tegmental area (VTA) (Fig. 3-7A-B) as well as TH staining in the corresponding striatal projection areas is dramatic (Fig. 3-7C-D). In addition, the olfactory
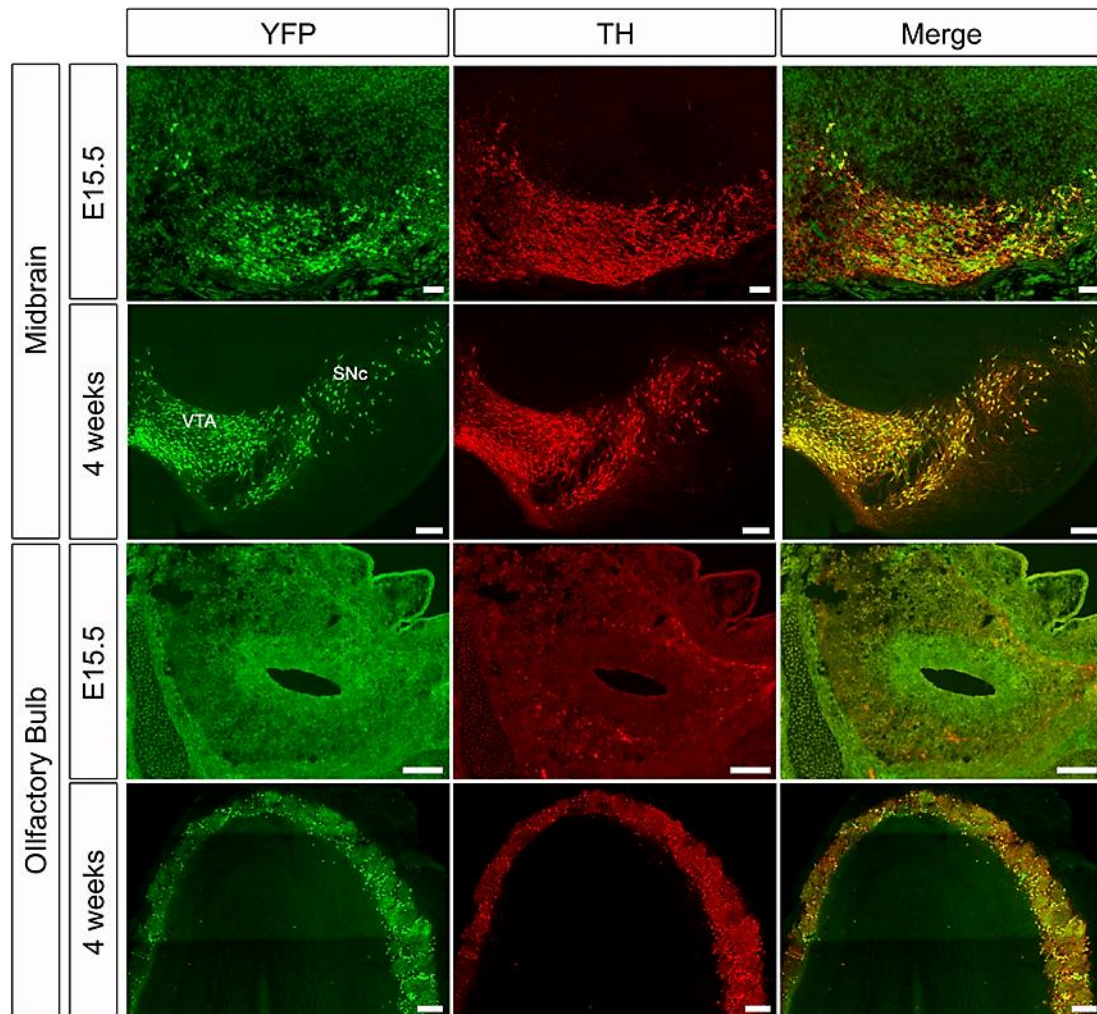
Fig. 3-6 Colocalisation of TH and YFP is delayed in OB DaNs. In the midbrain, TH-positive cells are co-expressing YFP at both E15.5 and 4 weeks of age (yellow in merged panel). In contrast, colocalisation of TH and YFP in the OB becomes apparent only at the age of 4 weeks. Scale bars: 100 µm.

tubercle (OT), located in the ventral striatum and innervated by VTA DaNs, shows lowered TH-TH-staining.

Respiratory chain defects in OB DaNs of MitoPark mice

Loss of TFAM is accompanied by loss of mtDNA encoded transcripts [32]. Consequently, respiratory chain defects become apparent in midbrain DaNs of 12-week-old MitoPark mice even before the onset of neurodegeneration [39]. In order to verify mitochondrial impairment in OB DaNs, a histochemical staining procedure for COX/SDH activity was performed (Fig. 3-7E). Sporadically, COX-deficient cells were found in the GL of the OB in MitoPark mice, however, no COX-deficient cells were observed in any of the control animals. These data reveal that COX-deficiency also occurs in OB DaNs of MitoPark mice after inactivating the Tfam gene driven by Dat-Cre recombination.
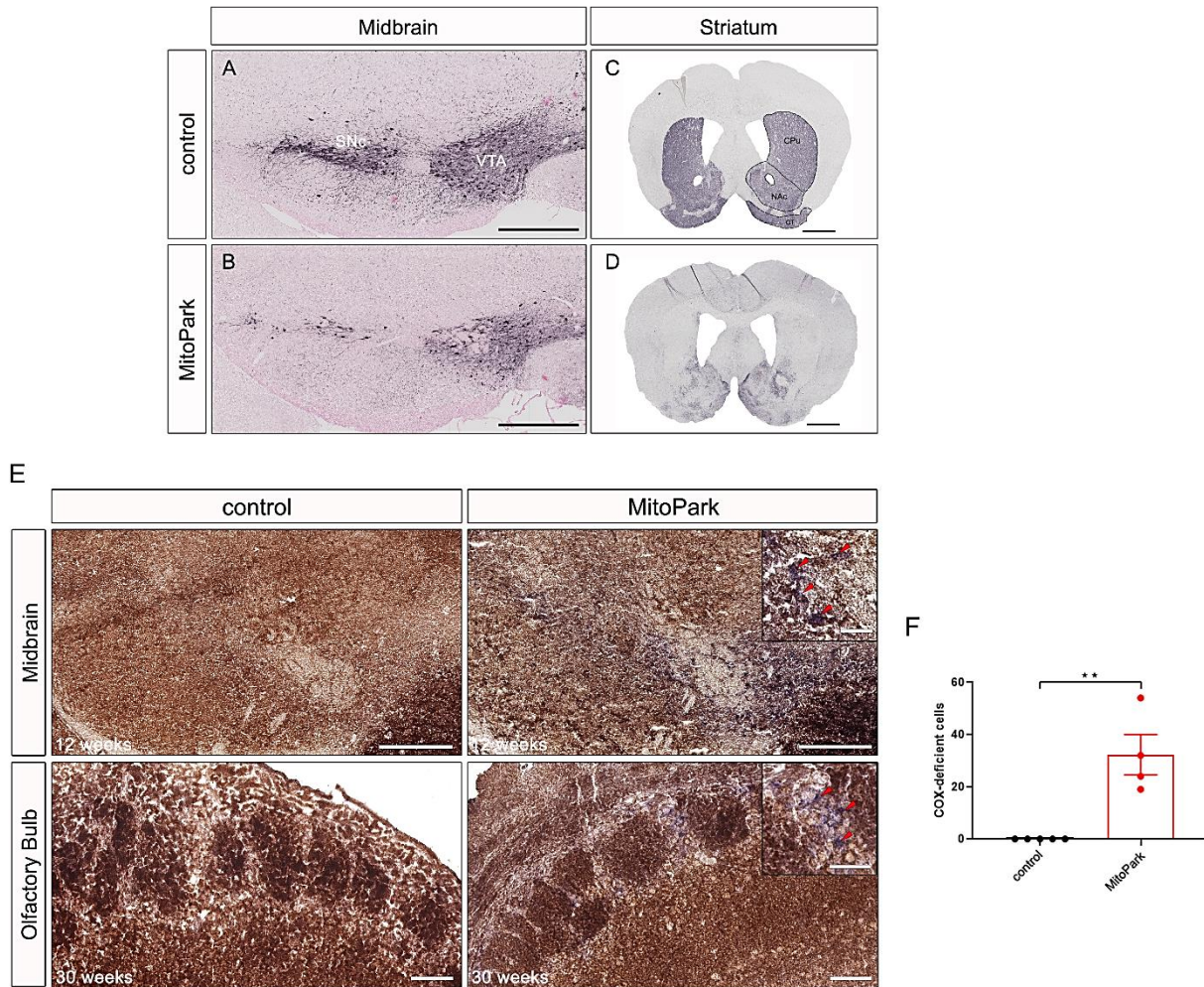
Fig. 3-7 Degeneration of midbrain DaNs and striatal projections in 30-week-old MitoPark mice. A, B) Tyrosine hydroxylase (TH) immunohistochemistry in the midbrain of MitoPark and age-matched control mice showing severe neuronal loss in the ventral tegmental area (VTA) and the substantia nigra pars compacta (SNc). C, D) Striatal staining presenting the reduction in TH-positive projection area in the nucleus accumbens (NAc), caudate putamen (CPu) as well as the olfactory tubercle (OT). Three control and four MitoPark mice were analyzed. E) COX-deficient DaNs in the OB of 30-week-old MitoPark mice. Neurons with reduced activity of cytochrome c oxidase (COX; brown) were unmasked by COX-SDH double staining (blue). In the midbrain, first COX-deficient cells become apparent at 12 weeks of age. Conversely, COX-deficient cells were found in the OB only after 30 weeks. F) COX-deficient cells in the OB of 30-week-old MitoPark mice. Quantitative analysis revealed a significantly higher number of blue cells in the OB of MitoPark mice when compared to control animals. Control mice: black bar n=5; MitoPark mice: red bar n=4. Scale bars: 500 μm (A, B), 1 mm (C, D), midbrain 500 μm, enlarged 50 μm; olfactory bulb 100 μm, enlarged 50 μm (E).

MitoPark mice exhibit impaired odor detection

To assess OB functionality in MitoPark mice, the olfactory behavior of control and Mito Park mice was investigated at different stages. In the buried pellet test, the latency to locate a food pellet, either hidden underneath the bedding or visible on the surface, respectively, was tested (for details of this widely used test, see supplementary methods). There was no significant difference in the latency time to detect the buried food pellet between MitoPark and control mice in any of the investigated ages (Fig. 3-8-1A). However, at the age of 30 weeks, MitoPark mice took significantly longer to find the visible pellet (control 15.14 ± 5.21 s, MitoPark 134.65 ±

48.14 s, two-way ANOVA, P<0.05), indicating that the severe motor impairment of 30-week-old MitoPark mice may influence the result rather than showing exclusively an affected ability for odor detection.

In order to analyze odor discrimination as well as odor detection more independent from motor performance, the odor discrimination test was carried out in 20- and 30-week-old MitoPark and control mice. Both non-social and social odors were presented consecutively three times each. Control animals revealed typical olfactory memory and discrimination. They presented habituation behavior to identical odors characterized by decreasing sniffing times as well as dishabituation to new odors with increasing sniffing times (Fig. 3-8A-D). For MitoPark mice, the time spent at the odors was dramatically reduced and they were not able to detect any of the presented odors. The time spent sniffing at the odor was significantly decreased in 20-week-old MitoPark mice for all odor types (Fig. 3-8C-D, water-1: two-way ANOVA, P<0.001, almond-1: P<0.01, banana-1: P<0.01, social 1-1: P<0.001). Furthermore, 30-week-old MitoPark mice spent no time at any of the presented odors (Fig. 3-8C-D). These results indicate that odor detection is fundamentally impaired in MitoPark mice.
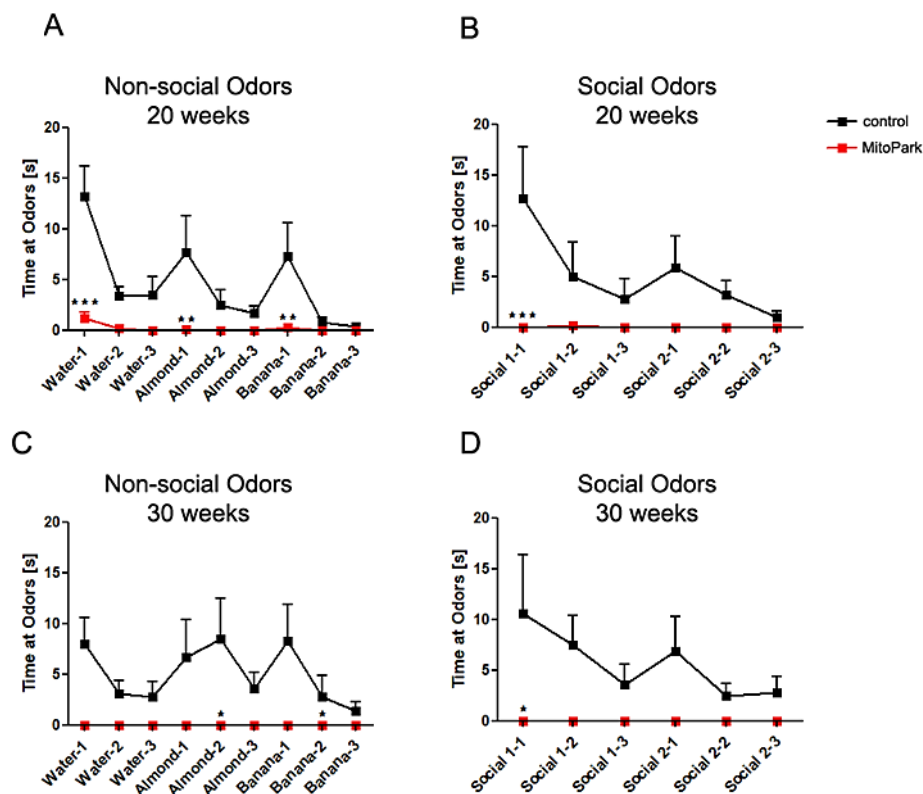
Fig. 3-8 Impaired odor detection in MitoPark mice. A-D) Time spent sniffing at the odor by 20 (A-B) and 30-week-old (C-D) MitoPark (red squares) and control mice (black squares). 20 weeks: (9-10 mice); 30 weeks: (5-6 mice).

Reduction of dopaminergic SCs in the OB of MitoPark mice

Soma size-based quantification was performed to examine the number of DaNs in the two main subpopulations (Fig. 3-9A-B). The number of SCs was higher compared to LACs in this area, in line with previously reported observations in wt mice [40]. The number of LACs and SCs did not differ between both groups at the age of 20 weeks, however, comparison of control and MitoPark mice showed a decreased number of SCs in 30-week old MitoPark (Fig. 3-9C, control: 351.25 ± 26.06, MitoPark: 228.67 ± 22.50, unpaired t-test, P<0.01). These results suggest that TFAM depletion in OB DaNs preferentially affects SC survival and that this may lead to the observed odor detection impairment. Alternatively, the continuous generation of progenitor cells could be affected and be the reason for the decreased SC number in MitoPark mice.
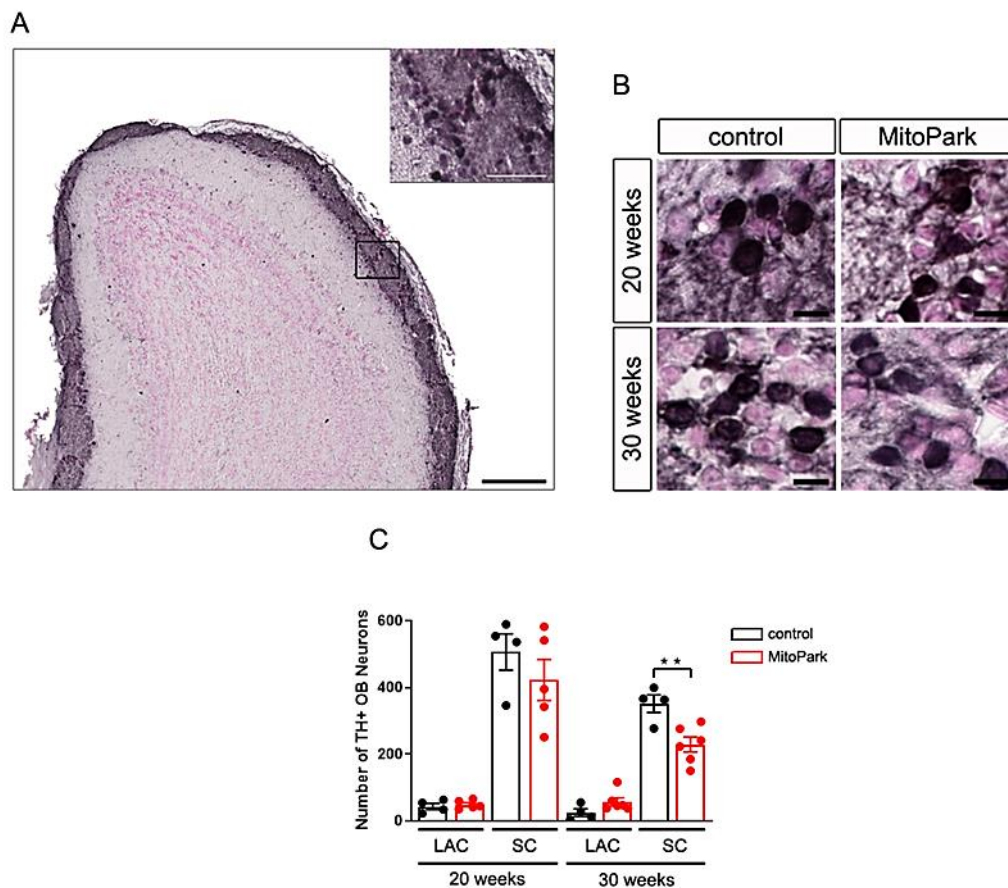
Fig. 3-9 Reduced proportion of SCs in the OB of MitoPark mice. A) Tyrosine hydroxylase (TH) immunohistochemistry of the OB and the enlarged glomerular layer. B) TH staining in MitoPark and age-matched control mice. C) Quantification of DaN subpopulations showed an increase in the proportion of LACs and a reduction in SCs in the OB of 30-week-old MitoPark mice. The fraction of SCs was higher compared to LACs (20 weeks, control 92.14 ± 1.32 % SCs vs. 7.86 ± 1.32 % LACs, one-way ANOVA, P<0.0001; MitoPark 89.69 ± 2.92 SCs vs. 10.31 ± 2.92 % LACs, P<0.0001; 30 weeks, control 93.92 ± 2.59 % SCs vs. 6.08 ± 2.59 % LACs, P<0.0001; MitoPark 80.37 ± 2.43 % SCs vs. 19.63 ± 2.43 % LACs, P<0.0001). Values are illustrated as percentage from total DaN number. Control mice: black bars, 20 weeks n=4, 30 weeks n=4; MitoPark mice: red bars, 20 weeks n=5, 30 weeks n=6. Scale bars: 200 µm and 50 µm (A), 10 µm (B).

Number of PAX6+ DaNs is not altered in the OB of MitoPark mice

In contrast to LACs, SCs can be newly generated even postnatally. To investigate if the reduced number of SCs in MitoPark mice is caused by an alteration in progenitor cell differentiation, PAX6 immunohistochemistry was performed in the OB (Fig. 3-10A). The transcription factor PAX6 is postnatally expressed in progenitor cells of the subventricular zone to mediate their dopaminergic fate [21–23, 41–43] and remains expressed in DaN progenitors after arriving in the OB [44–46]. In addition, PAX6 has recently been used by Höglinger and colleagues as a marker for neurogenic progenitors within the rostral migratory stream, which gives rise to DaNs in the OB [47]. In contrast, PAX6 expression in cells already established during development decreased over time with no colocalization in neurons [48]. This makes PAX6 an ideal marker for adult-born DaNs in the mouse OB. The amount of TH-positive neurons also expressing PAX6 did not differ between MitoPark and control mice (Fig. 3-10B, 20 weeks: control 65.66 ± 1.79 %, MitoPark 66.55 ± 3.76 %; 30 weeks; control 75.30 ± 1.17 %, MitoPark 72.54 ± 1.59 %, one-way ANOVA, n.s.). These data reveal that DaN progenitor cell differentiation in the OB is not impaired in MitoPark mice.

MitoPark mice show increased progenitor cell mobilization in the SVZ

To further assess whether OB progenitor cell proliferation is affected earlier in the lineage of these neurons, PAX6 expression in the dorsal SVZ was studied (Fig. 3-10C). At 20 weeks of age, there was no difference between MitoPark and control animals (Fig. 3-10D, control 37.69 ± 10.00 %, MitoPark 38.48 ± 3.71 %). However, 30-week-old MitoPark mice revealed a significantly increased number of PAX6-expressing cells when compared to 20-week-old MitoPark mice and age-matched control animals (MitoPark: 20 weeks 38.48 ± 3.71 %, 30 weeks 80.80 ± 16.63 %, one-way ANOVA, P<0.05; 30 weeks: control 24.02 ± 3.65 %, one-way ANOVA, P<0.01). These results indicate an enhanced mobilization of progenitor cells in the dorsal SVZ, probably induced by the decline of SCs in the OB.

Discussion

In contrast to the midbrain, OB DaNs reveal no Dat-Cre expression during embryonic development (Fig. 3-6). Moreover, RNA in situ hybridization data [38] suggest that the Dat gene only starts to be expressed in OB DaNs in the second postnatal week. Subsequently, cells with respiratory chain deficits become apparent in OB DaNs only in 30-week-old MitoPark mice (Fig. 3-7E), i.e. 28 weeks after TFAM inactivation at around P14, whereas midbrain DaNs uniformly present COX deficiency already after 12 weeks of age [39], i.e. 13 weeks after TFAM inactivation at around E15.5. This reveals a surprisingly different response of different DaN populations to inactivation of mitochondrial gene expression.
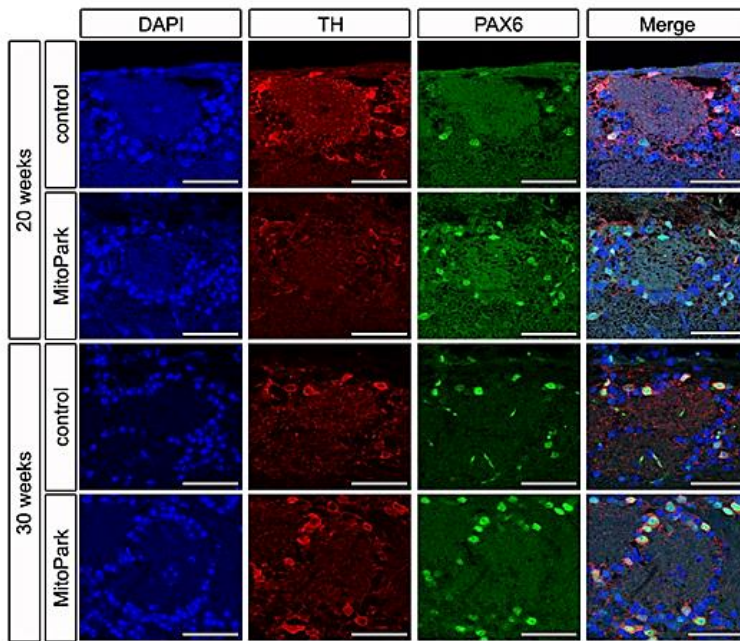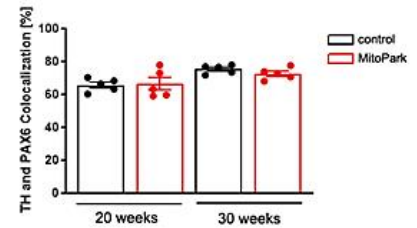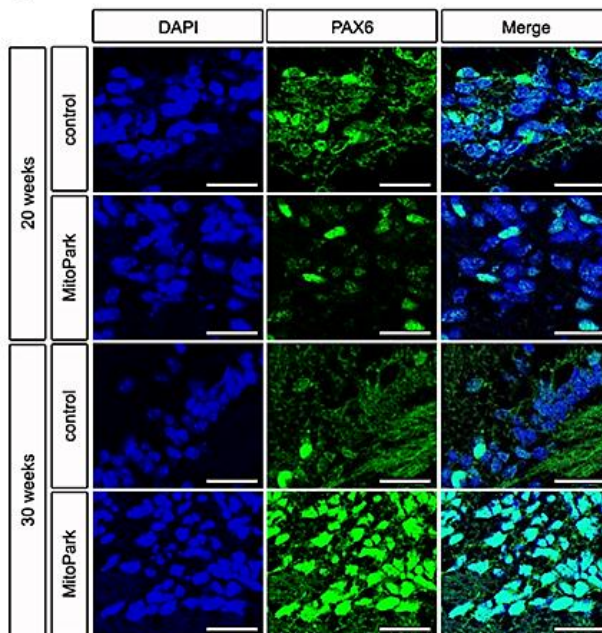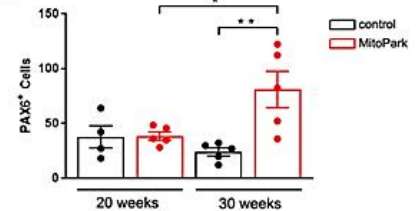
Fig. 3-10 No change in the amount of PAX6-expressing DaNs in the OB but in the amount of progenitor cells in the SVZ of MitoPark mice. A) Merged tyrosine hydroxylase and PAX6 immunofluorescent staining presents newborn OB DaNs in 20- and 30-week-old MitoPark and age-matched control mice. B) Quantitative analysis of PAX6-expressing DaN number revealed no difference between MitoPark and control animals. Control mice: black bars, 20 weeks n=5, 30 weeks n=5; MitoPark mice: red bars, 20 weeks n=5, 30 weeks n=5. Increase of PAX6-expressing progenitor cells in the SVZ of MitoPark mice. C) Combined nuclear (DAPI) and immunofluorescent PAX6 staining depicts the distribution of progenitor cells in MitoPark and age-matched control mice in the SVZ. D) Quantitative analysis showed an enhanced number of progenitor cells in 30-week-old MitoPark mice. Control mice: black bars, 20 weeks n=4, 30 weeks n=5; MitoPark mice: red bars, 20 weeks n=5, 30 weeks n=5. Scale bars: 50 μm (A), 25 μm (B).

To inspect MitoPark mice for OB functionality, olfactory behavior was investigated. The widely used buried pellet test did not reveal olfactory dysfunction in MitoPark mice (Fig. 3-8-1A-B), but this may rather be a consequence of the motor impairment at 30 weeks of age. It further has to be noted, that the outcome of the buried food pellet test does not exclusively depend on the detection of odors. As a consequence of the bradykinesia, MitoPark mice have to be supplied with moistened food pellets on the surface of the bedding from an age of 15 weeks onward. MitoPark mice are thereby trained to seek for food at the surface by housing conditions. Furthermore, the animals were not food deprived, since this would be ethically not permitted with MitoPark mice. In fact, these animals could even suffer from an enhanced desire for food, since they start losing weight at 20 weeks of age [49]. Thereby, the buried food pellet test might not be an appropriate test to analyze odor detection impairment in MitoPark mice.

It has further been shown that OB DaNs are involved in olfactory discrimination [7, 50, 51]. In order to analyze discrimination as wells as detection more independently from motor performance and food seeking, the odor discrimination test was performed (Fig. 3-8A D). Already 20-week-old MitoPark mice show sharply reduced times spent at all presented odors. After 30 weeks of age, no sniffing time is observed at all, indicating a severe impairment in fundamental odor detection. Noteworthy, the ability of MitoPark mice to move was still sufficient to localize the presented odors (video sequences, not shown).

In order to investigate the number of DaNs in the GL, soma size based quantification was performed. Intriguingly, only a reduced number of SCs is found in 30-week-old MitoPark mice, whereas LACs were unaffected (Fig. 3-9C). In the midbrain of MitoPark mice, both SNc and VTA DaNs present mitochondrial dysfunction at 12 weeks of age, followed by progressive neurodegeneration, with SNc neurons being more affected [32]. This selective vulnerability is one hallmark for PD in patients [52] and raises the question which cell type-specific factors render SNc DaNs vulnerable to mitochondrial dysfunction. Much research has been conducted characterizing neuroanatomical as well as electrophysiological properties of midbrain and OB DaNs. On the one hand, complex axonal morphology might play an essential role regarding the time course of degeneration. SNc DaNs show an extremely large arborization with an estimated number of 100.000 – 250.000 synapses per neuron [53], compared to both VTA and OB DaNs, with the SCs even being anaxonic [14]. The extended branching results in an extreme bioenergetic demand, leaving SNc DaNs working on a tight energy budget [54], especially when facing additional stressors, such as mitochondrial dysfunction. On the other hand, all three DaN populations are characterized as autonomous pacemakers [40, 55, 56]. The pacemaking machinery of VTA and OB DaNs is mainly driven by a persistent sodium current [40, 57, 58]. Conversely, SNc pacemaker activity is associated with Ca2+ influx through plasma membrane $Ca_v1.3$ channels, postulated to cause oxidant stress in the mitochondrial compartment [59, 60]. Combined with low intrinsic calcium buffering capacities, mitochondrial

dysfunction leads to an oxidized RedOx-system and hyperpolarized membrane potential in mitochondria of SNc DaNs, which thereby causes neuron death [39].

SCs and LACs differ in various aspects, including morphology, functionality and neurogenic potential. SCs are anaxonic and thereby generate somatic action potentials with a low firing rate. In contrast, the wide-branching LACs do have an axon and a high firing frequency [19]. SCs are typically type 1 periglomerular cells [61–65]. They receive olfactory nerve and dendrodendritic synapses, which in turn lead to the inhibition of mitral cells [66], the principal output neurons of the OB. A reduced number or functional changes of SCs in MitoPark mice could thereby cause temporal shifts in mitral cell activity, previously shown to impair olfactory-related behaviors [67].

In addition, anaxonic SCs are even continuously formed via adult neurogenesis, whereas LACs are exclusively established during embryonic development [15–19]. Consequently, affected neuronal replenishment of SCs could be the explanation for the reduced number of SCs. OB progenitor cells are created in the SVZ of the lateral ventricles and tangentially migrate along the rostral migratory stream, before they enter the OB [68]. Those progenitor cells are characterized by the expression of PAX6. Interestingly, MitoPark mice reveal an increased mobilization of PAX6-expressing cells in the SVZ at 30 weeks of age (Fig. 3-10C-D), indicating a potential compensatory upregulation of progenitor cells. However, the amount of PAX6 expressing DaNs in the OB is stable (Fig. 3-10A-B). This gives reason to suppose that either the death rate of SCs is so high that the number of replenished neurons in the OB cannot compensate for this, or that the upregulation of progenitor cells in the SVZ is not a direct cause of the reduced SC number. In addition, even though the time line of RMS migration is very well established, there is no evidence to when DAT expression is initiated in OB progenitor cells. Potentially, new but not fully matured neurons are more vulnerable to the TFAM knockout due to early DAT expression and die even before reaching the OB.

Besides the reduced number of SCs it is likely that the severe olfactory dysfunction is caused by other factors. So far no direct link between the midbrain and the OB could be demonstrated [69, 70]. However, a recent study discovered the existence of axonal projections from SNc DaNs to the OB and the ablation of this connectivity resulted in impaired olfactory perception [71]. At 30 weeks of age, MitoPark mice reveal a severe degeneration of SNc DaNs (Fig. 3-7B). Therefore, the absence of these nigro-bulbar connections could contribute to the olfactory dysfunction in MitoPark mice. More precisely, the loss of SNc-OB projections might lead to Ca2+-induced hyperactivity of mitral cells caused by the missing dopaminergic inhibition, as recently demonstrated in a 6 OHDA induced PD mouse model [72]. However, Zhang et al. did not show any data concerning the dopaminergic projection area in the striatum after partial depletion of SNc DaNs, though striatal denervation is likewise affecting olfactory behavior [73].

Since MitoPark mice reveal the degeneration of SNc DaNs as well as corresponding striatal fibres, we postulate that, besides the decreased number of SCs, olfactory dysfunction might be caused by the degeneration of the complete nigro-striatal system. Moreover, the loss of the nigro-striatal system might be the reason for the increased mobilization of progenitor cells in the SVZ observed in 30-week-old MitoPark mice, as shown likewise after 6-OHDA lesioning [74]. Noteworthy, DaNs from the VTA innervate the SVZ and are involved in proliferation of progenitor cells [75]. Increased progenitor cell mobilization may thereby also have its reason in a compensatory upregulation due to the loss of VTA DaNs. More importantly, the SNc, the VTA as well as the striatum further possess dopaminergic projections to higher olfactory brain regions, such as the piriform cortex and the olfactory tubercle [76–78]. Therefore, a prospective disconnection between the nigro-striatal system as well as the VTA and higher olfactory centers might importantly contribute to the impaired olfactory-related behavior in MitoPark mice.

Apart from the dopaminergic system, serotonin could also play a role in the olfactory dysfunction of MitoPark mice. Serotonergic neurons from the raphe nuclei are innervating all layers of the OB [79–81] and deafferentiation of corresponding fibres causes anosmia and OB atrophy [82]. Furthermore, mice that are deficient for PTEN-induced kinase 1 (PINK1), mutations of which make up 1-2% of the familiar forms of PD, possess a decreased serotonergic innervation in the GL, leading to an impaired olfactory behavior [83]. Besides the SNc, the raphe nuclei are also affected in PD patients, with a loss of serotonergic neurons and its projections [84, 85]. However, altered serotonin transporter activities in PD patients failed to correlate with olfactory dysfunction [86], leaving the role of serotonergic neurons in PD-related anosmia unclear.

Our data provide new insights into olfactory dysfunction and adaptations of adult neurogenesis in response to genetic depletion of the dopaminergic system. Furthermore, we show that dopaminergic neurons located in the olfactory bulb reveal a high robustness towards mitochondrial impairment, in striking contrast to their midbrain counterparts.

Acknowledgements

Financial Disclosures

References

1.   Tysnes O-B, Storstein A. Epidemiology of Parkinson's disease. J Neur Transm. 2017; 124:901–5. doi:10.1007/s00702-017-1686-y.

2.   Michel PP, Hirsch EC, Hunot S. Understanding Dopaminergic Cell Death Pathways in Parkinson Disease. Neuron. 2016; 90:675–91. doi: 10.1016/j.neuron.2016.03.038.

3.   Haehner A, Hummel T, Reichmann H. Olfactory dysfunction as a diagnostic marker for Parkinson's disease. Expert Rev Neurother. 2009; 9:1773–9. doi:10.1586/ern.09.115.

4.   Doty RL. Olfaction in Parkinson's disease and related disorders. Neurobiol Dis. 2012; 46:527–52. doi: 10.1016/j.nbd.2011.10.026.

5.   Klingelhoefer L, Reichmann H. Pathogenesis of Parkinson disease--the gut-brain axis and environmental factors. Nature Rev Neurol. 2015; 11:625–36. doi:10.1038/nrneurol.2015.197.

6.   Cave JW, Baker H. Dopamine systems in the forebrain. Adv Exp Med Biol. 2009:15–35.

7.   Tillerson JL, Caudle WM, Parent JM, Gong C, Schallert T, Miller GW. Olfactory discrimination deficits in mice lacking the dopamine transporter or the D2 dopamine receptor. Behav Brain Res. 2006; 172:97–105. doi: 10.1016/j.bbr.2006.04.025.

8.   Escanilla O, Yuhas C, Marzan D, Linster C. Dopaminergic modulation of olfactory bulb processing affects odor discrimination learning in rats. Behav Neurosci. 2009; 123:828–33. doi:10.1037/a0015855.

9.   Berkowicz DA, Trombley PQ. Dopaminergic modulation at the olfactory nerve synapse. Brain Research. 2000:90–9.

10.   Wachowiak M, McGann JP, Heyward PM, Shao Z, Puche AC, Shipley MT. Inhibition corrected of olfactory receptor neuron input to olfactory bulb glomeruli mediated by suppression of presynaptic calcium influx. J Neurophysiol. 2005; 94:2700–12. doi:10.1152/jn.00286.2005.

11.   Nagayama S, Homma R, Imamura F. Neuronal organization of olfactory bulb circuits. Front Neur Circ. 2014; 8:98. doi:10.3389/fncir.2014.00098.

12.   Banerjee A, Marbach F, Anselmi F, Koh MS, Davis MB, Garcia da Silva P, et al. An Interglomerular Circuit Gates Glomerular Output and Implements Gain Control in the Mouse Olfactory Bulb. Neuron. 2015; 87:193–207. doi: 10.1016/j.neuron.2015.06.019.

13.   Liu S, Plachez C, Shao Z, Puche A, Shipley MT. Olfactory bulb short axon cell release of GABA and dopamine produces a temporally biphasic inhibition-excitation response in external tufted cells. J Neurosci. 2013; 33:2916–26. doi:10.1523/JNEUROSCI.3607-12.2013.

14. Pignatelli A, Belluzzi O. Dopaminergic Neurones in the Main Olfactory Bulb: An Overview from an Electrophysiological Perspective. Front Neuroanat. 2017; 11:7. doi:10.3389/fnana.2017.00007.

15. Kosaka K, Hama K, Nagatsu I, Wu J-Y, Ottersen OP, Storm-Mathisen J, Kosaka T. Postnatal development of neurons containing both catecholaminergic and GABAergic traits in the rat main olfactory bulb. Brain Res. 1987; 403:355–60. doi:10.1016/0006-8993(87)90075-8.

16. Vergano-Vera E, Yusta-Boyo MJ, Castro F de, Bernad A, Pablo F de, Vicario-Abejón C. Generation of GABAergic and dopaminergic interneurons from endogenous embryonic olfactory bulb precursor cells. Development. 2006:4367–79.

17. Bovetti S, Veyrac A, Peretto P, Fasolo A, Marchis S de. Olfactory enrichment influences adult neurogenesis modulating GAD67 and plasticity-related molecules expression in newborn cells of the olfactory bulb. PLoS ONE. 2009;4: e6359. doi: 10.1371/journal.pone.0006359.

18. Kosaka T, Kosaka K. Two types of tyrosine hydroxylase positive GABAergic juxtaglomerular neurons in the mouse main olfactory bulb are different in their time of origin. Neurosci Res. 2009; 64:436–41. doi: 10.1016/j.neures.2009.04.018.

19. Galliano E, Franzoni E, Breton M, Chand AN, Byrne DJ, Murthy VN, Grubb MS. Embryonic and postnatal neurogenesis produce functionally distinct subclasses of dopaminergic neuron. Elife 2018. doi:10.7554/eLife.32373.

20. Fiorelli R, Azim K, Fischer B, Raineteau O. Adding a spatial dimension to postnatal ventricular-subventricular zone neurogenesis. Development. 2015; 142:2109–20. doi:10.1242/dev.119966.

21. Merkle FT, Mirzadeh Z, Alvarez-Buylla A. Mosaic organization of neural stem cells in the adult brain. Science. 2007; 317:381–4. doi:10.1126/science.1144914.

22. Young KM, Fogarty M, Kessaris N, Richardson WD. Subventricular zone stem cells are heterogeneous with respect to their embryonic origins and neurogenic fates in the adult olfactory bulb. J Neurosci. 2007; 27:8286–96. doi:10.1523/JNEUROSCI.0476-07.2007.

23. Brill MS, Snapyan M, Wohlfrom H, Ninkovic J, Jawerka M, Mastick GS, et al. A dlx2- and pax6-dependent transcriptional code for periglomerular neuron specification in the adult olfactory bulb. J Neurosci. 2008; 28:6439–52. doi:10.1523/JNEUROSCI.0700-08.2008.

24. Codega P, Silva-Vargas V, Paul A, Maldonado-Soto AR, Deleo AM, Pastrana E, Doetsch F. Prospective identification and purification of quiescent adult neural stem cells from their in vivo niche. Neuron. 2014; 82:545–59. doi: 10.1016/j.neuron.2014.02.039.

25. Bonaguidi MA, Stadel RP, Berg DA, Sun J, Ming G-l, Song H. Diversity of Neural Precursors in the Adult Mammalian Brain. Cold Spring Harb Perspect Biol. 2016;8: a018838. doi:10.1101/cshperspect.a018838.

26. Mundiñano I-C, Caballero M-C, Ordóñez C, Hernandez M, DiCaudo C, Marcilla I, et al. Increased dopaminergic cells and protein aggregates in the olfactory bulb of patients with neurodegenerative disorders. Acta Neuropathol. 2011; 122:61–74. doi:10.1007/s00401-011-0830-2.

27. Huisman E, Uylings HBM, Hoogland PV. Gender-related changes in increase of dopaminergic neurons in the olfactory bulb of Parkinson's disease patients. Mov Disord. 2008; 23:1407–13. doi:10.1002/mds.22009.

28. Cave JW, Fujiwara N, Weibman AR, Baker H. Cytoarchitectural changes in the olfactory bulb of Parkinson's disease patients. NPJ Parkinsons Dis. 2016; 2:16011. doi:10.1038/npjparkd.2016.11.

29.   Dölle C, Flønes I, Nido GS, Miletic H, Osuagwu N, Kristoffersen S, et al. Defective mitochondrial DNA homeostasis in the substantia nigra in Parkinson disease. Nat Comm. 2016; 7:13548. doi:10.1038/ncomms13548.

30.   Campbell CT, Kolesar JE, Kaufman BA. Mitochondrial transcription factor A regulates mitochondrial transcription initiation, DNA packaging, and genome copy number. Biochim Biophys Acta. 2012; 1819:921–9. doi: 10.1016/j.bbagrm.2012.03.002.

31.   Gustafsson CM, Falkenberg M, Larsson N-G. Maintenance and Expression of Mammalian Mitochondrial DNA. Annu Rev Biochem. 2016; 85:133–60. doi:10.1146/annurev-biochem-060815-014402.

32.   Ekstrand MI, Terzioglu M, Galter D, Zhu S, Hofstetter C, Lindqvist E, et al. Progressive parkinsonism in mice with respiratory-chain-deficient dopamine neurons. PNAS. 2007; 104:1325–30. doi:10.1073/pnas.0605208103.

33.   Ekstrand MI, Galter D. The MitoPark Mouse – An animal model of Parkinson's disease with impaired respiratory chain function in dopamine neurons. Park Rel Dis. 2009;15: S185-S188. doi:10.1016/S1353-8020(09)70811-9.

34.   Sciacco M, Bonilla E. Cytochemistry and immunocytochemistry of mitochondria in tissue sections. Met Enzymol. 1996; 264:509–21.

35.   Bonzano S, Bovetti S, Gendusa C, Peretto P, Marchis S de. Adult Born Olfactory Bulb Dopaminergic Interneurons: Molecular Determinants and Experience-Dependent Plasticity. Frontier Neurosci. 2016; 10:189. doi:10.3389/fnins.2016.00189.

36.   Srinivas S, Watanabe T, Lin C-S, William CM, Tanabe Y, Jessell TM, Costantini F. Cre reporter strains produced by targeted insertion of EYFP and ECFP into the ROSA26 locus. BMC Dev Biol. 2001; 1:4. doi:10.1186/1471-213X-1-4.

37.   Vaswani AR, Weykopf B, Hagemann C, Fried H-U, Brüstle O, Blaess S. Correct setup of the substantia nigra requires Reelin-mediated fast, laterally-directed migration of dopaminergic neurons. Elife 2019. doi:10.7554/eLife.41623.

38.   Allen Institute. Allen Developing Brain Atlas. 2015. http://developingmouse.brain-map.org. Accessed 10th July 2019.

39.   Ricke KM, Paß T, Kimoloi S, Fährmann K, Jüngst C, Schauss A, et al. Mitochondrial Dysfunction Combined with High Calcium Load Leads to Impaired Antioxidant Defense Underlying the Selective Loss of Nigral Dopaminergic Neurons. J Neurosci. 2020; 40:1975–86. doi:10.1523/JNEUROSCI.1345-19.2019.

40.   Pignatelli A, Kobayashi K, Okano H, Belluzzi O. Functional properties of dopaminergic neurones in the mouse olfactory bulb. J Physiol. 2005; 564:501–14. doi:10.1113/jphysiol.2005.084632.

41.   Hack MA, Saghatelyan A, Chevigny A de, Pfeifer A, Ashery-Padan R, Lledo P-M, Götz M. Neuronal fate determinants of adult olfactory bulb neurogenesis. Nat Neurosci. 2005; 8:865–72. doi:10.1038/nn1479.

42.   Chevigny A de, Core N, Follert P, Wild S, Bosio A, Yoshikawa K, et al. Dynamic expression of the pro-dopaminergic transcription factors Pax6 and Dlx2 during postnatal olfactory bulb neurogenesis. Front Cell Neurosci. 2012; 6:6. doi:10.3389/fncel.2012.00006.

43.   Curto GG, Nieto-Estévez V, Hurtado-Chong A, Valero J, Gómez C, Alonso JR, et al. Pax6 is essential for the maintenance and multi-lineage differentiation of neural stem cells, and for neuronal incorporation into the adult olfactory bulb. Stem Cells Dev. 2014; 23:2813–30. doi:10.1089/scd.2014.0058.

44.   Kohwi M, Osumi N, Rubenstein JLR, Alvarez-Buylla A. Pax6 is required for making specific subpopulations of granule and periglomerular neurons in the olfactory bulb. J Neurosci. 2005; 25:6997–7003. doi:10.1523/JNEUROSCI.1435-05.2005.

45.   Ninkovic J, Pinto L, Petricca S, Lepier A, Sun J, Rieger MA, et al. The transcription factor Pax6 regulates survival of dopaminergic olfactory bulb neurons via crystallin αA. Neuron. 2010; 68:682–94. doi: 10.1016/j.neuron.2010.09.030.

46.   Agoston Z, Heine P, Brill MS, Grebbin BM, Hau A-C, Kallenborn-Gerhardt W, et al. Meis2 is a Pax6 co-factor in neurogenesis and dopaminergic periglomerular fate specification in the adult olfactory bulb. Development. 2014; 141:28–38. doi:10.1242/dev.097295.

47.   Schweyer K, Rüschoff-Steiner C, Arias-Carrión O, Oertel WH, Rösler TW, Höglinger GU. Neuronal precursor cells with dopaminergic commitment in the rostral migratory stream of the mouse. Sci Rep. 2019; 9:13359. doi:10.1038/s41598-019-49920-5.

48.   Duan D, Fu Y, Paxinos G, Watson C. Spatiotemporal expression patterns of Pax6 in the brain of embryonic, newborn, and adult mice. Brain Struct Funct. 2013; 218:353–72. doi:10.1007/s00429-012-0397-2.

49.   Galter D, Pernold K, Yoshitake T, Lindqvist E, Hoffer B, Kehr J, et al. MitoPark mice mirror the slow progression of key symptoms and L-DOPA response in Parkinson's disease. Genes, Brain and Behavior. 2010; 9:173–81. doi:10.1111/j.1601-183X.2009.00542. x.

50.   Kruzich PJ, Grandy DK. Dopamine D2 receptors mediate two-odor discrimination and reversal learning in C57BL/6 mice. BMC Neurosci. 2004; 5:12. doi:10.1186/1471-2202-5-12.

51.   Pavlis M, Feretti C, Levy A, Gupta N, Linster C. l-DOPA improves odor discrimination learning in rats. Physiol Behav. 2006; 87:109–13. doi: 10.1016/j.physbeh.2005.09.011.

52.   Giguère N, Burke Nanni S, Trudeau L-E. On Cell Loss and Selective Vulnerability of Neuronal Populations in Parkinson's Disease. Front Neurol. 2018; 9:455. doi:10.3389/fneur.2018.00455.

53.   Bolam JP, Pissadaki EK. Living on the edge with too many mouths to feed: why dopamine neurons die. Mov Disord. 2012; 27:1478–83. doi:10.1002/mds.25135.

54.   Pacelli C, Giguère N, Bourque M-J, Lévesque M, Slack RS, Trudeau L-É. Elevated Mitochondrial Bioenergetics and Axonal Arborization Size Are Key Contributors to the Vulnerability of Dopamine Neurons. Curr Biol. 2015; 25:2349–60. doi: 10.1016/j.cub.2015.07.050.

55.   Grace AA. Dopamine system dysregulation by the ventral subiculum as the common pathophysiological basis for schizophrenia psychosis, psychostimulant abuse, and stress. Neurotox Res. 2010; 18:367–76. doi:10.1007/s12640-010-9154-6.

56.   Dragicevic E, Schiemann J, Liss B. Dopamine midbrain neurons in health and Parkinson's disease: emerging roles of voltage-gated calcium channels and ATP-sensitive potassium channels. Neurosci. 2015; 284:798–814. doi: 10.1016/j.neuroscience.2014.10.037.

57.   Khaliq ZM, Bean BP. Pacemaking in dopaminergic ventral tegmental area neurons: depolarizing drive from background and voltage-dependent sodium conductances. J Neurosci. 2010; 30:7401–13. doi:10.1523/JNEUROSCI.0143-10.2010.

58.   Pignatelli A, Iseppe AF, Gambardella C, Borin M, Belluzzi O, editors. Pacemaker Currents in Dopaminergic Neurones of the Mice Olfactory Bulb: Intech Open; 2012.

59.   Guzman JN, Sanchez-Padilla J, Wokosin D, Kondapalli J, Ilijic E, Schumacker PT, Surmeier DJ. Oxidant stress evoked by pacemaking in dopaminergic neurons is attenuated by DJ-1. Nature. 2010; 468:696–700. doi:10.1038/nature09536.

60.   Guzman JN, Ilijic E, Yang B, Sanchez-Padilla J, Wokosin D, Galtieri D, et al. Systemic isradipine treatment diminishes calcium-dependent mitochondrial oxidant stress. J Clin Invest. 2018; 128:2266–80. doi:10.1172/JCI95898.

61.   Koster NL, Norman AB, Richtand NM, Nickell WT, Puche AC, Pixley SK, Shipley MT. Olfactory receptor neurons express D2 dopamine receptors. J Comp Neurol. 1999; 411:666–73.

62.   Wachowiak M, Cohen LB. Presynaptic inhibition of primary olfactory afferents mediated by different mechanisms in lobster and turtle. J Neurosci. 1999; 19:8808–17.

63.   Ennis M, Zhou FM, Ciombor KJ, Aroniadou-Anderjaska V, Hayar A, Borrelli E, et al. Dopamine D2 receptor-mediated presynaptic inhibition of olfactory nerve terminals. J Neurophysiol. 2001; 86:2986–97. doi:10.1152/jn.2001.86.6.2986.

64.   Parrish-Aungst S, Shipley MT, Erdelyi F, Szabo G, Puche AC. Quantitative analysis of neuronal diversity in the mouse olfactory bulb. J Comp Neurol. 2007; 501:825–36. doi:10.1002/cne.21205.

65.   Maher BJ, Westbrook GL. Co-transmission of dopamine and GABA in periglomerular cells. J Neurophysiol. 2008; 99:1559–64. doi:10.1152/jn.00636.2007.

66.   Wachowiak M, Shipley MT. Coding and synaptic processing of sensory information in the glomerular layer of the olfactory bulb. Sem Cell Dev Biol. 2006; 17:411–23. doi: 10.1016/j.semcdb.2006.04.007.

67.   Rebello MR, McTavish TS, Willhite DC, Short SM, Shepherd GM, Verhagen JV. Perception of odors linked to precise timing in the olfactory system. PLoS Biol. 2014;12: e1002021. doi: 10.1371/journal.pbio.1002021.

68.   Sun W, Kim H, Moon Y. Control of neuronal migration through rostral migration stream in mice. Anat Cell Biol. 2010; 43:269–79. doi:10.5115/acb.2010.43.4.269.

69.   McLean JH, Shipley MT. Postmitotic, postmigrational expression of tyrosine hydroxylase in olfactory bulb dopaminergic neurons. J Neurosci. 1988; 8:3658–69.

70.   Shipley MT, Ennis M. Functional organization of olfactory system. J Neurobiol. 1996; 30:123–76. doi:10.1002/(SICI)1097-4695(199605)30:1<123::AID-NEU11>3.0.CO;2-N.

71.   Höglinger GU, Alvarez-Fischer D, Arias-Carrión O, Djufri M, Windolph A, Keber U, et al. A new dopaminergic nigro-olfactory projection. Acta Neuropathol. 2015; 130:333–48. doi: 10.1007/s00401-015-1451-y.

72.   Zhang W, Sun C, Shao Y, Zhou Z, Hou Y, Li A. Partial depletion of dopaminergic neurons in the substantia nigra impairs olfaction and alters neural activity in the olfactory bulb. Sci Rep. 2019; 9:254. doi: 10.1038/s41598-018-36538-2.

73.   Valle-Leija P, Drucker-Colín R. Unilateral olfactory deficit in a hemiparkinson's disease mouse model. Neuroreport. 2014; 25:948–53. doi: 10.1097/WNR.0000000000000218.

74.   Winner B, Geyer M, Couillard-Despres S, Aigner R, Bogdahn U, Aigner L, et al. Striatal deafferentation increases dopaminergic neurogenesis in the adult olfactory bulb. Exp Neurol. 2006; 197:113–21. doi: 10.1016/j.expneurol.2005.08.028.

75.   Lennington JB, Pope S, Goodheart AE, Drozdowicz L, Daniels SB, Salamone JD, Conover JC. Midbrain dopamine neurons associated with reward processing innervate the neurogenic subventricular zone. J Neurosci. 2011; 31:13078–87. doi: 10.1523/JNEUROSCI.1197-11.2011.

76.   Xiong A, Wesson DW. Illustrated Review of the Ventral Striatum's Olfactory Tubercle. Chem Senses. 2016; 41:549–55. doi: 10.1093/chemse/bjw069.

77.   Zhang Z, Liu Q, Wen P, Zhang J, Rao X, Zhou Z, et al. Activation of the dopaminergic pathway from VTA to the medial olfactory tubercle generates odor-preference and reward. Elife 2017. doi: 10.7554/eLife.25423.

78.   Zhang Z, Zhang H, Wen P, Zhu X, Wang L, Liu Q, et al. Whole-Brain Mapping of the Inputs and Outputs of the Medial Part of the Olfactory Tubercle. Front Neur Circ. 2017; 11:52. doi: 10.3389/fncir.2017.00052.

79.   McLean JH, Shipley MT, Nickell WT, Aston-Jones G, Reyher CK. Chemoanatomical organization of the noradrenergic input from locus coeruleus to the olfactory bulb of the adult rat. J Comp Neurol. 1989; 285:339–49. doi: 10.1002/cne.902850305.

80.   Steinfeld R, Herb JT, Sprengel R, Schaefer AT, Fukunaga I. Divergent innervation of the olfactory bulb by distinct raphe nuclei. J Comp Neurol. 2015; 523:805–13. doi:10.1002/cne.23713.

81.   Brunert D, Tsuno Y, Rothermel M, Shipley MT, Wachowiak M. Cell-Type-Specific Modulation of Sensory Responses in Olfactory Bulb Circuits by Serotonergic Projections from the Raphe Nuclei. J Neurosci. 2016; 36:6820–35. doi:10.1523/JNEUROSCI.3667-15.2016.

82.   Moriizumi T, Tsukatani T, Sakashita H, Miwa T. Olfactory disturbance induced by deafferentation of serotonergic fibers in the olfactory bulb. Neuroscience. 1994; 61:733–8. doi:10.1016/0306-4522(94)90396-4.

83.   Glasl L, Kloos K, Giesert F, Roethig A, Di Benedetto B, Kühn R, et al. Pink1-deficiency in mice impairs gait, olfaction and serotonergic innervation of the olfactory bulb. Exp Neurol. 2012; 235:214–27. doi: 10.1016/j.expneurol.2012.01.002.

84.   Halliday GM, Blumbergs PC, Cotton RGH, Blessing WW, Geffen LB. Loss of brainstem serotonin- and substance P-containing neurons in Parkinson's disease. Brain Res. 1990; 510:104–7. doi:10.1016/0006-8993(90)90733-R.

85.   Politis M, Wu K, Loane C, Kiferle L, Molloy S, Brooks DJ, Piccini P. Staging of serotonergic dysfunction in Parkinson's disease: an in vivo 11C-DASB PET study. Neurobiol Dis. 2010; 40:216–21. doi: 10.1016/j.nbd.2010.05.028.

86.   Pagano G, Niccolini F, Fusar-Poli P, Politis M. Serotonin transporter in Parkinson's disease: A meta-analysis of positron emission tomography studies. Ann Neurol. 2017; 81:171–80. doi:10.1002/ana.24859.

Video Legends

Video 1: Odor Discrimination Test of a 30-week-old MitoPark mouse. Movement and sniffing behavior of the test mouse are shown during the presentation of a new odor via a cotton swab in an open cage. While the MitoPark mouse's ability to move was sufficient to discover the cotton swab, the sniffing behavior appeared undirected. The mouse did not locate the swab at any time in the presented video sequence.

Video 2: Odor Discrimination Test of a 30-week-old control mouse. Movement and sniffing behavior of the test mouse are shown while a new odor is presented via a cotton swab in an open cage. The control mouse shows a normal olfactory behavior. In particular, a targeted sniffing behavior is seen, followed by the rapid detection of the odor's source.

Supplementary Material
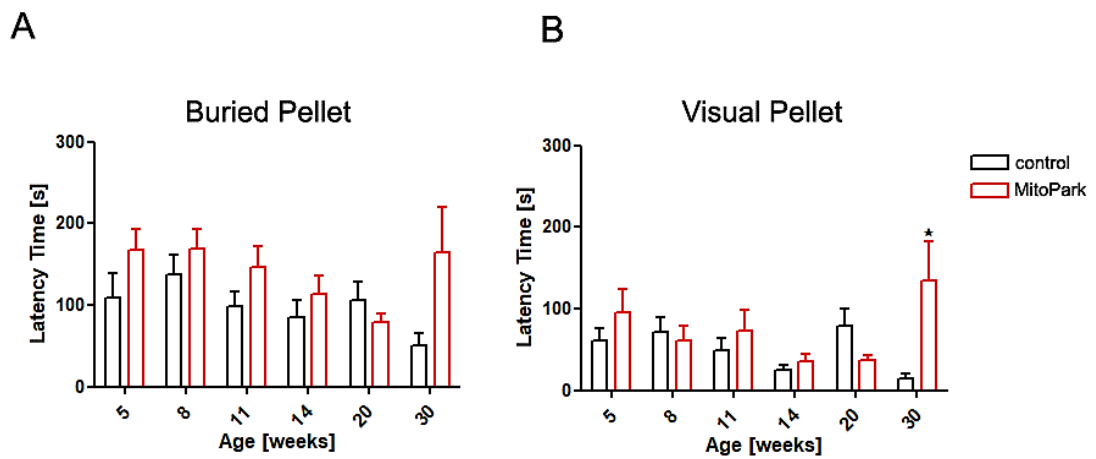
Fig. 3-8-1 No significant difference in buried food pellet detection between MitoPark and control mice. A) Latency time of MitoPark (red bars) and age-matched control mice (black bars) to the buried and B) unburied food pellet (n = 5-23 mice).

3.3 Preserved Striatal Innervation and Motor Function Despite Severe Neurodegeneration of Nigral Dopaminergic Neurons Upon Slow Progressive Impairment of mtDNA Replication

Short title: Impaired mtDNA Replication in Dopaminergic Neurons

Thomas Paß[1], Konrad Ricke[1], Olivier Baris[1] and Rudolf J. Wiesner[1,2]

[1]Center for Physiology and Pathophysiology, Institute of Vegetative Physiology, University of Cologne, Cologne, Germany

[2]Cologne Excellence Cluster on Cellular Stress Responses in Aging-associated Diseases (CECAD), University of Cologne, Cologne, Germany

Corresponding author:

Thomas Paß, M. Sc.
thomas.pass@uk-koeln.de
ORCID-ID: 0000-0002-9915-7360

or

Prof. Dr. Rudolf Wiesner
Institute of Vegetative Physiology,
University of Köln,
Robert-Koch-Str. 39
50931 Köln
Germany
rudolf.wiesner@uni-koeln.de

Abstract

Mitochondrial dysfunction in midbrain dopaminergic neurons (DaNs) is a central feature of Parkinson's disease (PD), including the common idiopathic as well as those rare familial forms induced by mutations in the Parkin, Pink1, LRRK2 or DJ-1 genes. Mitochondrial dysfunction is probably caused by the accumulation of mitochondrial DNA (mtDNA) deletions, as shown post-mortem in elderly humans as well as in PD patients. Motor symptoms are caused by DaN loss, especially in the *substantia nigra pars compacta* (SNc), while those in the neighboring *ventral tegmental area* (VTA) are largely spared. In order to accelerate the accumulation of mtDNA deletions, we generated mice in which the DaNs express a mutated, dominant-negative variant of the mitochondrial helicase Twinkle (K320E), leading to mtDNA deletions in patients. K320E-Twinkle[DaN] mice show no motor decline even at the age of 20 months, although DaN number in both SNc and VTA was severely reduced. Surprisingly, the corresponding striatal projection areas, the *caudate putamen* (CPu) and the *nucleus accumbens* (NAcc), were differentially affected. In stark contrast to other genetically and chemically induced mitochondrial PD models described in the literature, fibres in the NAcc innervated by the VTA were dramatically reduced, causing a depressive-like behavior in these animals. Despite the severe neurodegeneration, the SNc-innervated CPu of homozygous K320E-Twinkle[DaN] mice still possessed ~80% of dopaminergic projections, which was sufficient to maintain voluntary movement control. Our data reveal that, although both surviving VTA and SNc DaNs show normal expression levels of complex IV, only SNc DaNs were able to compensate for neurodegeneration by preserved striatal innervation when facing slow and progressive impairment of mtDNA replication.

Key words: Parkinson's disease, mitochondrial dysfunction, midbrain, dopaminergic neurons, striatum

Introduction

Parkinson's disease (PD) is characterized by the progressive loss of midbrain dopaminergic neuron (DaNs) in the substantia nigra pars compacta (SNc), while the neighboring ventral tegmental area (VTA) is largely spared. The depletion of dopamine in the dorsal striatum leads to the cardinal motor symptoms of PD, including tremor, rigidity, bradykinesia and postural instability (Michel et al. 2016). Besides the movement disorder, non-motor symptoms, such as gastrointestinal dysfunction, loss of smell, sleep disturbances, anxiety and depression, are frequently reported to precede and accompany the neurodegenerative disease (Reijnders et al. 2008; Kurtis et al. 2013; Simuni and Fernandez 2013; Fasano et al. 2015). While being important for diagnosis, motor symptoms only arise after 30-50% of SNc DaNs and up to 80% of striatal dopamine are already gone (Obeso et al. 2017). Up to now, available drugs and treatments can then only dampen the symptoms for a foreseeable time. Therefore, medications which both stop the ongoing loss of DaNs and promote striatal innervation of the surviving DaNs are urgently needed.

Mitochondrial dysfunction in DaNs is a central feature of PD, including the common idiopathic as well as those rare familial forms caused by mutations in the Parkin, Pink1, LRRK2 or DJ-1 genes (Park et al. 2018; Chen et al. 2019). With increasing age, DaNs accumulate mitochondrial DNA (mtDNA) deletions, which are even further elevated in PD and thought to be a key process in the pathogenesis of the neuronal loss (Bender et al. 2006; Kraytsberg et al. 2006; Meissner et al. 2008; Elstner et al. 2011; Dölle et al. 2016). We could already show that the enhanced accumulation of mtDNA deletions is driven by the metabolism of catecholamines (Neuhaus et al. 2014; Neuhaus et al. 2017), explaining why dopamine-producing cells are hot spots for such alterations in the mtDNA.

In order to investigate the impact of mtDNA deletions on the function of various tissues, we generated mice in which a mutated, dominant-negative variant of the mitochondrial helicase Twinkle (K320E mutation) is expressed in a cell-specific manner. The equivalent mutation of twinkle is found in patients with the sensory ataxic neuropathy with dysarthria and ophtalmoparesis (SANDO) syndrome (Hanisch et al. 2015), leading to progressive external ophthalmoplegia (PEO) and is accompanied by the accumulation of multiple mtDNA deletions in skeletal muscle (Hudson et al. 2005). In addition, the brain has been reported to reveal high amounts of mutated mtDNA as well in a patient with PEO (Suomalainen et al. 1992). Our lab already reported the mitochondrial defects in various tissues upon the expression of K320E (Baris et al. 2015; Weiland et al. 2018; Holzer et al. 2019). In order to investigate the impact of the increased accumulation of mtDNA deletions in DaNs on neuronal survival, mitochondrial function and motor behavior, we generated mice in which K320E is expressed in DaNs.

Materials and Methods

Experimental model

All experiments were conducted in agreement with European and German guidelines and approved by local authorities (LANUV NRW, Recklinghausen, Germany; 84-02.04.2013-A141, 81-02.04.2018-A210). Experiments were carried out with male or female mice of the strain C57/BL6N. For depressive state only group-housed animals were used to avoid possible effects induced by social deprivation. Heterozygous (K320E/WtDaN) and homozygous (K320E/K320EDaN) K320E-TwinkleDaN mice were generated by crossing DAT cre mice (Cre-gene inserted upstream of the translation start codon in exon 2 of the DAT gene, (Ekstrand et al. 2007)) with R26-K320E-TwinkleloxP/+ mice. DAT cre mice had been kindly provided by Nils-Göran Larsson (Karolinska Institutet, Sweden). Generation of R26-K320E-TwinkleloxP/+ mice has been described previously (Baris et al. 2015). Mice were genotyped by PCR using genomic DNA isolated from ear punches. Primer sequences and PCR conditions are available upon request.

Histology

All immunohistochemical approaches were performed on 5 μm paraffin sections. Striatal tyrosine hydroxylase (TH) immunoreactivity was assayed using a TH antibody (polyclonal rabbit, Abcam, #ab112, 1:750) and a biotinylated secondary antibody (donkey anti-rabbit, dianova, #111-065-006, 1:500). Fluorescence stainings of midbrain sections were performed with primary antibodies against TH (polyclonal rabbit, Abcam, #ab112, 1:1500) and mitochondrial complex IV subunit 1 (mtCOI, monoclonal mouse, Abcam, #ab14705, 1:1000) and fluorochrome-conjugated secondary antibodies (Goat anti-rabbit TRITC-conjugated, AffiniPure, #111-025-144, 1:2000, Goat anti-mouse DyLight488-conjugated, Jackson-ImmunoResearch, #115-485-003, 1:400). Visualization of Cytochrome c Oxidase (COX) deficiency was performed by COX-SDH enzymatic activity staining at Bregma -3.08 mm similar to (Aradjanski et al. 2017), but incubation with SDH solution was performed for 180 min.

For densitometric analysis of striatal sections, bright-field microscopy was used (Slide Scanner, SCN400, Leica) equipped with a 40x objective. High resolution images from striatal sections at Bregma +0.74 mm were generated by the Leica SlidePath Gateway and the Microsoft Image Composite Editor software. TH-positive striatal fibre density was determined by optical density analysis using ImageJ-software with two sections per mouse. Non-specific background signal of the corpus callosum was subtracted from the striatal optical density values. Fluorescence images were obtained with an inverse confocal microscope (TCS SP8 gSTED, Leica) with a 40x oil objective at Bregma -3.08 mm. mtCOI-signal intensity was measured in the somata of TH-positive neurons. Fluorescent intensity was normalized to the

mtCOI-signal of TH-positive cells from the same objective slide using a tissue slice which was not incubated with the primary antibody against mtCOI (negative control).

Immunohistochemistry

Anaesthetized mice (ketamine/xylazine: 100/10 mg/kg body weight, intraperitoneally) were intracardially perfused with PBS (GIBCO; 140 mM NaCl, 10 mM sodium phosphate, 2.68 mM KCl, pH 7.4) for 3 min and 4% PFA in PBS for 15 min. Brains were dissected and immersion-fixed in 4% PFA in PBS overnight. Afterwards tissues were dehydrated in a series of ethanol solutions (ethanol percentages are given): 70%, 90%, 2x 100% (15 min each), 100% (30 min) and 100% (45 min, Leica ASP300, CMMC Tissue Embedding Facility) and embedded in paraffin (Leica EG1150 H, CMMC Tissue Embedding Facility). Coronal 5 µm striatal sections were cut with a microtome (Leica RM2125 RTS). Sections were deparaffinized in xylene (2x5 min), washed in a series of ethanol solutions (100%, 95%, 70% and 50%, 1 min each) and afterwards washed in ddH$_2$O (5 min). For epitope retrieval, sections were heated in citrate buffer (10 mM citric acid monohydrate, pH 6) using a microwave oven.

Brightfield microscopy: Sections were washed in TBS (10 mM Tris base, 150 mM NaCl, pH 7.6, 3x5 min), quenched with 0.3% H$_2$O$_2$/TBS solution and washed again in TBS (3x5 min). Subsequently, sections were blocked in 10% normal goat serum in TBS (45 min, RT) and afterwards incubated with the tyrosine hydroxylase (TH) antibody (polyclonal rabbit, Abcam, #ab112, 1:750 in 3% skim milk powder/TBS, overnight, 4°C). After another TBS washing step (3x5 min), sections were incubated with the secondary biotinylated antibody (donkey anti-rabbit, dianova, #111-065-006, 1:500 in 3% skim milk powder/TBS, 30 min, RT), followed by avidin/biotin Vectastain Elite ABC HRP Kit (Vector Laboratories). Visualization was performed by using DAB solution (0.46 mM 3,3'-Diaminobenzidine tetrahydrochloride, 7.3 mM Imidazole, 15.2 mM Ammonium nickel (II) sulfate hexahydrate, 0.015% H$_2$O$_2$ in TBS, pH 7.1, 6 min). Following a short washing in ddH$_2$O (1 sec), sections were dehydrated in 50%, 70% (1 sec each), 95% and 100% ethanol (1 min each), cleared in xylene (2x10 min) and mounted with Entellan.

Fluorescence stainings

Sections were rinsed in 0.5% Tween20 in TBS (3x5 min) after the epitope retrieval and incubated with the primary antibodies (TH polyclonal rabbit, Abcam, #ab112, 1:750, mitochondrial complex IV subunit 1 (mtCOI) monoclonal mouse, Abcam, #ab14705, 1:1000 in Dako antibody diluent, overnight, 4°C). Sections were washed in 0.5% Tween20 in TBS (3x5 min) and incubated with fluorochrome-conjugated secondary antibodies (Goat anti-rabbit TRITC-conjugated, AffiniPure, #111-025-144, 1:1000, Goat anti-mouse DyLight488-conjugated, Jackson-ImmunoResearch, #115-485-003, 1:400, overnight, 4°C). Following

another washing step in 0.5% Tween20 in TBS (3x5 min), midbrain sections were counterstained with DAPI (1 µg/mL in ddH$_2$O, 1 min), washed again in 0.5% Tween20 in TBS (3x5 min) and mounted with Fluoromount. At each time point, immunofluorescent stainings were performed with all sections at the same time.

Stereological quantification of dopaminergic neurons

For the counting of DaNs, tyrosine hydroxylase stainings of serial coronal paraffin midbrain sections were performed similar to stainings in the striatum. Sections were incubated with DAB solution (0.46 mM 3,3'-Diaminobenzidine tetrahydrochloride, 7.3 mM Imidazole, 15.2 mM Ammonium nickel (II) sulfate hexahydrate, 0.015% H2O2 in TBS, pH 7.1) for 14 min and counterstained with nuclear fast red (NFR, 0.1% in 5% aluminium sulfate dissolved 1:5 in ddH2O). Stereological quantification of DaNs was conducted with the physical fractionator approach, which is typically used for the quantification of large neuron numbers in brain nuclei using thin, paired tissue sections (Gundersen et al., 1988; Ma et al., 2003; Glaser et al., 2007). The region of interest was confined either to the SNc or to the VTA using the mouse brain atlas (Paxinos and Franklin, 2001) on sections between Bregma -2.54 mm and -3.88 mm. Neurons Q were only counted, if their TH- and NFR-positive profiles appeared in the reference section but not in the lookup section. In addition, neurons had to be located either within the counting frame, or touching the open frame, but not touching the forbidden frame. The height sampling fraction hsf (section thickness/dissection height = 5 µm/5 µm = 1) and the area sampling fraction asf (area of counting frame/area of sampling grid = 42.9 µm²/191.82 µm² = 0.223647) were given as constants. The section sampling fraction ssf was set by the number of sections between the analyzed section pairs (typically 27 sections). Total dopaminergic neuron numbers N were calculated by means of the following formula (Dorph-Petersen et al., 2001; Howard and Reed, 2005): N = Q x 1/hsf x 1/asf x 1/ssf.

COX-SDH staining

Visualization of Cytochrome c Oxidase (COX) deficiency was performed by COX-SDH enzymatic activity staining (Sciacco and Bonilla 1996). COX is respiratory chain (RC) complex IV which is partially encoded by mtDNA, while succinate dehydrogenase (SDH), complex II, is entirely encoded by nuclear DNA. Impaired integrity of mtDNA results in COX-deficiency, but sustained SDH-activity. Cells with decreased COX-activity will stain blue for SDH, while cells with normal COX-activity will appear brown. Following dissection, brains were embedded (O.C.T. Tissue-Tek), frozen on dry ice and stored at -80 °C. Cryostat (Leica CM3050 S) sections of 7 µm were stored at -80 °C. Coronal midbrain cryosections at Bregma -3.08 mm were air dried and treated with COX incubation solution (100 µM Cytochrome C, 4 mM diaminobenzidine, 4400 U catalase in 0.1 M phosphate buffer) for 40 min at 37 °C. Afterwards, sections were washed in ddH2O (3x30 sec) and treated with SDH incubation solution (1.5 mM

Nitroblue tetrazolium, 130 mM sodium succinate, 200 µM phenazine methosulfate, 1 mM sodium azide) for 180 min at 37 °C. Sections were washed again in ddH2O (3x30 sec), dehydrated in 95% (2x2 min) and 100% ethanol (10 min), air dried and mounted with glycerol-gelatine.

Behavioral Tests

Beam Break Experiment

Spontaneous horizontal as well as vertical movement of mice was tested by performing the open field test. The activity measurements were done in home-made beam break detector cages. Before individual mice were transferred, the experimental cages were cleaned with ethanol. Horizontal and vertical movement were detected by infrared beams. Interruptions on the horizontal and vertical level were recorded during a tracking period of 60 minutes. The total counts after 60 minutes are presented as percentages of control animals. All experiments were conducted between 12:00 and 17:00 p.m.

Tail Suspension Test

The tail suspension test was used to inspect K320E-TwinkleDaN mice for depressive-like behavior. The test was performed in accordance with (Can et al. 2012) with minor modifications. Before testing, mice were kept individually in a new cage for 30 min in the experimental room. Mice were suspended for 6 min by using laboratory tape (1.91 cm width, Roti®-Tape-marking tapes, Carl Roth). Each trial was performed with one mouse only. In order to prevent animals from climbing their tails, clear hollow home-made cylinders were placed around their tails. Each session was recorded by a video camera. The time of immobility was calculated for each video by measuring the time of active movement and its subtraction from the total recording time. Active movement has been defined as the condition when at least three paws are in motion. Immobility time was presented in relation to the body weight at the time of the behavioral testing. Values were normalized to relative data from control animals. The observer was blinded concerning the genotype of the animals.

Sugar Preference

Another test to assess depression-related behavior in rodents is the sugar preference test. Together with their littermates, animals were transferred into a new cage for 24 h. During this time, mice are offered two bottles with 200 ml, one with 5% sucrose solution and the other with tap water. After the habituation phase, the littermates were transferred back to the regular cages and the experimental mice were kept single-housed for another 24 h. The amount of consumed water and sucrose solution was measured and presented in relation to the body weight at the time of the behavioral testing. Values were normalized to relative data from control animals. To avoid influences that might occur by the preference of a bottle's position,

the order of the bottles had been changed randomly after the habituation phase. Mice were not deprived of food or water prior to the test. All experiments were conducted on the weekend, ensuring a quiet environment for the tested animals. For normalization of behavioral data, the body weight of K320E-Twinkle[DaN] and control mice was determined.

Statistics

Statistical analysis was done with GraphPad Prism 8 for Windows. Quantified data in the figures and in the text is presented as mean + SEM. Relative data is shown as percentage of control experiments. Values of sample size (n) refer to mouse numbers. Unpaired *t* tests, one-way or two-way ANOVA with *post hoc* comparisons (Bonferroni *post hoc* test) were used to determine differences between groups. A significance level of 0.05 was accepted for all statistical tests. Asterisks mark P-values of 0.05 (*), 0.01 (**), 0.001 (***) or 0.0001 (****). Hashtags were analogously used in order to visualize P-values of 0.05 (**#**), 0.01 (**##**), 0.001 (**###**) or 0.0001 (**####**) between groups of different time points.

Results

Motor activity is not impaired in K320E-Twinkle[DaN] mice

In order to investigate the impact of the mutated TWINKLE helicase on DaN functionality and motor behavior, motor function was assayed in a bream break setup in 10- and 20-month-old K320E-Twinkle[DaN] and control mice (Fig. 3-11A). There was no significant difference in the activity, neither at the horizontal nor vertical level, between K320E-Twinkle[DaN] and control animals at both ages (Fig. 3-11B, 10 months: horizontal control 100.00 ± 11.54 %, K320E/Wt[DaN] 105.69 ± 11.08 %, K320E/K320E[DaN] 118.30 ± 9.29 %, vertical control 100.00 ± 18.97 %, K320E/Wt[DaN] 77.15 ± 11.15 %, K320E/K320E[DaN] 102.96 ± 15.94 %; 20 months: horizontal control 100.00 ± 6.30 %, K320E/Wt[DaN] 116.87 ± 11.48 %, K320E/K320E[DaN] 114.65 ± 19.42 %, vertical control 100.00 ± 10.74 %, K320E/Wt[DaN] 120.54 ± 21.32 %, K320E/K320E[DaN] 92.75 ± 26.33 %; one-way ANOVA, n.s.).

Severe loss of midbrain DaNs

The absent motor phenotype in K320E-Twinkle[DaN] mice indicates that midbrain DaNs are not affected by the impairment of the mtDNA replication machinery. To verify the survival of DaNs

A

B
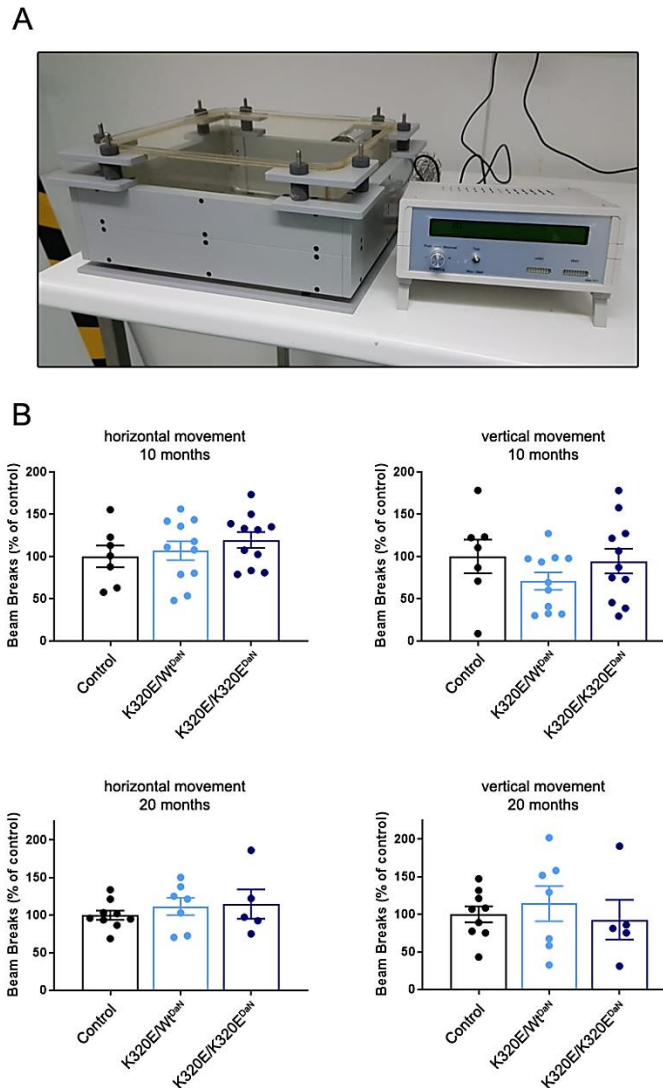
Fig. 3-11 No differences in spontaneous motor activity between K320E-Twinkle^{DaN} and control mice. A) Beam break cage with connected motor activity reading device. B) Beam break events are shown on the horizontal and vertical level. Quantitative data revealed no difference between K320E-Twinkle^{DaN} and control animals at 10 as well as 20 months of age (control mice n = 7-9, K320E/Wt^{DaN} mice n = 7-11, K320E/K320E^{DaN} mice n = 4-11).

despite the presence of the mutated TWINKLE, stereological cell quantification of midbrain sections was performed (Fig 3-12A). At the age of 5 months, no difference in the number of TH-positive cells was found between K320E-Twinkle^{DaN} and control mice (Fig. 3-12B, control 100.00 ± 4.33 %, K320E/Wt^{DaN} 108.03 ± 5.67 %, K320E/K320E^{DaN} 96.35 ± 8.67 %, one-way ANOVA, n.s.). However, 10-month-old hetero- and homozygous K320E-Twinkle^{DaN} mice both showed decreased DaN amounts when compared to control animals (control 100.00 ± 8.43 %, K320E/Wt^{DaN} 66.83 ± 6.12 %, one-way ANOVA, $P=0.0039$; K320E/K320E^{DaN} 42.85 ± 3.19 %, one-way ANOVA, $P<0.0001$), with the homozygous expressers being more affected than the heterozygous ones (one-way ANOVA, $P=0.0473$). In addition, when compared to 5-month-old individuals, the relative number of TH-positive cells was significantly reduced in hetero- and homozygous K320E-Twinkle^{DaN} mice of 10 months of age (K320E/Wt^{DaN}, unpaired *t*-test,

p=0.0014, K320E/K320E[DaN], unpaired *t*-test, P=0.0022). At the age of 20 months, the relative DaN number was further decreased in both hetero- and homozygous K320E-Twinkle[DaN] mice compared to control animals (control 100.00 ± 8.42 %, K320E/Wt[DaN] 58.62 ± 0.95 %, one-way ANOVA, P=0.0019; K320E/K320E[DaN] 23.05 ± 3.24 %, one-way ANOVA, P<0.0001). Again, homozygous K320E-Twinkle[DaN] mice revealed a lower number of TH-positive cells than heterozygous animals (one-way ANOVA, P=0.0077). Moreover, the relative DaN number of
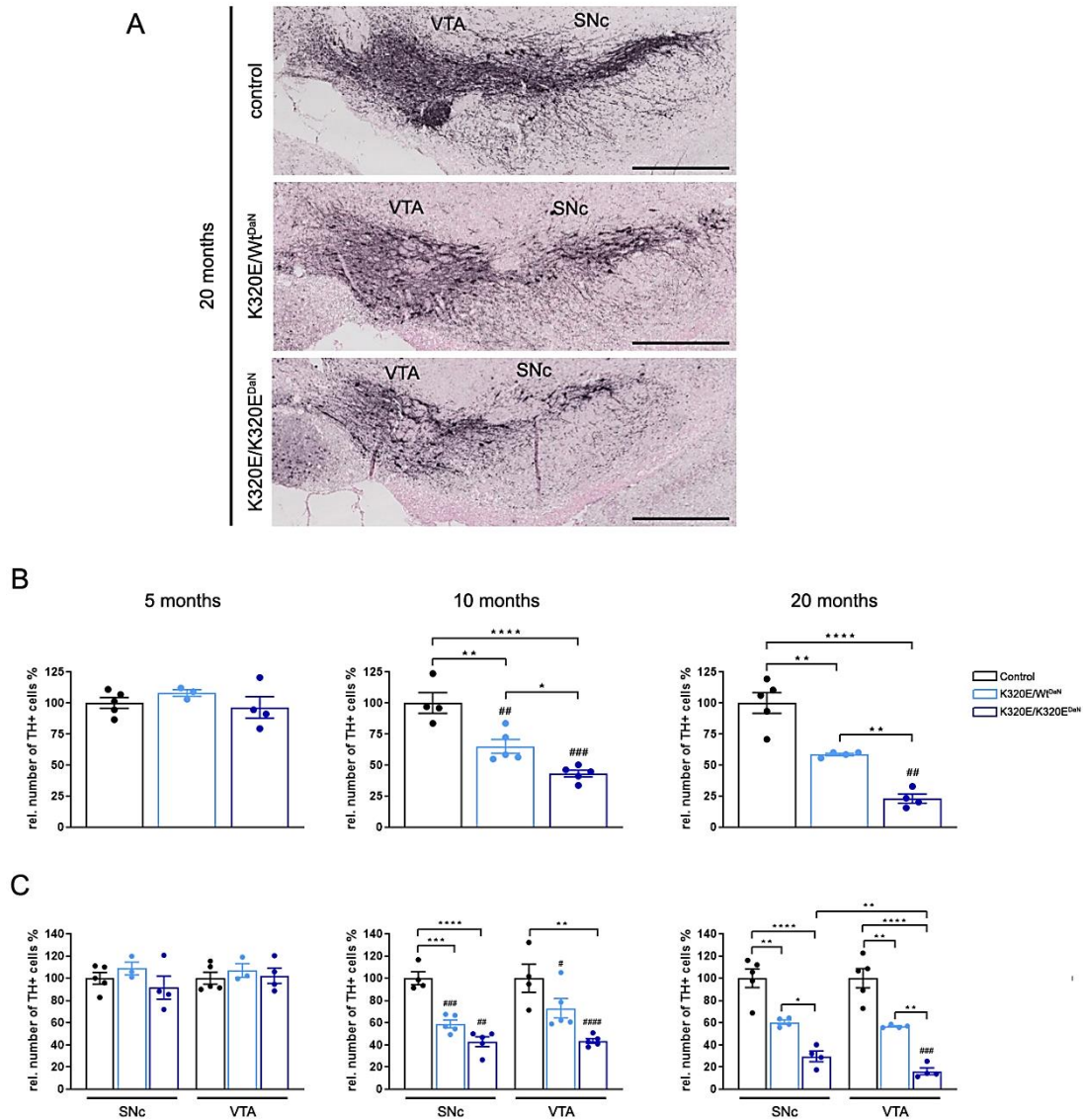
Fig. 3-12 K320E-Twinkle[DaN] mice show loss of TH-positive cells in both VTA and SNc. A) Immunohistochemical staining of Tyrosine hydroxylase (TH)-positive neurons in the ventral tegmental area (VTA) and the substantia nigra pars compacta (SNc) in 20-month-old hetero- and homozygous K320E-Twinkle[DaN] mice as well as age-matched control animals. Scale bar, 500 μm. B) Stereological quantification of TH-positive neurons in the midbrain revealed unaltered cell numbers between K320E-Twinkle[DaN] and control mice at the age of 5 months. After 10-month-old K320E-Twinkle[DaN] mice showed decreased numbers of TH-positive cells with the homozygous expressers being more affected. The number of TH-positive cells was further reduced in 20-month-old homozygous K320E-Twinkle[DaN] mice after 20 months of age (control mice n = 4-5, K320E/Wt[DaN] mice n = 3-5, K320E/K320E[DaN] mice n = 4-5). C) Region-specific differentiation of TH-positive neurons revealed VTA and SNc being similarly affected in K320E-Twinkle[DaN] animals. However, homozygous expressers showed less TH-positive cells in the VTA than the SNc after 20 months of age. # indicates significance compared to individuals of prior time point. Data are represented as mean ± SEM; * p < 0.05, ** p < 0.01, *** p < 0.001, **** p < 0.0001, ## p < 0.01, ### p < 0.001.

homozygous K320E-Twinkle[DaN] mice was further decreased compared to 10-month-old animals (10 months 42.85 ± 3.19 %, 20 months 23.05 ± 3.24 %, unpaired *t*-test, P=0.0028).

Reduced DaN number in both VTA and SNc

The selective cell death in PD patients as well as the differential vulnerability upon mitochondrial damage of SNc DaNs is highly conserved (Obeso et al. 2017). In order to investigate if the slow impairment of mtDNA replication in DaNs leads to region-specific loss, midbrain DaN numbers were further divided into the SNc and the VTA (Fig. 3-12C). In 5-month-old animals, no changes in the number of TH-positive cells were found between K320E-TwinkleDaN and control mice as well as between SNc and VTA (control SNc 100.00 ± 5.19 % VTA 100.00 ± 5.35 %, K320E/WtDaN SNc 108.87 ± 5.67 % VTA 106.97 ± 6.10 %, K320E/K320EDaN SNc 91.57 ± 10.33 % VTA 102.33 ± 6.97 %; two-way ANOVA, n.s.). Region-specific quantification of DaNs in hetero- and homozygous K320E-TwinkleDaN mice at the age of 10 months revealed that neurodegeneration was similarly present in both SNc and VTA (K320E/WtDaN SNc 59.43 ± 4.01 % VTA 76.15 ± 9.47 %, K320E/K320EDaN SNc 41.16 ± 4.62 % VTA 44.99 ± 1.93 %; two-way ANOVA, n.s.). After 20 months, TH-positive cells were lost to a similar extent in the SNc and the VTA of heterozygous K320E-TwinkleDaN mice (K320E/WtDaN SNc 60.50 ± 1.82 % VTA 56.68 ± 0.60 %, two-way ANOVA, n.s.). However, homozygous K320E-TwinkleDaN mice revealed an even stronger degeneration of DaNs in the VTA compared to the SNc (K320E/K320EDaN SNc 29.64 ± 4.18 % VTA 16.25 ± 2.76 %, two-way ANOVA, P=0.0027). In addition, the VTA DaN number of 20-month-old homozygous K320E-TwinkleDaN mice was further decreased when compared to 10-month-old individuals (10 months 44.99 ± 1.93 %, 20 months 16.25 ± 2.76 %, unpaired t test, P=0.0001), whereas the amount of SNc DaNs did not significantly change (10 months 41.16 ± 4.62 %, 20 months 29.64 ± 4.18 %, unpaired t test, n.s.).

Decrease of mitochondrially deficient DaNs with age

To confirm that neurodegeneration is linked to mitochondrial dysfunction, enzymatic cytochrome c oxidase (COX) activity was analyzed by histochemistry in midbrain sections of K320E-Twinkle[DaN] mice. 10-month-old hetero- and homozygous K320E-Twinkle[DaN] mice revealed blue, COX-deficient cells in both the SNc and the VTA (Fig. 3-13A, representative images). Interestingly, almost no blue cells could be detected after 20 months of age (Fig. 3-13B, representative images). For quantitative analysis, we further investigated the expression level of the mtDNA-encoded subunit I of COX (mtCOI), which is essential for COX activity and assembly, in the somata of DaNs in K320E-Twinkle[DaN] and control mice by immunofluorescent stainings (Fig. 3-14A). At the age of 5 months, fluorescent intensity of mtCOI was decreased in the somata of DaNs in the VTA of both hetero- and homozygous

K320E-Twinkle^{DaN} mice when compared to control animals (Fig. 3-14B, control 388.67 ± 16.63 %, K320E/Wt^{DaN} 275.46 ± 16.36 %, one-way ANOVA, P=0.0001; K320E/K320E^{DaN} 311.16 ± 21.03 %, one-way ANOVA, P=0.0062). The same was true for DaNs in the SNc (control 468.30 ± 23.20 %, K320E/Wt^{DaN} 266.32 ± 17.36 %, one-way ANOVA, P<0.0001; K320E/K320E^{DaN} 329.92 ± 24.20 %, one-way ANOVA, P<0.0001). Interestingly, mtCOI expression was higher in VTA than in SNc DaNs for control animals (two-way ANOVA, P=0.0051), whereas there was no difference between the midbrain regions in the mutants. However, after 10 months, fluorescence intensity of mtCOI was only reduced in the VTA of homozygous K320E-Twinkle^{DaN} mice (control 308.94 ± 12.22 %, K320E/Wt^{DaN} 268.40 ± 23.04 %, one-way ANOVA, n.s.; K320E/K320E^{DaN} 223.84 ± 14.06 %, one-way ANOVA, P=0.0033). No reduction in mtCOI expression became apparent for the SNc in any of the K320E-Twinkle^{DaN} mice (control 276.91 ± 9.47 %, K320E/Wt^{DaN} 242.57 ± 15.64 %, one-way ANOVA, n.s.; K320E/K320E^{DaN} 249.50 ± 21.06 %, one-way ANOVA, n.s.). Finally, hetero- and homozygous 20-month-old K320E-Twinkle^{DaN} mice revealed similar mtCOI fluorescent intensities in DaNs of both VTA and SNc (VTA: control 309.43 ± 10.06 %, K320E/Wt^{DaN} 307.55 ± 17.30 %, one-way ANOVA, n.s.; K320E/K320E^{DaN} 305.78 ± 19.17 %, one-way ANOVA, n.s.; SNc: control 295.90 ± 9.26 %, K320E/Wt^{DaN} 273.37 ± 16.99 %, one-way ANOVA, n.s.; K320E/K320E^{DaN} 283.98 ± 15.09 %, one-way ANOVA, n.s.).
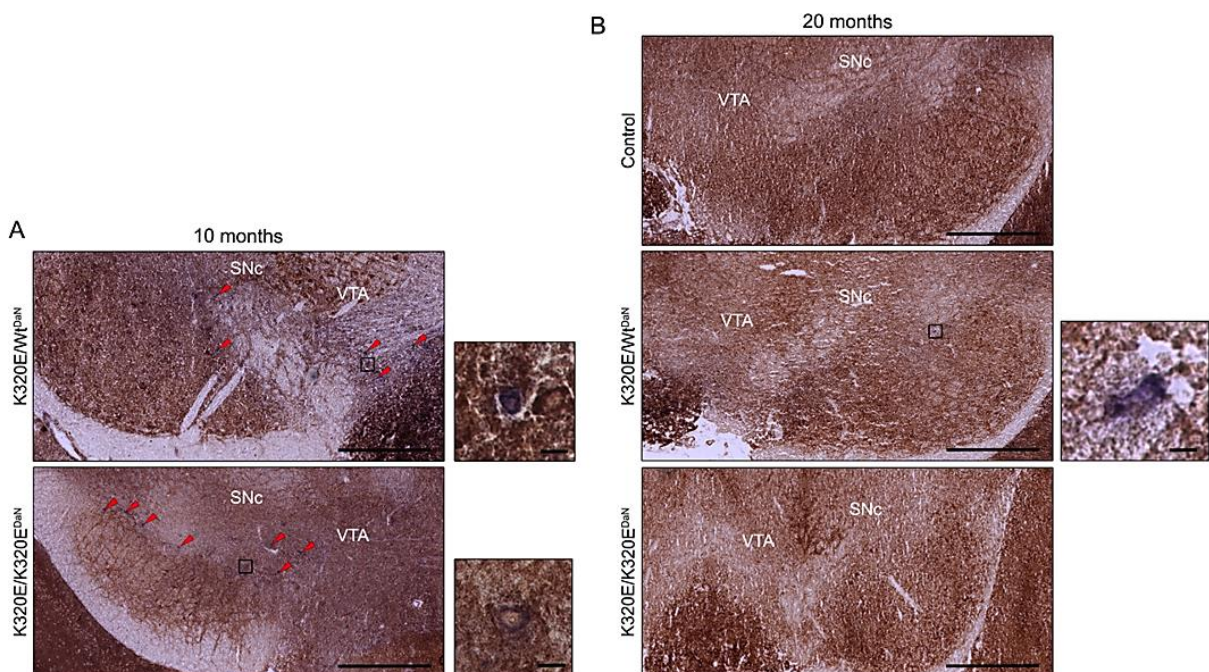
Fig. 3-13 COX-deficient cells in the midbrain of 10-month-old K320E-Twinkle^{DaN}. A) Cells with reduced COX activity (blue, highlighted by red arrowheads) were unmasked by COX-SDH staining in the midbrain of 10-months-old hetero- and homozygous K320E-Twinkle^{DaN} mice. B) After 20 months, almost no blue cells could be detected in mutant mice. Scale bars, 500 µm, single neuron presentation with 10 µm.

Fig. 3-14 Higher proportion of DaNs with normal complex IV expression in K320E-Twinkle[DaN] mice with increasing age. A) The immunofluorescent signal of subunit I of complex IV (mtCOI; green) was analyzed in the cell bodies of TH-positive (red) neurons in the ventral tegmental area (VTA) and the substantia nigra pars compacta (SNc) of 5-, 10- and 20-month-old control, hetero- and homozygous K320E-Twinkle[DaN] mice. Scale bars, 50 µm. B) The normalized fluorescence intensity of the mtCOI-staining (norm. mtCOI FI) was reduced in both the VTA and the SNc of 5-month-old hetero- and homozygous K320E-Twinkle[DaN] mice (n = 57-96 cells of 5 mice each). At 10 months of age, no difference could be found in the SNc. In contrast, TH-positive neurons in the VTA of homozygous K320E-Twinkle[DaN] animals showed decreased mtCOI fluorescent intensity (n = 67-84 cells of 3-5 mice). After 20 months, the mtCOI signal was similar in both the SNc and the VTA of hetero- and homozygous K320E-Twinkle[DaN] mice when compared to control animals (n = 58-100 cells of 4-5 mice). Data are represented as mean ± SEM; ** p < 0.01, *** p < 0.001.

Dopaminergic SNc projections are less affected than VTA projections in K320E-Twinkle[DaN] mice

Despite the severe loss of midbrain DaNs, and especially those which are located in the SNc, the motor activity of K320E-TwinkleDaN mice was not impaired. Apparently, sufficient levels of dopamine are still released by dopaminergic projections in the dorsal striatum in order to maintain directed movement. To test this hypothesis, we performed TH-based immunohistochemical analyses of striatal sections in K320E-TwinkleDaN and control mice (Fig. 3-15A). The striatum was further divided into the dorsal caudate putamen (CPu), where most of the SNc DaNs are projecting to (Liss and Roeper 2008), and the nucleus accumbens (NAcc), which is mostly innervated by VTA DaNs (Miller et al. 1997; Watabe-Uchida et al. 2012). Although DaN numbers were unaltered at this age, 5-month-old homozygous K320E-TwinkleDaN mice revealed a slight decrease of the TH-positive fibre density in the CPu compared to control animals (Fig. 3-15B, control 100.00 ± 1.38 %, K320E/K320EDaN 82.66 ± 5.71 %, one-way ANOVA, P=0.0240). In contrast, dopaminergic projections in the NAcc were not affected (control 100.00 ± 7.90 %, K320E/K320EDaN 95.35 ± 1.59 %, one-way ANOVA, n.s.). Due to the mild decrease of TH-positive fibres in the CPu, whole striatum quantification of fibre density was significantly reduced as well (control 100.00 ± 1.93 %, K320E/K320EDaN 86.80 ± 4.13 %, one-way ANOVA, P=0.0430). There were no differences between heterozygous K320E-TwinkleDaN and control mice for any of the projection areas (Striatum
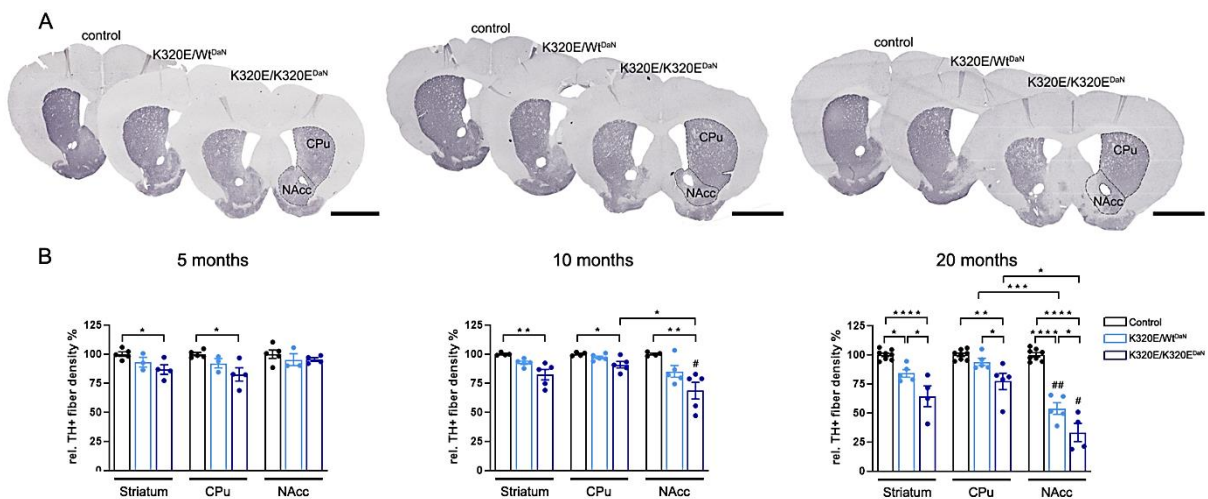
Fig. 3-15 Severe loss of TH-positive fibre density in the NAcc of K320E-Twinkle[DaN] mice. A) Immunohistochemical staining of TH-positive fibres in the striatum of 5-, 10- and 20-month-old hetero- and homozygous K320E-Twinkle[DaN] and control mice. The striatum is divided into the dorsal caudate putamen (CPu) with dopaminergic projections originating from the SNc, and the ventral nucleus accumbens (NAcc), which is innervated by fibres of VTA DaNs. Scale bar, 2000 μm. B) Quantification of the TH-positive fibre density revealed an age-dependent loss in the NAcc of K320E-Twinkle[DaN] mice. Whereas at 5 months of age, a reduction of fibre density was only present in the CPu of homozygous K320E-Twinkle[DaN] mice, 10-month-old animals showed a loss of fibre density in the NAcc, which was even stronger when compared to the CPu. At the age of 20 months, the selective loss of TH-positive fibres in the NAcc became apparent in both hetero- and homozygous K320E-Twinkle[DaN] animals (control mice n = 4-8, K320E/Wt[DaN] mice n = 3-5, K320E/K320E[DaN] mice n = 4-5). # indicates significance compared to individuals of the prior time point. Data are represented as mean ± SEM; * p < 0.05, ** p < 0.01, *** p < 0.001, **** p < 0.0001, # p < 0.05, ## p < 0.01.

93.14 ± 4.11 %, CPu 92.10 ± 3.96 %, NAcc 95.27 ± 5.14 %, one-way ANOVA, n.s.). After 10 months of age, the density of TH-positive fibres were still slightly affected in the CPu (control 100.00 ± 0.70 %, K320E/K320EDaN 90.94 ± 1.92 %, one-way ANOVA, P=0.0213) and striatum (control 100.00 ± 0.57 %, K320E/K320EDaN 82.30 ± 4.43 %, one-way ANOVA, P=0.0045) of homozygous K320E-TwinkleDaN compared to control animals, but did not show further reduction compared to 5-month-old individuals (CPu, unpaired t test, n.s.; striatum, unpaired t test, n.s.). Interestingly, dopaminergic innervation of the NAcc was significantly reduced (control 100.00 ± 0.74 %, K320E/K320EDaN 68.62 ± 7.21 %, one-way ANOVA, P=0.0067) and even more affected when compared to the CPu (two-way ANOVA, P=0.0330). The reduction in the NAcc was further enhanced compared to 5-month-old individuals (K320E/K320EDaN 5 months NAcc 95.27 ± 5.14 %, 10 months 68.62 ± 7.21 %, unpaired t-test, P=0.0146). Again, no differences were found between heterozygous K320E-TwinkleDaN and control mice for any of the observed projection areas (striatum 92.54 ± 1.39 %, CPu 97.23 ± 1.03 %, NAcc 85.23 ± 4.93 %, one-way ANOVA, n.s.). At the age of 20 months, heterozygous K320E-TwinkleDaN mice showed a decreased fibre density in the NAcc (control 100.00 ± 1.80 %, K320E/WtDaN 53.92 ± 4.95 %, one-way ANOVA, P<0.0001), but not in the CPu (control 100.00 ± 1.51 %, K320E/WtDaN 94.02 ± 2.99 %, one-way ANOVA, n.s.) when compared to control animals. Due to the decrease of TH-positive fibres in the NAcc, whole striatum quantification of fibre density was significantly reduced as well (control 100.00 ± 1.52 %, K320E/WtDaN 84.07 ± 3.14 %, one-way ANOVA, P=0.0333). Homozygous K320E-TwinkleDaN mice revealed a significant fibre loss in all three projection areas (striatum, control 100.00 ± 1.52 %, K320E/K320EDaN 64.36 ± 8.90 %, one-way ANOVA, P<0.0001, CPu control 100.00 ± 1.51 %, K320E/K320EDaN 77.23 ± 6.92 %, one-way ANOVA, P=0.0017, NAcc control 100.00 ± 1.80 %, K320E/K320EDaN 33.34 ± 7.84 %, one-way ANOVA, P<0.0001). However, the NAcc showed a stronger decrease in TH-positive fibres than the CPu for both hetero- and homozygous K320E-TwinkleDaN mice (K320E/WtDaN two-way ANOVA, P=0.0006; K320E/K320EDaN two-way ANOVA, P=0.0175). Moreover, the loss of the dopaminergic projections in the NAcc of both mutants was stronger when compared to 10-month-old individuals (K320E/WtDaN 10 months 85.23 ± 4.93 %, 20 months 53.92 ± 4.95 %, unpaired t test, P=0.0021; K320E/K320EDaN 10 months 68.62 ± 7.21 %, 20 months 33.34 ± 7.84 %, unpaired t test, P=0.0131).

K320E-Twinkle[DaN] mice show depressive-like behavior

The loss of VTA DaNs as well as their projections to the NAcc may cause a depression-related phenotype (Brown et al. 2012; Furlanetti et al. 2016). In order to inspect our K320E-TwinkleDaN mice for depressive-like behavior, the tail suspension test as well as the sugar preference test were carried out initially (Fig. 3-16A). No difference was found in the body weight between the genetic groups at 10 and 20 months of age (Fig. 3-16B, 10 months: control
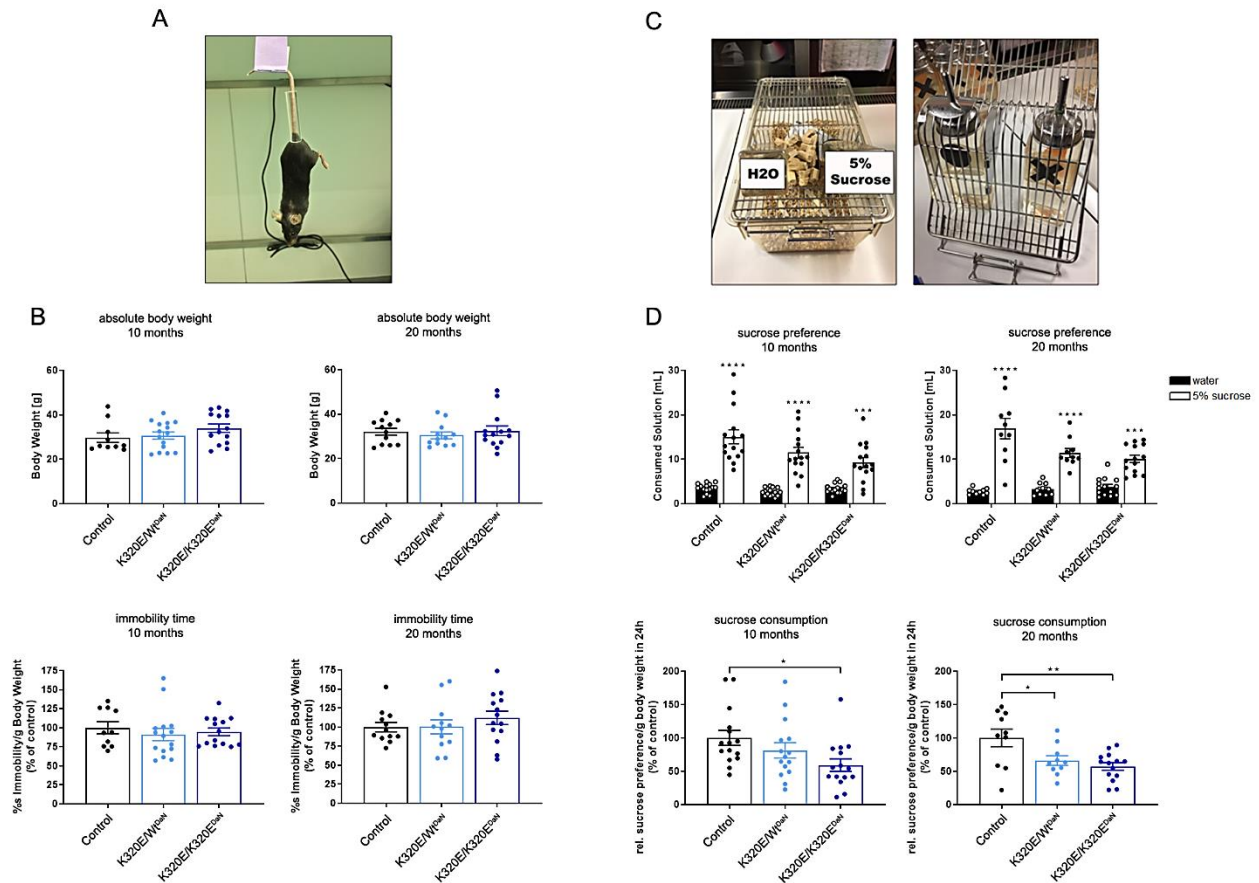
Fig. 3-16 Decreased sugar consumption but unaltered immobility time of K320E-Twinkle[DaN] mice. A) Exemplary representation of a test mouse during the tail suspension test. B) Quantitative data showed no differences in the body weight of K320E-Twinkle[DaN] mice compared to control animals. However, the time to reach immobility did not significantly differ between K320E-Twinkle[DaN] and control mice for both ages (n = 10-15). C) Sugar preference test setup presenting an experimental, marked cage equipped with one bottle of tap water and one bottle of 5% sucrose solution. D) Quantitative data revealed sugar preference for all animals, but reduced sucrose consumption of both hetero- and homozygous 20-month-old K320E-Twinkle[DaN] mice compared to control animals. At the age of 10 months, homozygous K320E-Twinkle[DaN] mice already showed less sucrose consumption when compared to control animals (n = 10-15). Data are represented as mean ± SEM; * p < 0.05, ** p < 0.01, *** p < 0.001, **** p < 0.0001.

29.70 ± 2.15 g, K320E/WtDaN 30.63 ± 1.62 g, K320E/K320EDaN 33.99 ± 1.89 g, one-way ANOVA, n.s.; 20 months: control 32.08 ± 1.56 g, K320E/WtDaN 30.45 ± 1.51 g, K320E/K320EDaN 32.49 ± 2.17 g, one-way ANOVA, n.s). Neither 10- nor 20-month-old K320E-TwinkleDaN mice showed an alteration in the relative immobility time when compared to control animals (10 months: control 100.00 ± 7.91 %, K320E/WtDaN 91.06 ± 8.09 %, K320E/K320EDaN 94.55 ± 5.00 %, one-way ANOVA, n.s.; 20 months: control 100.00 ± 6.29 %, K320E/WtDaN 100.26 ± 9.26 %, K320E/K320EDaN 112.09 ± 8.71 %, one-way ANOVA, n.s.).

The sugar preference test (Fig. 3-16C) revealed a significant preference for the 5% sucrose solution compared to normal tap water in all genetic groups at the age of 10 months (Fig. 3-16D, control: water 3.51 ± 0.27 mL, 5% sucrose 15.05 ± 1.57 mL, two-way ANOVA, P<0.0001; K320E/WtDaN: water 2.65 ± 0.22 mL, 5% sucrose 11.48 ± 1.21 mL, two-way

ANOVA, P<0.0001; K320E/K320EDaN: water 3.43 ± 0.27 mL, 5% sucrose 9.27 ± 1.13 mL, two-way ANOVA, P=0.0006). The same was true for 20-month-old animals (control: water 3.08 ± 0.38 mL, 5% sucrose 16.36 ± 2.15 mL, two-way ANOVA, P<0.0001; K320E/WtDaN: water 3.72 ± 0.47 mL, 5% sucrose 11.07 ± 0.87 mL, two-way ANOVA, P<0.0001; K320E/K320EDaN: water 3.83 ± 0.51 mL, 5% sucrose 9.88 ± 0.80 mL, two-way ANOVA, P=0.0003). However, relative as well as normalized sucrose consumption was significantly reduced in 10-month-old homozygous K320E-TwinkleDaN mice when compared to control animals (control 100.00 ± 11.18 %, K320E/K320EDaN 59.21 ± 9.33 %, one-way ANOVA, P=0.0302), in contrast to heterozygous mutants (K320E/WtDaN 81.33 ± 11.46 %, one-way ANOVA, n.s.). After 20 months of age, both hetero- and homozygous K320E-TwinkleDaN animals showed a decrease in sucrose consumption compared to control mice (control 100.00 ± 13.23 %, K320E/WtDaN 66.26 ± 6.57 %, one-way ANOVA, P=0.0430; K320E/K320EDaN 58.25 ± 5.61 %, one-way ANOVA, P=0.0040).

Discussion

In this study, the impact of the increased accumulation of mtDNA deletions in DaNs on neuronal survival, mitochondrial function and behavior was investigated by generating mice, which express a mutated variant of Twinkle (K320E) exclusively in DaNs. As a first step, the voluntary movement behavior of hetero- and homozygous K320E-TwinkleDaN mice was investigated, showing no differences compared to control animals even at the age of 20 months (Fig. 3-11B). However, stereological quantification of midbrain DaNs revealed a severe neurodegeneration in both mutant genotypes, whereas it was most pronounced in homozygous expressers (Fig. 3-12B). Region-specific differentiation further disclosed that neurodegeneration was not selective for the SNc (Fig. 3-12C). In PD, motor symptoms start to arise when ~30-50% of SNc DaNs are gone (Obeso et al. 2017). PD-related mouse models show impaired motor activity at a DaN loss rate of ~40-55% upon genetic interference (Wakamatsu et al. 2007; Lu et al. 2009; Chen et al. 2012; Rousseaux et al. 2012) and ~60% when pharmacologically induced, respectively (Crocker et al. 2003; Becker et al. 2018; Zeng et al. 2018). We have already shown that MitoPark mice, which are lacking the TFAM protein, essential for transcription and maintenance of the mtDNA, exclusively in DaNs, present a motor decline being visible at the age of 14 weeks and even more severe at 20 weeks, when ~68% of SNc DaNs are lost due to a detrimental imbalance in the mitochondrial redox system (Ricke et al. 2020). Homozygous K320E-TwinkleDaN mice, however, revealed normal motor function with only ~30% of neurons left. Golden et al. (2013) already reported about the compensatory capacity of SNc DaNs. After the early developmental destruction of DaNs, 10% of SNc DaNs were sufficient to ensure movement control, probably due to an enhanced sensitization of striatal dopamine receptors. Nevertheless, to our knowledge, homozygous K320E-

TwinkleDaN mice are the first PD-related mouse model showing motor behavior compensation in aging mice despite the degeneration of SNc DaNs by ~70%.

Next, we wanted to investigate if the loss of DaNs in K320E-TwinkleDaN mice has been induced by mitochondrial dysfunction upon impairment of the mtDNA replication machinery. Indeed, COX-deficient cells as well as reduced complex IV expression levels were found in both hetero- and homozygous animals at the age of 5 and 10 months (Fig. 3-13 and 3-14B). Interestingly, we observed a decline in the number of mitochondrial-deficient DaNs with increasing age. Eventually, at the age of 20 months, DaNs expressed normal complex IV levels in both SNc and VTA, indicating that the surviving DaN populations successfully adapted to the impaired mtDNA replication. One adaptation could be an extremely efficient mitochondrial quality control mechanism, which enables the surviving DaN populations to both detect and remove dysfunctional mitochondria and those which surpassed a certain threshold of mtDNA deletions, respectively.

In PD as well as related animal models, the loss of SNc DaNs is accompanied by the reduced innervation of the dorsal striatum, the CPu, whereas the ventral NAcc is spared (Miller et al. 1997; Ekstrand et al. 2007; Villalba et al. 2009; Boix et al. 2015). In fact, it has been shown that dopaminergic striatal nerve terminals degenerate even before their cell bodies (Chu et al. 2012; Kordower et al. 2013). To examine to what extent striatal innervation is affected in K320E-TwinkleDaN mice, densitometric analysis of dopaminergic terminals was performed. Surprisingly, 77% of striatal fibres were still preserved in the CPu of homozygous mutants despite the severe neurodegeneration (Fig. 3-15B), which is sufficient to maintain voluntary movement control. This imbalance between the number of SNc DaNs and its projections points to compensatory axonal sprouting. Given the unique morphological architecture of these neurons, any additional spread of their axon terminals would be astonishing. The axon of a single SNc DaN is estimated to give rise to up to 245,000 synapses in rats and 2.4 million synapses in humans, respectively (Bolam and Pissadaki 2012). The massive arborization of concurrently unmyelinated axons (Braak et al. 2004) is accompanied by an extremely high energetic demand in order to maintain ion homeostasis for action potential propagation and synaptic processes (Pacelli et al. 2015). In our homozygous K320E-TwinkleDaN mice, the surviving ~30% of SNc DaNs consequently have to deal with even higher energetic demands and therefore rely on the increased supply of functioning mitochondria. Again, efficient mitochondrial quality control is of great importance in these neurons. Furthermore, the enhanced synaptic energy supply of dopaminergic terminals in homozygous K320E-TwinkleDaN mice might be further counteracted by an increased mobilization of astrocytes, which feed synapses with energy substrates from blood vessels on demand (Tsacopoulos and Magistretti 1996; Simard et al. 2003; Stobart and Anderson 2013).

To further unravel compensatory adaptations on a cellular level as well as to confirm the presence of mtDNA deletions in the surviving population of SNc DaNs, transcriptomic analysis of isolated DaNs will be performed after DAT-specific fluorescent activated cell sorting. Increased axonal arborization will be analyzed in future experiments by fluorescent labeling of single SNc DaNs and subsequent morphological analysis using acute midbrain slices of 20-month-old K320E-TwinkleDaN and control mice. At the same time, electrophysiological recordings will be performed to unmask potential adaptations of single SNc DaNs in order to preserve synaptic activity in the risen amount of axon terminals per cell. It is likely, that surviving neurons might disclose increased burst activities as observed in PD patients (Zaghloul et al. 2009).

Noteworthy, VTA DaNs were additionally affected besides the SNc in K320E-TwinkleDaN mice (Fig. 3-12B). Interestingly, the number of VTA DaNs was even lower compared to the SNc in homozygous mutants at the age of 20 months. Administration of the ubiquitin proteasome system inhibitor lactacystin, which has been used to model nigrostriatal degeneration in rats, was reported to decrease the number of VTA DaNs by ~32%, whereas loss of SNc DaNs was ~54% (Harrison et al. 2016). Interestingly, overexpression of the human amyloid precursor protein led to an age-dependent loss of VTA DaNs, whereas the SNc was spared (Nobili et al. (2016). Hence, to our knowledge, K320E-TwinkleDaN mice are the first PD-related model revealing a similar (heterozygous) and even enhanced (homozygous) loss rate of VTA DaNs. In contrast to projections from SNc DaNs, fibres originating from the VTA were severely reduced (Fig. 3-15B). It has been shown that both the loss of VTA DaNs and dopaminergic fibres in the NAcc lead to depressive behavior (Brown et al. 2012; Furlanetti et al. 2016; Nobili et al. 2017). We therefore verified, if this behavior is manifested in our K320E-TwinkleDaN mice in consequence of the loss of the mesolimbic pathway. No abnormalities became apparent in the tail suspension test (Fig. 3-16B), whereas the test's outcome could be influenced by its dependence on the stress condition as well as motor performance, as even increased spontaneous motor activity was observed for several mutant mice. In addition, the loss of VTA DaNs might have modified the activity of the amygdala, which is innervated by the VTA and controlling anxiety behavior (Brinley-Reed and McDonald 1999; Bissière et al. 2003; Kröner et al. 2005). This could have led to decreased fear in K320E-TwinkleDaN mice which in turn might have distorted the measured immobility time. However, depressive-like behavior was detected by reduced sugar preference in K320E-TwinkleDaN mice (Fig. 3-16D). Furthermore, social behavior in K320E-TwinkleDaN mice could be altered, since optogenetic approaches have highlighted the importance of VTA DaNs projecting to the medial prefrontal cortex for social interaction in mice (Chaudhury et al. 2013; Friedman et al. 2014). Social behavior will therefore be assessed by performing the three chamber test.

Here, we present the first genetic animal model for depression that is induced by the loss of the dopaminergic mesolimbic pathway upon mitochondrial dysfunction. Moreover, our data showing preserved motor function and CPu innervation despite severe SNc DaN degeneration in homozygous K320E-TwinkleDaN mice could be of great importance. Understanding, how small amounts of surviving SNc DaNs can counteract mtDNA deletions as well as mitochondrial dysfunction with increasing age, and maintain synaptic processes in the dorsal striatum although facing an energetic mammoth task, might help to find new pathways to prevent the loss of SNc DaNs and motor symptoms in PD.

Acknowledgements

Financial Disclosures

References

Aradjanski, Marijana; Dogan, Sukru Anil; Lotter, Stephan; Wang, Shuaiyu; Hermans, Steffen; Wibom, Rolf et al. (2017): DARS2 protects against neuroinflammation and apoptotic neuronal loss, but is dispensable for myelin producing cells. Hum Mol Genet 26 (21), pp. 4181–4189. DOI: 10.1093/hmg/ddx307.

Baris, Olivier R.; Ederer, Stefan; Neuhaus, Johannes F. G.; Kleist-Retzow, Jürgen-Christoph von; Wunderlich, Claudia M.; Pal, Martin et al. (2015): Mosaic Deficiency in Mitochondrial Oxidative Metabolism Promotes Cardiac Arrhythmia during Aging. Cell Met 21 (5), pp. 667–677. DOI: 10.1016/j.cmet.2015.04.005.

Becker, Birte; Demirbas, Melek; Johann, Sonja; Zendedel, Adib; Beyer, Cordian; Clusmann, Hans et al. (2018): Effect of Intrastriatal 6-OHDA Lesions on Extrastriatal Brain Structures in the Mouse. In Mol Neurobiol 55 (5), pp. 4240–4252. DOI: 10.1007/s12035-017-0637-9.

Bender, Andreas; Krishnan, Kim J.; Morris, Christopher M.; Taylor, Geoffrey A.; Reeve, Amy K.; Perry, Robert H. et al. (2006): High levels of mitochondrial DNA deletions in substantia nigra neurons in aging and Parkinson disease. Nat Genet 38 (5), pp. 515–517. DOI: 10.1038/ng1769.

Bissière, Stephanie; Humeau, Yann; Lüthi, Andreas (2003): Dopamine gates LTP induction in lateral amygdala by suppressing feedforward inhibition. Nat Neurosci 6 (6), pp. 587–592. DOI: 10.1038/nn1058.

Boix, Jordi; Padel, Thomas; Paul, Gesine (2015): A partial lesion model of Parkinson's disease in mice--characterization of a 6-OHDA-induced medial forebrain bundle lesion. Behav Brain Res 284, pp. 196–206. DOI: 10.1016/j.bbr.2015.01.053.

Bolam, J. Paul; Pissadaki, Eleftheria K. (2012): Living on the edge with too many mouths to feed: why dopamine neurons die. Mov Disord 27 (12), pp. 1478–1483. DOI: 10.1002/mds.25135.

Braak, Heiko; Ghebremedhin, Estifanos; Rüb, Udo; Bratzke, Hansjürgen; Del Tredici, Kelly (2004): Stages in the development of Parkinson's disease-related pathology. Cell Tissue Res 318 (1), pp. 121–134. DOI: 10.1007/s00441-004-0956-9.

Brinley-Reed, Margaret; McDonald, Alexander J. (1999): Evidence that dopaminergic axons provide a dense innervation of specific neuronal subpopulations in the rat basolateral amygdala. Brain Res 850 (1-2), pp. 127–135. DOI: 10.1016/S0006-8993(99)02112-5.

Brown, C. A.; Campbell, M. C.; Karimi, M.; Tabbal, S. D.; Loftin, S. K.; Tian, L. L. et al. (2012): Dopamine pathway loss in nucleus accumbens and ventral tegmental area predicts apathetic behavior in MPTP-lesioned monkeys. Exp Neurol 236 (1), pp. 190–197. DOI: 10.1016/j.expneurol.2012.04.025.

Can, Adem; Dao, David T.; Terrillion, Chantelle E.; Piantadosi, Sean C.; Bhat, Shambhu; Gould, Todd D. (2012): The tail suspension test. J Vis Exp (59), e3769. DOI: 10.3791/3769.

Chaudhury, Dipesh; Walsh, Jessica J.; Friedman, Allyson K.; Juarez, Barbara; Ku, Stacy M.; Koo, Ja Wook et al. (2013): Rapid regulation of depression-related behaviours by control of midbrain dopamine neurons. Nature 493 (7433), pp. 532–536. DOI: 10.1038/nature11713.

Chen, Chun; Turnbull, Doug M.; Reeve, Amy K. (2019): Mitochondrial Dysfunction in Parkinson's Disease-Cause or Consequence? In Biology 8 (2). DOI: 10.3390/biology8020038.

Chen, C-Y; Weng, Y-H; Chien, K-Y; Lin, K-J; Yeh, T-H; Cheng, Y-P et al. (2012): (G2019S) LRRK2 activates MKK4-JNK pathway and causes degeneration of SN dopaminergic neurons in a transgenic mouse model of PD. Cell Death Differ 19 (10), pp. 1623–1633. DOI: 10.1038/cdd.2012.42.

Chu, Yaping; Morfini, Gerardo A.; Langhamer, Lori B.; He, Yinzhen; Brady, Scott T.; Kordower, Jeffrey H. (2012): Alterations in axonal transport motor proteins in sporadic and experimental Parkinson's disease. Brain 135 (Pt 7), pp. 2058–2073. DOI: 10.1093/brain/aws133.

Crocker, Stephen J.; Smith, Patrice D.; Jackson-Lewis, Vernice; Lamba, Wiplore R.; Hayley, Shawn P.; Grimm, Erich et al. (2003): Inhibition of Calpains Prevents Neuronal and Behavioral Deficits in an MPTP Mouse Model of Parkinson's Disease. J Neurosci 23 (10), pp. 4081–4091. DOI: 10.1523/JNEUROSCI.23-10-04081.2003.

Dölle, Christian; Flønes, Irene; Nido, Gonzalo S.; Miletic, Hrvoje; Osuagwu, Nelson; Kristoffersen, Stine et al. (2016): Defective mitochondrial DNA homeostasis in the substantia nigra in Parkinson disease. Nat Commun 7, p. 13548. DOI: 10.1038/ncomms13548.

Ekstrand, Mats I.; Terzioglu, Mügen; Galter, Dagmar; Zhu, Shunwei; Hofstetter, Christoph; Lindqvist, Eva et al. (2007): Progressive parkinsonism in mice with respiratory-chain-deficient

dopamine neurons. Proc Natl Acad Sci 104 (4), pp. 1325–1330. DOI: 10.1073/pnas.0605208103.

Elstner, Matthias; Müller, Sarina K.; Leidolt, Lars; Laub, Christoph; Krieg, Lena; Schlaudraff, Falk et al. (2011): Neuromelanin, neurotransmitter status and brainstem location determine the differential vulnerability of catecholaminergic neurons to mitochondrial DNA deletions. Mol Brain 4, p. 43. DOI: 10.1186/1756-6606-4-43.

Fasano, Alfonso; Visanji, Naomi P.; Liu, Louis W. C.; Lang, Antony E.; Pfeiffer, Ronald F. (2015): Gastrointestinal dysfunction in Parkinson's disease. Lancet Neurol 14 (6), pp. 625–639. DOI: 10.1016/S1474-4422(15)00007-1.

Friedman, Allyson K.; Walsh, Jessica J.; Juarez, Barbara; Ku, Stacy M.; Chaudhury, Dipesh; Wang, Jing et al. (2014): Enhancing depression mechanisms in midbrain dopamine neurons achieves homeostatic resilience. Science 344 (6181), pp. 313–319. DOI: 10.1126/science.1249240.

Furlanetti, L. L.; Coenen, V. A.; Döbrössy, M. D. (2016): Ventral tegmental area dopaminergic lesion-induced depressive phenotype in the rat is reversed by deep brain stimulation of the medial forebrain bundle. Behav Brain Res 299, pp. 132–140. DOI: 10.1016/j.bbr.2015.11.036.

Golden, Judith P.; Demaro, Joseph A.; Knoten, Amanda; Hoshi, Masato; Pehek, Elizabeth; Johnson, Eugene M. et al. (2013): Dopamine-dependent compensation maintains motor behavior in mice with developmental ablation of dopaminergic neurons. J Neurosci 33 (43), pp. 17095–17107. DOI: 10.1523/JNEUROSCI.0890-13.2013.

Hanisch, Frank; Kornhuber, Malte; Alston, Charlotte L.; Taylor, Robert W.; Deschauer, Marcus; Zierz, Stephan (2015): SANDO syndrome in a cohort of 107 patients with CPEO and mitochondrial DNA deletions. J Neurol Neurosurg Psychiatry 86 (6), pp. 630–634. DOI: 10.1136/jnnp-2013-306748.

Holzer, Tatjana; Probst, Kristina; Etich, Julia; Auler, Markus; Georgieva, Veronika S.; Bluhm, Björn et al. (2019): Respiratory chain inactivation links cartilage-mediated growth retardation to mitochondrial diseases. J Cell Biol 218 (6), pp. 1853–1870. DOI: 10.1083/jcb.201809056.

Hudson, G.; Deschauer, M.; Busse, K.; Zierz, S.; Chinnery, P. F. (2005): Sensory ataxic neuropathy due to a novel C10Orf2 mutation with probable germline mosaicism. Neurology 64 (2), pp. 371–373. DOI: 10.1212/01.WNL.0000149767.51152.83.

Kordower, Jeffrey H.; Olanow, C. Warren; Dodiya, Hemraj B.; Chu, Yaping; Beach, Thomas G.; Adler, Charles H. et al. (2013): Disease duration and the integrity of the nigrostriatal system in Parkinson's disease. Brain 136 (Pt 8), pp. 2419–2431. DOI: 10.1093/brain/awt192.

Kraytsberg, Yevgenya; Kudryavtseva, Elena; McKee, Ann C.; Geula, Changiz; Kowall, Neil W.; Khrapko, Konstantin (2006): Mitochondrial DNA deletions are abundant and cause functional impairment in aged human substantia nigra neurons. Nat Genet 38 (5), pp. 518–520. DOI: 10.1038/ng1778.

Kröner, Sven; Rosenkranz, J. Amiel; Grace, Anthony A.; Barrionuevo, German (2005): Dopamine modulates excitability of basolateral amygdala neurons in vitro. J Neurophysiol 93 (3), pp. 1598–1610. DOI: 10.1152/jn.00843.2004.

Kurtis, Monica M.; Rodriguez-Blazquez, Carmen; Martinez-Martin, Pablo (2013): Relationship between sleep disorders and other non-motor symptoms in Parkinson's disease. Parkinsonism Relat Disord 19 (12), pp. 1152–1155. DOI: 10.1016/j.parkreldis.2013.07.026.

Liss, Birgit; Roeper, Jochen (2008): Individual dopamine midbrain neurons: functional diversity and flexibility in health and disease. Brain Res Rev 58 (2), pp. 314–321. DOI: 10.1016/j.brainresrev.2007.10.004.

Lu, Xiao-Hong; Fleming, Sheila M.; Meurers, Bernhard; Ackerson, Larry C.; Mortazavi, Farzad; Lo, Victor et al. (2009): Bacterial artificial chromosome transgenic mice expressing a truncated mutant parkin exhibit age-dependent hypokinetic motor deficits, dopaminergic neuron degeneration, and accumulation of proteinase K-resistant alpha-synuclein. J Neurosci 29 (7), pp. 1962–1976. DOI: 10.1523/JNEUROSCI.5351-08.2009.

Meissner, Christoph; Bruse, Petra; Mohamed, Salaheldien Ali; Schulz, Anja; Warnk, Hanne; Storm, Thilo; Oehmichen, Manfred (2008): The 4977 bp deletion of mitochondrial DNA in human skeletal muscle, heart and different areas of the brain: a useful biomarker or more? Exp Gerontol 43 (7), pp. 645–652. DOI: 10.1016/j.exger.2008.03.004.

Michel, Patrick P.; Hirsch, Etienne C.; Hunot, Stéphane (2016): Understanding Dopaminergic Cell Death Pathways in Parkinson Disease. Neuron 90 (4), pp. 675–691. DOI: 10.1016/j.neuron.2016.03.038.

Miller, G. W.; Staley, J. K.; Heilman, C. J.; Perez, J. T.; Mash, D. C.; Rye, D. B.; Levey, A. I. (1997): Immunochemical analysis of dopamine transporter protein in Parkinson's disease. Ann Neurol 41 (4), pp. 530–539. DOI: 10.1002/ana.410410417.

Neuhaus, Johannes F. G.; Baris, Olivier R.; Hess, Simon; Moser, Natasha; Schröder, Hannsjörg; Chinta, Shankar J. et al. (2014): Catecholamine metabolism drives generation of mitochondrial DNA deletions in dopaminergic neurons. Brain 137 (Pt 2), pp. 354–365. DOI: 10.1093/brain/awt291.

Neuhaus, Johannes Friedrich Georg; Baris, Olivier Richard; Kittelmann, Anne; Becker, Katrin; Rothschild, Markus Alexander; Wiesner, Rudolf Josef (2017): Catecholamine Metabolism Induces Mitochondrial DNA Deletions and Leads to Severe Adrenal Degeneration during Aging. Neuroendocrinology 104 (1), pp. 72–84. DOI: 10.1159/000444680.

Nobili, Annalisa; Latagliata, Emanuele Claudio; Viscomi, Maria Teresa; Cavallucci, Virve; Cutuli, Debora; Giacovazzo, Giacomo et al. (2017): Dopamine neuronal loss contributes to memory and reward dysfunction in a model of Alzheimer's disease. Nat Comm 8, p. 14727. DOI: 10.1038/ncomms14727.

Obeso, J. A.; Stamelou, M.; Goetz, C. G.; Poewe, W.; Lang, A. E.; Weintraub, D. et al. (2017): Past, present, and future of Parkinson's disease: A special essay on the 200th Anniversary of the Shaking Palsy. Mov Disord 32 (9), pp. 1264–1310. DOI: 10.1002/mds.27115.

Pacelli, Consiglia; Giguère, Nicolas; Bourque, Marie-Josée; Lévesque, Martin; Slack, Ruth S.; Trudeau, Louis-Éric (2015): Elevated Mitochondrial Bioenergetics and Axonal Arborization Size Are Key Contributors to the Vulnerability of Dopamine Neurons. Curr Biol 25 (18), pp. 2349–2360. DOI: 10.1016/j.cub.2015.07.050.

Park, Jin-Sung; Davis, Ryan L.; Sue, Carolyn M. (2018): Mitochondrial Dysfunction in Parkinson's Disease: New Mechanistic Insights and Therapeutic Perspectives. Curr Neurol Neurosci Rep 18 (5), p. 21. DOI: 10.1007/s11910-018-0829-3.

Reijnders, Jennifer S. A. M.; Ehrt, Uwe; Weber, Wim E. J.; Aarsland, Dag; Leentjens, Albert F. G. (2008): A systematic review of prevalence studies of depression in Parkinson's disease. Mov Disord 23 (2), 183-9; quiz 313. DOI: 10.1002/mds.21803.

Ricke, K. M.; Paß, T.; Kimoloi, S.; Fährmann, K.; Jüngst, C.; Schauss, A. et al. (2020): Mitochondrial Dysfunction Combined with High Calcium Load Leads to Impaired Antioxidant Defense Underlying the Selective Loss of Nigral Dopaminergic Neurons. J Neurosci (4), pp. 1–12.

Rousseaux, Maxime W. C.; Marcogliese, Paul C.; Qu, Dianbo; Hewitt, Sarah J.; Seang, Sarah; Kim, Raymond H. et al. (2012): Progressive dopaminergic cell loss with unilateral-to-bilateral progression in a genetic model of Parkinson disease. Proc Natl Acad Sci 109 (39), pp. 15918–15923. DOI: 10.1073/pnas.1205102109.

Sciacco, Monica; Bonilla, Eduardo (1996): [43] Cytochemistry and immunocytochemistry of mitochondria in tissue sections. In Giuseppe Attardi (Ed.): Mitochondrial biogenesis and genetics, vol. 264. San Diego, Calif.: Acad Press (Methods in Enzymology, 264), pp. 509–521.

Simard, Marie; Arcuino, Gregory; Takano, Takahiro; Liu, Qing Song; Nedergaard, Maiken (2003): Signaling at the Gliovascular Interface. J Neurosci 23 (27), pp. 9254–9262. DOI: 10.1523/JNEUROSCI.23-27-09254.2003.

Simuni, T.; Fernandez, H. H. (Eds.) (2013): Anxiety in Parkinson's disease. 2nd ed. New York: Humana Press (Parkinson's Disease and Nonmotor Dysfunction).

Stobart, Jillian L.; Anderson, Christopher M. (2013): Multifunctional role of astrocytes as gatekeepers of neuronal energy supply. Front Cell Neurosci 7, p. 38. DOI: 10.3389/fncel.2013.00038.

Suomalainen, A.; Majander, A.; Haltia, M.; Somer, H.; Lönnqvist, J.; Savontaus, M. L.; Peltonen, L. (1992): Multiple deletions of mitochondrial DNA in several tissues of a patient with severe retarded depression and familial progressive external ophthalmoplegia. J Clin Invest 90 (1), pp. 61–66. DOI: 10.1172/JCI115856.

Tsacopoulos, M.; Magistretti, P. J. (1996): Metabolic coupling between glia and neurons. J Neurosci 16 (3), pp. 877–885. DOI: 10.1523/JNEUROSCI.16-03-00877.1996.

Villalba, Rosa M.; Lee, Heyne; Smith, Yoland (2009): Dopaminergic denervation and spine loss in the striatum of MPTP-treated monkeys. Exp Neurol 215 (2), pp. 220–227. DOI: 10.1016/j.expneurol.2008.09.025.

Wakamatsu, Masaki; Ishii, Aiko; Ukai, Yuriko; Sakagami, Junko; Iwata, Shingo; Ono, Mieko et al. (2007): Accumulation of phosphorylated alpha-synuclein in dopaminergic neurons of transgenic mice that express human alpha-synuclein. J Neurosci Res 85 (8), pp. 1819–1825. DOI: 10.1002/jnr.21310.

Watabe-Uchida, Mitsuko; Zhu, Lisa; Ogawa, Sachie K.; Vamanrao, Archana; Uchida, Naoshige (2012): Whole-brain mapping of direct inputs to midbrain dopamine neurons. Neuron 74 (5), pp. 858–873. DOI: 10.1016/j.neuron.2012.03.017.

Weiland, Daniela; Brachvogel, Bent; Hornig-Do, Hue-Tran; Neuhaus, Johannes F. G.; Holzer, Tatjana; Tobin, Desmond J. et al. (2018): Imbalance of Mitochondrial Respiratory Chain Complexes in the Epidermis Induces Severe Skin Inflammation. J Invest Dermatol 138 (1), pp. 132–140. DOI: 10.1016/j.jid.2017.08.019.

Zaghloul, Kareem A.; Blanco, Justin A.; Weidemann, Christoph T.; McGill, Kathryn; Jaggi, Jurg L.; Baltuch, Gordon H.; Kahana, Michael J. (2009): Human substantia nigra neurons encode unexpected financial rewards. Science 323 (5920), pp. 1496–1499. DOI: 10.1126/science.1167342.

Zeng, Xian-Si; Geng, Wen-Shuo; Jia, Jin-Jing (2018): Neurotoxin-Induced Animal Models of Parkinson Disease: Pathogenic Mechanism and Assessment. ASN neuro 10, 1759091418777438. DOI: 10.1177/1759091418777438.

4   Discussion

Here, the results presented in each of the three manuscripts will be discussed in a coherent manner, in accordance with the key questions of the thesis. In particular, the first chapter focuses on the differences between distinct dopaminergic populations upon the loss of TFAM and thereby compares the outcomes of the first (3.1, Ricke, Paß et al. 2020) and the second manuscript (3.2, Paß et al. 2020). The second chapter, in turn, contrasts the well-known MitoPark model with our newly generated K320E-Twinkle[DaN] model in consideration of the data presented in the first and the third manuscript (3.3, Paß et al. *ready for submission*).

4.1   DaN Subpopulations Are Differently Affected Upon TFAM Depletion

In the MitoPark mouse model, midbrain SNc DaNs are severely affected upon the loss of TFAM, characterized by striatal denervation as well as neurodegeneration starting at the age of 12 weeks (Fig. 3-1A-D), as initially shown (Ekstrand et al. 2007). Breakdown of the nigrostriatal pathway consequently leads to progressive decline in motor activity (Fig. 3-1E). Conversely, VTA DaNs are relatively spared from neurodegeneration with more or less preserved striatal projections (Fig. 3-1A-D). One may argue that the differential susceptibility results from an incomplete penetrance of DatCre-mediated recombination in VTA DaNs and that TFAM inactivation is consequently absent in the surviving DaN population. However, both SNc and VTA DaNs consistently reveal DatCre-mediated recombination at E15.5, represented by YFP expression (Fig. 3-6), and no TH-positive but YFP-negative cells are apparent. In addition, at 12 weeks of age, SNc and VTA DaNs equally disclose mitochondrial impairment shown by low COX activity as well as reduced COXI expression (Fig. 3-2). This underscores the significance of cell type-specific factors concerning the selective vulnerability of SNc DaNs towards mitochondrial dysfunction.

In the OB of MitoPark mice, DaNs present low COX activity only at a relatively late age of 30 weeks (Fig. 3-7E). In contrast to the midbrain, where TFAM KO takes place during embryonic development at E15.5, in OB DaNs this occurs only at around two weeks after birth (P14) (Fig. 3-6). However, OB DaNs show mitochondrial impairment as a consequence after approximately 28 weeks, whereas midbrain DaNs reveal respiratory chain deficits already 13 weeks after the KO of TFAM. In addition, COX-deficient cells appear to be much less frequent in the OB when compared to midbrain. Thus, these distinct subpopulations of DaNs respond very differently to inactivation of mitochondrial gene expression.

While mitochondrial impairment of midbrain DaNs is followed by severe neurodegeneration in the SNc after 20 weeks, quantification of DaNs in the OB of MitoPark mice only revealed a reduced number of SCs after 30 weeks of age, whereas the amount of LACs did not change at all (Fig. 3-9C). Investigation at more extended time points was not possible due to the severe motor symptoms of these animals. It has to be noted, that regarding the *in situ* analysis it is

unclear whether COX deficiency in OB neurons of MitoPark mice is restricted to SCs, thereby explaining the decreased numbers of only this dopaminergic subtype, or whether it occurs to the same extent in both OB DaN populations.

OB as well as VTA DaNs differ from their vulnerable counterparts in the SNc regarding distinct cellular characteristics. Though each of these dopaminergic subtypes are reported to be pacemakers, VTA and OB DaNs mainly use sodium currents for autonomous oscillatory activity (Pignatelli et al. 2005; Khaliq and Bean 2010; Pignatelli and Belluzzi 2017). Conversely, pacemaking activity in SNc DaNs is associated with Ca^{2+} oscillations which are mainly provided by Ca_v1 (Chan et al. 2007), but also T-type (Guzman et al. 2018; Tabata et al. 2018) and R-Type (Benkert et al. 2019) Ca^{2+} channels, which was reported to be accompanied with enhanced oxidative stress (Guzman et al. 2010). Increased intrinsic Ca^{2+} levels are therefore thought to be a critical factor concerning the susceptibility of SNc DaNs to mitochondrial dysfunction (Surmeier, Guzman, and Sanchez-Padilla 2010; Surmeier et al. 2012; Duda, Potschke, and Liss 2016). In MitoPark mice, it has been shown that decreased I_h, which is associated with a rise in intracellular Ca^{2+} (Carbone et al. 2017), and upregulation of Ca_v1 channel subunits are preceding the death of SNc DaNs (Branch et al. 2016), which might be compensatory mechanisms to preserve neuronal function. This suggest a vicious circle for SNc DaNs with Ca^{2+} playing a crucial role. We could show that the mitochondrial redox system of MitoPark SNc DaNs is disturbed just before the onset of neurodegeneration, in contrast to spared VTA DaNs. Intriguingly, reducing both cytosolic as well as mitochondrial Ca^{2+} influx, normalizes the redox status of SNc DaNs (Fig. 3-4B). Ca^{2+} influx into SNc DaNs is counterbalanced by a high mitochondrial inner membrane potential even in the presence of mitochondrial dysfunction (Fig. 3-5D), but this might consequently further contribute to the detrimental imbalance in the mitochondrial redox system, which in turn eventually leads to neuron death. In order to prevent this, the presence of intracellular buffering proteins appear to be of great importance. In accordance with recent data supporting the neuroprotective role of the Ca^{2+} binding protein calbindin in MPTP-treated monkeys (Inoue et al. 2019), we found an age-dependent increase of the percentage of calbindin-expressing neurons within the surviving SNc DaNs of MitoPark mice (Fig. 3-3B). However, the mechanism of how calbindin might protect DaNs from cell death upon mitochondrial impairment is not fully understood and its potential neuroprotective effect still has to be investigated more closely.

Besides the electrophysiological differences, SNc DaNs further reveal a unique axon morphology. In contrast to VTA as well as OB DaNs, where SCs are even anaxonic (Pignatelli and Belluzzi 2017), DaNs originating from the SNc show an extremely large arborization including ~100,000-250,000 synapses in rats (Bolam and Pissadaki 2012), which implies an extremely high energetic demand already under physiological conditions (Pacelli et al. 2015).

Thus, SNc DaNs are particularly susceptible to additional stressors, especially when impairing energy supply, such as the loss of TFAM followed by mitochondrial dysfunction.

However, a higher vulnerability because of enhanced energetic demands or a special electrophysiological equipment might not apply to SCs in the OB, which are slightly reduced in numbers in 30-week-old MitoPark mice. LACs, which are spared, have an axon and show an even higher firing rate than SCs (Galliano et al. 2018). Thus, it is more likely that the lower number of SCs is due to other factors. In contrast to LACs, SCs are continuously generated via adult neurogenesis, already pointing to an intrinsic and permanently high susceptibility to cell death (Kosaka et al. 1987; Vergano-Vera et al. 2006; Bovetti et al. 2009; Kosaka and Kosaka 2009; Galliano et al. 2018). Although mobilization of progenitor cells in the SVZ of 30-week-old MitoPark mice is indeed increased (Fig. 3-10C-D), indicating a compensatory response due to increased death of SCs upon mitochondrial dysfunction, the amount of progenitor cells present in the OB is stable (Fig. 3-10A-B). Since it is not known when Dat expression is initiated during the development of OB progenitor cells, it is possible that new but not fully maturated neurons are more vulnerable to the TFAM KO and die during differentiation into a dopaminergic phenotype or even before reaching the OB along the RMS.

Despite the relatively low impact of TFAM depletion on OB DaNs, the moderately reduced numbers of SCs are associated with a severely impaired olfactory behavior (Fig. 3-8A-D) of MitoPark mice at the age of 30 weeks. This may be due to temporal shifts in mitral cell activity (Rebello et al. 2014) caused by the lower number or functional changes in SCs. However, loss of olfaction in MitoPark mice might be also directly linked to the preceding loss of the nigrostriatal system as well as VTA neurons, which have been shown to possess direct projections to higher olfactory brain regions, such as the piriform cortex and the olfactory tubercle (Hoglinger et al. 2015; Xiong and Wesson 2016; Zhang, Liu, et al. 2017; Zhang, Zhang, et al. 2017).

4.2 Comparison between MitoPark and K320E-Twinkle[DaN] Mice

The MitoPark mouse presents a well-established model in order to investigate potential mechanisms contributing to the selective loss of SNc DaNs and motor impairment upon mitochondrial dysfunction in PD. Regarding the disease course in humans, however, these animals reveal a very rapid and early-onset recapitulation of the key pathology. In addition, progressive loss of TFAM is most likely not reflecting the initial cause of mitochondrial dysfunction in SNc DaNs of PD patients. Since the elevated accumulation of deleted mtDNA molecules in SNc DaNs with increasing age has been associated with mitochondrial dysfunction and PD development (Bender et al. 2006; Kraytsberg et al. 2006; Elstner et al. 2011), K320E-Twinkle[DaN] mice were generated to investigate the impact of accumulating mtDNA deletions on DaN survival and its contribution to the development of a PD-like

phenotype. In the following, these two mouse models are compared concerning mitochondrial dysfunction, DaN survival, striatal innervation and motor impairment.

4.2.1 Mitochondrial Dysfunction

COX-deficient cells are consistently found in both the SNc and VTA of MitoPark mice at the early age of 12 weeks (Fig. 3-2C). In hetero- and homozygous K320E-Twinkle[DaN] mice, blue cells become visible in the SNc and VTA only after 10 months (Fig. 3-13A), but cells with low COX activity appear to be much less frequent than in the midbrain of MitoPark mice. TFAM is not only important for packaging, but also necessary for mtDNA transcription and is essential for the maintenance of mtDNA (Gustafsson, Falkenberg, and Larsson 2016). The disruption of *Tfam* in midbrain DaNs of MitoPark mice is accompanied with rapidly reduced mtDNA expression (Ekstrand et al. 2007) and causes the progressive loss of mtDNA encoded transcripts. Since the catalytic subunits of COX are encoded by mtDNA, COX deficiency is inevitable and observed in cells located in the SNc and VTA after 12 weeks of age. In contrast to the progressive depletion of mtDNA in the MitoPark model, various cell types have been shown to accumulate mtDNA deletions upon expression of *Twinkle* carrying the K320E mutation, also followed by COX deficiency (Baris et al. 2015; Weiland et al. 2018; Holzer et al. 2019). It is therefore likely that midbrain DaNs of hetero- and homozygous K320E-Twinkle[DaN] mice reveal accumulations of mtDNA deletions over time as well, but analysis of isolated DaNs will be necessary to confirm this. Accumulating deleted molecules upon impaired mtDNA replication is a stochastic event. The time point, at which the threshold for tolerable amounts of mtDNA deletions, which is thought to be around 60% of deleted molecules (Picard, Vincent, and Turnbull 2016), is exceeded and leads to COX deficiency, consequently varies from cell to cell. This is in line with the smaller number of blue cells in the SNc and VTA of 10-month-old K320E-Twinkle[DaN] mice compared to MitoPark animals. The exact mechanism, how K320E impairs the function of TWINKLE and how this contributes to the formation of mtDNA deletions, is still not known. According to the equivalent mutation found in patients with SANDO syndrome causing PEO, the helicase activity might be impaired by K320E through a stalled replication process, thereby promoting large mtDNA deletions to accumulate (Zeviani et al. 1989; Suomalainen et al. 1992; Suomalainen et al. 1997). Correspondingly, it is likely that K320E also belongs to mutations of the primase-like domain, which are suggested to disrupt oligomer formation of TWINKLE (Peter et al. 2019).

In accordance with the COX-SDH assay, DaNs located in the SNc and VTA present equally reduced complex IV expression in 12-week-old MitoPark mice (Fig. 3-2A-B), represented by COXI fluorescence intensity. In K320E-Twinkle[DaN] mice, however, the proportion of midbrain DaNs with reduced complex IV expression decreases with age (Fig. 3-14A-B). Whereas SNc as well as VTA DaNs show low COXI signal in both hetero- and homozygous K320E-Twinkle[DaN] mice at 5 months of age, reduced complex IV expression in 10-month-old

animals is only found in VTA DaNs of homozygous expressers. Eventually, after 20 months of age, normal levels of complex IV are present in both midbrain DaN populations. With regard to neurodegeneration being first detected in K320E-Twinkle[DaN] mice at 10 months of age (Fig. 3-12B-C), we hypothesize that DaNs showing decreased complex IV expression in 5-month-old animals are already perished at later ages and that surviving DaNs successfully adapted to the impaired mtDNA replication upon K320E mutation expression, respectively. This is underscored by the nearly complete absence of COX-deficient cells in the midbrain of K320E-Twinkle[DaN] mice after 20 months of age (Fig. 3-13B).

Thus, impairment of mtDNA replication allows DaNs to adapt, in contrast to rapid mtDNA as well as mtRNA depletion upon loss of TFAM, and therefore prevents mitochondrial dysfunction and eventually neuron death. One adaption of surviving DaNs might be an extremely efficient mitochondrial quality control. A fast detection and subsequent removal of defective mitochondria and those which surpass a certain threshold of deleted molecules, respectively, via mitophagy would be essential to maintain energy supply and thereby neuronal activity in these cells. Accordingly, a beneficial effect of mitophagy stimulation on reducing mtDNA deletion load has been reported in *Drosophila melanogaster* (Kandul et al. 2016). Conversely, reducing mitophagy favors the accumulation of mutant mtDNA molecules in *C. elegans* (Gitschlag et al. 2016). The importance of mitophagy for DaNs, especially in the SNc, is underscored by *PINK1* and *Parkin* mutations causing early-onset PD with selective loss of SNc DaNs (Kilarski et al. 2012; Truban et al. 2017). In addition, DaN-specific autophagy-deficient mice reveal neurodegeneration exclusively in the SNc, accompanied with Lewy pathology and motor deficits (Sato et al. 2018). It might further be possible that surviving DaNs are able to detect the deletion load within mitochondria and rather selectively degrade deleted molecules via the formation of MDVs in order to prevent the loss of whole organelles. Keeping deleted mtDNA molecules at low levels might be assisted by increasing mtDNA copy number, as previously indicated (Trifunovic et al. 2004; Perier et al. 2013). Thereby, sufficient numbers of wild-type mtDNA could be maintained, as was reported in SNc DaNs of healthy individuals during aging (Dolle et al. 2016).

4.2.2 Neurodegeneration

The consistent mitochondrial dysfunction of midbrain DaNs in MitoPark mice is followed by the selective loss of SNc DaNs, according to the pathology in PD patients, at 20 weeks of age (Fig. 3-1D). There is no indication for neurodegeneration of DaNs in hetero- and homozygous K320E-Twinkle[DaN] mice of the same age (Fig. 3-12B-C). Intriguingly, 10-month-old K320E-Twinkle[DaN] mice reveal DaN loss occurring to a similar extent in SNc and VTA, and homozygous expressers are more affected than heterozygous animals. At 20 months of age, homozygous K320E-Twinkle[DaN] mice show further degeneration of DaNs, with the number of DaNs in the VTA being even lower than in the SNc. Thus, there is no selective death of SNc

DaNs in the K320E-Twinkle[DaN] model. Like for the MitoPark model, one may argue that the surviving DaNs in the midbrain of K320E-Twinkle[DaN] mice do not express the K320E mutation as a result of incomplete DatCre-mediated recombination. However, this seems rather unlikely, since DatCre-mediated recombination represented by YFP expression is consistently present in both midbrain neuron populations during embryonic development (Fig. 3-6), and the same DatCre line was used for generating K320E-Twinkle[DaN] mice.

Depending on the perspective, the similar degeneration of SNc and VTA DaNs in our K320E-Twinkle[DaN] mice either point to enhanced VTA DaN vulnerability or decreased SNc DaN vulnerability. When comparing with the selective loss of SNc DaNs presented in MitoPark mice or in other numerous genetically as well as pharmacologically induced PD mouse models and with the well-established susceptibility of SNc DaNs to mitochondrial dysfunction, it is more likely that, in our model, SNc DaNs indeed successfully prevent death for a period of time by unknown compensatory mechanisms upon slow accumulation of mtDNA defects.

4.2.3 Striatal Fibre Density

In MitoPark mice, the progressive degeneration of SNc DaNs is accompanied by the loss of corresponding fibres projecting to the dorsal striatum (CPu, Fig. 3-1A). Moreover, striatal denervation of the CPu starts at about 12 weeks of age (Fig. 3-1C), indicating that axon terminals of SNc DaNs even die before their cell bodies. In line with this, reduced neuritic branching has been recently reported to precede neuron death of MitoPark SNc DaNs (Lynch et al. 2018). In fact, striatonigral dying-back of DaNs is believed to occur in PD patients as well (Cheng, Ulane, and Burke 2010; Chu et al. 2012; Kordower et al. 2013). Like in patients, fibres of VTA DaNs projecting to the NAcc are more or less preserved in the MitoPark model (Fig. 3-1B). Hetero- as well as homozygous K320E-Twinkle[DaN] mice show similarly severe degeneration of SNc and VTA DaNs. Intriguingly, striatal projections are differently affected (Fig. 3-15A-B). Whereas only ~33% (~54%) of dopaminergic fibres are left in the VTA-innervated NAcc, ~77% (~94%) of projections that originate from the SNc are still preserved in homozygous (heterozygous) K320E-Twinkle[DaN] mice at the age of 20 months. The severe loss of VTA DaNs as well as corresponding projections in the ventral striatum is associated with depressive-like behavior in both mutant genotypes, presented by reduced sugar preference (Fig. 3-16D), and thereby supports the contribution of the impaired dopaminergic mesolimbic pathway to PD-related depression.

Astoundingly, while only ~30% of SNc DaNs are left in 20-month-old homozygous K320E-Twinkle[DaN] mice, ~77% of striatal fibres in the corresponding projection area are still preserved. This imbalance points to compensatory axonal sprouting, which would imply an enormous energetic task with regard to the massive axonal arborization and energetic needs these neurons already have (Bolam and Pissadaki 2012; Pacelli et al. 2015). Thus, the small

population of surviving SNc DaNs relies on a fast and proper axonal transport machinery, which is affected in MitoPark mice (Sterky et al. 2011), in order to ensure synaptic supply with a large number of functioning mitochondria. This further underscores the importance of efficient mitochondrial quality control. Correspondingly, generation of new mitochondria is of great importance as well. In fact, increased levels of prokineticin-2 are found in PD patients as well as MitoPark mice and prokineticin-2 has been shown to slow down DaN degeneration by promoting mitochondrial biogenesis (Gordon et al. 2016). Moreover, compensatory responses could arise in the dopaminergic environment, such as enhanced mobilization of astrocytes in the dorsal striatum, which feed presynaptic terminals of SNc DaNs with energy substrates from blood vessels (Tsacopoulos and Magistretti 1996; Simard et al. 2003; Stobart and Anderson 2013) and consequently support the maintenance of neuronal activity.

Besides energetic requirements, electrophysiological properties might change as well upon increased axonal arborization. Surviving SNc DaNs could thereby show increased burst activity, as it is also observed in PD patients (Zaghloul et al. 2009), in order to ensure action potential propagation throughout the more branched axon. It is likely that in this case, ion channel physiology is modified as well to enable increased neuronal activity. In MitoPark mice, for instance, decreased I_h and upregulation of Ca_v1 channel subunits are preceding the death of SNc DaNs (Branch et al. 2016). Enhanced bursting of the surviving SNc DaNs of K320E-Twinkle[DaN] mice would imply even higher Ca^{2+} oscillations and would require further buffering of intracellular Ca^{2+} levels through Ca^{2+}-binding proteins or mitochondria, assuming that pacemaker activity in the surviving SNc DaN population is still primarily dependent on Ca_v channels. Furthermore, K-ATP channel expression or channel sensitivity could be decreased in order to prevent breakdown of SNc DaN activity following the enhanced energetic demands, as previously shown (Liss et al. 2005). Additional investigations are necessary to confirm compensatory axonal sprouting as well as electrophysiological modifications of surviving SNc DaNs in order to preserve striatal DA supply in K320E-Twinkle[DaN] mice.

4.2.4   Motor Impairment

The progressive loss of the dopaminergic nigrostriatal pathway in MitoPark mice is accompanied with a continuous decline in motor activity, becoming first apparent at 14 weeks of age (Fig. 3-1E). Reduced motor performance is explained by the corresponding lack of striatal DA, as previously shown (Ekstrand et al. 2007), which is essential for voluntary movement control (Wichmann and DeLong 1996). Despite the severe loss of SNc DaNs, K320E-Twinkle[DaN] mice, however, still reveal normal motor behavior at the age of 20 months (Fig. 3-11B). In PD, motor symptoms start to occur when ~30-50% of SNc DaNs are perished (Obeso et al. 2017). PD-related mouse models reveal a comparable range, with impaired motor performance at a DaN loss rate of ~40-55% upon genetic interference (Wakamatsu et al. 2007; Lu et al. 2009; Chen et al. 2012; Rousseaux et al. 2012) and ~60% when

pharmacologically induced (Crocker et al. 2003; Becker et al. 2018; Zeng, Geng, and Jia 2018). Given that already ~70% of SNc DaNs are lost in homozygous K320E-Twinkle[DaN] mice, absent motor impairment is surprising. In contrast to other PD-related mouse models, however, SNc DaN projections of K320E-Twinkle[DaN] mice are only mildly affected. Thus, the relatively preserved innervation of the dorsal striatum by dopaminergic projections is likely to maintain sufficient DA levels to ensure motor activity in these animals.

4.3 Clinical Relevance

The MitoPark mouse model mimics pathophysiological key features of PD, including dopaminergic denervation of the dorsal striatum (Fig. 3-1C) preceding the progressive as well
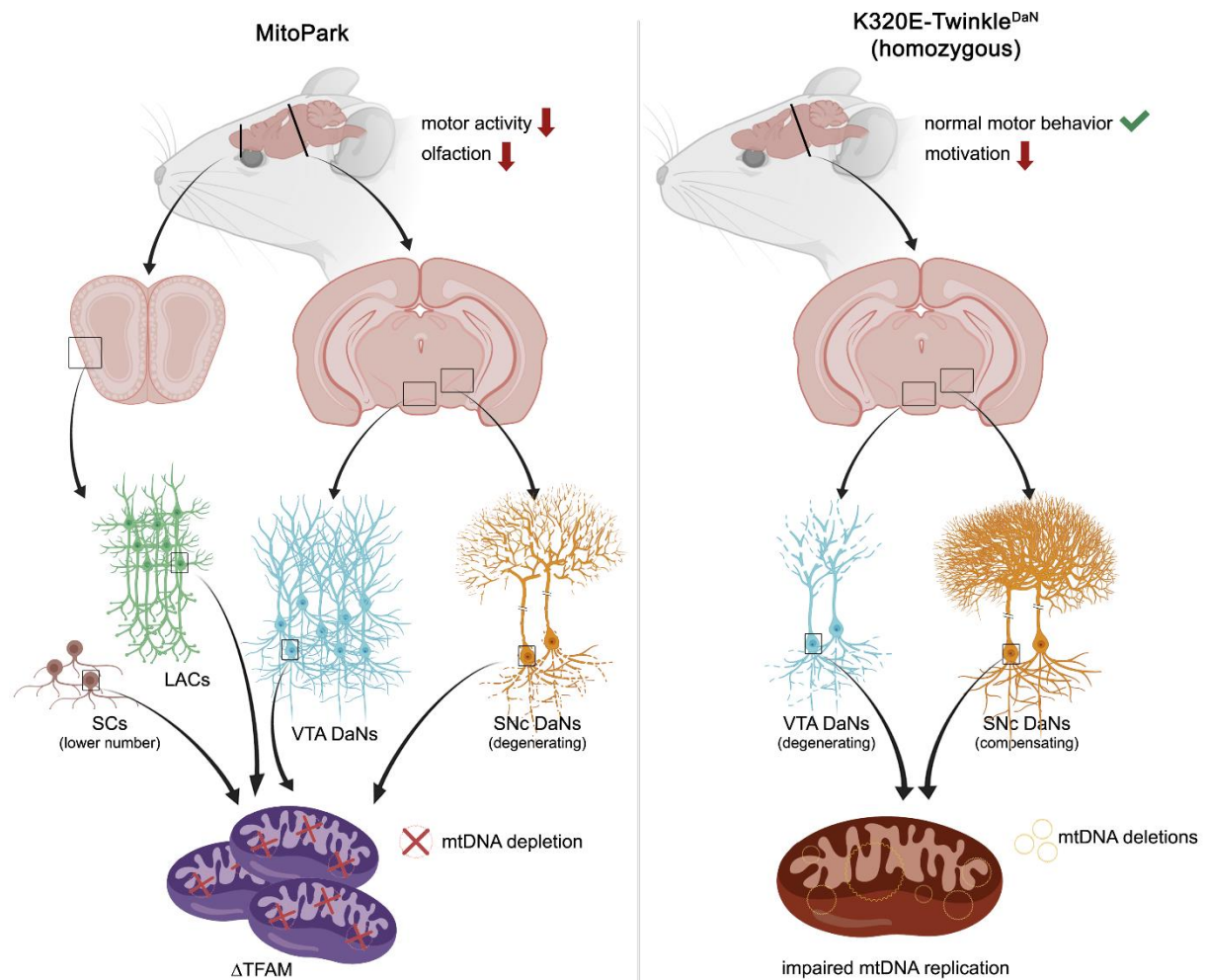
Fig. 4-1 Schematic summary of the presented manuscripts. In MitoPark mice, DaN-specific TFAM KO leads to mitochondrial dysfunction, followed by the selective loss of SNc DaNs in the midbrain, causing progressive motor decline. In contrast, VTA DaNs are more or less spared. In the OB, only SCs are mildly affected in numbers, which is associated with olfactory dysfunction. Impaired mitochondrial function (highlighted by blue mitochondria representing COX-deficiency according to COX/SDH histochemistry) is due to mtDNA depletion. In K320E-Twinkle[DaN] mice, impaired mtDNA replication in DaNs results in severe degeneration of both SNc and VTA DaNs. Whereas loss of the dopaminergic mesolimbic pathway is linked to decreased motivation and depressive-like behavior, respectively, SNc DaN projections in the dorsal striatum are preserved, indicating compensatory axonal sprouting. Surviving midbrain DaNs reveal normal mitochondrial function. This implies cellular adaptation mechanisms, especially for highly energy consuming SNc DaNs, which might be able to maintain low levels of mtDNA deletions and high levels of wild-type mtDNA, respectively, in order to prevent mitochondrial impairment (Figure was generated by using Photoshop CS2 and appropriate templates from BioRender).

as selective loss of SNc DaNs (Fig. 3-1D) upon mitochondrial dysfunction (Fig. 3-2A-C), causing impaired motor behavior (Fig. 3-1E). Thus, this mouse model is suitable for preclinical testing of drugs that may have the potential to slow down the death of SNc DaNs, due to mitochondrial impairment, and to improve motor performance, respectively, as done by a variety of studies (Le Poul et al. 2012; Zhang et al. 2012; Smith et al. 2014; Gordon et al. 2016; Ay et al. 2017; Langley et al. 2017; Hsieh et al. 2020). MitoPark mice further respond to L-DOPA treatment (Galter et al. 2010) and present behavioral as well as biochemical characteristics of long-term L-DOPA treatment in PD patients (Gellhaar et al. 2015).

Conversely, these animals can be used to confirm pathways that might exacerbate SNc DaN degeneration or the motor phenotype (Gellhaar et al. 2015; Langley et al. 2018), and which can in turn be blocked or downregulated. However, in contrast to patients suffering from idiopathic PD, MitoPark mice reveal early-onset and much faster neurodegeneration. In consequence, drugs that are used to treat MitoPark mice will only be able to slow down but may not stop the loss of SNc DaNs. In addition, the rapid disease progression in MitoPark mice might obscure the contribution of potential compensatory processes occurring in humans, which might eventually become part of disease pathology. Olfactory dysfunction occurs in the late disease stage of MitoPark mice (Fig. 3-8A-D) and thereby renders these animals an inappropriate tool to study hyposmia as a prodromal symptom that arises before motor deficits in PD patients.

Reduced TFAM expression and decreasing copies of mtDNA have been reported in SNc DaNs of PD patients (Grunewald et al. 2016). However, TFAM inactivation in DaNs and the consequently ongoing depletion of mtDNA as well as mtRNA in MitoPark mice, do not reflect the pathophysiological mechanism in humans. In PD patients, mitochondrial dysfunction of SNc DaNs rather results from decreasing levels of wild-type mtDNA upon failed copy number elevation (Dolle et al. 2016) and the concurrently increased accumulation of mtDNA deletions over time (Bender et al. 2006; Kraytsberg et al. 2006; Elstner et al. 2011). Hence, K320E-Twinkle[DaN] mice have been generated to study the impact of accumulating mtDNA deletions on survival as well mitochondrial function of DaNs. On the one hand, hetero- and homozygous mutants reveal neurodegeneration of both SNc and VTA DaNs to a similar extent (Fig. 3-12C) after 20 months of age, which disqualifies this model concerning the investigation of drug effects on the selective loss of SNc DaNs. In addition, the absent motor phenotype in these animals does not allow any treatment testing in order to improve motor symptoms. On the other hand, degeneration of the dopaminergic mesolimbic pathway causing depressive-like behavior of K320E-Twinkle[DaN] mice implies the potential of using anti-depressant agents as well as studying depressive states that are independent of serotonergic signalling.

More importantly, however, the K320E-Twinkle[DaN] model offers the chance to identify which cellular mechanisms are responsible for cell death prevention in SNc DaNs of high age despite impaired mtDNA replication. Furthermore, transcriptome as well as proteome analysis of surviving SNc DaNs could unravel pathways that enable axonal sprouting in order to preserve striatal innervation and thereby DA supply, and that consequently ensure compensation of lost DaNs and normal motor function. PD patients are mostly diagnosed when motor symptoms become apparent. At this point, up to ~50% of SNc DaNs are already irreversibly lost (Obeso et al. 2017). Until today, drugs, such as L-DOPA or MAO$_B$ inhibitors, and surgical treatments, including DBS of the STN, can only dampen the outcome of the disease for a certain period of time. However, the origin of motor symptoms, the loss of the nigrostriatal system, cannot be stopped. Thus, novel therapeutic interventions are highly needed. Deciphering the compensatory adaptations of the surviving population of SNc DaNs in K320E-Twinkle[DaN] mice could therefore provide novel targets to both slow down degeneration of SNc DaNs as well as preserve dopaminergic innervation of the dorsal striatum. One may still argue, that those SNc DaNs, which survived in our model, do not express the mutated variant of TWINKLE. Assuming that this is true, it is still astounding how few aged SNc DaNs are able to compensate the severe neuron loss and maintain normal motor function. In this context, pharmacological stimulation of the ongoing pathways in surviving SNc DaNs of K320E-Twinkle[DaN] mice might help to boost resilience in remaining neurons of PD patients, preserving striatal innervation and recovering motor performance. The K320E-Twinkle[DaN] model might therefore host the potential to rescue motor symptoms and DA supply in the dorsal striatum via cellular modification of remaining SNc DaNs, even when neurodegeneration is ongoing.

5   Conclusion

A key role of mitochondrial dysfunction for the selective degeneration of SNc DaNs in PD is confirmed by complex I impairing toxins, high accumulation of mtDNA deletions as well as the variety of mitochondrial-related monogenic mutations in familial forms of PD. However, we showed that distinct DaN populations respond differently to impaired mitochondrial function, underscoring the importance of additional cell-type specific factors for the selective vulnerability of SNc DaNs in PD, such as ion channel equipment, axonal architecture and energetic demands. In the OB, only SCs are mildly affected upon TFAM inactivation following mitochondrial dysfunction. The associated olfactory dysfunction suggests a putative role for OB DaN functionality in the development of PD-related hyposmia. In the midbrain, SNc DaNs selectively degenerate in a striatonigral manner upon the rapid depletion of mtDNA, accompanied by progressive motor decline. Neuron death of MitoPark mice is caused by a detrimental imbalance in the mitochondrial redox system which is triggered by elevated intracellular Ca^{2+} loads. In contrast, neighboring VTA DaNs and corresponding striatal projections are more or less spared. At the same time, the newly generated K320E-Twinkle^{DaN} model demonstrates that SNc DaNs possess a great potential for adaptation to mtDNA defects, provided they only accumulate slowly over time. They can further compensate severe neurodegeneration through preserved striatal innervation, which is associated with normal motor behavior, whereas VTA DaNs do not. Thus, the small number of remaining SNc DaNs in PD patients might also be able to recover motor performance by axonal re-innervation of the dorsal striatum following stimulation of compensatory mechanisms that are ongoing in surviving SNc DaNs of aged K320E-Twinkle^{DaN} mice.

6   References

Abbott, R. D., G. W. Ross, L. R. White, C. M. Tanner, K. H. Masaki, J. S. Nelson, J. D. Curb, and H. Petrovitch. 2005. 'Excessive daytime sleepiness and subsequent development of Parkinson disease', *Neurology*, 65: 1442-6.

Ahlskog, J. E., and M. D. Muenter. 2001. 'Frequency of levodopa-related dyskinesias and motor fluctuations as estimated from the cumulative literature', *Mov Disord*, 16: 448-58.

Airaksinen, M. S., H. Thoenen, and M. Meyer. 1997. 'Vulnerability of midbrain dopaminergic neurons in calbindin-D28k-deficient mice: lack of evidence for a neuroprotective role of endogenous calbindin in MPTP-treated and weaver mice', *Eur J Neurosci*, 9: 120-7.

Alam, Z. I., A. Jenner, S. E. Daniel, A. J. Lees, N. Cairns, C. D. Marsden, P. Jenner, and B. Halliwell. 1997. 'Oxidative DNA damage in the parkinsonian brain: an apparent selective increase in 8-hydroxyguanine levels in substantia nigra', *J Neurochem*, 69: 1196-203.

Alberico, S. L., M. D. Cassell, and N. S. Narayanan. 2015. 'The Vulnerable Ventral Tegmental Area in Parkinson's Disease', *Basal Ganglia*, 5: 51-55.

Albin, R. L., A. B. Young, and J. B. Penney. 1989. 'The functional anatomy of basal ganglia disorders', *Trends Neurosci*, 12: 366-75.

Alcalay, R. N., E. Caccappolo, H. Mejia-Santana, M. X. Tang, L. Rosado, B. M. Ross, M. Verbitsky, S. Kisselev, E. D. Louis, C. Comella, A. Colcher, D. Jennings, M. A. Nance, S. B. Bressman, W. K. Scott, C. Tanner, S. Mickel, H. Andrews, C. Waters, S. Fahn, L. Cote, S. Frucht, B. Ford, M. Rezak, K. Novak, J. H. Friedman, R. Pfeiffer, L. Marsh, B. Hiner, A. Siderowf, R. Ottman, K. Marder, and L. N. Clark. 2010. 'Frequency of known mutations in early-onset Parkinson disease: implication for genetic counseling: the consortium on risk for early onset Parkinson disease study', *Arch Neurol*, 67: 1116-22.

Allen Institute. 2020. 'Allen Brain Atlas', Allen Institute, Accessed 1st April. https://mouse.brain-map.org/.

Amo, T., S. Saiki, T. Sawayama, S. Sato, and N. Hattori. 2014. 'Detailed analysis of mitochondrial respiratory chain defects caused by loss of PINK1', *Neurosci Lett*, 580: 37-40.

Andreyev, A. Y., Y. E. Kushnareva, and A. A. Starkov. 2005. 'Mitochondrial metabolism of reactive oxygen species', *Biochemistry (Mosc)*, 70: 200-14.

Aquino, C. C., and S. H. Fox. 2015. 'Clinical spectrum of levodopa-induced complications', *Mov Disord*, 30: 80-9.

Aron, A. R., D. M. Herz, P. Brown, B. U. Forstmann, and K. Zaghloul. 2016. 'Frontosubthalamic Circuits for Control of Action and Cognition', *J Neurosci*, 36: 11489-95.

Ashrafi, G., J. S. Schlehe, M. J. LaVoie, and T. L. Schwarz. 2014. 'Mitophagy of damaged mitochondria occurs locally in distal neuronal axons and requires PINK1 and Parkin', *J Cell Biol*, 206: 655-70.

Ay, M., J. Luo, M. Langley, H. Jin, V. Anantharam, A. Kanthasamy, and A. G. Kanthasamy. 2017. 'Molecular mechanisms underlying protective effects of quercetin against mitochondrial dysfunction and progressive dopaminergic neurodegeneration in cell culture and MitoPark transgenic mouse models of Parkinson's Disease', *J Neurochem*, 141: 766-82.

Banerjee, A., F. Marbach, F. Anselmi, M. S. Koh, M. B. Davis, P. Garcia da Silva, K. Delevich, H. K. Oyibo, P. Gupta, B. Li, and D. F. Albeanu. 2015. 'An Interglomerular Circuit Gates Glomerular Output and Implements Gain Control in the Mouse Olfactory Bulb', *Neuron*, 87: 193-207.

Bannwarth, S., S. Ait-El-Mkadem, A. Chaussenot, E. C. Genin, S. Lacas-Gervais, K. Fragaki, L. Berg-Alonso, Y. Kageyama, V. Serre, D. G. Moore, A. Verschueren, C. Rouzier, I. Le Ber, G. Auge, C. Cochaud, F. Lespinasse, K. N'Guyen, A. de Septenville, A. Brice, P. Yu-Wai-Man, H. Sesaki, J. Pouget, and V. Paquis-Flucklinger. 2014. 'A mitochondrial origin for frontotemporal dementia and amyotrophic lateral sclerosis through CHCHD10 involvement', *Brain*, 137: 2329-45.

Barbeau, A., M. Roy, G. Bernier, G. Campanella, and S. Paris. 1987. 'Ecogenetics of Parkinson's disease: prevalence and environmental aspects in rural areas', *Can J Neurol Sci*, 14: 36-41.

Baris, O. R., S. Ederer, J. F. Neuhaus, J. C. von Kleist-Retzow, C. M. Wunderlich, M. Pal, F. T. Wunderlich, V. Peeva, G. Zsurka, W. S. Kunz, T. Hickethier, A. C. Bunck, F. Stockigt, J. W. Schrickel, and R. J. Wiesner. 2015. 'Mosaic Deficiency in Mitochondrial Oxidative Metabolism Promotes Cardiac Arrhythmia during Aging', *Cell Metab*, 21: 667-77.

Basso, V., E. Marchesan, and E. Ziviani. 2020. 'A trio has turned into a quartet: DJ-1 interacts with the IP3R-Grp75-VDAC complex to control ER-mitochondria interaction', *Cell Calcium*, 87: 102186.

Beach, T. G., C. H. Adler, L. I. Sue, L. Vedders, L. Lue, C. L. White Iii, H. Akiyama, J. N. Caviness, H. A. Shill, M. N. Sabbagh, and D. G. Walker. 2010. 'Multi-organ distribution of phosphorylated alpha-synuclein histopathology in subjects with Lewy body disorders', *Acta Neuropathol*, 119: 689-702.

Becker, B., M. Demirbas, S. Johann, A. Zendedel, C. Beyer, H. Clusmann, S. J. Haas, A. Wree, S. K. H. Tan, and M. Kipp. 2018. 'Effect of Intrastriatal 6-OHDA Lesions on Extrastriatal Brain Structures in the Mouse', *Mol Neurobiol*, 55: 4240-52.

Beilina, A., I. N. Rudenko, A. Kaganovich, L. Civiero, H. Chau, S. K. Kalia, L. V. Kalia, E. Lobbestael, R. Chia, K. Ndukwe, J. Ding, M. A. Nalls, Consortium International Parkinson's Disease Genomics, Consortium North American Brain Expression, M. Olszewski, D. N. Hauser, R. Kumaran, A. M. Lozano, V. Baekelandt, L. E. Greene, J. M. Taymans, E. Greggio, and M. R. Cookson. 2014. 'Unbiased screen for interactors of leucine-rich repeat kinase 2 supports a common pathway for sporadic and familial Parkinson disease', *Proc Natl Acad Sci U S A*, 111: 2626-31.

Bell, Julia, and A. J. Clark. 1926. 'A Pedigree of Paralysis Agitans', *Annals of Eugenics*, 1: 455-64.

Benarroch, E. E. 2016. 'Intrinsic circuits of the striatum: Complexity and clinical correlations', *Neurology*, 86: 1531-42.

Bender, A., K. J. Krishnan, C. M. Morris, G. A. Taylor, A. K. Reeve, R. H. Perry, E. Jaros, J. S. Hersheson, J. Betts, T. Klopstock, R. W. Taylor, and D. M. Turnbull. 2006. 'High levels of mitochondrial DNA deletions in substantia nigra neurons in aging and Parkinson disease', *Nat Genet*, 38: 515-7.

Bendor, J. T., T. P. Logan, and R. H. Edwards. 2013. 'The function of alpha-synuclein', *Neuron*, 79: 1044-66.

Benkert, J., S. Hess, S. Roy, D. Beccano-Kelly, N. Wiederspohn, J. Duda, C. Simons, K. Patil, A. Gaifullina, N. Mannal, E. Dragicevic, D. Spaich, S. Muller, J. Nemeth, H. Hollmann, N. Deuter, Y. Mousba, C. Kubisch, C. Poetschke, J. Striessnig, O. Pongs, T. Schneider, R. Wade-Martins, S. Patel, R. Parlato, T. Frank, P. Kloppenburg, and B. Liss. 2019. 'Cav2.3 channels contribute to dopaminergic neuron loss in a model of Parkinson's disease', *Nat Commun*, 10: 5094.

Berg, D., C. H. Adler, B. R. Bloem, P. Chan, T. Gasser, C. G. Goetz, G. Halliday, A. E. Lang, S. Lewis, Y. Li, I. Liepelt-Scarfone, I. Litvan, K. Marek, C. Maetzler, T. Mi, J. Obeso, W. Oertel, C. W. Olanow, W. Poewe, S. Rios-Romenets, E. Schaffer, K. Seppi, B. Heim, E. Slow, M. Stern, I. O. Bledsoe, G. Deuschl, and R. B. Postuma. 2018. 'Movement disorder society criteria for clinically established early Parkinson's disease', *Mov Disord*, 33: 1643-46.

Berg, D., R. B. Postuma, C. H. Adler, B. R. Bloem, P. Chan, B. Dubois, T. Gasser, C. G. Goetz, G. Halliday, L. Joseph, A. E. Lang, I. Liepelt-Scarfone, I. Litvan, K. Marek, J. Obeso, W. Oertel, C. W. Olanow, W. Poewe, M. Stern, and G. Deuschl. 2015. 'MDS research criteria for prodromal Parkinson's disease', *Mov Disord*, 30: 1600-11.

Bergman, H., T. Wichmann, B. Karmon, and M. R. DeLong. 1994. 'The primate subthalamic nucleus. II. Neuronal activity in the MPTP model of parkinsonism', *J Neurophysiol*, 72: 507-20.

Berkowicz, D. A., and P. Q. Trombley. 2000. 'Dopaminergic modulation at the olfactory nerve synapse', *Brain Res*, 855: 90-9.

Betarbet, R., T. B. Sherer, G. MacKenzie, M. Garcia-Osuna, A. V. Panov, and J. T. Greenamyre. 2000. 'Chronic systemic pesticide exposure reproduces features of Parkinson's disease', *Nat Neurosci*, 3: 1301-6.

Bhatia, K. P., P. Bain, N. Bajaj, R. J. Elble, M. Hallett, E. D. Louis, J. Raethjen, M. Stamelou, C. M. Testa, and G. Deuschl. 2018. 'Consensus Statement on the classification of tremors. from the task force on tremor of the International Parkinson and Movement Disorder Society', *Mov Disord*, 33: 75-87.

Biglan, K. M., D. Oakes, A. E. Lang, R. A. Hauser, K. Hodgeman, B. Greco, J. Lowell, R. Rockhill, I. Shoulson, C. Venuto, D. Young, and T. Simuni. 2017. 'A novel design of a Phase III trial of isradipine in early Parkinson disease (STEADY-PD III)', *Ann Clin Transl Neurol*, 4: 360-68.

Biskup, S., D. J. Moore, F. Celsi, S. Higashi, A. B. West, S. A. Andrabi, K. Kurkinen, S. W. Yu, J. M. Savitt, H. J. Waldvogel, R. L. Faull, P. C. Emson, R. Torp, O. P. Ottersen, T. M. Dawson, and V. L. Dawson. 2006. 'Localization of LRRK2 to membranous and vesicular structures in mammalian brain', *Ann Neurol*, 60: 557-69.

Boeckel, G. R., and B. E. Ehrlich. 2018. 'NCS-1 is a regulator of calcium signaling in health and disease', *Biochim Biophys Acta Mol Cell Res*, 1865: 1660-67.

Bolam, J. P., and E. K. Pissadaki. 2012. 'Living on the edge with too many mouths to feed: why dopamine neurons die', *Mov Disord*, 27: 1478-83.

Bologna, M., G. Paparella, A. Fasano, M. Hallett, and A. Berardelli. 2020. 'Evolving concepts on bradykinesia', *Brain*, 143: 727-50.

Bonaguidi, M. A., R. P. Stadel, D. A. Berg, J. Sun, G. L. Ming, and H. Song. 2016. 'Diversity of Neural Precursors in the Adult Mammalian Brain', *Cold Spring Harb Perspect Biol*, 8: a018838.

Bonifati, V., P. Rizzu, M. J. van Baren, O. Schaap, G. J. Breedveld, E. Krieger, M. C. Dekker, F. Squitieri, P. Ibanez, M. Joosse, J. W. van Dongen, N. Vanacore, J. C. van Swieten, A. Brice, G. Meco, C. M. van Duijn, B. A. Oostra, and P. Heutink. 2003. 'Mutations in the DJ-1 gene associated with autosomal recessive early-onset parkinsonism', *Science*, 299: 256-9.

116

Bosco, D. A., D. M. Fowler, Q. Zhang, J. Nieva, E. T. Powers, P. Wentworth, Jr., R. A. Lerner, and J. W. Kelly. 2006. 'Elevated levels of oxidized cholesterol metabolites in Lewy body disease brains accelerate alpha-synuclein fibrilization', *Nat Chem Biol*, 2: 249-53.

Bostan, A. C., and P. L. Strick. 2018. 'The basal ganglia and the cerebellum: nodes in an integrated network', *Nat Rev Neurosci*, 19: 338-50.

Bovetti, S., A. Veyrac, P. Peretto, A. Fasolo, and S. De Marchis. 2009. 'Olfactory enrichment influences adult neurogenesis modulating GAD67 and plasticity-related molecules expression in newborn cells of the olfactory bulb', *PLoS One*, 4: e6359.

Braak, H., K. Del Tredici, U. Rub, R. A. de Vos, E. N. Jansen Steur, and E. Braak. 2003. 'Staging of brain pathology related to sporadic Parkinson's disease', *Neurobiol Aging*, 24: 197-211.

Braak, H., E. Ghebremedhin, U. Rub, H. Bratzke, and K. Del Tredici. 2004. 'Stages in the development of Parkinson's disease-related pathology', *Cell Tissue Res*, 318: 121-34.

Branch, S. Y., C. Chen, R. Sharma, J. D. Lechleiter, S. Li, and M. J. Beckstead. 2016. 'Dopaminergic Neurons Exhibit an Age-Dependent Decline in Electrophysiological Parameters in the MitoPark Mouse Model of Parkinson's Disease', *J Neurosci*, 36: 4026-37.

Breen, D. P., G. M. Halliday, and A. E. Lang. 2019. 'Gut-brain axis and the spread of alpha-synuclein pathology: Vagal highway or dead end?', *Mov Disord*, 34: 307-16.

Brichta, L., P. Greengard, and M. Flajolet. 2013. 'Advances in the pharmacological treatment of Parkinson's disease: targeting neurotransmitter systems', *Trends Neurosci*, 36: 543-54.

Brill, M. S., M. Snapyan, H. Wohlfrom, J. Ninkovic, M. Jawerka, G. S. Mastick, R. Ashery-Padan, A. Saghatelyan, B. Berninger, and M. Gotz. 2008. 'A dlx2- and pax6-dependent transcriptional code for periglomerular neuron specification in the adult olfactory bulb', *J Neurosci*, 28: 6439-52.

Brown, C. A., M. C. Campbell, M. Karimi, S. D. Tabbal, S. K. Loftin, L. L. Tian, S. M. Moerlein, and J. S. Perlmutter. 2012. 'Dopamine pathway loss in nucleus accumbens and ventral tegmental area predicts apathetic behavior in MPTP-lesioned monkeys', *Exp Neurol*, 236: 190-7.

Cadenas, E., and K. J. Davies. 2000. 'Mitochondrial free radical generation, oxidative stress, and aging', *Free Radic Biol Med*, 29: 222-30.

Caesar, M., S. Zach, C. B. Carlson, K. Brockmann, T. Gasser, and F. Gillardon. 2013. 'Leucine-rich repeat kinase 2 functionally interacts with microtubules and kinase-dependently modulates cell migration', *Neurobiol Dis*, 54: 280-8.

Cai, Q., H. M. Zakaria, A. Simone, and Z. H. Sheng. 2012. 'Spatial parkin translocation and degradation of damaged mitochondria via mitophagy in live cortical neurons', *Curr Biol*, 22: 545-52.

Cannon, J. R., V. Tapias, H. M. Na, A. S. Honick, R. E. Drolet, and J. T. Greenamyre. 2009. 'A highly reproducible rotenone model of Parkinson's disease', *Neurobiol Dis*, 34: 279-90.

Cao, M., I. Milosevic, S. Giovedi, and P. De Camilli. 2014. 'Upregulation of Parkin in endophilin mutant mice', *J Neurosci*, 34: 16544-9.

Carbone, C., A. Costa, G. Provensi, G. Mannaioni, and A. Masi. 2017. 'The Hyperpolarization-Activated Current Determines Synaptic Excitability, Calcium Activity and Specific Viability of Substantia Nigra Dopaminergic Neurons', *Front Cell Neurosci*, 11: 187.

Catoni, C., T. Cali, and M. Brini. 2019. 'Calcium, Dopamine and Neuronal Calcium Sensor 1: Their Contribution to Parkinson's Disease', *Front Mol Neurosci*, 12: 55.

Catterall, W. A., E. Perez-Reyes, T. P. Snutch, and J. Striessnig. 2005. 'International Union of Pharmacology. XLVIII. Nomenclature and structure-function relationships of voltage-gated calcium channels', *Pharmacol Rev*, 57: 411-25.

Cave, J. W., and H. Baker. 2009. 'Dopamine systems in the forebrain', *Adv Exp Med Biol*, 651: 15-35.

Cave, J. W., N. Fujiwara, A. R. Weibman, and H. Baker. 2016. 'Cytoarchitectural changes in the olfactory bulb of Parkinson's disease patients', *NPJ Parkinsons Dis*, 2: 16011.

Chan, C. S., J. N. Guzman, E. Ilijic, J. N. Mercer, C. Rick, T. Tkatch, G. E. Meredith, and D. J. Surmeier. 2007. ''Rejuvenation' protects neurons in mouse models of Parkinson's disease', *Nature*, 447: 1081-6.

Chan, N. C., A. M. Salazar, A. H. Pham, M. J. Sweredoski, N. J. Kolawa, R. L. Graham, S. Hess, and D. C. Chan. 2011. 'Broad activation of the ubiquitin-proteasome system by Parkin is critical for mitophagy', *Hum Mol Genet*, 20: 1726-37.

Chaugule, V. K., L. Burchell, K. R. Barber, A. Sidhu, S. J. Leslie, G. S. Shaw, and H. Walden. 2011. 'Autoregulation of Parkin activity through its ubiquitin-like domain', *EMBO J*, 30: 2853-67.

Chen, C. Y., Y. H. Weng, K. Y. Chien, K. J. Lin, T. H. Yeh, Y. P. Cheng, C. S. Lu, and H. L. Wang. 2012. '(G2019S) LRRK2 activates MKK4-JNK pathway and causes degeneration of SN dopaminergic neurons in a transgenic mouse model of PD', *Cell Death Differ*, 19: 1623-33.

Cheng, H. C., C. M. Ulane, and R. E. Burke. 2010. 'Clinical progression in Parkinson disease and the neurobiology of axons', *Ann Neurol*, 67: 715-25.

Cherra, S. J., 3rd, E. Steer, A. M. Gusdon, K. Kiselyov, and C. T. Chu. 2013. 'Mutant LRRK2 elicits calcium imbalance and depletion of dendritic mitochondria in neurons', *Am J Pathol*, 182: 474-84.

Choi, W. S., E. Lee, J. Lim, and Y. J. Oh. 2008. 'Calbindin-D28K prevents drug-induced dopaminergic neuronal death by inhibiting caspase and calpain activity', *Biochem Biophys Res Commun*, 371: 127-31.

Chu, C. T., J. Ji, R. K. Dagda, J. F. Jiang, Y. Y. Tyurina, A. A. Kapralov, V. A. Tyurin, N. Yanamala, I. H. Shrivastava, D. Mohammadyani, K. Z. Q. Wang, J. Zhu, J. Klein-Seetharaman, K. Balasubramanian, A. A. Amoscato, G. Borisenko, Z. Huang, A. M. Gusdon, A. Cheikhi, E. K. Steer, R. Wang, C. Baty, S. Watkins, I. Bahar, H. Bayir, and V. E. Kagan. 2013. 'Cardiolipin externalization to the outer mitochondrial membrane acts as an elimination signal for mitophagy in neuronal cells', *Nat Cell Biol*, 15: 1197-205.

Chu, Y., G. A. Morfini, L. B. Langhamer, Y. He, S. T. Brady, and J. H. Kordower. 2012. 'Alterations in axonal transport motor proteins in sporadic and experimental Parkinson's disease', *Brain*, 135: 2058-73.

Chung, W. G., C. L. Miranda, and C. S. Maier. 2007. 'Epigallocatechin gallate (EGCG) potentiates the cytotoxicity of rotenone in neuroblastoma SH-SY5Y cells', *Brain Res*, 1176: 133-42.

Cicchetti, F., J. Drouin-Ouellet, and R. E. Gross. 2009. 'Environmental toxins and Parkinson's disease: what have we learned from pesticide-induced animal models?', *Trends Pharmacol Sci*, 30: 475-83.

Clayton, D. A. 1982. 'Replication of animal mitochondrial DNA', *Cell*, 28: 693-705.

Cleary, D. R., A. M. Raslan, J. E. Rubin, D. Bahgat, A. Viswanathan, M. M. Heinricher, and K. J. Burchiel. 2013. 'Deep brain stimulation entrains local neuronal firing in human globus pallidus internus', *J Neurophysiol*, 109: 978-87.

Codega, P., V. Silva-Vargas, A. Paul, A. R. Maldonado-Soto, A. M. Deleo, E. Pastrana, and F. Doetsch. 2014. 'Prospective identification and purification of quiescent adult neural stem cells from their in vivo niche', *Neuron*, 82: 545-59.

Collier, T. J., N. M. Kanaan, and J. H. Kordower. 2017. 'Aging and Parkinson's disease: Different sides of the same coin?', *Mov Disord*, 32: 983-90.

Collin, F. 2019. 'Chemical Basis of Reactive Oxygen Species Reactivity and Involvement in Neurodegenerative Diseases', *Int J Mol Sci*, 20.

Cookson, M. R. 2012. 'Parkinsonism due to mutations in PINK1, parkin, and DJ-1 and oxidative stress and mitochondrial pathways', *Cold Spring Harb Perspect Med*, 2: a009415.

———. 2016. 'Cellular functions of LRRK2 implicate vesicular trafficking pathways in Parkinson's disease', *Biochem Soc Trans*, 44: 1603-10.

Crocker, S. J., P. D. Smith, V. Jackson-Lewis, W. R. Lamba, S. P. Hayley, E. Grimm, S. M. Callaghan, R. S. Slack, E. Melloni, S. Przedborski, G. S. Robertson, H. Anisman, Z. Merali, and D. S. Park. 2003. 'Inhibition of calpains prevents neuronal and behavioral deficits in an MPTP mouse model of Parkinson's disease', *J Neurosci*, 23: 4081-91.

Cui, G., S. B. Jun, X. Jin, M. D. Pham, S. S. Vogel, D. M. Lovinger, and R. M. Costa. 2013. 'Concurrent activation of striatal direct and indirect pathways during action initiation', *Nature*, 494: 238-42.

Cui, M., R. Aras, W. V. Christian, P. M. Rappold, M. Hatwar, J. Panza, V. Jackson-Lewis, J. A. Javitch, N. Ballatori, S. Przedborski, and K. Tieu. 2009. 'The organic cation transporter-3 is a pivotal modulator of neurodegeneration in the nigrostriatal dopaminergic pathway', *Proc Natl Acad Sci U S A*, 106: 8043-8.

Dagda, R. K., J. Zhu, S. M. Kulich, and C. T. Chu. 2008. 'Mitochondrially localized ERK2 regulates mitophagy and autophagic cell stress: implications for Parkinson's disease', *Autophagy*, 4: 770-82.

Damier, P., E. C. Hirsch, Y. Agid, and A. M. Graybiel. 1999. 'The substantia nigra of the human brain. II. Patterns of loss of dopamine-containing neurons in Parkinson's disease', *Brain*, 122 (Pt 8): 1437-48.

Dave, K. D., S. De Silva, N. P. Sheth, S. Ramboz, M. J. Beck, C. Quang, R. C. Switzer, 3rd, S. O. Ahmad, S. M. Sunkin, D. Walker, X. Cui, D. A. Fisher, A. M. McCoy, K. Gamber, X. Ding, M. S. Goldberg, S. A. Benkovic, M. Haupt, M. A. Baptista, B. K. Fiske, T. B. Sherer, and M. A. Frasier. 2014. 'Phenotypic characterization of recessive gene knockout rat models of Parkinson's disease', *Neurobiol Dis*, 70: 190-203.

Davis, R. L., S. L. Wong, P. J. Carling, T. Payne, C. M. Sue, and O. Bandmann. 2020. 'Serum FGF-21, GDF-15, and blood mtDNA copy number are not biomarkers of Parkinson disease', *Neurol Clin Pract*, 10: 40-46.

de Bie, R. M. A., C. E. Clarke, A. J. Espay, S. H. Fox, and A. E. Lang. 2020. 'Initiation of pharmacological therapy in Parkinson's disease: when, why, and how', *Lancet Neurol*.

De Simoni, S., D. Linard, E. Hermans, B. Knoops, and J. Goemaere. 2013. 'Mitochondrial peroxiredoxin-5 as potential modulator of mitochondria-ER crosstalk in MPP+-induced cell death', *J Neurochem*, 125: 473-85.

Deas, E., H. Plun-Favreau, S. Gandhi, H. Desmond, S. Kjaer, S. H. Loh, A. E. Renton, R. J. Harvey, A. J. Whitworth, L. M. Martins, A. Y. Abramov, and N. W. Wood. 2011. 'PINK1 cleavage at position A103 by the mitochondrial protease PARL', *Hum Mol Genet*, 20: 867-79.

Delcambre, Sylvie, Yannic Nonnenmacher, and Karsten Hiller. 2016. 'Dopamine Metabolism and Reactive Oxygen Species Production.' in Lori M. Buhlman (ed.), *Mitochondrial Mechanisms of Degeneration and Repair in Parkinson's Disease* (Springer International Publishing: Cham).

DeLong, M. R. 1990. 'Primate models of movement disorders of basal ganglia origin', *Trends Neurosci*, 13: 281-5.

Devi, L., V. Raghavendran, B. M. Prabhu, N. G. Avadhani, and H. K. Anandatheerthavarada. 2008. 'Mitochondrial import and accumulation of alpha-synuclein impair complex I in human dopaminergic neuronal cultures and Parkinson disease brain', *J Biol Chem*, 283: 9089-100.

Dexter, D. T., C. J. Carter, F. R. Wells, F. Javoy-Agid, Y. Agid, A. Lees, P. Jenner, and C. D. Marsden. 1989. 'Basal Lipid Peroxidation in Substantia Nigra Is Increased in Parkinson's Disease', *Journal of Neurochemistry*, 52: 381-89.

Di Fonzo, A., A. Bordoni, M. Crimi, G. Sara, R. Del Bo, N. Bresolin, and G. P. Comi. 2003. 'POLG mutations in sporadic mitochondrial disorders with multiple mtDNA deletions', *Hum Mutat*, 22: 498-9.

Di Maio, R., P. J. Barrett, E. K. Hoffman, C. W. Barrett, A. Zharikov, A. Borah, X. Hu, J. McCoy, C. T. Chu, E. A. Burton, T. G. Hastings, and J. T. Greenamyre. 2016. 'alpha-Synuclein binds to TOM20 and inhibits mitochondrial protein import in Parkinson's disease', *Sci Transl Med*, 8: 342ra78.

Dias, V., E. Junn, and M. M. Mouradian. 2013. 'The role of oxidative stress in Parkinson's disease', *J Parkinsons Dis*, 3: 461-91.

Dickson, D. W. 2012. 'Parkinson's disease and parkinsonism: neuropathology', *Cold Spring Harb Perspect Med*, 2.

Diepenbroek, M., N. Casadei, H. Esmer, T. C. Saido, J. Takano, P. J. Kahle, R. A. Nixon, M. V. Rao, R. Melki, L. Pieri, S. Helling, K. Marcus, R. Krueger, E. Masliah, O. Riess, and S. Nuber. 2014. 'Overexpression of the calpain-specific inhibitor calpastatin reduces human alpha-Synuclein processing, aggregation and synaptic impairment in [A30P]alphaSyn transgenic mice', *Hum Mol Genet*, 23: 3975-89.

Doder, M., E. A. Rabiner, N. Turjanski, A. J. Lees, and D. J. Brooks. 2003. 'Tremor in Parkinson's disease and serotonergic dysfunction: an 11C-WAY 100635 PET study', *Neurology*, 60: 601-5.

Doherty, K. M., L. Silveira-Moriyama, L. Parkkinen, D. G. Healy, M. Farrell, N. E. Mencacci, Z. Ahmed, F. M. Brett, J. Hardy, N. Quinn, T. J. Counihan, T. Lynch, Z. V. Fox, T. Revesz, A. J. Lees, and J. L. Holton. 2013. 'Parkin disease: a clinicopathologic entity?', *JAMA Neurol*, 70: 571-9.

Dolle, C., I. Flones, G. S. Nido, H. Miletic, N. Osuagwu, S. Kristoffersen, P. K. Lilleng, J. P. Larsen, O. B. Tysnes, K. Haugarvoll, L. A. Bindoff, and C. Tzoulis. 2016. 'Defective mitochondrial DNA homeostasis in the substantia nigra in Parkinson disease', *Nat Commun*, 7: 13548.

Dopeso-Reyes, I. G., A. J. Rico, E. Roda, S. Sierra, D. Pignataro, M. Lanz, D. Sucunza, L. Chang-Azancot, and J. L. Lanciego. 2014. 'Calbindin content and differential vulnerability of midbrain efferent dopaminergic neurons in macaques', *Front Neuroanat*, 8: 146.

Doty, R. L. 2012. 'Olfaction in Parkinson's disease and related disorders', *Neurobiol Dis*, 46: 527-52.

Dragicevic, E., C. Poetschke, J. Duda, F. Schlaudraff, S. Lammel, J. Schiemann, M. Fauler, A. Hetzel, M. Watanabe, R. Lujan, R. C. Malenka, J. Striessnig, and B. Liss. 2014. 'Cav1.3 channels control D2-autoreceptor responses via NCS-1 in substantia nigra dopamine neurons', *Brain*, 137: 2287-302.

Duda, J., C. Potschke, and B. Liss. 2016. 'Converging roles of ion channels, calcium, metabolic stress, and activity pattern of Substantia nigra dopaminergic neurons in health and Parkinson's disease', *J Neurochem*, 139 Suppl 1: 156-78.

Duncan, G. W., T. K. Khoo, A. J. Yarnall, J. T. O'Brien, S. Y. Coleman, D. J. Brooks, R. A. Barker, and D. J. Burn. 2014. 'Health-related quality of life in early Parkinson's disease: the impact of nonmotor symptoms', *Mov Disord*, 29: 195-202.

Durcan, T. M., M. Y. Tang, J. R. Perusse, E. A. Dashti, M. A. Aguileta, G. L. McLelland, P. Gros, T. A. Shaler, D. Faubert, B. Coulombe, and E. A. Fon. 2014. 'USP8 regulates mitophagy by removing K6-linked ubiquitin conjugates from parkin', *EMBO J*, 33: 2473-91.

Duty, S., and P. Jenner. 2011. 'Animal models of Parkinson's disease: a source of novel treatments and clues to the cause of the disease', *Br J Pharmacol*, 164: 1357-91.

Ehringer, H., and O. Hornykiewicz. 1998. 'Distribution of noradrenaline and dopamine (3-hydroxytyramine) in the human brain and their behavior in diseases of the extrapyramidal system', *Parkinsonism Relat Disord*, 4: 53-7.

Ekstrand, M. I., M. Terzioglu, D. Galter, S. Zhu, C. Hofstetter, E. Lindqvist, S. Thams, A. Bergstrand, F. S. Hansson, A. Trifunovic, B. Hoffer, S. Cullheim, A. H. Mohammed, L. Olson, and N. G. Larsson. 2007. 'Progressive parkinsonism in mice with respiratory-chain-deficient dopamine neurons', *Proc Natl Acad Sci U S A*, 104: 1325-30.

Elstner, M., S. K. Muller, L. Leidolt, C. Laub, L. Krieg, F. Schlaudraff, B. Liss, C. Morris, D. M. Turnbull, E. Masliah, H. Prokisch, T. Klopstock, and A. Bender. 2011. 'Neuromelanin, neurotransmitter status and brainstem location determine the differential vulnerability of catecholaminergic neurons to mitochondrial DNA deletions', *Mol Brain*, 4: 43.

Escanilla, O., C. Yuhas, D. Marzan, and C. Linster. 2009. 'Dopaminergic modulation of olfactory bulb processing affects odor discrimination learning in rats', *Behav Neurosci*, 123: 828-33.

Esteves, A. R., I. Gozes, and S. M. Cardoso. 2014. 'The rescue of microtubule-dependent traffic recovers mitochondrial function in Parkinson's disease', *Biochim Biophys Acta*, 1842: 7-21.

Esteves, A. R., G. Fernandes M, D. Santos, C. Januario, and S. M. Cardoso. 2015. 'The Upshot of LRRK2 Inhibition to Parkinson's Disease Paradigm', *Mol Neurobiol*, 52: 1804-20.

Fahn, S., L. R. Libsch, and R. W. Cutler. 1971. 'Monoamines in the human neostriatum: topographic distribution in normals and in Parkinson's disease and their role in akinesia, rigidity, chorea, and tremor', *J Neurol Sci*, 14: 427-55.

Fahn, S., D. Oakes, I. Shoulson, K. Kieburtz, A. Rudolph, A. Lang, C. W. Olanow, C. Tanner, and K. Marek. 2004. 'Levodopa and the progression of Parkinson's disease', *N Engl J Med*, 351: 2498-508.

Fallon, L., C. M. Belanger, A. T. Corera, M. Kontogiannea, E. Regan-Klapisz, F. Moreau, J. Voortman, M. Haber, G. Rouleau, T. Thorarinsdottir, A. Brice, P. M. van Bergen En Henegouwen, and E. A. Fon. 2006. 'A regulated interaction with the UIM protein Eps15 implicates parkin in EGF receptor trafficking and PI(3)K-Akt signalling', *Nat Cell Biol*, 8: 834-42.

Fallon, L., F. Moreau, B. G. Croft, N. Labib, W. J. Gu, and E. A. Fon. 2002. 'Parkin and CASK/LIN-2 associate via a PDZ-mediated interaction and are co-localized in lipid rafts and postsynaptic densities in brain', *J Biol Chem*, 277: 486-91.

Faull, R. L., and R. Laverty. 1969. 'Changes in dopamine levels in the corpus striatum following lesions in the substantia nigra', *Exp Neurol*, 23: 332-40.

Fearnley, J. M., and A. J. Lees. 1990. 'Striatonigral degeneration. A clinicopathological study', *Brain*, 113 (Pt 6): 1823-42.

Ferreira, M., T. Evangelista, L. S. Almeida, J. Martins, M. C. Macario, E. Martins, A. Moleirinho, L. Azevedo, L. Vilarinho, and F. M. Santorelli. 2011. 'Relative frequency of known causes of multiple mtDNA deletions: two novel POLG mutations', *Neuromuscul Disord*, 21: 483-8.

Ferris, C. F., M. Marella, B. Smerkers, T. M. Barchet, B. Gershman, A. Matsuno-Yagi, and T. Yagi. 2013. 'A phenotypic model recapitulating the neuropathology of Parkinson's disease', *Brain Behav*, 3: 351-66.

Fiorelli, R., K. Azim, B. Fischer, and O. Raineteau. 2015. 'Adding a spatial dimension to postnatal ventricular-subventricular zone neurogenesis', *Development*, 142: 2109-20.

Fleming, S. M., C. Zhu, P. O. Fernagut, A. Mehta, C. D. DiCarlo, R. L. Seaman, and M. F. Chesselet. 2004. 'Behavioral and immunohistochemical effects of chronic intravenous and subcutaneous infusions of varying doses of rotenone', *Exp Neurol*, 187: 418-29.

Flones, I. H., E. Fernandez-Vizarra, M. Lykouri, B. Brakedal, G. O. Skeie, H. Miletic, P. K. Lilleng, G. Alves, O. B. Tysnes, K. Haugarvoll, C. Dolle, M. Zeviani, and C. Tzoulis. 2018. 'Neuronal complex I deficiency occurs throughout the Parkinson's disease brain, but is not associated with neurodegeneration or mitochondrial DNA damage', *Acta Neuropathol*, 135: 409-25.

Floor, E., and M. G. Wetzel. 1998. 'Increased protein oxidation in human substantia nigra pars compacta in comparison with basal ganglia and prefrontal cortex measured with an improved dinitrophenylhydrazine assay', *J Neurochem*, 70: 268-75.

Ford, C. P. 2014. 'The role of D2-autoreceptors in regulating dopamine neuron activity and transmission', *Neuroscience*, 282: 13-22.

Fukui, H., and C. T. Moraes. 2009. 'Mechanisms of formation and accumulation of mitochondrial DNA deletions in aging neurons', *Hum Mol Genet*, 18: 1028-36.

Funayama, M., K. Ohe, T. Amo, N. Furuya, J. Yamaguchi, S. Saiki, Y. Li, K. Ogaki, M. Ando, H. Yoshino, H. Tomiyama, K. Nishioka, K. Hasegawa, H. Saiki, W. Satake, K. Mogushi, R. Sasaki, Y. Kokubo, S. Kuzuhara, T. Toda, Y. Mizuno, Y. Uchiyama, K. Ohno, and N. Hattori. 2015. 'CHCHD2 mutations in autosomal dominant late-onset Parkinson's disease: a genome-wide linkage and sequencing study', *Lancet Neurol*, 14: 274-82.

Furlanetti, L. L., V. A. Coenen, and M. D. Dobrossy. 2016. 'Ventral tegmental area dopaminergic lesion-induced depressive phenotype in the rat is reversed by deep brain stimulation of the medial forebrain bundle', *Behav Brain Res*, 299: 132-40.

Gagliardi, M., G. Iannello, C. Colica, G. Annesi, and A. Quattrone. 2017. 'Analysis of CHCHD2 gene in familial Parkinson's disease from Calabria', *Neurobiol Aging*, 50: 169 e5-69 e6.

Gainetdinov, R. R., F. Fumagalli, S. R. Jones, and M. G. Caron. 1997. 'Dopamine transporter is required for in vivo MPTP neurotoxicity: evidence from mice lacking the transporter', *J Neurochem*, 69: 1322-5.

Galliano, E., E. Franzoni, M. Breton, A. N. Chand, D. J. Byrne, V. N. Murthy, and M. S. Grubb. 2018. 'Embryonic and postnatal neurogenesis produce functionally distinct subclasses of dopaminergic neuron', *Elife*, 7.

Galter, D., K. Pernold, T. Yoshitake, E. Lindqvist, B. Hoffer, J. Kehr, N. G. Larsson, and L. Olson. 2010. 'MitoPark mice mirror the slow progression of key symptoms and L-DOPA response in Parkinson's disease', *Genes Brain Behav*, 9: 173-81.

Gatt, A. P., O. F. Duncan, J. Attems, P. T. Francis, C. G. Ballard, and J. M. Bateman. 2016. 'Dementia in Parkinson's disease is associated with enhanced mitochondrial complex I deficiency', *Mov Disord*, 31: 352-9.

Geisler, S., K. M. Holmstrom, D. Skujat, F. C. Fiesel, O. C. Rothfuss, P. J. Kahle, and W. Springer. 2010. 'PINK1/Parkin-mediated mitophagy is dependent on VDAC1 and p62/SQSTM1', *Nat Cell Biol*, 12: 119-31.

Gellhaar, S., D. Marcellino, M. B. Abrams, and D. Galter. 2015. 'Chronic L-DOPA induces hyperactivity, normalization of gait and dyskinetic behavior in MitoPark mice', *Genes Brain Behav*, 14: 260-70.

German, D. C., K. F. Manaye, P. K. Sonsalla, and B. A. Brooks. 1992. 'Midbrain dopaminergic cell loss in Parkinson's disease and MPTP-induced parkinsonism: sparing of calbindin-D28k-containing cells', *Ann N Y Acad Sci*, 648: 42-62.

Ghandili, M., and S. Munakomi. 2020. 'Neuroanatomy, Putamen.' in, *StatPearls* (StatPearls Publishing

StatPearls Publishing LLC.: Treasure Island (FL)).

Gitschlag, B. L., C. S. Kirby, D. C. Samuels, R. D. Gangula, S. A. Mallal, and M. R. Patel. 2016. 'Homeostatic Responses Regulate Selfish Mitochondrial Genome Dynamics in C. elegans', *Cell Metab*, 24: 91-103.

Gomez-Lazaro, M., N. A. Bonekamp, M. F. Galindo, J. Jordan, and M. Schrader. 2008. '6-Hydroxydopamine (6-OHDA) induces Drp1-dependent mitochondrial fragmentation in SH-SY5Y cells', *Free Radic Biol Med*, 44: 1960-9.

Gordon, R., M. L. Neal, J. Luo, M. R. Langley, D. S. Harischandra, N. Panicker, A. Charli, H. Jin, V. Anantharam, T. M. Woodruff, Q. Y. Zhou, A. G. Kanthasamy, and A. Kanthasamy. 2016. 'Prokineticin-2 upregulation during neuronal injury mediates a compensatory protective response against dopaminergic neuronal degeneration', *Nat Commun*, 7: 12932.

Grace, A. A., and B. S. Bunney. 1984. 'The control of firing pattern in nigral dopamine neurons: single spike firing', *J Neurosci*, 4: 2866-76.

Greenamyre, J. T., J. R. Cannon, R. Drolet, and P. G. Mastroberardino. 2010. 'Lessons from the rotenone model of Parkinson's disease', *Trends Pharmacol Sci*, 31: 141-2; author reply 42-3.

Greene, A. W., K. Grenier, M. A. Aguileta, S. Muise, R. Farazifard, M. E. Haque, H. M. McBride, D. S. Park, and E. A. Fon. 2012. 'Mitochondrial processing peptidase regulates PINK1 processing, import and Parkin recruitment', *EMBO Rep*, 13: 378-85.

Greene, J. G., R. Dingledine, and J. T. Greenamyre. 2005. 'Gene expression profiling of rat midbrain dopamine neurons: implications for selective vulnerability in parkinsonism', *Neurobiol Dis*, 18: 19-31.

Greggio, E., S. Jain, A. Kingsbury, R. Bandopadhyay, P. Lewis, A. Kaganovich, M. P. van der Brug, A. Beilina, J. Blackinton, K. J. Thomas, R. Ahmad, D. W. Miller, S. Kesavapany, A. Singleton, A. Lees, R. J. Harvey, K. Harvey, and M. R. Cookson. 2006. 'Kinase activity is required for the toxic effects of mutant LRRK2/dardarin', *Neurobiol Dis*, 23: 329-41.

Grenier, K., M. Kontogiannea, and E. A. Fon. 2014. 'Short mitochondrial ARF triggers Parkin/PINK1-dependent mitophagy', *J Biol Chem*, 289: 29519-30.

Grenier, K., G. L. McLelland, and E. A. Fon. 2013. 'Parkin- and PINK1-Dependent Mitophagy in Neurons: Will the Real Pathway Please Stand Up?', *Front Neurol*, 4: 100.

Grimm, J., A. Mueller, F. Hefti, and A. Rosenthal. 2004. 'Molecular basis for catecholaminergic neuron diversity', *Proc Natl Acad Sci U S A*, 101: 13891-6.

Grunewald, A., K. A. Rygiel, P. D. Hepplewhite, C. M. Morris, M. Picard, and D. M. Turnbull. 2016. 'Mitochondrial DNA Depletion in Respiratory Chain-Deficient Parkinson Disease Neurons', *Ann Neurol*, 79: 366-78.

Gu, G., P. E. Reyes, G. T. Golden, R. L. Woltjer, C. Hulette, T. J. Montine, and J. Zhang. 2002. 'Mitochondrial DNA deletions/rearrangements in parkinson disease and related neurodegenrial disorders', *J Neuropathol Exp Neurol*, 61: 634-9.

Guardia-Laguarta, C., E. Area-Gomez, C. Rub, Y. Liu, J. Magrane, D. Becker, W. Voos, E. A. Schon, and S. Przedborski. 2014. 'alpha-Synuclein is localized to mitochondria-associated ER membranes', *J Neurosci*, 34: 249-59.

Gustafsson, C. M., M. Falkenberg, and N. G. Larsson. 2016. 'Maintenance and Expression of Mammalian Mitochondrial DNA', *Annu Rev Biochem*, 85: 133-60.

Guttman, M., I. Boileau, J. Warsh, J. A. Saint-Cyr, N. Ginovart, T. McCluskey, S. Houle, A. Wilson, E. Mundo, P. Rusjan, J. Meyer, and S. J. Kish. 2007. 'Brain serotonin transporter binding in non-depressed patients with Parkinson's disease', *Eur J Neurol*, 14: 523-8.

Guzman, J. N., E. Ilijic, B. Yang, J. Sanchez-Padilla, D. Wokosin, D. Galtieri, J. Kondapalli, P. T. Schumacker, and D. J. Surmeier. 2018. 'Systemic isradipine treatment diminishes calcium-dependent mitochondrial oxidant stress', *J Clin Invest*, 128: 2266-80.

Guzman, J. N., J. Sanchez-Padilla, C. S. Chan, and D. J. Surmeier. 2009. 'Robust pacemaking in substantia nigra dopaminergic neurons', *J Neurosci*, 29: 11011-9.

Guzman, J. N., J. Sanchez-Padilla, D. Wokosin, J. Kondapalli, E. Ilijic, P. T. Schumacker, and D. J. Surmeier. 2010. 'Oxidant stress evoked by pacemaking in dopaminergic neurons is attenuated by DJ-1', *Nature*, 468: 696-700.

Haehner, A., T. Hummel, and H. Reichmann. 2009. 'Olfactory dysfunction as a diagnostic marker for Parkinson's disease', *Expert Rev Neurother*, 9: 1773-9.

Hahn, P. J., G. S. Russo, T. Hashimoto, S. Miocinovic, W. Xu, C. C. McIntyre, and J. L. Vitek. 2008. 'Pallidal burst activity during therapeutic deep brain stimulation', *Exp Neurol*, 211: 243-51.

Halliday, G. M., P. C. Blumbergs, R. G. Cotton, W. W. Blessing, and L. B. Geffen. 1990. 'Loss of brainstem serotonin- and substance P-containing neurons in Parkinson's disease', *Brain Res*, 510: 104-7.

Halliday, G. M., D. A. McRitchie, H. Cartwright, R. Pamphlett, M. A. Hely, and J. G. Morris. 1996. 'Midbrain neuropathology in idiopathic Parkinson's disease and diffuse Lewy body disease', *J Clin Neurosci*, 3: 52-60.

Hanisch, F., M. Kornhuber, C. L. Alston, R. W. Taylor, M. Deschauer, and S. Zierz. 2015. 'SANDO syndrome in a cohort of 107 patients with CPEO and mitochondrial DNA deletions', *J Neurol Neurosurg Psychiatry*, 86: 630-4.

Hattori, N., M. Tanaka, T. Ozawa, and Y. Mizuno. 1991. 'Immunohistochemical studies on complexes I, II, III, and IV of mitochondria in Parkinson's disease', *Ann Neurol*, 30: 563-71.

Hedrich, K., C. Eskelson, B. Wilmot, K. Marder, J. Harris, J. Garrels, H. Meija-Santana, P. Vieregge, H. Jacobs, S. B. Bressman, A. E. Lang, M. Kann, G. Abbruzzese, P. Martinelli, E. Schwinger, L. J. Ozelius, P. P. Pramstaller, C. Klein, and P. Kramer. 2004. 'Distribution, type, and origin of Parkin mutations: review and case studies', *Mov Disord*, 19: 1146-57.

Heikkila, R. E., W. J. Nicklas, I. Vyas, and R. C. Duvoisin. 1985. 'Dopaminergic toxicity of rotenone and the 1-methyl-4-phenylpyridinium ion after their stereotaxic administration to rats: implication for the mechanism of 1-methyl-4-phenyl-1,2,3,6-tetrahydropyridine toxicity', *Neurosci Lett*, 62: 389-94.

Hierro, A., A. L. Rojas, R. Rojas, N. Murthy, G. Effantin, A. V. Kajava, A. C. Steven, J. S. Bonifacino, and J. H. Hurley. 2007. 'Functional architecture of the retromer cargo-recognition complex', *Nature*, 449: 1063-7.

Hindle, S., F. Afsari, M. Stark, C. A. Middleton, G. J. Evans, S. T. Sweeney, and C. J. Elliott. 2013. 'Dopaminergic expression of the Parkinsonian gene LRRK2-G2019S leads to non-autonomous visual neurodegeneration, accelerated by increased neural demands for energy', *Hum Mol Genet*, 22: 2129-40.

Hoglinger, G. U., D. Alvarez-Fischer, O. Arias-Carrion, M. Djufri, A. Windolph, U. Keber, A. Borta, V. Ries, R. K. Schwarting, D. Scheller, and W. H. Oertel. 2015. 'A new dopaminergic nigro-olfactory projection', *Acta Neuropathol*, 130: 333-48.

Holt, I. J., A. E. Harding, and J. A. Morgan-Hughes. 1988. 'Deletions of muscle mitochondrial DNA in patients with mitochondrial myopathies', *Nature*, 331: 717-9.

Holzer, T., K. Probst, J. Etich, M. Auler, V. S. Georgieva, B. Bluhm, C. Frie, J. Heilig, A. Niehoff, J. Nuchel, M. Plomann, J. M. Seeger, H. Kashkar, O. R. Baris, R. J. Wiesner, and B. Brachvogel. 2019. 'Respiratory chain inactivation links cartilage-mediated growth retardation to mitochondrial diseases', *J Cell Biol*, 218: 1853-70.

Hsieh, C. H., A. Shaltouki, A. E. Gonzalez, A. Bettencourt da Cruz, L. F. Burbulla, E. St Lawrence, B. Schule, D. Krainc, T. D. Palmer, and X. Wang. 2016. 'Functional Impairment in Miro Degradation and Mitophagy Is a Shared Feature in Familial and Sporadic Parkinson's Disease', *Cell Stem Cell*, 19: 709-24.

Hsieh, T. H., C. W. Kuo, K. H. Hsieh, M. J. Shieh, C. W. Peng, Y. C. Chen, Y. L. Chang, Y. Z. Huang, C. C. Chen, P. K. Chang, K. Y. Chen, and H. Y. Chen. 2020. 'Probiotics Alleviate the Progressive Deterioration of Motor Functions in a Mouse Model of Parkinson's Disease', *Brain Sci*, 10.

Hu, D., X. Sun, X. Liao, X. Zhang, S. Zarabi, A. Schimmer, Y. Hong, C. Ford, Y. Luo, and X. Qi. 2019. 'Alpha-synuclein suppresses mitochondrial protease ClpP to trigger mitochondrial oxidative damage and neurotoxicity', *Acta Neuropathol*, 137: 939-60.

Hudson, G., M. Deschauer, K. Busse, S. Zierz, and P. F. Chinnery. 2005. 'Sensory ataxic neuropathy due to a novel C10Orf2 mutation with probable germline mosaicism', *Neurology*, 64: 371-3.

Huisman, E., H. B. Uylings, and P. V. Hoogland. 2008. 'Gender-related changes in increase of dopaminergic neurons in the olfactory bulb of Parkinson's disease patients', *Mov Disord*, 23: 1407-13.

Hutchison, W. D., A. M. Lozano, K. D. Davis, J. A. Saint-Cyr, A. E. Lang, and J. O. Dostrovsky. 1994. 'Differential neuronal activity in segments of globus pallidus in Parkinson's disease patients', *Neuroreport*, 5: 1533-7.

Huynh, D. P., D. R. Scoles, D. Nguyen, and S. M. Pulst. 2003. 'The autosomal recessive juvenile Parkinson disease gene product, parkin, interacts with and ubiquitinates synaptotagmin XI', *Hum Mol Genet*, 12: 2587-97.

Ikebe, S., M. Tanaka, K. Ohno, W. Sato, K. Hattori, T. Kondo, Y. Mizuno, and T. Ozawa. 1990. 'Increase of deleted mitochondrial DNA in the striatum in Parkinson's disease and senescence', *Biochem Biophys Res Commun*, 170: 1044-8.

'Impact of deprenyl and tocopherol treatment on Parkinson's disease in DATATOP patients requiring levodopa. Parkinson Study Group'. 1996. *Ann Neurol*, 39: 37-45.

Inoue, K. I., S. Miyachi, K. Nishi, H. Okado, Y. Nagai, T. Minamimoto, A. Nambu, and M. Takada. 2019. 'Recruitment of calbindin into nigral dopamine neurons protects against MPTP-Induced parkinsonism', *Mov Disord*, 34: 200-09.

Irrcher, I., H. Aleyasin, E. L. Seifert, S. J. Hewitt, S. Chhabra, M. Phillips, A. K. Lutz, M. W. Rousseaux, L. Bevilacqua, A. Jahani-Asl, S. Callaghan, J. G. MacLaurin, K. F. Winklhofer, P. Rizzu, P. Rippstein, R. H. Kim, C. X. Chen, E. A. Fon, R. S. Slack, M. E. Harper, H. M. McBride, T. W. Mak, and D. S. Park. 2010. 'Loss of the Parkinson's disease-linked gene DJ-1 perturbs mitochondrial dynamics', *Hum Mol Genet*, 19: 3734-46.

'Isradipine Versus Placebo in Early Parkinson Disease: A Randomized Trial'. 2020. *Ann Intern Med*.

Janetzky, B., S. Hauck, M. B. Youdim, P. Riederer, K. Jellinger, F. Pantucek, R. Zochling, K. W. Boissl, and H. Reichmann. 1994. 'Unaltered aconitase activity, but decreased complex I activity in substantia nigra pars compacta of patients with Parkinson's disease', *Neurosci Lett*, 169: 126-8.

Jansen, I. E., J. M. Bras, S. Lesage, C. Schulte, J. R. Gibbs, M. A. Nalls, A. Brice, N. W. Wood, H. Morris, J. A. Hardy, A. B. Singleton, T. Gasser, P. Heutink, M. Sharma, and Ipdgc. 2015. 'CHCHD2 and Parkinson's disease', *Lancet Neurol*, 14: 678-9.

Javitch, J. A., R. J. D'Amato, S. M. Strittmatter, and S. H. Snyder. 1985. 'Parkinsonism-inducing neurotoxin, N-methyl-4-phenyl-1,2,3,6 -tetrahydropyridine: uptake of the metabolite N-methyl-4-phenylpyridine by dopamine neurons explains selective toxicity', *Proc Natl Acad Sci U S A*, 82: 2173-7.

Jenner, P., and C. W. Olanow. 1996. 'Oxidative stress and the pathogenesis of Parkinson's disease', *Neurology*, 47: S161-70.

Jeon, B. S., V. Jackson-Lewis, and R. E. Burke. 1995. '6-Hydroxydopamine lesion of the rat substantia nigra: time course and morphology of cell death', *Neurodegeneration*, 4: 131-7.

Jiang, H., Y. Ren, E. Y. Yuen, P. Zhong, M. Ghaedi, Z. Hu, G. Azabdaftari, K. Nakaso, Z. Yan, and J. Feng. 2012. 'Parkin controls dopamine utilization in human midbrain dopaminergic neurons derived from induced pluripotent stem cells', *Nat Commun*, 3: 668.

Jin, S. M., M. Lazarou, C. Wang, L. A. Kane, D. P. Narendra, and R. J. Youle. 2010. 'Mitochondrial membrane potential regulates PINK1 import and proteolytic destabilization by PARL', *J Cell Biol*, 191: 933-42.

Joch, M., A. R. Ase, C. X. Chen, P. A. MacDonald, M. Kontogiannea, A. T. Corera, A. Brice, P. Seguela, and E. A. Fon. 2007. 'Parkin-mediated monoubiquitination of the PDZ protein PICK1 regulates the activity of acid-sensing ion channels', *Mol Biol Cell*, 18: 3105-18.

Johnson, M. E., and L. Bobrovskaya. 2015. 'An update on the rotenone models of Parkinson's disease: their ability to reproduce the features of clinical disease and model gene-environment interactions', *Neurotoxicology*, 46: 101-16.

Kalia, L. V., and A. E. Lang. 2015. 'Parkinson's disease', *Lancet*, 386: 896-912.

Kandul, N. P., T. Zhang, B. A. Hay, and M. Guo. 2016. 'Selective removal of deletion-bearing mitochondrial DNA in heteroplasmic Drosophila', *Nat Commun*, 7: 13100.

Kane, L. A., M. Lazarou, A. I. Fogel, Y. Li, K. Yamano, S. A. Sarraf, S. Banerjee, and R. J. Youle. 2014. 'PINK1 phosphorylates ubiquitin to activate Parkin E3 ubiquitin ligase activity', *J Cell Biol*, 205: 143-53.

Kazlauskaite, A., C. Kondapalli, R. Gourlay, D. G. Campbell, M. S. Ritorto, K. Hofmann, D. R. Alessi, A. Knebel, M. Trost, and M. M. Muqit. 2014. 'Parkin is activated by PINK1-dependent phosphorylation of ubiquitin at Ser65', *Biochem J*, 460: 127-39.

Keeney, P. M., J. Xie, R. A. Capaldi, and J. P. Bennett, Jr. 2006. 'Parkinson's disease brain mitochondrial complex I has oxidatively damaged subunits and is functionally impaired and misassembled', *J Neurosci*, 26: 5256-64.

Kerenyi, L., G. A. Ricaurte, D. J. Schretlen, U. McCann, J. Varga, W. B. Mathews, H. T. Ravert, R. F. Dannals, J. Hilton, D. F. Wong, and Z. Szabo. 2003. 'Positron emission tomography of striatal serotonin transporters in Parkinson disease', *Arch Neurol*, 60: 1223-9.

Khaliq, Z. M., and B. P. Bean. 2010. 'Pacemaking in dopaminergic ventral tegmental area neurons: depolarizing drive from background and voltage-dependent sodium conductances', *J Neurosci*, 30: 7401-13.

Khoo, T. K., A. J. Yarnall, G. W. Duncan, S. Coleman, J. T. O'Brien, D. J. Brooks, R. A. Barker, and D. J. Burn. 2013. 'The spectrum of nonmotor symptoms in early Parkinson disease', *Neurology*, 80: 276-81.

Kilarski, L. L., J. P. Pearson, V. Newsway, E. Majounie, M. D. Knipe, A. Misbahuddin, P. F. Chinnery, D. J. Burn, C. E. Clarke, M. H. Marion, A. J. Lewthwaite, D. J. Nicholl, N. W. Wood, K. E. Morrison, C. H. Williams-Gray, J. R. Evans, S. J. Sawcer, R. A. Barker, M. M. Wickremaratchi, Y. Ben-Shlomo, N. M. Williams, and H. R. Morris. 2012. 'Systematic review and UK-based study of PARK2 (parkin), PINK1, PARK7 (DJ-1) and LRRK2 in early-onset Parkinson's disease', *Mov Disord*, 27: 1522-9.

Kilbride, S. M., J. E. Telford, and G. P. Davey. 2020. 'Complex I Controls Mitochondrial and Plasma Membrane Potentials in Nerve Terminals', *Neurochem Res*.

Kim, S. E., J. Y. Choi, Y. S. Choe, Y. Choi, and W. Y. Lee. 2003. 'Serotonin transporters in the midbrain of Parkinson's disease patients: a study with 123I-beta-CIT SPECT', *J Nucl Med*, 44: 870-6.

Kim, S. J., Y. J. Park, I. Y. Hwang, M. B. Youdim, K. S. Park, and Y. J. Oh. 2012. 'Nuclear translocation of DJ-1 during oxidative stress-induced neuronal cell death', *Free Radic Biol Med*, 53: 936-50.

Kita, H., and T. Kita. 2011. 'Role of Striatum in the Pause and Burst Generation in the Globus Pallidus of 6-OHDA-Treated Rats', *Front Syst Neurosci*, 5: 42.

Kitada, T., S. Asakawa, N. Hattori, H. Matsumine, Y. Yamamura, S. Minoshima, M. Yokochi, Y. Mizuno, and N. Shimizu. 1998. 'Mutations in the parkin gene cause autosomal recessive juvenile parkinsonism', *Nature*, 392: 605-8.

Klein, C., K. Hedrich, C. Wellenbrock, M. Kann, J. Harris, K. Marder, A. E. Lang, E. Schwinger, L. J. Ozelius, P. Vieregge, P. P. Pramstaller, and P. L. Kramer. 2003. 'Frequency of parkin mutations in late-onset Parkinson's disease', *Ann Neurol*, 54: 415-6; author reply 16-7.

Kondapalli, C., A. Kazlauskaite, N. Zhang, H. I. Woodroof, D. G. Campbell, R. Gourlay, L. Burchell, H. Walden, T. J. Macartney, M. Deak, A. Knebel, D. R. Alessi, and M. M. Muqit. 2012. 'PINK1 is activated by mitochondrial membrane potential depolarization and stimulates Parkin E3 ligase activity by phosphorylating Serine 65', *Open Biol*, 2: 120080.

Kordower, J. H., C. W. Olanow, H. B. Dodiya, Y. Chu, T. G. Beach, C. H. Adler, G. M. Halliday, and R. T. Bartus. 2013. 'Disease duration and the integrity of the nigrostriatal system in Parkinson's disease', *Brain*, 136: 2419-31.

Kosaka, K., K. Hama, I. Nagatsu, J. Y. Wu, O. P. Ottersen, J. Storm-Mathisen, and T. Kosaka. 1987. 'Postnatal development of neurons containing both catecholaminergic and GABAergic traits in the rat main olfactory bulb', *Brain Res*, 403: 355-60.

Kosaka, T., and K. Kosaka. 2009. 'Two types of tyrosine hydroxylase positive GABAergic juxtaglomerular neurons in the mouse main olfactory bulb are different in their time of origin', *Neurosci Res*, 64: 436-41.

Koschak, A., D. Reimer, I. Huber, M. Grabner, H. Glossmann, J. Engel, and J. Striessnig. 2001. 'alpha 1D (Cav1.3) subunits can form l-type Ca2+ channels activating at negative voltages', *J Biol Chem*, 276: 22100-6.

Kostic, M., M. H. Ludtmann, H. Bading, M. Hershfinkel, E. Steer, C. T. Chu, A. Y. Abramov, and I. Sekler. 2015. 'PKA Phosphorylation of NCLX Reverses Mitochondrial Calcium Overload and Depolarization, Promoting Survival of PINK1-Deficient Dopaminergic Neurons', *Cell Rep*, 13: 376-86.

Koyano, F., K. Okatsu, H. Kosako, Y. Tamura, E. Go, M. Kimura, Y. Kimura, H. Tsuchiya, H. Yoshihara, T. Hirokawa, T. Endo, E. A. Fon, J. F. Trempe, Y. Saeki, K. Tanaka, and N. Matsuda. 2014. 'Ubiquitin is phosphorylated by PINK1 to activate parkin', *Nature*, 510: 162-6.

Kraytsberg, Y., E. Kudryavtseva, A. C. McKee, C. Geula, N. W. Kowall, and K. Khrapko. 2006. 'Mitochondrial DNA deletions are abundant and cause functional impairment in aged human substantia nigra neurons', *Nat Genet*, 38: 518-20.

Krebiehl, G., S. Ruckerbauer, L. F. Burbulla, N. Kieper, B. Maurer, J. Waak, H. Wolburg, Z. Gizatullina, F. N. Gellerich, D. Woitalla, O. Riess, P. J. Kahle, T. Proikas-Cezanne, and R. Kruger. 2010. 'Reduced basal autophagy and impaired mitochondrial dynamics due to loss of Parkinson's disease-associated protein DJ-1', *PLoS One*, 5: e9367.

Krishnan, K. J., A. K. Reeve, D. C. Samuels, P. F. Chinnery, J. K. Blackwood, R. W. Taylor, S. Wanrooij, J. N. Spelbrink, R. N. Lightowlers, and D. M. Turnbull. 2008. 'What causes mitochondrial DNA deletions in human cells?', *Nat Genet*, 40: 275-9.

Kudin, A. P., N. Y. Bimpong-Buta, S. Vielhaber, C. E. Elger, and W. S. Kunz. 2004. 'Characterization of superoxide-producing sites in isolated brain mitochondria', *J Biol Chem*, 279: 4127-35.

Kudin, A. P., G. Debska-Vielhaber, and W. S. Kunz. 2005. 'Characterization of superoxide production sites in isolated rat brain and skeletal muscle mitochondria', *Biomed Pharmacother*, 59: 163-8.

Kussmaul, L., and J. Hirst. 2006. 'The mechanism of superoxide production by NADH:ubiquinone oxidoreductase (complex I) from bovine heart mitochondria', *Proc Natl Acad Sci U S A*, 103: 7607-12.

Lammel, S., A. Hetzel, O. Hackel, I. Jones, B. Liss, and J. Roeper. 2008. 'Unique properties of mesoprefrontal neurons within a dual mesocorticolimbic dopamine system', *Neuron*, 57: 760-73.

Lang, A. E. 2011. 'A critical appraisal of the premotor symptoms of Parkinson's disease: potential usefulness in early diagnosis and design of neuroprotective trials', *Mov Disord*, 26: 775-83.

Lang, Y., D. Gong, and Y. Fan. 2015. 'Calcium channel blocker use and risk of Parkinson's disease: a meta-analysis', *Pharmacoepidemiol Drug Saf*, 24: 559-66.

Langley, M., A. Ghosh, A. Charli, S. Sarkar, M. Ay, J. Luo, J. Zielonka, T. Brenza, B. Bennett, H. Jin, S. Ghaisas, B. Schlichtmann, D. Kim, V. Anantharam, A. Kanthasamy, B. Narasimhan, B. Kalyanaraman, and A. G. Kanthasamy. 2017. 'Mito-Apocynin Prevents Mitochondrial Dysfunction, Microglial Activation, Oxidative Damage, and Progressive Neurodegeneration in MitoPark Transgenic Mice', *Antioxid Redox Signal*, 27: 1048-66.

Langley, M. R., S. Ghaisas, M. Ay, J. Luo, B. N. Palanisamy, H. Jin, V. Anantharam, A. Kanthasamy, and A. G. Kanthasamy. 2018. 'Manganese exposure exacerbates progressive motor deficits and neurodegeneration in the MitoPark mouse model of Parkinson's disease: Relevance to gene and environment interactions in metal neurotoxicity', *Neurotoxicology*, 64: 240-55.

Langston, J. W., and P. A. Ballard, Jr. 1983. 'Parkinson's disease in a chemist working with 1-methyl-4-phenyl-1,2,5,6-tetrahydropyridine', *N Engl J Med*, 309: 310.

Langston, J. W., P. Ballard, J. W. Tetrud, and I. Irwin. 1983. 'Chronic Parkinsonism in humans due to a product of meperidine-analog synthesis', *Science*, 219: 979-80.

Langston, J. W., L. S. Forno, J. Tetrud, A. G. Reeves, J. A. Kaplan, and D. Karluk. 1999. 'Evidence of active nerve cell degeneration in the substantia nigra of humans years after 1-methyl-4-phenyl-1,2,3,6-tetrahydropyridine exposure', *Ann Neurol*, 46: 598-605.

Lautenschlager, J., C. F. Kaminski, and G. S. Kaminski Schierle. 2017. 'alpha-Synuclein - Regulator of Exocytosis, Endocytosis, or Both?', *Trends Cell Biol*, 27: 468-79.

Lautenschlager, J., A. D. Stephens, G. Fusco, F. Strohl, N. Curry, M. Zacharopoulou, C. H. Michel, R. Laine, N. Nespovitaya, M. Fantham, D. Pinotsi, W. Zago, P. Fraser, A. Tandon, P. St George-Hyslop, E. Rees, J. J. Phillips, A. De Simone, C. F. Kaminski, and G. S. K. Schierle. 2018. 'C-terminal calcium binding of alpha-synuclein modulates synaptic vesicle interaction', *Nat Commun*, 9: 712.

Law, B. M., V. A. Spain, V. H. Leinster, R. Chia, A. Beilina, H. J. Cho, J. M. Taymans, M. K. Urban, R. M. Sancho, M. Blanca Ramirez, S. Biskup, V. Baekelandt, H. Cai, M. R. Cookson, D. C. Berwick, and K. Harvey. 2014. 'A direct interaction between leucine-rich repeat kinase 2 and specific beta-tubulin isoforms regulates tubulin acetylation', *J Biol Chem*, 289: 895-908.

Lazarou, M., S. M. Jin, L. A. Kane, and R. J. Youle. 2012. 'Role of PINK1 binding to the TOM complex and alternate intracellular membranes in recruitment and activation of the E3 ligase Parkin', *Dev Cell*, 22: 320-33.

Lazarou, M., D. A. Sliter, L. A. Kane, S. A. Sarraf, C. Wang, J. L. Burman, D. P. Sideris, A. I. Fogel, and R. J. Youle. 2015. 'The ubiquitin kinase PINK1 recruits autophagy receptors to induce mitophagy', *Nature*, 524: 309-14.

Le Poul, E., C. Bolea, F. Girard, S. Poli, D. Charvin, B. Campo, J. Bortoli, A. Bessif, B. Luo, A. J. Koser, L. M. Hodge, K. M. Smith, A. G. DiLella, N. Liverton, F. Hess, S. E. Browne, and I. J. Reynolds. 2012. 'A potent and selective metabotropic glutamate receptor 4 positive allosteric modulator improves movement in rodent models of Parkinson's disease', *J Pharmacol Exp Ther*, 343: 167-77.

Lee, R. G., M. Sedghi, M. Salari, A. J. Shearwood, M. Stentenbach, A. Kariminejad, H. Goullee, O. Rackham, N. G. Laing, H. Tajsharghi, and A. Filipovska. 2018. 'Early-onset Parkinson disease caused by a mutation in CHCHD2 and mitochondrial dysfunction', *Neurol Genet*, 4: e276.

Lee, Y., D. A. Stevens, S. U. Kang, H. Jiang, Y. I. Lee, H. S. Ko, L. A. Scarffe, G. E. Umanah, H. Kang, S. Ham, T. I. Kam, K. Allen, S. Brahmachari, J. W. Kim, S. Neifert, S. P. Yun, F. C. Fiesel, W. Springer, V. L. Dawson, J. H. Shin, and T. M. Dawson. 2017. 'PINK1 Primes Parkin-Mediated Ubiquitination of PARIS in Dopaminergic Neuronal Survival', *Cell Rep*, 18: 918-32.

Lestienne, P., J. Nelson, P. Riederer, K. Jellinger, and H. Reichmann. 1990. 'Normal Mitochondrial Genome in Brain from Patients with Parkinson's Disease and Complex I Defect', *Journal of Neurochemistry*, 55: 1810-12.

Levitt, P., J. E. Pintar, and X. O. Breakefield. 1982. 'Immunocytochemical demonstration of monoamine oxidase B in brain astrocytes and serotonergic neurons', *Proc Natl Acad Sci U S A*, 79: 6385-9.

Lill, C. M. 2016. 'Genetics of Parkinson's disease', *Mol Cell Probes*, 30: 386-96.

Lin, C. H., P. I. Tsai, R. M. Wu, and C. T. Chien. 2010. 'LRRK2 G2019S mutation induces dendrite degeneration through mislocalization and phosphorylation of tau by recruiting autoactivated GSK3ss', *J Neurosci*, 30: 13138-49.

Lin, W., and U. J. Kang. 2008. 'Characterization of PINK1 processing, stability, and subcellular localization', *J Neurochem*, 106: 464-74.

Liss, B., O. Haeckel, J. Wildmann, T. Miki, S. Seino, and J. Roeper. 2005. 'K-ATP channels promote the differential degeneration of dopaminergic midbrain neurons', *Nat Neurosci*, 8: 1742-51.

Liss, B., and J. Roeper. 2001. 'Molecular physiology of neuronal K-ATP channels (review)', *Mol Membr Biol*, 18: 117-27.

———. 2008. 'Individual dopamine midbrain neurons: functional diversity and flexibility in health and disease', *Brain Res Rev*, 58: 314-21.

Liu, J. P. 2014. 'Molecular mechanisms of ageing and related diseases', *Clin Exp Pharmacol Physiol*, 41: 445-58.

Liu, S., C. Plachez, Z. Shao, A. Puche, and M. T. Shipley. 2013. 'Olfactory bulb short axon cell release of GABA and dopamine produces a temporally biphasic inhibition-excitation response in external tufted cells', *J Neurosci*, 33: 2916-26.

Lowes, H., A. Pyle, M. Santibanez-Koref, and G. Hudson. 2020. 'Circulating cell-free mitochondrial DNA levels in Parkinson's disease are influenced by treatment', *Mol Neurodegener*, 15: 10.

Lu, X. H., S. M. Fleming, B. Meurers, L. C. Ackerson, F. Mortazavi, V. Lo, D. Hernandez, D. Sulzer, G. R. Jackson, N. T. Maidment, M. F. Chesselet, and X. W. Yang. 2009. 'Bacterial artificial chromosome transgenic mice expressing a truncated mutant parkin exhibit age-dependent hypokinetic motor deficits, dopaminergic neuron degeneration, and accumulation of proteinase K-resistant alpha-synuclein', *J Neurosci*, 29: 1962-76.

Lu, X., J. S. Kim-Han, S. Harmon, S. E. Sakiyama-Elbert, and K. L. O'Malley. 2014. 'The Parkinsonian mimetic, 6-OHDA, impairs axonal transport in dopaminergic axons', *Mol Neurodegener*, 9: 17.

Lu, Y. W., and E. K. Tan. 2008. 'Molecular biology changes associated with LRRK2 mutations in Parkinson's disease', *J Neurosci Res*, 86: 1895-901.

Ludtmann, M. H. R., P. R. Angelova, M. H. Horrocks, M. L. Choi, M. Rodrigues, A. Y. Baev, A. V. Berezhnov, Z. Yao, D. Little, B. Banushi, A. S. Al-Menhali, R. T. Ranasinghe, D. R. Whiten, R. Yapom, K. S. Dolt, M. J. Devine, P. Gissen, T. Kunath, M. Jaganjac, E. V. Pavlov, D. Klenerman, A. Y. Abramov, and S. Gandhi. 2018. 'alpha-synuclein oligomers interact with ATP synthase and open the permeability transition pore in Parkinson's disease', *Nat Commun*, 9: 2293.

Luthman, J., A. Fredriksson, E. Sundstrom, G. Jonsson, and T. Archer. 1989. 'Selective lesion of central dopamine or noradrenaline neuron systems in the neonatal rat: motor behavior and monoamine alterations at adult stage', *Behav Brain Res*, 33: 267-77.

Lynch, W. B., C. W. Tschumi, A. L. Sharpe, S. Y. Branch, C. Chen, G. Ge, S. Li, and M. J. Beckstead. 2018. 'Progressively disrupted somatodendritic morphology in dopamine neurons in a mouse Parkinson's model', *Mov Disord*, 33: 1928-37.

Mahul-Mellier, A. L., J. Burtscher, N. Maharjan, L. Weerens, M. Croisier, F. Kuttler, M. Leleu, G. W. Knott, and H. A. Lashuel. 2020. 'The process of Lewy body formation, rather than simply alpha-synuclein fibrillization, is one of the major drivers of neurodegeneration', *Proc Natl Acad Sci U S A*, 117: 4971-82.

Mann, V. M., J. M. Cooper, S. E. Daniel, K. Srai, P. Jenner, C. D. Marsden, and A. H. Schapira. 1994. 'Complex I, iron, and ferritin in Parkinson's disease substantia nigra', *Ann Neurol*, 36: 876-81.

Mann, V. M., J. M. Cooper, D. Krige, S. E. Daniel, A. H. Schapira, and C. D. Marsden. 1992. 'Brain, skeletal muscle and platelet homogenate mitochondrial function in Parkinson's disease', *Brain*, 115 (Pt 2): 333-42.

Maraganore, D. M., K. Wilkes, T. G. Lesnick, K. J. Strain, M. de Andrade, W. A. Rocca, J. H. Bower, J. E. Ahlskog, S. Lincoln, and M. J. Farrer. 2004. 'A limited role for DJ1 in Parkinson disease susceptibility', *Neurology*, 63: 550-3.

Marella, M., B. B. Seo, E. Nakamaru-Ogiso, J. T. Greenamyre, A. Matsuno-Yagi, and T. Yagi. 2008. 'Protection by the NDI1 gene against neurodegeneration in a rotenone rat model of Parkinson's disease', *PLoS One*, 3: e1433.

Martinez-Martin, P., C. Rodriguez-Blazquez, M. M. Kurtis, and K. R. Chaudhuri. 2011. 'The impact of non-motor symptoms on health-related quality of life of patients with Parkinson's disease', *Mov Disord*, 26: 399-406.

Martinez, T. N., and J. T. Greenamyre. 2012. 'Toxin models of mitochondrial dysfunction in Parkinson's disease', *Antioxid Redox Signal*, 16: 920-34.

Masi, A., R. Narducci, E. Landucci, F. Moroni, and G. Mannaioni. 2013. 'MPP(+) -dependent inhibition of Ih reduces spontaneous activity and enhances EPSP summation in nigral dopamine neurons', *Br J Pharmacol*, 169: 130-42.

Masi, A., R. Narducci, F. Resta, C. Carbone, K. Kobayashi, and G. Mannaioni. 2015. 'Differential contribution of Ih to the integration of excitatory synaptic inputs in substantia nigra pars compacta and ventral tegmental area dopaminergic neurons', *Eur J Neurosci*, 42: 2699-706.

Matsuda, N., S. Sato, K. Shiba, K. Okatsu, K. Saisho, C. A. Gautier, Y. S. Sou, S. Saiki, S. Kawajiri, F. Sato, M. Kimura, M. Komatsu, N. Hattori, and K. Tanaka. 2010. 'PINK1 stabilized by mitochondrial depolarization recruits Parkin to damaged mitochondria and activates latent Parkin for mitophagy', *J Cell Biol*, 189: 211-21.

McLelland, G. L., V. Soubannier, C. X. Chen, H. M. McBride, and E. A. Fon. 2014. 'Parkin and PINK1 function in a vesicular trafficking pathway regulating mitochondrial quality control', *EMBO J*, 33: 282-95.

Melov, S., J. A. Schneider, P. E. Coskun, D. A. Bennett, and D. C. Wallace. 1999. 'Mitochondrial DNA rearrangements in aging human brain and in situ PCR of mtDNA', *Neurobiol Aging*, 20: 565-71.

Meng, H., C. Yamashita, K. Shiba-Fukushima, T. Inoshita, M. Funayama, S. Sato, T. Hatta, T. Natsume, M. Umitsu, J. Takagi, Y. Imai, and N. Hattori. 2017. 'Loss of Parkinson's disease-associated protein CHCHD2 affects mitochondrial crista structure and destabilizes cytochrome c', *Nat Commun*, 8: 15500.

Merkle, F. T., Z. Mirzadeh, and A. Alvarez-Buylla. 2007. 'Mosaic organization of neural stem cells in the adult brain', *Science*, 317: 381-4.

Michel, P. P., E. C. Hirsch, and S. Hunot. 2016. 'Understanding Dopaminergic Cell Death Pathways in Parkinson Disease', *Neuron*, 90: 675-91.

Milusheva, E., M. Baranyi, A. Kittel, B. Sperlagh, and E. S. Vizi. 2005. 'Increased sensitivity of striatal dopamine release to H2O2 upon chronic rotenone treatment', *Free Radic Biol Med*, 39: 133-42.

Miriyala, S., A. K. Holley, and D. K. St Clair. 2011. 'Mitochondrial superoxide dismutase--signals of distinction', *Anticancer Agents Med Chem*, 11: 181-90.

Mizuno, Y., S. Ohta, M. Tanaka, S. Takamiya, K. Suzuki, T. Sato, H. Oya, T. Ozawa, and Y. Kagawa. 1989. 'Deficiencies in complex I subunits of the respiratory chain in Parkinson's disease', *Biochem Biophys Res Commun*, 163: 1450-5.

Mortiboys, H., K. K. Johansen, J. O. Aasly, and O. Bandmann. 2010. 'Mitochondrial impairment in patients with Parkinson disease with the G2019S mutation in LRRK2', *Neurology*, 75: 2017-20.

Muller, E. J., and P. A. Robinson. 2018. 'Suppression of Parkinsonian Beta Oscillations by Deep Brain Stimulation: Determination of Effective Protocols', *Front Comput Neurosci*, 12: 98.

Mundinano, I. C., M. C. Caballero, C. Ordonez, M. Hernandez, C. DiCaudo, I. Marcilla, M. E. Erro, M. T. Tunon, and M. R. Luquin. 2011. 'Increased dopaminergic cells and protein aggregates in the olfactory bulb of patients with neurodegenerative disorders', *Acta Neuropathol*, 122: 61-74.

Murphy, M. P. 2009. 'How mitochondria produce reactive oxygen species', *Biochem J*, 417: 1-13.

Nagayama, S., R. Homma, and F. Imamura. 2014. 'Neuronal organization of olfactory bulb circuits', *Front Neural Circuits*, 8: 98.

Nambu, A., H. Tokuno, and M. Takada. 2002. 'Functional significance of the cortico-subthalamo-pallidal 'hyperdirect' pathway', *Neurosci Res*, 43: 111-7.

Nandipati, S., and I. Litvan. 2016. 'Environmental Exposures and Parkinson's Disease', *Int J Environ Res Public Health*, 13.

Narendra, D. P., S. M. Jin, A. Tanaka, D. F. Suen, C. A. Gautier, J. Shen, M. R. Cookson, and R. J. Youle. 2010. 'PINK1 is selectively stabilized on impaired mitochondria to activate Parkin', *PLoS Biol*, 8: e1000298.

Neuhaus, J. F., O. R. Baris, S. Hess, N. Moser, H. Schroder, S. J. Chinta, J. K. Andersen, P. Kloppenburg, and R. J. Wiesner. 2014. 'Catecholamine metabolism drives generation of mitochondrial DNA deletions in dopaminergic neurons', *Brain*, 137: 354-65.

References

Neuhaus, J. F., O. R. Baris, A. Kittelmann, K. Becker, M. A. Rothschild, and R. J. Wiesner. 2017. 'Catecholamine Metabolism Induces Mitochondrial DNA Deletions and Leads to Severe Adrenal Degeneration during Aging', *Neuroendocrinology*, 104: 72-84.

Nicklas, W. J., I. Vyas, and R. E. Heikkila. 1985. 'Inhibition of NADH-linked oxidation in brain mitochondria by 1-methyl-4-phenyl-pyridine, a metabolite of the neurotoxin, 1-methyl-4-phenyl-1,2,5,6-tetrahydropyridine', *Life Sci*, 36: 2503-8.

Nissanka, N., S. R. Bacman, M. J. Plastini, and C. T. Moraes. 2018. 'The mitochondrial DNA polymerase gamma degrades linear DNA fragments precluding the formation of deletions', *Nat Commun*, 9: 2491.

Nobili, A., E. C. Latagliata, M. T. Viscomi, V. Cavallucci, D. Cutuli, G. Giacovazzo, P. Krashia, F. R. Rizzo, R. Marino, M. Federici, P. De Bartolo, D. Aversa, M. C. Dell'Acqua, A. Cordella, M. Sancandi, F. Keller, L. Petrosini, S. Puglisi-Allegra, N. B. Mercuri, R. Coccurello, N. Berretta, and M. D'Amelio. 2017. 'Dopamine neuronal loss contributes to memory and reward dysfunction in a model of Alzheimer's disease', *Nat Commun*, 8: 14727.

Obeso, J. A., M. C. Rodriguez-Oroz, M. Rodriguez, J. L. Lanciego, J. Artieda, N. Gonzalo, and C. W. Olanow. 2000. 'Pathophysiology of the basal ganglia in Parkinson's disease', *Trends Neurosci*, 23: S8-19.

Obeso, J. A., M. Stamelou, C. G. Goetz, W. Poewe, A. E. Lang, D. Weintraub, D. Burn, G. M. Halliday, E. Bezard, S. Przedborski, S. Lehericy, D. J. Brooks, J. C. Rothwell, M. Hallett, M. R. DeLong, C. Marras, C. M. Tanner, G. W. Ross, J. W. Langston, C. Klein, V. Bonifati, J. Jankovic, A. M. Lozano, G. Deuschl, H. Bergman, E. Tolosa, M. Rodriguez-Violante, S. Fahn, R. B. Postuma, D. Berg, K. Marek, D. G. Standaert, D. J. Surmeier, C. W. Olanow, J. H. Kordower, P. Calabresi, A. H. V. Schapira, and A. J. Stoessl. 2017. 'Past, present, and future of Parkinson's disease: A special essay on the 200th Anniversary of the Shaking Palsy', *Mov Disord*, 32: 1264-310.

Orenstein, S. J., S. H. Kuo, I. Tasset, E. Arias, H. Koga, I. Fernandez-Carasa, E. Cortes, L. S. Honig, W. Dauer, A. Consiglio, A. Raya, D. Sulzer, and A. M. Cuervo. 2013. 'Interplay of LRRK2 with chaperone-mediated autophagy', *Nat Neurosci*, 16: 394-406.

Ortner, N. J., G. Bock, A. Dougalis, M. Kharitonova, J. Duda, S. Hess, P. Tuluc, T. Pomberger, N. Stefanova, F. Pitterl, T. Ciossek, H. Oberacher, H. J. Draheim, P. Kloppenburg, B. Liss, and J. Striessnig. 2017. 'Lower Affinity of Israldipine for L-Type Ca(2+) Channels during Substantia Nigra Dopamine Neuron-Like Activity: Implications for Neuroprotection in Parkinson's Disease', *J Neurosci*, 37: 6761-77.

Ozawa, T., M. Tanaka, S. Ikebe, K. Ohno, T. Kondo, and Y. Mizuno. 1990. 'Quantitative determination of deleted mitochondrial DNA relative to normal DNA in parkinsonian striatum by a kinetic PCR analysis', *Biochem Biophys Res Commun*, 172: 483-9.

Pacelli, C., N. Giguere, M. J. Bourque, M. Levesque, R. S. Slack, and L. E. Trudeau. 2015. 'Elevated Mitochondrial Bioenergetics and Axonal Arborization Size Are Key Contributors to the Vulnerability of Dopamine Neurons', *Curr Biol*, 25: 2349-60.

Paillusson, S., P. Gomez-Suaga, R. Stoica, D. Little, P. Gissen, M. J. Devine, W. Noble, D. P. Hanger, and C. C. J. Miller. 2017. 'alpha-Synuclein binds to the ER-mitochondria tethering protein VAPB to disrupt Ca(2+) homeostasis and mitochondrial ATP production', *Acta Neuropathol*, 134: 129-49.

Paisan-Ruiz, C., S. Jain, E. W. Evans, W. P. Gilks, J. Simon, M. van der Brug, A. Lopez de Munain, S. Aparicio, A. M. Gil, N. Khan, J. Johnson, J. R. Martinez, D. Nicholl, I. Marti Carrera, A. S. Pena, R. de Silva, A. Lees, J. F. Marti-Masso, J. Perez-Tur, N. W. Wood, and A. B. Singleton. 2004. 'Cloning of the gene containing mutations that cause PARK8-linked Parkinson's disease', *Neuron*, 44: 595-600.

Pan, H. S., and J. R. Walters. 1988. 'Unilateral lesion of the nigrostriatal pathway decreases the firing rate and alters the firing pattern of globus pallidus neurons in the rat', *Synapse*, 2: 650-6.

Panneton, W. M., V. B. Kumar, Q. Gan, W. J. Burke, and J. E. Galvin. 2010. 'The neurotoxicity of DOPAL: behavioral and stereological evidence for its role in Parkinson disease pathogenesis', *PLoS One*, 5: e15251.

Parent, M., M. J. Wallman, D. Gagnon, and A. Parent. 2011. 'Serotonin innervation of basal ganglia in monkeys and humans', *J Chem Neuroanat*, 41: 256-65.

Parisiadou, L., C. Xie, H. J. Cho, X. Lin, X. L. Gu, C. X. Long, E. Lobbestael, V. Baekelandt, J. M. Taymans, L. Sun, and H. Cai. 2009. 'Phosphorylation of ezrin/radixin/moesin proteins by LRRK2 promotes the rearrangement of actin cytoskeleton in neuronal morphogenesis', *J Neurosci*, 29: 13971-80.

Park, J. S., N. F. Blair, and C. M. Sue. 2015. 'The role of ATP13A2 in Parkinson's disease: Clinical phenotypes and molecular mechanisms', *Mov Disord*, 30: 770-9.

Park, J. S., B. Koentjoro, R. L. Davis, and C. M. Sue. 2016. 'Loss of ATP13A2 impairs glycolytic function in Kufor-Rakeb syndrome patient-derived cell models', *Parkinsonism Relat Disord*, 27: 67-73.

Park, J. S., B. Koentjoro, D. Veivers, A. Mackay-Sim, and C. M. Sue. 2014. 'Parkinson's disease-associated human ATP13A2 (PARK9) deficiency causes zinc dyshomeostasis and mitochondrial dysfunction', *Hum Mol Genet*, 23: 2802-15.

Parker, W. D., Jr., S. J. Boyson, and J. K. Parks. 1989. 'Abnormalities of the electron transport chain in idiopathic Parkinson's disease', *Ann Neurol*, 26: 719-23.

Parkinson, J. 2002. 'An essay on the shaking palsy. 1817', *J Neuropsychiatry Clin Neurosci*, 14: 223-36; discussion 22.

Paulus, W., and K. Jellinger. 1991. 'The neuropathologic basis of different clinical subgroups of Parkinson's disease', *J Neuropathol Exp Neurol*, 50: 743-55.

Perez Carrion, M., F. Pischedda, A. Biosa, I. Russo, L. Straniero, L. Civiero, M. Guida, C. J. Gloeckner, N. Ticozzi, C. Tiloca, C. Mariani, G. Pezzoli, S. Duga, I. Pichler, L. Pan, J. E. Landers, E. Greggio, M. W. Hess, S. Goldwurm, and G. Piccoli. 2018. 'The LRRK2 Variant E193K Prevents Mitochondrial Fission Upon MPP+ Treatment by Altering LRRK2 Binding to DRP1', *Front Mol Neurosci*, 11: 64.

Perez, F. A., and R. D. Palmiter. 2005. 'Parkin-deficient mice are not a robust model of parkinsonism', *Proc Natl Acad Sci U S A*, 102: 2174-9.

Perier, C., A. Bender, E. Garcia-Arumi, M. J. Melia, J. Bove, C. Laub, T. Klopstock, M. Elstner, R. B. Mounsey, P. Teismann, T. Prolla, A. L. Andreu, and M. Vila. 2013. 'Accumulation of mitochondrial DNA deletions within dopaminergic neurons triggers neuroprotective mechanisms', *Brain*, 136: 2369-78.

Peter, B., G. Farge, C. Pardo-Hernandez, S. Tangefjord, and M. Falkenberg. 2019. 'Structural basis for adPEO-causing mutations in the mitochondrial TWINKLE helicase', *Hum Mol Genet*, 28: 1090-99.

Pfeiffer, R. F. 2016. 'Non-motor symptoms in Parkinson's disease', *Parkinsonism Relat Disord*, 22 Suppl 1: S119-22.

Philippart, F., G. Destreel, P. Merino-Sepulveda, P. Henny, D. Engel, and V. Seutin. 2016. 'Differential Somatic Ca2+ Channel Profile in Midbrain Dopaminergic Neurons', *J Neurosci*, 36: 7234-45.

Philippart, F., and Z. M. Khaliq. 2018. 'Gi/o protein-coupled receptors in dopamine neurons inhibit the sodium leak channel NALCN', *Elife*, 7.

Picard, M., A. E. Vincent, and D. M. Turnbull. 2016. 'Expanding Our Understanding of mtDNA Deletions', *Cell Metab*, 24: 3-4.

Pickrell, A. M., C. H. Huang, S. R. Kennedy, A. Ordureau, D. P. Sideris, J. G. Hoekstra, J. W. Harper, and R. J. Youle. 2015. 'Endogenous Parkin Preserves Dopaminergic Substantia Nigral Neurons following Mitochondrial DNA Mutagenic Stress', *Neuron*, 87: 371-81.

Pickrell, A. M., M. Pinto, A. Hida, and C. T. Moraes. 2011. 'Striatal dysfunctions associated with mitochondrial DNA damage in dopaminergic neurons in a mouse model of Parkinson's disease', *J Neurosci*, 31: 17649-58.

Pignatelli, A., and O. Belluzzi. 2017. 'Dopaminergic Neurones in the Main Olfactory Bulb: An Overview from an Electrophysiological Perspective', *Front Neuroanat*, 11: 7.

Pignatelli, A., K. Kobayashi, H. Okano, and O. Belluzzi. 2005. 'Functional properties of dopaminergic neurones in the mouse olfactory bulb', *J Physiol*, 564: 501-14.

Pinto, M., A. M. Pickrell, X. Wang, S. R. Bacman, A. Yu, A. Hida, L. M. Dillon, P. D. Morton, T. R. Malek, S. L. Williams, and C. T. Moraes. 2017. 'Transient mitochondrial DNA double strand breaks in mice cause accelerated aging phenotypes in a ROS-dependent but p53/p21-independent manner', *Cell Death Differ*, 24: 288-99.

Podlesniy, P., J. Figueiro-Silva, A. Llado, A. Antonell, R. Sanchez-Valle, D. Alcolea, A. Lleo, J. L. Molinuevo, N. Serra, and R. Trullas. 2013. 'Low cerebrospinal fluid concentration of mitochondrial DNA in preclinical Alzheimer disease', *Ann Neurol*, 74: 655-68.

Podlesniy, P., M. Puigros, N. Serra, R. Fernandez-Santiago, M. Ezquerra, E. Tolosa, and R. Trullas. 2019. 'Accumulation of mitochondrial 7S DNA in idiopathic and LRRK2 associated Parkinson's disease', *EBioMedicine*, 48: 554-67.

Poetschke, C., E. Dragicevic, J. Duda, J. Benkert, A. Dougalis, R. DeZio, T. P. Snutch, J. Striessnig, and B. Liss. 2015. 'Compensatory T-type Ca2+ channel activity alters D2-autoreceptor responses of Substantia nigra dopamine neurons from Cav1.3 L-type Ca2+ channel KO mice', *Sci Rep*, 5: 13688.

Politis, M., K. Wu, C. Loane, D. J. Brooks, L. Kiferle, F. E. Turkheimer, P. Bain, S. Molloy, and P. Piccini. 2014. 'Serotonergic mechanisms responsible for levodopa-induced dyskinesias in Parkinson's disease patients', *J Clin Invest*, 124: 1340-9.

Politis, M., K. Wu, C. Loane, F. E. Turkheimer, S. Molloy, D. J. Brooks, and P. Piccini. 2010. 'Depressive symptoms in PD correlate with higher 5-HTT binding in raphe and limbic structures', *Neurology*, 75: 1920-7.

Post, M. R., O. J. Lieberman, and E. V. Mosharov. 2018. 'Can Interactions Between alpha-Synuclein, Dopamine and Calcium Explain Selective Neurodegeneration in Parkinson's Disease?', *Front Neurosci*, 12: 161.

Postuma, R. B., D. Aarsland, P. Barone, D. J. Burn, C. H. Hawkes, W. Oertel, and T. Ziemssen. 2012. 'Identifying prodromal Parkinson's disease: pre-motor disorders in Parkinson's disease', *Mov Disord*, 27: 617-26.

Postuma, R. B., D. Berg, M. Stern, W. Poewe, C. W. Olanow, W. Oertel, J. Obeso, K. Marek, I. Litvan, A. E. Lang, G. Halliday, C. G. Goetz, T. Gasser, B. Dubois, P. Chan, B. R. Bloem, C. H. Adler, and G. Deuschl. 2015. 'MDS clinical diagnostic criteria for Parkinson's disease', *Mov Disord*, 30: 1591-601.

Postuma, R. B., A. E. Lang, J. F. Gagnon, A. Pelletier, and J. Y. Montplaisir. 2012. 'How does parkinsonism start? Prodromal parkinsonism motor changes in idiopathic REM sleep behaviour disorder', *Brain*, 135: 1860-70.

Pramstaller, P. P., M. G. Schlossmacher, T. S. Jacques, F. Scaravilli, C. Eskelson, I. Pepivani, K. Hedrich, S. Adel, M. Gonzales-McNeal, R. Hilker, P. L. Kramer, and C. Klein. 2005. 'Lewy body Parkinson's disease in a large pedigree with 77 Parkin mutation carriers', *Ann Neurol*, 58: 411-22.

Pryde, K. R., H. L. Smith, K. Y. Chau, and A. H. Schapira. 2016. 'PINK1 disables the anti-fission machinery to segregate damaged mitochondria for mitophagy', *J Cell Biol*, 213: 163-71.

Przedborski, S., M. Levivier, H. Jiang, M. Ferreira, V. Jackson-Lewis, D. Donaldson, and D. M. Togasaki. 1995. 'Dose-dependent lesions of the dopaminergic nigrostriatal pathway induced by intrastriatal injection of 6-hydroxydopamine', *Neuroscience*, 67: 631-47.

Puopolo, M., E. Raviola, and B. P. Bean. 2007. 'Roles of subthreshold calcium current and sodium current in spontaneous firing of mouse midbrain dopamine neurons', *J Neurosci*, 27: 645-56.

Pyle, A., H. Anugrha, M. Kurzawa-Akanbi, A. Yarnall, D. Burn, and G. Hudson. 2016. 'Reduced mitochondrial DNA copy number is a biomarker of Parkinson's disease', *Neurobiol Aging*, 38: 216.e7-16.e10.

Pyle, A., R. Brennan, M. Kurzawa-Akanbi, A. Yarnall, A. Thouin, B. Mollenhauer, D. Burn, P. F. Chinnery, and G. Hudson. 2015. 'Reduced cerebrospinal fluid mitochondrial DNA is a biomarker for early-stage Parkinson's disease', *Ann Neurol*, 78: 1000-4.

Pyle, A., H. Lowes, R. Brennan, M. Kurzawa-Akanbi, A. Yarnall, D. Burn, and G. Hudson. 2016. 'Reduced mitochondrial DNA is not a biomarker of depression in Parkinson's disease', *Mov Disord*, 31: 1923-24.

Ramonet, D., J. P. Daher, B. M. Lin, K. Stafa, J. Kim, R. Banerjee, M. Westerlund, O. Pletnikova, L. Glauser, L. Yang, Y. Liu, D. A. Swing, M. F. Beal, J. C. Troncoso, J. M. McCaffery, N. A. Jenkins, N. G. Copeland, D. Galter, B. Thomas, M. K. Lee, T. M. Dawson, V. L. Dawson, and D. J. Moore. 2011. 'Dopaminergic neuronal loss, reduced neurite complexity and autophagic abnormalities in transgenic mice expressing G2019S mutant LRRK2', *PLoS One*, 6: e18568.

Ramonet, D., A. Podhajska, K. Stafa, S. Sonnay, A. Trancikova, E. Tsika, O. Pletnikova, J. C. Troncoso, L. Glauser, and D. J. Moore. 2012. 'PARK9-associated ATP13A2 localizes to intracellular acidic vesicles and regulates cation homeostasis and neuronal integrity', *Hum Mol Genet*, 21: 1725-43.

Rana, M., I. de Coo, F. Diaz, H. Smeets, and C. T. Moraes. 2000. 'An out-of-frame cytochrome b gene deletion from a patient with parkinsonism is associated with impaired complex III assembly and an increase in free radical production', *Ann Neurol*, 48: 774-81.

Rayaprolu, S., Y. B. Seven, J. Howard, C. Duffy, M. Altshuler, C. Moloney, B. I. Giasson, and J. Lewis. 2018. 'Partial loss of ATP13A2 causes selective gliosis independent of robust lipofuscinosis', *Mol Cell Neurosci*, 92: 17-26.

Rebello, M. R., T. S. McTavish, D. C. Willhite, S. M. Short, G. M. Shepherd, and J. V. Verhagen. 2014. 'Perception of odors linked to precise timing in the olfactory system', *PLoS Biol*, 12: e1002021.

Reed, N. A., D. Cai, T. L. Blasius, G. T. Jih, E. Meyhofer, J. Gaertig, and K. J. Verhey. 2006. 'Microtubule acetylation promotes kinesin-1 binding and transport', *Curr Biol*, 16: 2166-72.

Reeve, A. K., K. J. Krishnan, J. L. Elson, C. M. Morris, A. Bender, R. N. Lightowlers, and D. M. Turnbull. 2008. 'Nature of mitochondrial DNA deletions in substantia nigra neurons', *Am J Hum Genet*, 82: 228-35.

Reich, S. G. 2020. 'Does This Patient Have Parkinson Disease or Essential Tremor?', *Clin Geriatr Med*, 36: 25-34.

Remy, P., M. Doder, A. Lees, N. Turjanski, and D. Brooks. 2005. 'Depression in Parkinson's disease: loss of dopamine and noradrenaline innervation in the limbic system', *Brain*, 128: 1314-22.

Ren, Jie, Ling Yuan, Wenbin Wang, Meiju Zhang, Qun Wang, Simin Li, Ling Zhang, and Kun Hu. 2019. 'Tricetin protects against 6-OHDA-induced neurotoxicity in Parkinson's disease model by

activating Nrf2/HO-1 signaling pathway and preventing mitochondria-dependent apoptosis pathway', *Toxicology and Applied Pharmacology*, 378: 114617.

Rhee, S. G., H. Z. Chae, and K. Kim. 2005. 'Peroxiredoxins: a historical overview and speculative preview of novel mechanisms and emerging concepts in cell signaling', *Free Radic Biol Med*, 38: 1543-52.

Richard, I. H., M. P. McDermott, R. Kurlan, J. M. Lyness, P. G. Como, N. Pearson, S. A. Factor, J. Juncos, C. Serrano Ramos, M. Brodsky, C. Manning, L. Marsh, L. Shulman, H. H. Fernandez, K. J. Black, M. Panisset, C. W. Christine, W. Jiang, C. Singer, S. Horn, R. Pfeiffer, D. Rottenberg, J. Slevin, L. Elmer, D. Press, H. C. Hyson, and W. McDonald. 2012. 'A randomized, double-blind, placebo-controlled trial of antidepressants in Parkinson disease', *Neurology*, 78: 1229-36.

Richter, F., M. Hamann, and A. Richter. 2007. 'Chronic rotenone treatment induces behavioral effects but no pathological signs of parkinsonism in mice', *J Neurosci Res*, 85: 681-91.

Riley, B. E., J. C. Lougheed, K. Callaway, M. Velasquez, E. Brecht, L. Nguyen, T. Shaler, D. Walker, Y. Yang, K. Regnstrom, L. Diep, Z. Zhang, S. Chiou, M. Bova, D. R. Artis, N. Yao, J. Baker, T. Yednock, and J. A. Johnston. 2013. 'Structure and function of Parkin E3 ubiquitin ligase reveals aspects of RING and HECT ligases', *Nat Commun*, 4: 1982.

Rizzo, G., M. Copetti, S. Arcuti, D. Martino, A. Fontana, and G. Logroscino. 2016. 'Accuracy of clinical diagnosis of Parkinson disease: A systematic review and meta-analysis', *Neurology*, 86: 566-76.

Rojo, A. I., C. Cavada, M. R. de Sagarra, and A. Cuadrado. 2007. 'Chronic inhalation of rotenone or paraquat does not induce Parkinson's disease symptoms in mice or rats', *Exp Neurol*, 208: 120-6.

Rousseaux, M. W., P. C. Marcogliese, D. Qu, S. J. Hewitt, S. Seang, R. H. Kim, R. S. Slack, M. G. Schlossmacher, D. C. Lagace, T. W. Mak, and D. S. Park. 2012. 'Progressive dopaminergic cell loss with unilateral-to-bilateral progression in a genetic model of Parkinson disease', *Proc Natl Acad Sci U S A*, 109: 15918-23.

Ruszkiewicz, J., and J. Albrecht. 2015. 'Changes in the mitochondrial antioxidant systems in neurodegenerative diseases and acute brain disorders', *Neurochem Int*, 88: 66-72.

Rylander, D., M. Parent, S. S. O'Sullivan, S. Dovero, A. J. Lees, E. Bezard, L. Descarries, and M. A. Cenci. 2010. 'Maladaptive plasticity of serotonin axon terminals in levodopa-induced dyskinesia', *Ann Neurol*, 68: 619-28.

Sarraf, S. A., M. Raman, V. Guarani-Pereira, M. E. Sowa, E. L. Huttlin, S. P. Gygi, and J. W. Harper. 2013. 'Landscape of the PARKIN-dependent ubiquitylome in response to mitochondrial depolarization', *Nature*, 496: 372-6.

Sato, S., M. Koike, M. Funayama, J. Ezaki, T. Fukuda, T. Ueno, Y. Uchiyama, and N. Hattori. 2016. 'Lysosomal Storage of Subunit c of Mitochondrial ATP Synthase in Brain-Specific Atp13a2-Deficient Mice', *Am J Pathol*, 186: 3074-82.

Sato, S., T. Uchihara, T. Fukuda, S. Noda, H. Kondo, S. Saiki, M. Komatsu, Y. Uchiyama, K. Tanaka, and N. Hattori. 2018. 'Loss of autophagy in dopaminergic neurons causes Lewy pathology and motor dysfunction in aged mice', *Sci Rep*, 8: 2813.

Sauer, H., and W. H. Oertel. 1994. 'Progressive degeneration of nigrostriatal dopamine neurons following intrastriatal terminal lesions with 6-hydroxydopamine: a combined retrograde tracing and immunocytochemical study in the rat', *Neuroscience*, 59: 401-15.

Scarffe, L. A., D. A. Stevens, V. L. Dawson, and T. M. Dawson. 2014. 'Parkin and PINK1: much more than mitophagy', *Trends Neurosci*, 37: 315-24.

Schapira, A. H. 1994. 'Evidence for mitochondrial dysfunction in Parkinson's disease--a critical appraisal', *Mov Disord*, 9: 125-38.

Schapira, A. H., J. M. Cooper, D. Dexter, P. Jenner, J. B. Clark, and C. D. Marsden. 1989. 'Mitochondrial complex I deficiency in Parkinson's disease', *Lancet*, 1: 1269.

Schapira, A. H., I. J. Holt, M. Sweeney, A. E. Harding, P. Jenner, and C. D. Marsden. 1990. 'Mitochondrial DNA analysis in Parkinson's disease', *Mov Disord*, 5: 294-7.

Schapira, A. H., V. M. Mann, J. M. Cooper, D. Dexter, S. E. Daniel, P. Jenner, J. B. Clark, and C. D. Marsden. 1990. 'Anatomic and disease specificity of NADH CoQ1 reductase (complex I) deficiency in Parkinson's disease', *J Neurochem*, 55: 2142-5.

Schiemann, J., F. Schlaudraff, V. Klose, M. Bingmer, S. Seino, P. J. Magill, K. A. Zaghloul, G. Schneider, B. Liss, and J. Roeper. 2012. 'K-ATP channels in dopamine substantia nigra neurons control bursting and novelty-induced exploration', *Nat Neurosci*, 15: 1272-80.

Schuepbach, W. M., J. Rau, K. Knudsen, J. Volkmann, P. Krack, L. Timmermann, T. D. Halbig, H. Hesekamp, S. M. Navarro, N. Meier, D. Falk, M. Mehdorn, S. Paschen, M. Maarouf, M. T. Barbe, G. R. Fink, A. Kupsch, D. Gruber, G. H. Schneider, E. Seigneuret, A. Kistner, P. Chaynes, F. Ory-Magne, C. Brefel Courbon, J. Vesper, A. Schnitzler, L. Wojtecki, J. L. Houeto, B. Bataille,

D. Maltete, P. Damier, S. Raoul, F. Sixel-Doering, D. Hellwig, A. Gharabaghi, R. Kruger, M. O. Pinsker, F. Amtage, J. M. Regis, T. Witjas, S. Thobois, P. Mertens, M. Kloss, A. Hartmann, W. H. Oertel, B. Post, H. Speelman, Y. Agid, C. Schade-Brittinger, and G. Deuschl. 2013. 'Neurostimulation for Parkinson's disease with early motor complications', *N Engl J Med*, 368: 610-22.

Scott, W. K., L. H. Yamaoka, J. M. Stajich, B. L. Scott, J. M. Vance, A. D. Roses, M. A. Pericak-Vance, R. L. Watts, M. Nance, J. Hubble, W. Koller, M. B. Stern, A. Colcher, F. H. Allen, Jr., B. C. Hiner, J. Jankovic, W. Ondo, N. G. Laing, F. Mastaglia, C. Goetz, E. Pappert, G. W. Small, D. Masterman, J. L. Haines, and T. L. Davies. 1999. 'The alpha-synuclein gene is not a major risk factor in familial Parkinson disease', *Neurogenetics*, 2: 191-2.

Seaman, M. N. 2012. 'The retromer complex - endosomal protein recycling and beyond', *J Cell Sci*, 125: 4693-702.

Seibenhener, M. L., and M. C. Wooten. 2015. 'Use of the Open Field Maze to measure locomotor and anxiety-like behavior in mice', *J Vis Exp*: e52434.

Shannak, K., A. Rajput, B. Rozdilsky, S. Kish, J. Gilbert, and O. Hornykiewicz. 1994. 'Noradrenaline, dopamine and serotonin levels and metabolism in the human hypothalamus: observations in Parkinson's disease and normal subjects', *Brain Res*, 639: 33-41.

Sheng, Z., S. Zhang, D. Bustos, T. Kleinheinz, C. E. Le Pichon, S. L. Dominguez, H. O. Solanoy, J. Drummond, X. Zhang, X. Ding, F. Cai, Q. Song, X. Li, Z. Yue, M. P. van der Brug, D. J. Burdick, J. Gunzner-Toste, H. Chen, X. Liu, A. A. Estrada, Z. K. Sweeney, K. Scearce-Levie, J. G. Moffat, D. S. Kirkpatrick, and H. Zhu. 2012. 'Ser1292 autophosphorylation is an indicator of LRRK2 kinase activity and contributes to the cellular effects of PD mutations', *Sci Transl Med*, 4: 164ra61.

Shin, J. H., H. S. Ko, H. Kang, Y. Lee, Y. I. Lee, O. Pletinkova, J. C. Troconso, V. L. Dawson, and T. M. Dawson. 2011. 'PARIS (ZNF746) repression of PGC-1alpha contributes to neurodegeneration in Parkinson's disease', *Cell*, 144: 689-702.

Shoffner, J. M., M. T. Lott, A. M. Lezza, P. Seibel, S. W. Ballinger, and D. C. Wallace. 1990. 'Myoclonic epilepsy and ragged-red fiber disease (MERRF) is associated with a mitochondrial DNA tRNA(Lys) mutation', *Cell*, 61: 931-7.

Sian, J., D. T. Dexter, A. J. Lees, S. Daniel, Y. Agid, F. Javoy-Agid, P. Jenner, and C. D. Marsden. 1994. 'Alterations in glutathione levels in Parkinson's disease and other neurodegenerative disorders affecting basal ganglia', *Ann Neurol*, 36: 348-55.

Simard, M., G. Arcuino, T. Takano, Q. S. Liu, and M. Nedergaard. 2003. 'Signaling at the gliovascular interface', *J Neurosci*, 23: 9254-62.

Singh, A., P. Verma, A. Raju, and K. P. Mohanakumar. 2019. 'Nimodipine attenuates the parkinsonian neurotoxin, MPTP-induced changes in the calcium binding proteins, calpain and calbindin', *J Chem Neuroanat*, 95: 89-94.

Sironi, F., P. Primignani, S. Ricca, S. Tunesi, M. Zini, S. Tesei, R. Cilia, G. Pezzoli, M. Seia, and S. Goldwurm. 2013. 'DJ1 analysis in a large cohort of Italian early onset Parkinson Disease patients', *Neurosci Lett*, 557 Pt B: 165-70.

Smith, G. A., J. Jansson, E. M. Rocha, T. Osborn, P. J. Hallett, and O. Isacson. 2016. 'Fibroblast Biomarkers of Sporadic Parkinson's Disease and LRRK2 Kinase Inhibition', *Mol Neurobiol*, 53: 5161-77.

Smith, K. M., S. E. Browne, S. Jayaraman, C. J. Bleickardt, L. M. Hodge, E. Lis, L. Yao, S. L. Rittle, N. Innocent, D. E. Mullins, G. Boykow, I. J. Reynolds, D. Hill, E. M. Parker, and R. A. Hodgson. 2014. 'Effects of the selective adenosine A2A receptor antagonist, SCH 412348, on the parkinsonian phenotype of MitoPark mice', *Eur J Pharmacol*, 728: 31-8.

Sofic, E., K. W. Lange, K. Jellinger, and P. Riederer. 1992. 'Reduced and oxidized glutathione in the substantia nigra of patients with Parkinson's disease', *Neurosci Lett*, 142: 128-30.

Soloway, S. B. 1976. 'Naturally occurring insecticides', *Environ Health Perspect*, 14: 109-17.

Sonia Angeline, M., P. Chaterjee, K. Anand, R. K. Ambasta, and P. Kumar. 2012. 'Rotenone-induced parkinsonism elicits behavioral impairments and differential expression of parkin, heat shock proteins and caspases in the rat', *Neuroscience*, 220: 291-301.

Sonntag, K. C., B. Song, N. Lee, J. H. Jung, Y. Cha, P. Leblanc, C. Neff, S. W. Kong, B. S. Carter, J. Schweitzer, and K. S. Kim. 2018. 'Pluripotent stem cell-based therapy for Parkinson's disease: Current status and future prospects', *Prog Neurobiol*, 168: 1-20.

Soong, N. W., D. R. Hinton, G. Cortopassi, and N. Arnheim. 1992. 'Mosaicism for a specific somatic mitochondrial DNA mutation in adult human brain', *Nat Genet*, 2: 318-23.

Soto-Otero, R., E. Mendez-Alvarez, A. Hermida-Ameijeiras, A. M. Munoz-Patino, and J. L. Labandeira-Garcia. 2000. 'Autoxidation and neurotoxicity of 6-hydroxydopamine in the presence of some antioxidants: potential implication in relation to the pathogenesis of Parkinson's disease', *J Neurochem*, 74: 1605-12.

Soubannier, V., G. L. McLelland, R. Zunino, E. Braschi, P. Rippstein, E. A. Fon, and H. M. McBride. 2012. 'A vesicular transport pathway shuttles cargo from mitochondria to lysosomes', *Curr Biol*, 22: 135-41.

Spillantini, M. G., M. L. Schmidt, V. M. Lee, J. Q. Trojanowski, R. Jakes, and M. Goedert. 1997. 'Alpha-synuclein in Lewy bodies', *Nature*, 388: 839-40.

Stafa, K., E. Tsika, R. Moser, A. Musso, L. Glauser, A. Jones, S. Biskup, Y. Xiong, R. Bandopadhyay, V. L. Dawson, T. M. Dawson, and D. J. Moore. 2014. 'Functional interaction of Parkinson's disease-associated LRRK2 with members of the dynamin GTPase superfamily', *Hum Mol Genet*, 23: 2055-77.

Sterio, D., A. Beric, M. Dogali, E. Fazzini, G. Alfaro, and O. Devinsky. 1994. 'Neurophysiological properties of pallidal neurons in Parkinson's disease', *Ann Neurol*, 35: 586-91.

Sterky, F. H., S. Lee, R. Wibom, L. Olson, and N. G. Larsson. 2011. 'Impaired mitochondrial transport and Parkin-independent degeneration of respiratory chain-deficient dopamine neurons in vivo', *Proc Natl Acad Sci U S A*, 108: 12937-42.

Stevens, D. A., Y. Lee, H. C. Kang, B. D. Lee, Y. I. Lee, A. Bower, H. Jiang, S. U. Kang, S. A. Andrabi, V. L. Dawson, J. H. Shin, and T. M. Dawson. 2015. 'Parkin loss leads to PARIS-dependent declines in mitochondrial mass and respiration', *Proc Natl Acad Sci U S A*, 112: 11696-701.

Stobart, J. L., and C. M. Anderson. 2013. 'Multifunctional role of astrocytes as gatekeepers of neuronal energy supply', *Front Cell Neurosci*, 7: 38.

Su, Y. C., and X. Qi. 2013. 'Inhibition of excessive mitochondrial fission reduced aberrant autophagy and neuronal damage caused by LRRK2 G2019S mutation', *Hum Mol Genet*, 22: 4545-61.

Sugiura, A., G. L. McLelland, E. A. Fon, and H. M. McBride. 2014. 'A new pathway for mitochondrial quality control: mitochondrial-derived vesicles', *EMBO J*, 33: 2142-56.

Suleiman, J., N. Hamwi, and A. W. El-Hattab. 2018. 'ATP13A2 novel mutations causing a rare form of juvenile-onset Parkinson disease', *Brain Dev*, 40: 824-26.

Suomalainen, A., A. Majander, M. Haltia, H. Somer, J. Lonnqvist, M. L. Savontaus, and L. Peltonen. 1992. 'Multiple deletions of mitochondrial DNA in several tissues of a patient with severe retarded depression and familial progressive external ophthalmoplegia', *J Clin Invest*, 90: 61-6.

Suomalainen, A., A. Majander, M. Wallin, K. Setala, K. Kontula, H. Leinonen, T. Salmi, A. Paetau, M. Haltia, L. Valanne, J. Lonnqvist, L. Peltonen, and H. Somer. 1997. 'Autosomal dominant progressive external ophthalmoplegia with multiple deletions of mtDNA: clinical, biochemical, and molecular genetic features of the 10q-linked disease', *Neurology*, 48: 1244-53.

Surmeier, D. J., J. N. Guzman, and J. Sanchez-Padilla. 2010. 'Calcium, cellular aging, and selective neuronal vulnerability in Parkinson's disease', *Cell Calcium*, 47: 175-82.

Surmeier, D. J., J. N. Guzman, J. Sanchez-Padilla, and J. A. Goldberg. 2010. 'What causes the death of dopaminergic neurons in Parkinson's disease?', *Prog Brain Res*, 183: 59-77.

Surmeier, D. J., J. N. Guzman, J. Sanchez, and P. T. Schumacker. 2012. 'Physiological phenotype and vulnerability in Parkinson's disease', *Cold Spring Harb Perspect Med*, 2: a009290.

Tabata, Y., Y. Imaizumi, M. Sugawara, T. Andoh-Noda, S. Banno, M. Chai, T. Sone, K. Yamazaki, M. Ito, K. Tsukahara, H. Saya, N. Hattori, J. Kohyama, and H. Okano. 2018. 'T-type Calcium Channels Determine the Vulnerability of Dopaminergic Neurons to Mitochondrial Stress in Familial Parkinson Disease', *Stem Cell Reports*, 11: 1171-84.

Taguchi, T., M. Ikuno, M. Hondo, L. K. Parajuli, K. Taguchi, J. Ueda, M. Sawamura, S. Okuda, E. Nakanishi, J. Hara, N. Uemura, Y. Hatanaka, T. Ayaki, S. Matsuzawa, M. Tanaka, O. M. A. El-Agnaf, M. Koike, M. Yanagisawa, M. T. Uemura, H. Yamakado, and R. Takahashi. 2020. 'alpha-Synuclein BAC transgenic mice exhibit RBD-like behaviour and hyposmia: a prodromal Parkinson's disease model', *Brain*, 143: 249-65.

Taira, T., Y. Saito, T. Niki, S. M. Iguchi-Ariga, K. Takahashi, and H. Ariga. 2004. 'DJ-1 has a role in antioxidative stress to prevent cell death', *EMBO Rep*, 5: 213-8.

Tang, F. L., W. Liu, J. X. Hu, J. R. Erion, J. Ye, L. Mei, and W. C. Xiong. 2015. 'VPS35 Deficiency or Mutation Causes Dopaminergic Neuronal Loss by Impairing Mitochondrial Fusion and Function', *Cell Rep*, 12: 1631-43.

Telford, J. E., S. M. Kilbride, and G. P. Davey. 2009. 'Complex I is rate-limiting for oxygen consumption in the nerve terminal', *J Biol Chem*, 284: 9109-14.

Thiele, S. L., R. Warre, and J. E. Nash. 2012. 'Development of a unilaterally-lesioned 6-OHDA mouse model of Parkinson's disease', *J Vis Exp*.

Thomas, J. M., T. Li, W. Yang, F. Xue, P. S. Fishman, and W. W. Smith. 2016. '68 and FX2149 Attenuate Mutant LRRK2-R1441C-Induced Neural Transport Impairment', *Front Aging Neurosci*, 8: 337.

Thyagarajan, D., S. Bressman, C. Bruno, S. Przedborski, S. Shanske, T. Lynch, S. Fahn, and S. DiMauro. 2000. 'A novel mitochondrial 12SrRNA point mutation in parkinsonism, deafness, and neuropathy', *Ann Neurol*, 48: 730-6.

Tillerson, J. L., W. M. Caudle, J. M. Parent, C. Gong, T. Schallert, and G. W. Miller. 2006. 'Olfactory discrimination deficits in mice lacking the dopamine transporter or the D2 dopamine receptor', *Behav Brain Res*, 172: 97-105.

Trempe, J. F., V. Sauve, K. Grenier, M. Seirafi, M. Y. Tang, M. Menade, S. Al-Abdul-Wahid, J. Krett, K. Wong, G. Kozlov, B. Nagar, E. A. Fon, and K. Gehring. 2013. 'Structure of parkin reveals mechanisms for ubiquitin ligase activation', *Science*, 340: 1451-5.

Trifunovic, A., A. Wredenberg, M. Falkenberg, J. N. Spelbrink, A. T. Rovio, C. E. Bruder, Y. M. Bohlooly, S. Gidlof, A. Oldfors, R. Wibom, J. Tornell, H. T. Jacobs, and N. G. Larsson. 2004. 'Premature ageing in mice expressing defective mitochondrial DNA polymerase', *Nature*, 429: 417-23.

Truban, D., X. Hou, T. R. Caulfield, F. C. Fiesel, and W. Springer. 2017. 'PINK1, Parkin, and Mitochondrial Quality Control: What can we Learn about Parkinson's Disease Pathobiology?', *J Parkinsons Dis*, 7: 13-29.

Tsacopoulos, M., and P. J. Magistretti. 1996. 'Metabolic coupling between glia and neurons', *J Neurosci*, 16: 877-85.

Ungerstedt, U. 1968. '6-Hydroxy-dopamine induced degeneration of central monoamine neurons', *Eur J Pharmacol*, 5: 107-10.

Valente, E. M., P. M. Abou-Sleiman, V. Caputo, M. M. Muqit, K. Harvey, S. Gispert, Z. Ali, D. Del Turco, A. R. Bentivoglio, D. G. Healy, A. Albanese, R. Nussbaum, R. Gonzalez-Maldonado, T. Deller, S. Salvi, P. Cortelli, W. P. Gilks, D. S. Latchman, R. J. Harvey, B. Dallapiccola, G. Auburger, and N. W. Wood. 2004. 'Hereditary early-onset Parkinson's disease caused by mutations in PINK1', *Science*, 304: 1158-60.

van Duijn, C. M., M. C. Dekker, V. Bonifati, R. J. Galjaard, J. J. Houwing-Duistermaat, P. J. Snijders, L. Testers, G. J. Breedveld, M. Horstink, L. A. Sandkuijl, J. C. van Swieten, B. A. Oostra, and P. Heutink. 2001. 'Park7, a novel locus for autosomal recessive early-onset parkinsonism, on chromosome 1p36', *Am J Hum Genet*, 69: 629-34.

Vergano-Vera, E., M. J. Yusta-Boyo, F. de Castro, A. Bernad, F. de Pablo, and C. Vicario-Abejon. 2006. 'Generation of GABAergic and dopaminergic interneurons from endogenous embryonic olfactory bulb precursor cells', *Development*, 133: 4367-79.

Vijayakumar, D., and J. Jankovic. 2016. 'Drug-Induced Dyskinesia, Part 1: Treatment of Levodopa-Induced Dyskinesia', *Drugs*, 76: 759-77.

Vilarino-Guell, C., C. Wider, O. A. Ross, J. C. Dachsel, J. M. Kachergus, S. J. Lincoln, A. I. Soto-Ortolaza, S. A. Cobb, G. J. Wilhoite, J. A. Bacon, B. Behrouz, H. L. Melrose, E. Hentati, A. Puschmann, D. M. Evans, E. Conibear, W. W. Wasserman, J. O. Aasly, P. R. Burkhard, R. Djaldetti, J. Ghika, F. Hentati, A. Krygowska-Wajs, T. Lynch, E. Melamed, A. Rajput, A. H. Rajput, A. Solida, R. M. Wu, R. J. Uitti, Z. K. Wszolek, F. Vingerhoets, and M. J. Farrer. 2011. 'VPS35 mutations in Parkinson disease', *Am J Hum Genet*, 89: 162-7.

Vitek, J. L., J. Zhang, T. Hashimoto, G. S. Russo, and K. B. Baker. 2012. 'External pallidal stimulation improves parkinsonian motor signs and modulates neuronal activity throughout the basal ganglia thalamic network', *Exp Neurol*, 233: 581-6.

Vives-Bauza, C., C. Zhou, Y. Huang, M. Cui, R. L. de Vries, J. Kim, J. May, M. A. Tocilescu, W. Liu, H. S. Ko, J. Magrane, D. J. Moore, V. L. Dawson, R. Grailhe, T. M. Dawson, C. Li, K. Tieu, and S. Przedborski. 2010. 'PINK1-dependent recruitment of Parkin to mitochondria in mitophagy', *Proc Natl Acad Sci U S A*, 107: 378-83.

Voigt, D. D., C. M. Nascimento, R. B. de Souza, P. H. Cabello Acero, M. Campos Junior, C. P. da Silva, J. S. Pereira, A. L. Rosso, M. A. Araujo Leite, L. F. R. Vasconcellos, M. V. Della Coletta, D. J. da Silva, D. H. Nicaretta, A. P. Goncalves, J. M. Dos Santos, V. Calassara, C. B. Santos-Reboucas, and M. M. G. Pimentel. 2019. 'CHCHD2 mutational screening in Brazilian patients with familial Parkinson's disease', *Neurobiol Aging*, 74: 236 e7-36 e8.

Wachowiak, M., J. P. McGann, P. M. Heyward, Z. Shao, A. C. Puche, and M. T. Shipley. 2005. 'Inhibition of olfactory receptor neuron input to olfactory bulb glomeruli mediated by suppression of presynaptic calcium influx', *J Neurophysiol*, 94: 2700-12.

Waddington, J. L. 1980. 'Effects of nomifensine and desipramine on the sequelae of intracerebrally-injected 6-OHDA and 5,6-DHT', *Pharmacol Biochem Behav*, 13: 915-7.

Wakamatsu, M., A. Ishii, Y. Ukai, J. Sakagami, S. Iwata, M. Ono, K. Matsumoto, A. Nakamura, N. Tada, K. Kobayashi, T. Iwatsubo, and M. Yoshimoto. 2007. 'Accumulation of phosphorylated alpha-synuclein in dopaminergic neurons of transgenic mice that express human alpha-synuclein', *J Neurosci Res*, 85: 1819-25.

Wallace, D. C., G. Singh, M. T. Lott, J. A. Hodge, T. G. Schurr, A. M. Lezza, L. J. Elsas, 2nd, and E. K. Nikoskelainen. 1988. 'Mitochondrial DNA mutation associated with Leber's hereditary optic neuropathy', *Science*, 242: 1427-30.

Wallman, M. J., D. Gagnon, and M. Parent. 2011. 'Serotonin innervation of human basal ganglia', *Eur J Neurosci*, 33: 1519-32.

References

Wang, M. J., H. Y. Huang, T. L. Chiu, H. F. Chang, and H. R. Wu. 2019. 'Peroxiredoxin 5 Silencing Sensitizes Dopaminergic Neuronal Cells to Rotenone via DNA Damage-Triggered ATM/p53/PUMA Signaling-Mediated Apoptosis', *Cells*, 9.

Wang, W., X. Wang, H. Fujioka, C. Hoppel, A. L. Whone, M. A. Caldwell, P. J. Cullen, J. Liu, and X. Zhu. 2016. 'Parkinson's disease-associated mutant VPS35 causes mitochondrial dysfunction by recycling DLP1 complexes', *Nat Med*, 22: 54-63.

Wang, X., K. Becker, N. Levine, M. Zhang, A. P. Lieberman, D. J. Moore, and J. Ma. 2019. 'Pathogenic alpha-synuclein aggregates preferentially bind to mitochondria and affect cellular respiration', *Acta Neuropathol Commun*, 7: 41.

Wang, X., M. H. Yan, H. Fujioka, J. Liu, A. Wilson-Delfosse, S. G. Chen, G. Perry, G. Casadesus, and X. Zhu. 2012. 'LRRK2 regulates mitochondrial dynamics and function through direct interaction with DLP1', *Hum Mol Genet*, 21: 1931-44.

Watabe-Uchida, M., L. Zhu, S. K. Ogawa, A. Vamanrao, and N. Uchida. 2012. 'Whole-brain mapping of direct inputs to midbrain dopamine neurons', *Neuron*, 74: 858-73.

Wauer, T., and D. Komander. 2013. 'Structure of the human Parkin ligase domain in an autoinhibited state', *EMBO J*, 32: 2099-112.

Weiland, D., B. Brachvogel, H. T. Hornig-Do, J. F. G. Neuhaus, T. Holzer, D. J. Tobin, C. M. Niessen, R. J. Wiesner, and O. R. Baris. 2018. 'Imbalance of Mitochondrial Respiratory Chain Complexes in the Epidermis Induces Severe Skin Inflammation', *J Invest Dermatol*, 138: 132-40.

West, A. B., D. J. Moore, S. Biskup, A. Bugayenko, W. W. Smith, C. A. Ross, V. L. Dawson, and T. M. Dawson. 2005. 'Parkinson's disease-associated mutations in leucine-rich repeat kinase 2 augment kinase activity', *Proc Natl Acad Sci U S A*, 102: 16842-7.

Wichmann, T., H. Bergman, P. A. Starr, T. Subramanian, R. L. Watts, and M. R. DeLong. 1999. 'Comparison of MPTP-induced changes in spontaneous neuronal discharge in the internal pallidal segment and in the substantia nigra pars reticulata in primates', *Exp Brain Res*, 125: 397-409.

Wichmann, T., and M. R. DeLong. 1996. 'Functional and pathophysiological models of the basal ganglia', *Curr Opin Neurobiol*, 6: 751-8.

Wirth, C., U. Brandt, C. Hunte, and V. Zickermann. 2016. 'Structure and function of mitochondrial complex I', *Biochim Biophys Acta*, 1857: 902-14.

Xi, Y., D. Feng, K. Tao, R. Wang, Y. Shi, H. Qin, M. P. Murphy, Q. Yang, and G. Zhao. 2018. 'MitoQ protects dopaminergic neurons in a 6-OHDA induced PD model by enhancing Mfn2-dependent mitochondrial fusion via activation of PGC-1alpha', *Biochim Biophys Acta Mol Basis Dis*, 1864: 2859-70.

Xiong, A., and D. W. Wesson. 2016. 'Illustrated Review of the Ventral Striatum's Olfactory Tubercle', *Chem Senses*, 41: 549-55.

Xu, W., and D. Lipscombe. 2001. 'Neuronal Ca(V)1.3alpha(1) L-type channels activate at relatively hyperpolarized membrane potentials and are incompletely inhibited by dihydropyridines', *J Neurosci*, 21: 5944-51.

Young, K. M., M. Fogarty, N. Kessaris, and W. D. Richardson. 2007. 'Subventricular zone stem cells are heterogeneous with respect to their embryonic origins and neurogenic fates in the adult olfactory bulb', *J Neurosci*, 27: 8286-96.

Yu, H., D. Sternad, D. M. Corcos, and D. E. Vaillancourt. 2007. 'Role of hyperactive cerebellum and motor cortex in Parkinson's disease', *Neuroimage*, 35: 222-33.

Yuan, H. H., R. J. Chen, Y. H. Zhu, C. L. Peng, and X. R. Zhu. 2013. 'The neuroprotective effect of overexpression of calbindin-D(28k) in an animal model of Parkinson's disease', *Mol Neurobiol*, 47: 117-22.

Yue, M., K. M. Hinkle, P. Davies, E. Trushina, F. C. Fiesel, T. A. Christenson, A. S. Schroeder, L. Zhang, E. Bowles, B. Behrouz, S. J. Lincoln, J. E. Beevers, A. J. Milnerwood, A. Kurti, P. J. McLean, J. D. Fryer, W. Springer, D. W. Dickson, M. J. Farrer, and H. L. Melrose. 2015. 'Progressive dopaminergic alterations and mitochondrial abnormalities in LRRK2 G2019S knock-in mice', *Neurobiol Dis*, 78: 172-95.

Zaghloul, K. A., J. A. Blanco, C. T. Weidemann, K. McGill, J. L. Jaggi, G. H. Baltuch, and M. J. Kahana. 2009. 'Human substantia nigra neurons encode unexpected financial rewards', *Science*, 323: 1496-9.

Zeng, X. S., W. S. Geng, and J. J. Jia. 2018. 'Neurotoxin-Induced Animal Models of Parkinson Disease: Pathogenic Mechanism and Assessment', *ASN Neuro*, 10: 1759091418777438.

Zeviani, M., C. T. Moraes, S. DiMauro, H. Nakase, E. Bonilla, E. A. Schon, and L. P. Rowland. 1988. 'Deletions of mitochondrial DNA in Kearns-Sayre syndrome', *Neurology*, 38: 1339-46.

Zeviani, M., S. Servidei, C. Gellera, E. Bertini, S. DiMauro, and S. DiDonato. 1989. 'An autosomal dominant disorder with multiple deletions of mitochondrial DNA starting at the D-loop region', *Nature*, 339: 309-11.

Zhang, Y., J. Gao, K. K. Chung, H. Huang, V. L. Dawson, and T. M. Dawson. 2000. 'Parkin functions as an E2-dependent ubiquitin- protein ligase and promotes the degradation of the synaptic vesicle-associated protein, CDCrel-1', *Proc Natl Acad Sci U S A*, 97: 13354-9.

Zhang, Y., A. C. Granholm, K. Huh, L. Shan, O. Diaz-Ruiz, N. Malik, L. Olson, B. J. Hoffer, C. R. Lupica, A. F. Hoffman, and C. M. Backman. 2012. 'PTEN deletion enhances survival, neurite outgrowth and function of dopamine neuron grafts to MitoPark mice', *Brain*, 135: 2736-49.

Zhang, Z., Q. Liu, P. Wen, J. Zhang, X. Rao, Z. Zhou, H. Zhang, X. He, J. Li, Z. Zhou, X. Xu, X. Zhang, R. Luo, G. Lv, H. Li, P. Cao, L. Wang, and F. Xu. 2017. 'Activation of the dopaminergic pathway from VTA to the medial olfactory tubercle generates odor-preference and reward', *Elife*, 6.

Zhang, Z., H. Zhang, P. Wen, X. Zhu, L. Wang, Q. Liu, J. Wang, X. He, H. Wang, and F. Xu. 2017. 'Whole-Brain Mapping of the Inputs and Outputs of the Medial Part of the Olfactory Tubercle', *Front Neural Circuits*, 11: 52.

Zhong, P., Z. Hu, H. Jiang, Z. Yan, and J. Feng. 2017. 'Dopamine Induces Oscillatory Activities in Human Midbrain Neurons with Parkin Mutations', *Cell Rep*, 19: 1033-44.

Zhou, C., Y. Huang, Y. Shao, J. May, D. Prou, C. Perier, W. Dauer, E. A. Schon, and S. Przedborski. 2008. 'The kinase domain of mitochondrial PINK1 faces the cytoplasm', *Proc Natl Acad Sci U S A*, 105: 12022-7.

Zhu, J. H., C. Horbinski, F. Guo, S. Watkins, Y. Uchiyama, and C. T. Chu. 2007. 'Regulation of autophagy by extracellular signal-regulated protein kinases during 1-methyl-4-phenylpyridinium-induced cell death', *Am J Pathol*, 170: 75-86.

Zimprich, A., A. Benet-Pages, W. Struhal, E. Graf, S. H. Eck, M. N. Offman, D. Haubenberger, S. Spielberger, E. C. Schulte, P. Lichtner, S. C. Rossle, N. Klopp, E. Wolf, K. Seppi, W. Pirker, S. Presslauer, B. Mollenhauer, R. Katzenschlager, T. Foki, C. Hotzy, E. Reinthaler, A. Harutyunyan, R. Kralovics, A. Peters, F. Zimprich, T. Brucke, W. Poewe, E. Auff, C. Trenkwalder, B. Rost, G. Ransmayr, J. Winkelmann, T. Meitinger, and T. M. Strom. 2011. 'A mutation in VPS35, encoding a subunit of the retromer complex, causes late-onset Parkinson disease', *Am J Hum Genet*, 89: 168-75.

Zimprich, A., S. Biskup, P. Leitner, P. Lichtner, M. Farrer, S. Lincoln, J. Kachergus, M. Hulihan, R. J. Uitti, D. B. Calne, A. J. Stoessl, R. F. Pfeiffer, N. Patenge, I. C. Carbajal, P. Vieregge, F. Asmus, B. Muller-Myhsok, D. W. Dickson, T. Meitinger, T. M. Strom, Z. K. Wszolek, and T. Gasser. 2004. 'Mutations in LRRK2 cause autosomal-dominant parkinsonism with pleomorphic pathology', *Neuron*, 44: 601-7.

Danksagung

Abschließend möchte ich die Gelegenheit nutzen, um „Danke" zu sagen. Auf verschiedenste Art und Weise durfte ich auf die stetige Unterstützung einer Reihe wunderbarer Menschen zählen. Ein dickes Dankeschön an…

Rudi… für das Vertrauen, das du von Tag eins an in mich gesetzt hast… für die Chance, in einem Beruf aufgehen zu können… für deine wissenschaftliche Expertise… für deine unglaubliche Ruhe und Erfahrung… für die zunehmende Unabhängigkeit, die du mir durch eigenständiges Schreiben von Paper und diverser TVAs antrainiert hast… die wissenschaftliche Integration außerhalb unserer AG… für den Freiraum, mich wissenschaftlich weiterzuentwickeln... für die hoffentlich weitere gemeinsame Zeit.

Konrad… für die unglaublich einfache Eingewöhnungsphase… für deine tägliche Unterstützung innerhalb und außerhalb des Labors… für deine Ruhe und Geduld… für deine wahnsinnige Struktur und Organisation … für den Mut und Zuspruch, den du mir immer gibst… für die Integration in den Turtle-Clan… für den Tipp, zu rennen, sobald es nach Mandeln riecht.

Olivier… for infecting me with your joy in this profession… for your scientific mentoring… for your humor to make things easy and overcome difficult situations… for the unforgotten jam session.

Sammy… for introducing the Kenyan way of life… for sharing your insanely giant scientific knowledge… for all the discussions about "propagandas", mtDNA and of course the "aliens".

unser Wiesner-Team: **David**, **Julia**, **Jana**, **Katrin**, **Nadine**, **Ruth**, **Ayesha**, aber auch **Diana** und Ehemalige, wie **Tran** und vor allem **Anja**… dafür, dass sich Arbeit nicht wie solche anfühlt… für ein unglaublich geiles Arbeitsklima… für eure tägliche Unterstützung, Beratung und Aufmunterung… auf eine hoffentlich weitere Zeit und ein paar feuchtfröhliche Konferenzen… in diesem Sinne: *tengo un cacahuete en mi capucha.*

meine Azubis: **Steffen**, **Katrin**, **Robin**, **Klara**… für die unzähligen Stunden, die ihr am Mikrotom und über den Färbekammern hingt und dabei trotzdem immer gut gelaunt wart. Ohne euch wäre die Doktorarbeit in dieser Zeit niemals möglich gewesen.

unsere Werkstatt-Jungs… für die verschiedensten, eigens angefertigten Apparaturen für meine Verhaltensexperimente.

the **Mito-RTG**, being led by **Elena** and **Jürgen**. For introducing me to the mitochondrial network in Cologne and beyond… for the MitoClubs and retreats… for the scientific feedback and mentoring whenever asked, especially to my tutors **Sandra** & **Peter**… but also **Katerina** and **Claudia**… für eure unglaublich beständige und freundliche Art… für die sofortige Hilfe und Unterstützung in vielfältiger Weise rund um die Promotion.

Christian… für deine große Unterstützung bei den Multiphotonenexperimenten… deine immer freundliche Art, vor allem bei der Beantwortung jeder meiner mittlerweile 1.000 Mails bezüglich der Anpassung einer Mikroskopbuchung.

meine **Freunde**, allen voran meinen **Kegelclub**… für eure schonungslos ehrliche und erdende Freundschaft vom Kindergarten an… für eine unglaublich schöne Zeit voll von skurrilen Geschichten, die hoffentlich in Zukunft noch weitergesponnen werden können.

meine **Familie**… dafür, dass ihr euch stets mein wissenschaftliches Gerede anzuhören und zu ertragen wisst… speziell an Michael, dass ich jetzt immer das Meer in euren Köpfen rauschen höre, sobald ich von der Arbeit spreche… dafür, dass ihr immer da wart, seid und hoffentlich noch lange sein werdet.

und schließlich an **Iris**… für jeden Tag, den ich mit dir verbringen darf… für deinen unnachgiebigen Versuch mir „aufgehängt" beizubringen… für die Bemühung, mir immer gespannt zuzuhören… für das Teilen meiner Freude in guten Zeiten… für den Trost und die Aufmunterung in schweren Zeiten… dafür, dass du immer an meiner Seite bist, seit nun unfassbaren zehn Jahren… und für das „Ja".

Erklärung

Hiermit versichere ich an Eides statt, dass ich die vorliegende Dissertation selbstständig und ohne die Benutzung anderer als der angegebenen Hilfsmittel und Literatur angefertigt habe. Alle Stellen, die wörtlich oder sinngemäß aus veröffentlichten und nicht veröffentlichten Werken dem Wortlaut oder dem Sinn nach entnommen wurden, sind als solche kenntlich gemacht. Ich versichere an Eides statt, dass diese Dissertation noch keiner anderen Fakultät oder Universität zur Prüfung vorgelegen hat; dass sie - abgesehen von unten angegebenen Teilpublikationen und eingebundenen Artikeln und Manuskripten - noch nicht veröffentlicht worden ist sowie, dass ich eine Veröffentlichung der Dissertation vor Abschluss der Promotion nicht ohne Genehmigung des Promotionsausschusses vornehmen werde. Die Bestimmungen dieser Ordnung sind mir bekannt. Darüber hinaus erkläre ich hiermit, dass ich die Ordnung zur Sicherung guter wissenschaftlicher Praxis und zum Umgang mit wissenschaftlichem Fehlverhalten der Universität zu Köln gelesen und sie bei der Durchführung der Dissertation zugrundeliegenden Arbeiten und der schriftlich verfassten Dissertation beachtet habe und verpflichte mich hiermit, die dort genannten Vorgaben bei allen wissenschaftlichen Tätigkeiten zu beachten und umzusetzen. Ich versichere, dass die eingereichte elektronische Fassung der eingereichten Druckfassung vollständig entspricht.

Curriculum Vitae

Thomas Paß
Weyerstraße 77
D-50676 Köln
0170 2053913
thomas.pass@uk-koeln.de

Date and Place of Birth:
2nd of March 1992 in Coesfeld
Nationality:
German

Publication List

2020	Konrad M. Ricke*, **Thomas Paß***, Sammy Kimoloi, Kai Fährmann, Christian Jüngst, Astrid Schauss, Olivier R. Baris, Marijana Aradjanski, Aleksandra Trifunovic, Therese M. Eriksson Faelker, Matteo Bergami and Rudolf J. Wiesner
	Mitochondrial Dysfunction Combined with High Calcium Load Leads to Impaired Antioxidant Defense Underlying the Selective Loss of Nigral Dopaminergic Neurons
	Journal of Neuroscience, 26 February 2020, 40 (9) 1975-1986
2020	**Thomas Paß**, Marlene Aßfalg, Marianna Tolve, Sandra Blaess, Markus Rothermel, Rudolf J. Wiesner and Konrad M. Ricke
	The Impact of Mitochondrial Dysfunction on Dopaminergic Neurons in the Olfactory Bulb and Odor Detection
	Molecular Neurobiology, 21 June 2020, 57 (9), 3646-3657
2020	Sammy Kimoloi, Rafael Oexner, David Pla-Martin, **Thomas Paß**, Martin H.J. Wiesen, Peter Zentis, Astrid Schauss, Olivier R. Baris and Rudolf J. Wiesner
	Extraocular muscle reveals selective vulnerability of Type IIB fibers to respiratory chain defects induced by mitochondrial DNA deletions
	Investigative Ophthalmology and Visual Science, in revision

Education

04/2017 – present	**PhD Position** | Rudolf Wiesner's lab | Center for Physiology and Pathophysiology | University Hospital of Cologne
10/2014 – 02/2017	**Master of Science** | Clinical and Experimental Neuroscience | University of Cologne | Grade: 1.7
10/2011 - 10/2014	**Bachelor of Science** | Biology | Heinrich-Heine University of Düsseldorf | Grade: 2.3 Emphasis on Neurobiology and Neurophysiology
06/2011	**General Matriculation Standard** | Abitur | Gymnasium Mariengarden | Borken Burlo

Research Experience

Master Thesis	"Subtype-specific Impact of Autophagy Inhibition on Distribution of the Adaptor Protein p62/SQSTM1 in Neurons"

| 07/2016 – 02/2017 | Investigation of molecular mechanisms underlying autophagy in distinct neuronal subtypes was performed. In particular, differential expression of the autophagy-related adaptor protein p62/SQSTM1 was analyzed in excitatory and inhibitory neurons using wildtype and autophagy-deficient primary neuronal culture. |
| Bachelor Thesis | Literature-based study of the impact of the astrocyte Na^+/K^+-ATPase on neuron-glia interactions. |

Internships

06/2016 - 02/2017	CECAD Research Center	**Dr. Natalia Kononenko**	Cologne	Internship and Master's Thesis
10/2015 - 12/2015	Institute of Neuropathology	**Prof. Dr. med. Astrid Jeibmann**	Münster	six-week	Preparation of a group internal paper: "Downregulation of IRP-1B Promotes Longevity of Aβ42 Expressing and Wildtype Drosophila Melanogaster in General and in Social Isolation"
09/2015 - 10/2015	Institute of Vegetative Physiology	**Prof. Dr. rer. nat. Rudolf J. Wiesner**	Cologne	six-week	Preparation of a group internal paper: "The Neuroprotective Role of Calbindin in Substantia Nigra Dopaminergic Respiratory-Chain-Deficient Neurons in a Mouse Model of Parkinson's Disease"
08/2013	Hospital Laboratory	St. Marien Hospital	Borken	four-week

Continuing Education

Graduate School	Graduate School for Biological Science (**GSfBS**)	since 05/2018
Animal Treatment	**Laboratory Animal Science Course**	Acquisition of general knowledge for performing animal experiments in mice and rats	FELASA B	University of Cologne	09/2017
Graduate Program	Integrated Research Training Group in Mitochondrial Biology (**mito-RTG**)	SFB-1218	since 04/2017

Further Information

Honorary Scientific Activity	**Organizing committee**	MitoChats	Scientific Symposium on Mitochondrial Biology	University of Cologne	10th-12th 07/2019
Honorary Position	**Chairman**	Pfarrjugend St. Ludgerus Borken	08/2013 – 08/2017 Youth group attendant	Pfarrjugend St. Ludgerus Borken	08/2008 - 08/2013
Language Skills Basic	German: Native language	**English**: safe in speech and writing	Latin, French:
Interests	Family and friends	Music	Sports

Cologne, 27th of April 2020   Thomas Paß